STUDY OF NEUTRINOLESS DOUBLE BETA DECAY WITHIN PHFB MODEL

THESIS SUBMITTED FOR THE AWARD OF THE DEGREE

OF

Doctor of Philosophy

In

Applied Physics

By

Yash Kaur Singh

Enrolment No.: 265/13

Under the Supervision of

Dr. Ramesh Chandra

Department of Applied Physics

School for Physical Sciences

Babasaheb Bhimrao Ambedkar University, Lucknow

U.P., (India) – 226025

2018

DEDICATED

TO

MY

LOVING

FAMILY

DECLARATION

I declare that the thesis titled "**Study of Neutrinoless Double Beta Decay Within PHFB Model**" has been prepared by me under the supervision of **Dr. Ramesh Chandra**, Assistant Professor, Department of Applied Physics, School for Physical Sciences, Babasaheb Bhimrao Ambedkar University, Lucknow. No part of this thesis has formed the basis for the award of any degree, diploma or fellowship previously. Further, I declare that the material embodied in the present work is based on original research work and the indebtedness to others has been duly acknowledged at relevant places. This is also declared that the thesis is essentially free from all kinds of plagiarism.

Yash Kaur Singh
24-09-2018

(Yash Kaur Singh)

Department of Applied Physics

School for Physical Sciences

Babasaheb Bhimrao Ambedkar University

Vidya Vihar, Raebareli Road

Lucknow, (U.P.), India- 226025

Date: 24th September, 2018

Place: Lucknow

CERTIFICATE

This is to certify that the thesis titled "**Study of Neutrinoless Double Beta Decay Within PHFB Model**" submitted by **Ms. Yash Kaur Singh** is an original research work and has not been previously submitted in part or full for the award of any other degree or diploma to this or any other university or institutions.

The thesis submitted to Babasaheb Bhimrao Ambedkar University, Lucknow satisfies all the requirements as stipulated in the *Doctor of Philosophy (Ph.D.) Regulations – 1999 as amended in 2010* and it is fit for submission and evaluation for the award of the degree of Doctor of Philosophy of the University.

Date: 24th September, 2018

Supervisor

Head of the Department

ACKNOWLEDGEMENT

First and foremost, I would like to thank the Almighty for His continuous showers of blessings throughout my research work without which it would not have been possible to begin this task. Thank you God for this day on which the research work stands successfully compiled in this thesis.

I feel obliged to take this opportunity to express my heartfelt reverences towards my supervisor and mentor Dr. Ramesh Chandra, Assistant Professor, for his invaluable guidance, vision, sincerity and motivation that kept me deeply inspired during whole course of research work. Besides guiding and encouraging me throughout this task, he was always there providing scholarly inputs and clarifying my doubts. Even the most stupid queries were met with amicable and positive disposition and with great sense of humor.

Next I would like to express my deep sense of gratitude towards my family. My father Shri Om Prakash Singh and Mother Smt. Sunita Singh have been constant torch bearers for me constantly encouraging and providing all necessary guidance, support and inspiration towards acquiring new skills. Support of my elder brother Mr. Kaushal Pal Singh as well as my sister Mrs. Mamta Singh needs no mention, without them it would have not been such a smooth task. I am highly indebted to all my family members, they helped me glide smoothly during times of despair.

I would like to express my deep gratitude to Dr. Devesh Kumar, Professor and Head of the Department, for his patient guidance, enthusiastic encouragement and useful critiques of this research work. His advice and assistance kept my progress on schedule and helped raise the bar to this satisfactory level.

I am highly grateful to the help and support provided by faculties of the department: Prof. B. C. Yadav, Dr. A. K. Yadav, Dr. K. B. Thapa and Dr. Devendra Singh for helping

me improve this task. I would like to pay my gratitude towards Prof. P. K. Rath, Lucknow University who continuously provided valuable suggestions and concise comments on given state of research work without which it would have been an impossible task. They were always available for fruitful discussions culminating into successful results. I feel extremely enlightened by the company of their thought provoking deliberations.

I would like to mention the help provided by my research group Mr. Vivek Kumar Nautiyal, Mr. Ratindra Gautam, Ms. Ruchi Mishra and Mrs. Nilima Das who were ever willing to lend helping hand even during odd hours. The help provided during course of Ph.D. research and manuscript preparation is highly acknowledged. Paucity of space does not allow me to mention the names of other researchers of the department, their support is highly acknowledged. I thank one and all who have directly or indirectly helped me or inspired me towards achievement of my goal.

Finally I would like to appreciate support and facilities extended by staff at Library and Computer Center of the Department as well as the University for aiding in literature survey and other requirements.

Yash Kaur Singh

(Yash Kaur Singh)

ABSTRACT

The study of nuclear $\beta\beta$ decay in general and neutrinoless double beta ($0\nu\beta\beta$) decay in particular has far reaching consequences in the panorama of lepton number violating processes. The confirmation of neutrino oscillation -one of the most captivating topics of Neutrino Physics- suggests that the neutrinos are massive. However, the actual mass of neutrinos can not be extracted from the oscillation data, which provide only mass-squared differences. On the other hand, the study of tritium single β decay and $\beta\beta$ decay together are capable to meet the above mentioned challenges. In fact, the $0\nu\beta^-\beta^-$ decay is the only potentially viable way to answer the question whether neutrinos are of Dirac or Majorana nature. The experimental observation of $0\nu\beta^-\beta^-$ decay will immediately imply the Majorana nature of neutrinos.

The $0\nu\beta^-\beta^-$ decay has not been experimentally observed hitherto, and only limits on half-lives of $0\nu\beta^-\beta^-$ decay are available. These half-life limits permit to extract limits on various effective lepton number violating parameters. One has to understand the mechanism of nuclear transition and evaluate the corresponding nuclear transition matrix elements (NTMEs) with high reliability in order to get accurate effective lepton number violating parameters. The $2\nu\beta^-\beta^-$ and $0\nu\beta^-\beta^-$ decays involve the same set of initial and final nuclear wave functions. The usual strategy is to first calculate NTMEs $M_{2\nu}$ for $2\nu\beta^-\beta^-$ decay. The $2\nu\beta^-\beta^-$ decay has been observed in eleven nuclei out of 35 possible candidates. The half-life of $2\nu\beta^-\beta^-$ decay is a product of accurately known phase space factor and NTME. One can extract NTMEs from the observed half-lives. A comparison between the theoretically calculated and experimentally extracted NTMEs provides a cross-check on the reliability of different nuclear models used for the calculation of NTMEs. It is observed in all cases of $2\nu\beta^-\beta^-$ decay that the NTMEs $M_{2\nu}$ are sufficiently quenched. The realization of this quenching mechanism is the main motive of all the theoretical

calculations. In the present work, the $2\nu\beta^-\beta^-$ decay for the $0^+ \rightarrow 2^+$ transition and $0\nu\beta^-\beta^-$ decay for the $0^+ \rightarrow 0^+$ transition have been studied.

PREFACE

The present thesis is on the study of $0\nu\beta^-\beta^-$ decay of ^{94,96}Zr, ^{100}Mo, ^{110}Pd, ^{128,130}Te and ^{150}Nd nuclei for the $0^+ \rightarrow 0^+$ transition. The half life of $2\nu\beta^-\beta^-$ decay for the $0^+ \rightarrow 0^+$ transition has been already measured for eleven nuclei and hence, the values of NTMEs $M_{2\nu}$ can be extracted directly from the observed half-lives of $2\nu\beta^-\beta^-$ decay. Consequently, the validity of different nuclear models employed for structure calculations can be tested by studying the $2\nu\beta^-\beta^-$ decay. The $0\nu\beta^-\beta^-$ decay is not observed so far. The aim of all the present experimental activities is to observe the $0\nu\beta^-\beta^-$ decay. As the $0\nu\beta^-\beta^-$ decay is not observed, the models predict the half-lives assuming certain value for the neutrino mass or extract limits on different effective gauge theoretical parameters from the experimentally observed limits on half-lives $T^{0\nu}_{1/2}$.

Nuclear models, which are generally used in the calculation of NTMEs of $2\nu\beta^-\beta^-$ decay, can be classified in to shell model and its variants, quasiparticle random phase approximations (QRPA) and its extensions and alternative models. The shell model is the best choice for the calculation of NTMEs. However, its application is limited only to *pf* shell nuclei, the study of which even requires a large number of basis states. In heavier nuclei, it is difficult to perform a reliable shell model calculations without severe truncation. The QRPA and its extensions are the commonly used models for the calculation of NTMEs. The QRPA calculations can be performed in large model spaces and this is the advantage over the shell model approach. Nevertheless, the extreme sensitivity of NTMEs to the strength of particle-particle interaction does not allow a reliable prediction of $2\nu\beta^-\beta^-$ decay rates. Moreover, the QRPA solutions collapse within the physical range of particle-particle strength parameter g_{pp}. Many extensions of the QRPA have been proposed to cure these problems, but none of them are free from ambiguities. The small predictive power of the QRPA is the main motivation to look for alternative

models. In the present work, we calculate NTMEs of $2\nu\beta^-\beta^-$ as well as $0\nu\beta^-\beta^-$ decay in Projected Hartree-Fock-Bogoliubov (PHFB) model using pairing plus multipole type of effective two-body interaction. This thesis contains following five chapters.

In Chapter 1, the literature survey on work done so far to study the $2\nu\beta^-\beta^-$ as well as $0\nu\beta^-\beta^-$ decay has been presented.

In Chapter 2, we present the theoretical formalism to calculate the nuclear spectroscopic properties, specifically, the yrast spectra, reduced $B(E2{:}0^+ \rightarrow 2^+)$ transition probabilities, deformation parameter β_2 and g-factors $g(2^+)$. The calculated spectroscopic properties of ^{94,96}Zr, ^{94,96,100}Mo, ^{100,104}Ru, ^{104,110}Pd, ^{110}Cd, ^{128,130}Te, ^{128,130}Xe, ^{150}Nd and ^{150}Sm nuclei are compared with the observed experimental data and there by, we check the "goodness of wave functions".

In Chapter 3, we calculate NTMEs $M_{2\nu}(2^+)$ and half-lives $T^{2\nu}_{1/2}(2^+)$ of $2\nu\beta^-\beta^-$ decay of ^{94,96}Zr, ^{100}Mo, ^{104}Ru, ^{110}Pd, ^{128,130}Te and ^{150}Nd nuclei for the $0^+ \rightarrow 2^+$ transition. We also examine the effect of deformation on NTMEs $M_{2\nu}(2^+)$.

In Chapter 4, we study the $0\nu\beta^-\beta^-$ decay of ^{94,96}Zr, ^{100}Mo, ^{110}Pd, ^{128,130}Te and ^{150}Nd nuclei for the $0^+ \rightarrow 0^+$ transition within mechanisms involving light Majorana neutrino mass and right handed current. We calculate the required NTMEs and extract limits on the effective light Majorana neutrino mass $< m_\nu >$, the effective weak coupling of right-handed leptonic current with right-handed hadronic current $< \lambda >$, and the effective weak coupling of right-handed leptonic current with left-handed hadronic current $< \eta >$ from the recent available limits on half-lives of $0\nu\beta^-\beta^-$ decay. In addition, we also investigate the role of deformation on NTMEs of $0\nu\beta^-\beta^-$ decay.

Finally, we conclude with Chapter 5 in which the most important aspects of nuclear structure in the context of PHFB model and uncertainties in NTMEs are discussed. We also suggest a number of necessary improvements to be incorporated in the PHFB model

for a more reliable study of $\beta^-\beta^-$ decay in general and $0\nu\beta^-\beta^-$ decay in particular.

LIST OF TABLES

2^+ transition of ^{94,96}Zr, ^{100}Mo, ^{104}Ru, ^{110}Pd, ^{128,130}Te and ^{150}Nd nuclei along with experimental half-lives $T^{2\nu}_{1/2}(2^+)$. "*" denotes the present calculation with average NTME.

Table 4.1: Theoretically calculated NTMEs M_α ($\alpha = \omega F$, qF, ωGT, qGT, qT, P, R) with the inclusion of SRC (SRC1, SRC2 and SRC3).

Table 4.2: Combination of NTMEs $M^{(0\nu)}$ and $M_{i\pm}$ ($i = 1, 2$). The values of $M^{(0\nu)}$ have been taken from Rath *et al.* (2013) and reevaluated at $g_A = 1.2701$.

Table 4.3: Change in the NTME M_α of $0\nu\beta^-\beta^-$decay (in %) due to the exchange of light Majorana neutrino, and admixture of $V - A$ and $V + A$ currents, with the inclusion of FNS and SRC (SRC1, SRC2, and SRC3) for all four parametrizations of the effective two-body interaction.

Table 4.4: Average values for NTMEs $\overline{M}_\alpha$ (uncertainty $\Delta\overline{M}_\alpha$) ($\alpha = \omega F$, qF, ωGT, qGT) for the $0\nu\beta^-\beta^-$ decay of ^{94,96}Zr, ^{100}Mo, ^{110}Pd, ^{128,130}Te and ^{150}Nd isotopes.

Table 4.5: Average values for NTMEs $\overline{M}_\alpha$ (uncertainty $\Delta\overline{M}_\alpha$) ($\alpha = qT$, P, R) for the $0\nu\beta^-\beta^-$ decay of ^{94,96}Zr, ^{100}Mo, ^{110}Pd, ^{128,130}Te and ^{150}Nd isotopes.

Table 4.6: Average nuclear structure factors $\overline{C}_{mm}$, $\overline{C}_{m\lambda}$, $\overline{C}_{m\eta}$, $\overline{C}_{\lambda\lambda}$, and $\overline{C}_{\eta\eta}$ for the $0\nu\beta^-\beta^-$ decay of ^{96}Zr, ^{100}Mo, ^{110}Pd, ^{130}Te and ^{150}Nd isotopes.

Table 4.7: Effective NTMEs $M^{(0\lambda)}_{eff}$ and $M^{(0\eta)}_{eff}$ along with $M^{(0\nu)}$ for the $0\nu\beta^-\beta^-$ decay of ^{96}Zr, ^{100}Mo, ^{110}Pd, ^{130}Te and ^{150}Nd isotopes.

Table 4.8: Experimental limits on half-lives $T^{(0\nu)}_{1/2}$ and the extracted on-axis limits on the effective mass of light neutrino $\langle m_\nu\rangle$, $\langle\lambda\rangle$, and $\langle\eta\rangle$ for the $0\nu\beta^-\beta^-$ decay of ^{96}Zr, ^{100}Mo, ^{110}Pd, ^{130}Te and ^{150}Nd isotopes. Predicted half-lives $T^{(0\nu)}_{1/2}$ of $0\nu\beta^-\beta^-$decay for two sets of parameters (i) $\langle m_\nu\rangle = 50$ meV (Case I) and (ii) $\langle m_\nu\rangle = 50$ meV, $\langle\lambda\rangle = 10^{-7}$ and $\langle\eta\rangle = 10^{-9}$ (Case II).

Table 4.9: Minimum and maximum values of D_α ($\alpha = \omega F$, qF, ωGT, qGT, qT, P, R) using all four parametrizations of the effective two-body interaction with the inclusion of

SRC (SRC1, SRC2, and SRC3).

LIST OF FIGURES

Fig. 3.1(h): NTMEs of $2\nu\beta^-\beta^-$ decay for the $0^+ \rightarrow 2^+$ transition of ^{150}Nd as a function of the difference in the deformation parameter $\Delta\beta_2$. "$\times$" denotes the value of calculated NTMEs for $\Delta\beta_2$ at $\zeta_{qq} = 1.0$.

TABLES OF CONTENTS

Chapter 1

Introduction

The story of neutrinos as well as weak interaction is rather checkered and quite exciting due to their enigmatic nature. In nature, the primordial neutrinos were produced during the first three minutes of the big-bang in which the universe was created 13.7 ± 0.2 Gyr ago. Among all the particles that constitute the Universe, neutrinos are the most common and the most weird particles. Billions of billion neutrinos are crossing our body per second but we never realize them. They are as near to nothing as anything. The first evidence for the physical existence of neutrinos came from the study of beta (β) decay. In order to explain the continuous β-spectrum, Pauli in 1930 proposed that in the β decay process, the electron is emitted together with a massless and chargeless particle of spin 1/2. He called this particle *neutron* (the neutral one). In 1932, J. Chadwick discovered a chargeless and spin 1/2 particle in the nuclear reaction

$$^4He +^9 Be \rightarrow^{12} C + n$$

However, this discovered particle was heavy and thus different than that of proposed by Pauli. This particle was given the name *neutron*. After the discovery of neutron, the particle proposed by Pauli was called *neutrino* (little neutron) by Enrico Fermi. In 1934, Fermi gave the first successful theory of β decay considering the neutrino. Experimentally the neutrino was detected by F. Reines and C. W. Cowan at Savannah River experiment in 1956.

Out of the four fundamental interactions, namely gravitation, electromagnetic, strong interaction and weak interaction, the weak interaction is closely related to the neutrino. In 1956, T. D. Lee and C. N. Yang, to resolve the $\tau - \theta$ puzzle, proposed for the first time that parity (P) might not be conserved in weak interaction. In 1957, C. S. Wu and co-workers of the National Bureau of Standards confirmed the parity violation in weak interaction through β decay of ^{60}Co. The experiment seemed also to prove that the charge symmetry (C) was violated. Leon M. Lederman, Melvin Schwartz and Jack Steinberger showed in 1962 that more than one type of neutrino exist by first detecting interactions of the muon neutrino. In 1975, a third type lepton, tau (τ), was discovered at Stanford Linear Accelerator. With the discovery of τ lepton it was natural to expect an associated neutrino. First evidence for this third type of neutrino came from the observation of missing energy and momentum in τ decays analogous to the β decay that had led to the discovery of the neutrino in first place. The direct observation of actual tau neutrino (ν_τ) interactions was achieved by DONUT collaboration at Fermilab in the year 2000.

Parity violation sets weak forces and the theories that explain them in a completely different footing than the other ones. In 1964, J. Cronin and his team showed that, in the decays of neutral kaons, not only the spatial symmetry P was violated but also the

combination CP was violated. Although this CP symmetry breaking is very tiny but could have created an initial asymmetry between matter and antimatter at the beginning of the universe. In 2004, the BaBar collaboration at SLAC National Accelerator Laboratory has observed that CP is violated in the decay of neutral B meson also.

The electromagnetic interaction and the weak interaction have been unified, known as electro-weak interaction, in the Standard Model (SM) due to works of S. L. Glashow (1961), S. Weinberg (1967) and A. Salam (1968). According to this theory, the photon, which is a boson, transports the electromagnetic interaction. For the transport of weak interaction, three other bosons $W^{\pm}$ and Z bosons are needed . In the β decay process, a neutron within nucleus transforms into a proton by emitting a W^{-} boson which, soon after, decays into an electron antineutrino pair. In the process of inverse β decay, a proton inside the nucleus transforms into a neutron by emitting a W^{+} boson. Carlo Rubbia and Simon van der Meer developed facility at CERN which first produced and detected $W^{\pm}$ and Z bosons. They were awarded the Nobel Prize for their leadership of this discovery experiment.

The SM of electroweak unification is a quantum field theory based on the gauge symmetry $\mathrm{SU(3)}_C \times \mathrm{SU(2)}_L \times \mathrm{U(1)}_Y$ in which $\mathrm{SU(3)}_C$ is the symmetry group of the strong interactions and $\mathrm{SU(2)}_L \times \mathrm{U(1)}_Y$ is the symmetry group of the electroweak interactions. The gauge sector of the SM is composed of eight gluons which are the gauge bosons of $\mathrm{SU(3)}_C$ and the photon (γ), $W^{\pm}$ and Z bosons which are the four gauge bosons of $\mathrm{SU(2)}_L \times \mathrm{U(1)}_Y$. The fermionic sector of SM contains 45 chiral fermions and their antiparticles which are

organized in three families. The particles in each family are as follows:

$$\begin{array}{ccc} 1^{st} \text{ family} & 2^{nd} \text{ family} & 3^{rd} \text{ family} \\ \begin{pmatrix} \nu_e \\ e^- \end{pmatrix}_L, e_R^-, \begin{pmatrix} u \\ d \end{pmatrix}_{L,R} & \begin{pmatrix} \nu_\mu \\ \mu^- \end{pmatrix}_L, \mu_R^-, \begin{pmatrix} c \\ s \end{pmatrix}_{L,R} & \begin{pmatrix} \nu_\tau \\ \tau^- \end{pmatrix}_L, \tau_R^-, \begin{pmatrix} t \\ b \end{pmatrix}_{L,R} \end{array} \tag{1.1}$$

The neutrinos are very elusive and hardly interact with the matter. Raymond Davis Jr. was the first person to look into the heart of a star by capturing the neutrinos produced in the sun's core and spread out across the space. In 1967, Raymond Davis started looking for neutrinos produced by the nuclear fusion reactions in the Sun's core using a huge tank of cleaning fluid (C_2Cl_4) which was placed deep underground to shield it from cosmic rays. However, he could only detect about one third of what was predicted by the theoretical calculation of John N. Bahcall using solar models. This discrepancy between experimental finding and theoretical calculation was called the "mystery of missing neutrinos". Other underground detectors also found similar neutrino shortfall. In 1957, Bruno Pontecorvo, inspired by the possibility of $K^0 - \overline{K}^0$ oscillation, proposed the possibility of transitions neutrino→antineutrino provided lepton number is not conserved [Pontecorvo (1957)]. This was the first idea about neutrino oscillation. Independently, Maki, Nakagawa and Sakata in 1962 proposed that neutrinos might change from one flavor into another (flavor oscillations) [Maki *et al.* (1962)]. Gradually, physicists started to suspect that neutrino oscillation could explain the mystery of missing neutrinos. The detectors could capture only one type of neutrino flavor, and neutrinos during their journey from the Sun to earth changed their flavor and escaped detection. According to the *SM* the neutrinos should have zero mass, however, there was no valid reason for the same. The

quantum theory requires that if neutrinos change flavor then they must have mass. The neutrino oscillations have been confirmed in atmospheric, solar, accelerator and reactor neutrinos and thereby establishing the fact that the neutrinos have mass.

1.1 Mass and nature of neutrinos

1.1.1 Nature of neutrinos

All known fundamental fermions other than neutrinos are Dirac particles due to the conservation of electric charge. It is well known that the massless neutrinos are Weyl particles and can be described by two component complex spinors. On the other hand, it is natural to treat the massive neutrinos like any other fermion and therefore they should be 4-component Dirac spinors. However, an important difference between the neutrinos and other fermions is that they are neutral particles. This suggests a new theoretical possibility that the neutrinos might also be 2-component Majorana spinors.

In chiral representation, the left and right handed particles are defined as

$$\psi_L = \frac{1-\gamma_5}{2}\psi \quad and \quad \psi_R = \frac{1+\gamma_5}{2}\psi. \tag{1.2}$$

Under combined operation of CP, the chiral fields transform as

$$CP\psi_L = \psi_R^C \quad and \quad CP\psi_R = \psi_L^C, \tag{1.3}$$

where $\psi^C = C\overline{\psi}^T = C\gamma_0\psi^*$ with $C = -i\gamma_2\gamma_0$. In this representation, the most general

mass term can be written in the form [Doi *et al.* (1985)]

$$\begin{aligned} L &= L_M + L_D \\ &= -\frac{1}{2} m_L \overline{\psi_L^C} \psi_L - \frac{1}{2} m_R \overline{\psi_R^C} \psi_R - \frac{1}{2} m_D \overline{\psi}_R \psi_L + h.c. \qquad (1.4) \\ &= \frac{1}{2} \left(\psi \quad \psi^C \right)_L^T C^{-1} \begin{pmatrix} m_L & m_D \\ m_D & m_R \end{pmatrix} \begin{pmatrix} \psi \\ \psi^C \end{pmatrix}_L + h.c. \\ &= \frac{1}{2} \Psi_L^T C^{-1} M \Psi_L \qquad (1.5) \end{aligned}$$

The two eigen values obtained by the diagonalization of the mass matrix are

$$m_{1,2} = \frac{1}{2} \left[(m_L + m_R) \pm \sqrt{(m_L + m_R)^2 + 4 m_D^2} \right]. \qquad (1.6)$$

From this analysis, the following possibilities emerge.

(i) The neutrons are Weyl particles if $m_L = m_R = m_D = 0$.

(ii) If $m_L = m_R = 0$, then $m_{1,2} = m_D$. In this case, the neutrinos are pure Dirac particles resulting from the superposition of a pair of degenerate Majorana neutrinos. Following Doi *et al.* (1983), this can be seen as follows.

The Lagrangian density for a Dirac field $\psi(\mathbf{x}, t)$ is given by

$$\begin{aligned} L &= \overline{\psi}(i\gamma_\mu \partial^\mu - m)\psi \qquad (1.7) \\ &= L_L(\eta) + L_R\left(\overline{\xi}\right) \qquad (1.8) \end{aligned}$$

with

$$\chi = \left(\eta + i\overline{\xi}\right)/\sqrt{2} \qquad \phi = -i\sigma_2 \left(\eta^* + i\overline{\xi}^*\right)/\sqrt{2}. \qquad (1.9)$$

Hence, a Dirac field ψ consists of two Majorana neutrinos

$$\psi = (N_1 + iN_2)/\sqrt{2}, \qquad (1.10)$$

where

$$N_1 = \begin{pmatrix} -i\sigma_2\eta^* \\ \\ \eta \end{pmatrix} \qquad N_2 = \begin{pmatrix} \xi \\ \\ i\sigma_2\xi^* \end{pmatrix}. \tag{1.11}$$

The fields N_1 and N_2 satisfy the Majorana condition

$$N_1 = C\overline{N}_1^T \qquad and \qquad N_2 = C\overline{N}_2^T. \tag{1.12}$$

Further, it is seen that η and ξ behave as left and right handed Majorana neutrinos with opposite CP phase. The Dirac neutrino may be expressed as a pair of degenerate Majorana neutrinos

$$\psi_L = \frac{N_{1L} + iN_{2L}}{\sqrt{2}} \quad and \quad \psi_R = \frac{(N_{1L})^C + i(N_{2L})^C}{\sqrt{2}}. \tag{1.13}$$

Moreover, a Dirac field can be constructed from two Majorana fields related to N_1 and N_2 by the orthogonal transformation

$$\begin{pmatrix} N_1(\alpha) \\ \\ N_2(\alpha) \end{pmatrix} = \begin{pmatrix} \cos\alpha & -\sin\alpha \\ \\ \sin\alpha & \cos\alpha \end{pmatrix} \begin{pmatrix} N_1 \\ \\ N_2 \end{pmatrix}. \tag{1.14}$$

Hence

$$\psi_\alpha = e^{i\alpha}\psi. \tag{1.15}$$

In case one uses a unitary transformation in Eq. (1.14), a Jauch field is obtained in which particles and antiparticles are mixed [Jauch (1954)]. In case the pair of neutrinos are of same flavor, the composed Dirac neutrino is called as an ordinary Dirac neutrino with definite lepton number L, which is conserved. On the other hand, if two or more flavors of neutrinos are involved, a Dirac neutrino is formed as

$$\psi = \nu_{eL} + (\nu_{\mu L})^C \quad and \quad L_M = -m\overline{\psi}\psi. \tag{1.16}$$

This Dirac neutrino is characterized by the combination of lepton numbers $L_e - L_\mu$, which is conserved. This type of Dirac neutrino is called the Konopinski-Mahmoud (KM) Dirac neutrino [Konopinski and Mahmoud (1953), Bilenky and Pontecorvo (1981), Kotani (1984), Petcov (1982), Leung and Petcov (1983), Valle (1983), Valle and Singer (1983), Wyler and Wolfstein (1983), Doi *et al.* (1984)].

(iii) If the Dirac mass $m_D = 0$, then $m_{1,2} = m_L$, m_R and neutrinos are of pure Majorana character [Doi *et al.* (1985)].

(iv) In case $m_D >> m_L$, m_R, then the neutrinos are of Pseudo-Dirac nature [Doi *et al.* (1985)].

In 1957, Bruno Pontecarvo (1957) and independently in 1962, Maki, Nakagawa and Sakata [Maki *et al.* (1962)] had already proposed that neutrinos might change from one flavor into another a phenomenon called neutrino oscillation given by

$$|\nu_\alpha\rangle = \sum_{i=1}^{n} U_{\alpha i} \, |\nu_i\rangle \, , \tag{1.17}$$

where the mixing matrix U is known as PMNS matrix after the names of Pontecorvo, Maki, Nakagawa and Sakata. The ν_α is a superposition of physical sates ν_i with masses m_i.

1.1.2 Mass of neutrinos

The classical way to determine the mass of electron neutrino ν_e is the investigation of the electron spectrum in β decay. The limit on the mass of ν_e obtained from tritium β decay experiments of Mainz [Kraus *et al.* (2005)] is $m_{\nu_e} \leq 2.3$ eV (95% CL). The upper limits obtained from Troitsk experiment [Aseev *et al.* (2011)] are $m_{\nu_e} \leq 2.12$ eV (95% CL) and

$m_{\nu_e} \leq 2.05$ eV (95% CL) using Bayesian statistics and Feldman and Cousins approach, respectively. The proposed KATRIN experiment is expected to reach a limit of 0.2 eV [Thümmler (2012)]. The limit on muon neutrino, ν_μ, is given by the two body decay of the $\pi^+ \rightarrow \mu^+ + \nu_\mu$. The study of pion decay into muon and ν_μ at PSI has yielded an upper limit on mass of muon neutrino $m_{\nu_\mu} < 0.19$ MeV (90% CL) [Groom *et al.* (2000)]. The investigation of τ-decays into 5 charged pions and ν_τ to extract the mass of tau neutrino ν_τ at ALEPH [Barate *et al.* (1998)] and OPAL [Ackerstaff *et al.* (1998)] has given limits $m_{\nu_\tau} < 18.2$ MeV (95% CL) and $m_{\nu_\tau} < 27.6$ MeV (95% CL), respectively.

Neutrino oscillations

Neutrino oscillations are peculiar quantum mechanical effect. It is hard to find a good macroscopic analogy of neutrino oscillation as it is concerned with the wave-particle duality of the matter. For massive neutrinos, the flavor eigenstates ν_α are not identical to the mass eigenstates ν_i. Instead, ν_α are the linear superposition of ν_i. During the propagation of neutrino beam, different components of the beam evolve differently, so that the probability of finding different flavor eigenstates in the beam varies with time. Assuming relativistic neutrinos and CP conservation, the quantum mechanical transition probability for the neutrino to oscillate from one flavor into another can be derived as [Bilenky *et al.* (1987)]

$$P(\nu_\alpha \rightarrow \nu_\beta) = \sum_i |U_{\beta i}|^2 |U_{\alpha i}|^2 + \mathrm{Re} \sum_{i \neq j} U_{\beta i} U^*_{\beta j} U^*_{\alpha i} U_{\alpha j} \exp\left(\frac{-it\Delta m^2_{ij}}{2E}\right) \qquad (1.18)$$

with $\Delta m_{ij}^2 = \left|m_i^2 - m_j^2\right|$. In the simple two-flavor mixing, the probability to find ν_β in a distance x with respect to a source of ν_α is given by

$$P(\nu_\alpha \rightarrow \nu_\beta) = \sin^2 2\theta \, \sin^2 \frac{\pi x}{L} \tag{1.19}$$

giving the oscillation length L in practical units as

$$L = \frac{4\pi E\hbar}{\Delta m^2 c^3} = 2.48 \left(\frac{E}{MeV}\right) \left(\frac{eV^2}{\Delta m^2}\right) m \tag{1.20}$$

From the above discussions it is concluded that the neutrino oscillations have been finally confirmed. Moreover, Barbeiri *et al.* (1998) and Barger *et al.* (1998) have shown that the oscillations among three neutrino species are sufficient to explain the solar and atmospheric neutrino puzzle. Considering the three generations for neutrinos and excluding the sterile neutrino, however no evidences exist to discard it, we have

$$|\nu_\alpha\rangle = \sum_{i=1}^{3} U_{\alpha i} \nu_i \tag{1.21}$$

where α, i and $U_{\alpha i}$ are the flavor index, mass index and unitary mixing matrix respectively. In case of Majorana neutrinos, the favorite parametrization of U is given in terms of three mixing angles θ_{12}, θ_{23} and θ_{13} and three CP phases as [Kobayashi and Maskawa (1973)]

$$U = \begin{pmatrix} c_{12}c_{13} & s_{12}c_{13}e^{-i\delta_{12}} & s_{13}e^{-i\delta_{13}} \\ -s_{12}c_{23}e^{i\delta_{12}} - c_{12}s_{23}s_{13}e^{i(\delta_{13}+\delta_{23})} & c_{12}c_{23} - s_{12}s_{23}s_{13}e^{i(\delta_{23}+\delta_{13}-\delta_{12})} & s_{23}c_{13}e^{i\delta_{23}} \\ s_{12}s_{23}e^{i(\delta_{13}+\delta_{23})} - c_{12}s_{23}s_{13}e^{i(\delta_{13}+\delta_{23})} & -c_{12}s_{23}e^{i\delta_{23}} - s_{12}c_{23}s_{13}e^{i(\delta_{13}-\delta_{12})} & c_{23}c_{13} \end{pmatrix} \tag{1.22}$$

with $c = \cos\theta$ and $s = \sin\theta$.

Reactor experiments: Reactor experiments come under the class of disappearance experiments looking for $\overline{\nu}_e \rightarrow \overline{\nu}_X$. In reactor experiments, one tries to prove that lesser

number of neutrinos of the same flavor reach the detector than what would be expected from the source. These reactor experiments measure all channels, e.g. $\nu_e \rightarrow \nu_\mu$, ν_τ etc. However, a precise knowledge of the neutrino flux is necessary which is a disadvantage of disappearance experiments. The reactor neutrino experiments have been nicely reviewed by Wen *et al.* (2017).

Several reactor experiments have been done in the past, namely ILL-Grenoble, Bugey, Rovno, Savannah River, Gösgen, Krasnojarsk and Buge III. New reactor experiments are CHOOZ, Palo Verdi, KamLAND, Daya Bay, Double Chooz, and RENO. The CHOOZ experiment (France) is located underground with a shielding of 300 m.w.e., reducing the background due to atmospheric muons by a factor of about 300. The detector is a homogeneous detector about 1030 m away from two reactors of total power 8.5 GW enlarging the sensitivity to smaller Δm^2. The Palo Verdi experiment near Phoenix, AZ (USA) consists of 12 t liquid scintillator also loaded with Gd. The experiment is located under a shielding of 46 m.w.e. in a distance of about 750 (829) m to three reactors with a total power of 10.2 GW. The CHOOZ and Palo Verde experiments used modern technologies of particle physics compared to the earlier experiments giving improved understanding of detector systematics and backgrounds. The third mixing angle θ_{13} is known to be extremely small from the limits obtained from CHOOZ and Palo Verde reactor experiment [Apollonio *et al.* (2003), Boehm *et al.* (2000)]. Three new experiments, namely Daya Bay, Double Chooz and RENO were built to measure the third mixing angle θ_{13}. The KamLAND detector was placed at a vertical overburden of 2,700 m.w.e. at the site of former Kamiokande experiment. In the KamLAND reactor experiment, it has been further observed that $\overline{\nu}_e$ oscillates as well [Eguchi *et al.* (2003)]. The mixing angle θ_{12} is obtained from the solar

neutrino experiment and KamLAND reactor experiment [Ahmed *et al.* (2001)]. A new multipurpose underground liquid scintillator detector JUNO is proposed for the determination of neutrino mass hierarchy as well as precision measurement of the oscillation parameters. The value of θ_{13} obtained from global fit of data from the reactor and accelerator experiments are $sin^2\theta_{13} = 0.0218^{+0.0010}_{-0.0010}$ and $0.0219^{+0.0011}_{-0.0010}$ [Gonzalez-Garcia *et al.* (2014)] for normal and inverted hierarchy hierarchy mass spectrums, respectively.

Solar neutrino oscillations: Solar neutrinos originate from the nuclear fusion powering the Sun and other stars. The mechanism by which stars, especially our Sun, generate their prodigious quantities of energy has long been of interest to scientists. In 1965 scientists began operating a detector that would detect neutrinos from the interior of the Sun and thereby confirm that the Sun's emitted energy is derived from the fusion of hydrogen into helium. The neutrinos were observed, but at a rate about 1/3 of that predicted by the Standard Solar Model. The oscillation between neutrino families could help to explain this neutrino deficit observed in solar neutrino flux and could be a good experimental tagging of the fact that neutrinos are massive.

The first observation of electron neutrino deficit was done in Chlorine experiment at Homestake mine. Three additional experiments, namely SAGE and GALLEX, using gallium as a neutrino target, and Kamiokande, using a water-Cerenkov detector, have also given evidence for solar-neutrino oscillation. The Super-Kamiokande experiment improved the accuracy in solar neutrino studies greatly using elastic scattering process. The SNO experiment has studied charged-current and neutral-current process in addition to elastic scattering process, and has shown that solar neutrinos change their flavors from

electron type to other active types [Ahmad *et al.* (2002)]. With these experiments, the decades-old solar neutrino problem that there is a deficit in the flux of neutrinos from the sun as compared to the predictions of the standard solar model championed by Bahcall and his collaborators [Bahcall *et al.* (1998)] and by many other groups, appears solved. The values of solar neutrino oscillation parameters obtained from the global fit of existing data for normal and inverted hierarchy hierarchy mass spectrums are [Gonzalez-Garcia *et al.* (2014)] as follows:

(i) Normal hierarchy mass spectrum ($m_1 < m_2 < m_3$)

$$\Delta m_s^2 = 7.5^{+0.19}_{-0.17} \times 10^{-5}\ \text{eV}^2 \qquad and \qquad sin^2\theta_{sun} = 0.304^{+0.013}_{-0.012} \tag{1.23}$$

(ii) Inverted hierarchy mass spectrum ($m_3 < m_1 < m_2$)

$$\Delta m_s^2 = 7.5^{+0.19}_{-0.17} \times 10^{-5}\ \text{eV}^2 \qquad and \qquad sin^2\theta_{sun} = 0.304^{+0.013}_{-0.012} \tag{1.24}$$

Atmospheric neutrino oscillations: Atmospheric neutrinos result from the interaction of cosmic rays with atoms in the Earth's atmosphere, creating showers of particles, many of which are unstable and produce neutrinos when they decay. Because of the well known nature of neutrino production, there should have been twice as many muon neutrinos as electron neutrinos from the atmosphere. In the observations made in Kamiokande [Fukuda *et al.* (1994)] and IMB [Becker-Szendy *et al.* (1995)] experiments, the measured ratio of these two types was much smaller. This became known as the "atmospheric neutrino anomaly". The Super-Kamiokande experiment [Fukuda *et al.* (1998), (1999)] confirms the indications of oscillations in earlier data from Kamiokande and IMB experiments. The K2K long base line probes the ν_μ disappearance and provides the first

confirmation of atmospheric neutrino oscillation [Ahn *et al.* (2002)]. The oscillation parameters are in agreement with those of solar neutrino experiments. This agreement based on CPT invariance shows that the matter effect on oscillation is well understood. The obtained atmospheric neutrino oscillation parameters from the global fit of existing data for normal and inverted hierarchy hierarchy mass spectrums are [Gonzalez-Garcia *et al.* (2014)]

(i) Normal hierarchy mass spectrum ($m_1 < m_2 < m_3$)

$$\Delta m_a^2 = 2.457^{+0.047}_{-0.047} \times 10^{-3}\ \text{eV}^2 \qquad and \qquad sin^2\theta_{atm} = 0.452^{+0.052}_{-0.028} \tag{1.25}$$

(ii) Inverted hierarchy mass spectrum ($m_3 < m_1 < m_2$)

$$\Delta m_a^2 = 2.449^{+0.048}_{-0.047} \times 10^{-3}\ \text{eV}^2 \qquad and \qquad sin^2\theta_{atm} = 0.579^{+0.025}_{-0.037} \tag{1.26}$$

However, these oscillation data provide only mass squared difference and the actual neutrino mass cannot be extracted. On the other hand, study of tritium single β decay and $\beta\beta$ decay together can provide sharpest limits on the mass and nature of the electron neutrino.

1.2 The Nuclear $\beta\beta$ decay

The nuclear $\beta\beta$ decay is a rare second order weak transition between two isobars having even Z–even N configuration and differing by two units in nuclear charge. The $\beta\beta$ decay candidates are stable against single β decay either due to energy conservation or angular momentum mismatch. There are two modes of $\beta\beta$ decay, namely two neutrino double beta ($2\nu\beta\beta$) decay and neutrinoless double beta ($0\nu\beta\beta$) decay. In $2\nu\beta\beta$ decay the parent

nucleus decays into daughter nucleus with the emission of two antineutrinos(neutrinos) along with two electrons(positrons) while in $0\nu\beta\beta$ decay no antineutrinos(neutrinos) are emitted. The $2\nu\beta\beta$ decay conserves the lepton number L exactly and is an allowed process within *SM*. On the other hand, $0\nu\beta\beta$ decay violates the lepton number by two units and has the potential to throw light on physics beyond the *SM*. The $2\nu\beta\beta$ decay can be classified into the following four categories on the basis of electron or positron emission.

$$\begin{aligned}
&(i) \quad {}^{A}_{Z}X \rightarrow {}^{A}_{Z+2}Y + 2e^{-} + 2\overline{\nu}_e && (double\ elctron\ emission)\\
&(ii) \quad {}^{A}_{Z}X \rightarrow {}^{A}_{Z-2}Y + 2e^{+} + 2\nu_e && (double\ positron\ emission)\\
&(iii) \quad e^{-} + {}^{A}_{Z}X \rightarrow {}^{A}_{Z-2}Y + e^{+} + 2\nu_e && (electron\ capture - positron\ emission)\\
&(iv) \quad 2e^{-} + {}^{A}_{Z}X \rightarrow {}^{A}_{Z-2}Y + 2\nu_e && (double\ electron\ capture)
\end{aligned} \tag{1.27}$$

The half-life of such decays was expected to be fairly long since they are low energy processes of second order in weak interaction. Maria Goepert-Mayer (1935) calculated the half-life for the $2\nu\beta^{-}\beta^{-}$ decay at the suggestion of Eugene P. Wigner. The calculated half-life was greater than 10^{17} years which is exceedingly slow even on the geological time scale.

The $0\nu\beta\beta$ decay was first considered by Racah in 1937 [Racah (1937)] and W. Furry in 1939 [Furry (1939)] as a tool to distinguish whether the neutrino is of Majorana (particle≡antiparticle) [Majorana (1937)] or Dirac (particle≠antiparticle) nature. The mechanism of $0\nu\beta^{-}\beta^{-}$ decay is based on the emission of an electron antineutrino $\overline{\nu}_e$ on the first decay vertex ($n \rightarrow p + e^{-} + \bar{\nu}_e$) and its absorption in the second vertex. The absorption part is an inverse beta decay ($n + \nu_e \rightarrow p + e^{-}$), where electron neutrino instead of antineutrino is required. The emission and absorption processes yield to exchange of

a virtual neutrino and the associated propagator produces a neutrino potential. Though, the conservation of energy and momentum required the emission of a neutrino in single β decay, there is no corresponding requirement for neutrinos in $0\nu\beta\beta$ decay. The energy and momentum could be conserved in this decay mode releasing two electrons only. There are also four $0\nu\beta\beta$ decay modes depending on whether electrons or positrons are emitted.

$$\begin{aligned}
&(i) \quad {}^{A}_{Z}X \rightarrow {}^{A}_{Z+2}Y + 2e^{-} && (double\ electron\ emission)\\
&(ii) \quad {}^{A}_{Z}X \rightarrow {}^{A}_{Z-2}Y + 2e^{+} && (double\ positron\ emission)\\
&(iii) \quad e^{-} + {}^{A}_{Z}X \rightarrow {}^{A}_{Z-2}Y + e^{+} && (electron\ capture - positron\ emission)\\
&(iv) \quad 2e^{-} + {}^{A}_{Z}X \rightarrow {}^{A}_{Z-2}Y^{*} && (double\ electron\ capture)
\end{aligned} \tag{1.28}$$

The first theoretical investigations of $\beta\beta$ decay were attempted by Zeldovich *et al.* (1954), Primakoff and Rosen [Primakoff (1952), Rosen and Primakoff (1959)]. It was then realized that $0\nu\beta^{-}\beta^{-}$ decay enjoys a substantial kinematical advantage ($\sim 10^{8}$) over the $2\nu\beta^{-}\beta^{-}$ decay. This attracted the attention of experimentalists as life-times of about 10^{15} y were within the reach of the then existing experimental capabilities. However, the $0\nu\beta\beta$ decay process was not observed even when this level was reached. Scientists interpreted this failure as a manifestation of the fact that the neutrino is a Dirac particle. However, this conclusion was premature. In fact, the discovery of parity violation in weak interactions combined with the fact that the neutrinos participating in weak interactions are always left handed, implied that $0\nu\beta\beta$ decay is helicity suppressed and perhaps unobservable if the neutrinos are very light even though they may be Majorana particles. This motivated the experimentalists to be quite pessimistic and the experimental activities subsided. Later on, it was conjectured theoretically that $0\nu\beta\beta$ decay is expected to proceed mainly via the small admixtures of right handed currents in the predominantly left handed

Lagrangian [Primakoff and Rosen (1961), (1969)] and consequently, the experimental activity was resumed in the 1960's. The $\beta\beta$ decay has been nicely reviewed theoretically as well as experimentally in refs. [Vergados (2002), Avignone *et al.* (2008), Vogel (2012), Ostrovskiy (2016), Henning (2016), Engel and Menéndez (2017)] and references there in.

1.2.1 $2\nu\beta^-\beta^-$ decay and validity of nuclear models

The inverse half-life of $2\nu\beta^-\beta^-$ decay for the $0^+ \rightarrow J_f^+$ transition is given by

$$\left[T_{1/2}^{2\nu}(0^+ \rightarrow\ J_f^+)\right]^{-1} = G_{2\nu}(J_f^+)\left|M_{2\nu}(J_f^+)\right|^2 \tag{1.29}$$

where

$$M_{2\nu}(J_f^+) = \frac{1}{\sqrt{s}}\sum_N \frac{\left\langle J_f^+ \left\| \boldsymbol{\sigma}\tau^+ \right\| 1_N^+ \right\rangle \left\langle 1_N^+ \left\| \boldsymbol{\sigma}\tau^+ \right\| 0^+ \right\rangle}{[E_N - (E_I + E_F)/2]^s} \tag{1.30}$$

with $s = \{1 + 2\delta_{J2}\}$ and the integrated kinematical factor $G_{2\nu}(J_f^+)$ can be calculated with good accuracy [Doi *et al* (1985), (1992)].

Out of 35 possible candidates, the $0^+ \rightarrow 0^+$transition of $2\nu\beta^-\beta^-$ decay has been observed for ^{48}Ca, ^{76}Ge, ^{82}Se, ^{96}Zr, ^{100}Mo, ^{116}Cd, ^{128,130}Te, ^{136}Xe, ^{150}Nd and ^{238}U nuclei [Saakyan (2013), Barabash (2015)] and limits on the half-lives $T_{1/2}^{2\nu}$ of a number of isotopes for the $0^+ \rightarrow 0^+$ and $0^+ \rightarrow 2^+$ transitions have already been given [Tretyak and Zdesenko (1995), (2002)]. The inverse half-life of $2\nu\beta^-\beta^-$ decay is a product of the phase space factor and model dependent nuclear transition matrix element (NTME) $M_{2\nu}$. The phase space factors have been calculated employing the exact Dirac wave functions in conjunction with finite nuclear size and screening effects [Kotila and Iachello (2012), Stoica and

Mirea (2013)]. Using the observed experimental half-lives for the $0^+ \rightarrow 0^+$ transition, the NTMEs $M_{2\nu}(0^+)$ has been extracted [Barabash (2015)] and in all cases of $2\nu\beta^-\beta^-$ decay, it has been observed that the NTMEs $M_{2\nu}(0^+)$ are sufficiently quenched [Barea *et al.* (2015)]. The main motive of all theoretical calculations is to understand the physical mechanism responsible for the observed suppression of $M_{2\nu}(0^+)$. Hence, the validity of different nuclear models can be tested by calculating $M_{2\nu}(0^+)$ and comparing them with the experimental value.

The calculation of NTME $M_{2\nu}$ is quite complex as it requires the knowledge of a complete set of states of the intermediate nucleus in addition to the initial and final nuclear states. In solving this problem, different models and nuclear structure scenarios have been applied. Over the past few years, several nuclear models have been employed to calculate the $2\nu\beta^-\beta^-$ decay rate in 2n mechanism. They can be broadly classified into three categories, namely shell model and its variants, quasiparticle random phase approximation (QRPA) and its extensions and alternative models. The details about these models -their advantages as well as shortcomings- have been discussed excellently by Suhonen and Civitarese (1998) and Faessler and Simkovic (1998). We briefly discuss in the below the relative applicability, success and failure of various models used so far to study the $\beta^-\beta^-$ decay processes for the sake of completeness.

Shell model and its variants

The shell model, which attempts to solve the nuclear many-body problem as exactly as possible, is the best choice for the calculation of the NTMEs for $2\nu\beta^-\beta^-$ and $0\nu\beta^-\beta^-$ decay. Beyond the pf-shell, the number of basis states increases so drastically that a few

years back it was not possible to perform a conventional shell model calculation without imposing certain truncation schemes. On the other hand, most of the $\beta\beta$ decay emitters are medium or heavy mass nuclei. Since a reliable shell-model calculation was difficult to perform, Vergados *et al.* (1976) and Haxton *et al.* (1984) have studied the $\beta^-\beta^-$ decay of ^{48}Ca, ^{76}Ge, ^{82}Se and ^{128,130}Te nuclei in weak coupling limit. The large scale shell model (LSSM) calculations by Skouras *et al.* (1983), Zhao and coworkers [(1990), (1993)], Caurier *et al.* [(1990), (1995), (1999)], Iwata *et al.* (2016), Nowacki *et al.* (2016) are more promising in nature. The $0\nu\beta^-\beta^-$ decay of ^{48}Ca has been studied by Retamosa *et al.* (1995) in lower *fp*-shell without any restriction. Ogawa *et al.* [Ogawa *et al.* (1989)] and Caurier *et al.* [Caurier *et al.* (1990)] have studied $2\nu\beta^-\beta^-$ decay of ^{48}Ca in full *fp*-shell. The calculations by Caurier *et al.* are more realistic in nature, in which the NTMEs of $2\nu\beta^-\beta^-$ as well as $0\nu\beta^-\beta^-$ decay of ^{82}Se is calculated exactly, and those of ^{76}Ge and ^{136}Xe are dealt with in a nearly exact manner [Caurier *et al.* (1996)]. Further, NTMEs of $2\nu\beta^-\beta^-$ and $0\nu\beta^-\beta^-$ decay have been calculated by Caurier *et al.* [Caurier *et al.* (1999)] for ^{48}Ca, ^{76}Ge, ^{82}Se , ^{124}Sn, ^{128,130}Te, ^{136}Xe nuclei. The conventional shell model and Monte-Carlo shell model (MCSM) [Koonin *et al.* (1997) and Radha *et al.* (1996), (1997)] have been tested against each other for the case of ^{48}Ca in complete *pf*-shell and ^{76}Ge in upper *fpg*-shell, and the agreement is interestingly significant. The interacting shell model (ISM) are based on direct diagonalization. It has been successfully applied to study the $0\nu\beta^-\beta^-$ decay of all the potential $\beta^-\beta^-$ emitters [Caurier *et al.* (2008), (2008*a*), Menendez *et al.* (2009), Horoi and Stoica (2010), Horoi and Brown (2013), Brown *et al.* (2014), (2015), Neacsu and Horoi (2015), Horoi and Neacsu (2016), Sen'kov *et al.* (2013), (2014), (2014*a*), (2016)].

In shell model calculations, the following features are observed in the case of $\beta^-\beta^-$ decay:

(i) The model space dependence of $2\nu\beta^-\beta^-$ decay matrix element in ^{48}Ca [Zhao *et al.* (1990)] and ^{92}Mo [Suhonen *et al.* (1997)] show that stringent truncation imposed on number of shell model basis states prevent configurations responsible for the reduction of NTMEs by destructive interference.

(ii) The omission of spin-orbit partners may also hinder the destructive interference between spin-flip and spin non-flip contributions leading to the suppression of NTMEs for $2\nu\beta^-\beta^-$ decay [Raduta *et al.* (1995), Civitarese *et al.* (1995) and Aunola *et al.* (1996)].

(iii) The renormalization of vector and axial vector weak interaction strengths g_V and g_A respectively due to nuclear medium effects results in $g_V/g_A \approx 1$. This leads to renormalization of Gamow-Teller operator, which is responsible for quenching of about 60%.

Thus, the mechanism responsible for the quenching of $2\nu\beta^-\beta^-$ decay strength is not well understood. The shell model calculations, besides being feasible for a limited number of nuclei due to a large number of basis states, fail to fulfil Ikeda sum rule by about 40 to 60 %.

QRPA and its extensions

Vogel and Zirnbauer were the first to provide an understanding of the observed suppression of $M_{2\nu}$ in the QRPA model [Vogel *et al.* (1986)]. It was observed that the quenching of $M_{2\nu}$ can be achieved by a proper inclusion of ground state correlations through the particle-particle interaction in the $S = 1$, $T = 0$ channel, and the calculated half-lives are in close agreement with all the experimental data. The QRPA frequently overestimates

the ground state correlations as a result of an increase in the strength of attractive proton-neutron interaction leading to the collapse of QRPA solutions. The physical value of this force is usually close to the point at which the QRPA solutions collapse. The origin of this unfortunate behavior is attributed to the quasi-boson approximation (QBA) of the QRPA operators violating the Pauli exclusion principle. With increase in ground state correlations, the violation of the exclusion principle is also increased. The most important proposals directed towards solving some of the inherent problems are as follows.

(i) Inclusion of proton-neutron pairing (full QRPA) [Cheoun *et al.* (1993), (1995)].

(ii) Renormalized QRPA in which violation of Pauli exclusion principle is restored (RQRPA) [Toivanen *et al.* (1995), (1997), Simkovic *et al.* (1997) and Krmpotic *et al.* (1997)] or full RQRPA [Schwieger *et al.* (1996), Šimkovic *et al.* (1997), (2008), (2009) and Stoica *et al.* (2001)].

(iii) Higher QRPA (HQRPA) [Raduta *et al.* (1991), Sambarato *et al.* (1997)], SQRPA [Stoica *et al.* (1993), (1994), (1995), (1996), (2000) and (2001)], SRQRPA [Bobyk *et al.* (2001)].

(iv) Multiple commutator method (MCM) [Suhonen *et al.* (1993), Civitarese *et al.* (1994) and Aunola *et al.* (1996)].

(v) Particle number projection (PQRPA) [Civitarese *et al.* (1990), (1991), Suhonen *et al.* (1992), Suhonen (1993), Krmpotic *et al.* (1993)].

(vi) Deformed QRPA [Šimkovic *et al.* (2004), Faessler *et al.* (2012), Fang *et al.* (2010), (2011), (2015), Mustonen and Engel (2013)].

(vii) QRPA with isospin restoration [Šimkovic *et al.* (2013)]

However, it is not clear which method is the best. Altogether, QRPA and its various

extensions with the ability to adjust one free parameter are able to explain the observed $2\nu\beta^-\beta^-$ decay rates.

Alternative models

The shell model and its variants as well as the QRPA and its extensions, besides having their own limitations, fail to fulfil the Ikeda sum rule. In the QRPA approach, a larger uncertainty may occur in deformed nuclei as deformation is usually ignored. This has been shown for ^{100}Mo and ^{150}Nd isotopes using QRPA [Suhonen *et al.* (1994)] and pseudo SU(3) model [Hirsch *et al.* (1995)]. The small predictive power of QRPA and its extensions is the main motivation for seeking an alternative description which might result in a more reliable approach for the study of nuclear $\beta^-\beta^-$ decay processes. These attempts have been summarized as alternative models. Under alternative models, one has

(i) Operator expansion method (OEM) [Ching *et al.* (1989), Simkovic (1989), Engel *et al.* (1992), Wu *et al.* (1991) and (1992), Hirsch *et al.* (1993), (1994), Muto (1993), Simkovic *et al.* (1998)].

(ii) Broken SU(4) symmetry [Bernabeu *et al.* (1990), Vladimirov *et al.* (1992), Moe and Vogel (1994) and Rumyantsev *et al.* (1995)].

(iii) Group theoretical studies in SU(2) [Hirsch *et al.* (1996)], SO(5) [Hirsch *et al.* (1997)], O(8) [Engel *et al.* (1997)] and the pseudo-SU(3) [Castanos *et al.* (1994) and Hirsch *et al.* (1995), (2002)].

(iv) two-vacua RPA (TVRPA) [Simkovic *et al.* (1994) and Teneva *et al.* (1995)].

(v) Single state dominance hypothesis (SSDH) [Ejiri *et al.* (1996), Civitarese *et al.* (1998) and (1999)].

(vi) Energy density functional (EDF) method [Rodríguez *et al.* (2010), Menéndez *et al.* (2014)]

(vii) Interacting boson model (IBM) [Barea *et al.* (2013), Iachello *et al.* (2011), (2011*a*), Barea and Iachello (2009), Yosida and Iachello (2013)].

(viii) IBM with isospin restoration [Barea *et al.* (2015)].

(ix) Projected Hartree-Fock-Bogoliubov (PHFB) method [Tomoda *et al.* (1985), (1986), Chandra *et al.* (2005), (2009), Rath *et al.* (2010), (2012), (2013), (2016)] .

1.2.2 $0\nu\beta^-\beta^-$ decay and physics beyond the *SM*

The $0\nu\beta^-\beta^-$ decay mode is far more interesting since it violates the conservation of lepton number L by two units ($\Delta L = 2$) and is not allowed in the *SM*. The emission of a neutrino and its absorption as an antineutrino demands that neutrino and antineutrino to be the same, which is not possible in the standard electroweak SU(2) $\times$ U(1) model. The violation of parity maximally in weak interactions adds an additional requirement that the Majorana neutrino emitted during the decay of the first neutron should reverse its helicity from right to left-handed. Such a reversal might be caused by the neutrino mass (m_ν) and/or might occur explicitly through an admixture of right-handed current in weak interactions. The Majorana mass term requires the breaking of lepton number L. However, the only gauge-anomaly free combination of quantum numbers in general gauge theories is $B - L$. Therefore, one considers the breaking of $B - L$ symmetry. The study of $\beta\beta$ decay in general and $0\nu\beta^-\beta^-$ decay in particular is a convenient tool to test the following important ramifications vis-a-vis constraints on parameters of various gauge theoretical models beyond the *SM,* namely (i) lepton number violation, (ii) mass

and charge conjugation properties of the electron-neutrino and (iii) possible right handed admixtures in the weak leptonic current.

The $0\nu\beta^-\beta^-$ decay is not observed so far and only limits on half-lives $T^{0\nu}_{1/2}$ are available. These limits have been presented in Table 1.2. The $0\nu\beta^-\beta^-$ decay can be studied mainly in three types of models, namely Left-right symmetric models (*LRSM*), Majoron models and R-parity violating as well as conserving Supersymmetric models (R_p-*MSSM*). Further, the $0\nu\beta^-\beta^-$ decay can verify issues like compositeness, leptoquarks, sterile neutrinos and violation of weak equivalence principle. In the following we discuss them briefly.

Hirsch *et al.* (1996) have calculated limits on various gauge parameters of the *LRSM*, such as light neutrino effective mass $\langle m_\nu \rangle < 0.56$ eV, effective coupling of right-handed leptonic current with right-handed nucleonic currents $\langle \lambda \rangle < 1.0 \times 10^{-6}$, effective coupling of right-handed leptonic current with left-handed nucleonic currents $\langle \eta \rangle < 5.5 \times 10^{-9}$, effective mass parameter of right handed heavy neutrino $\langle \xi \rangle < 1.7 \times 10^{-8}$ and mass of right handed W-boson $M_{W_R} \geq 1.1$ TeV for ^{76}Ge using half-life $T^{0\nu}_{1/2} \geq 7.4 \times 10^{24}$ yr [Balysh *et al.* (1995)]. Using the best fit limit of $T^{0\nu}_{1/2} = 1.19 \times 10^{25}$ for ^{76}Ge reported by Klapdor *et al.* (2004), the values of lepton number violating parameters are $\langle m_\nu \rangle = 0.44$ eV, $\langle \lambda \rangle = 7.86 \times 10^{-7}$, $\langle \eta \rangle = 4.35 \times 10^{-9}$ and $\langle \xi \rangle = 1.34 \times 10^{-8}$ for the NTMEs of Hirsch *et al.* (1996).

The limit on the effective Majoron-neutrino coupling constant $< g_M >$ can be obtained from the experimental half-life limit by calculating the NTMEs M_α. For the case of ^{76}Ge, using the NTMEs of Hirsch *et al.* (1996*a*) and half-life limit given by Klapdor *et al.* (2001), the limit on $< g_M >$ is $< 0.82 \times 10^{-4}$. The limit on $< g_M >$ obtained from the half-life limit given by NEMO 3 experiment [Arnold *et al.* (2006)] for ^{100}Mo nucleus is

$< (1.6 - 1.8) \times 10^{-4}$ using NTMEs of Rodin *et al.* (2005).

In the R_p violating minimal supersymmetric standard model (R_p-violating *MSSM*) [Hirsch *et al.* (1996*b*), Mohapatra (1991)], the exchange of gluinos, photinos etc. contributes to $0\nu\beta^-\beta^-$ decay , and leads to a very stringent limit on the first generation Yukawa coupling and combination of the intergeneration Yukawa couplings. Constraint on the Yukawa coupling constant is given as Hirsch *et al.* (1996*b*)

$$\lambda'_{11i}\lambda'_{1i1} \leq \epsilon'_i \left(\frac{\Lambda_{SUSY}}{100GeV}\right)^3 \tag{1.31}$$

Here, Λ_{SUSY} is effective SUSY breaking scale. The current upper bound for the R_p violating SUSY interaction constant λ'^2_{111} is $\leq 7.7 \times 10^{-6}$ [Faessler *et al.* (2008)] assuming masses of SUSY particles to be on the scale of 100 GeV for the case of ^{76}Ge using half-life limit given by Baudis *et al.* (1999) in Heidelberg-Moscow experiment.

Panella and Srivastava (1995) showed that the compositeness scenario can give additional contribution to $0\nu\beta^-\beta^-$ decay mediated by composite heavy Majorana neutrino and achieved bounds on the compositeness parameters from the non-observation of $0\nu\beta^-\beta^-$ decay. Panella *et al.* (1997) have obtained bound on coupling constant $|f| < 4.12$ for the compositeness scale $\Lambda_c = 1$ TeV using the lower bound on half-life $T^{0\nu}_{1/2}$ of $0\nu\beta^-\beta^-$ decay of ^{76}Ge obtained from Heidelberg-Moscow experiment [Maier *et al.* (1995)]. For the best fit value of $T^{0\nu}_{1/2}$ [Klapdor *et al.* (2004)], the coupling constant comes out to be $|f| = 3.42$.

Assuming that either scalar or vector leptoquarks (LQ) contribute $0\nu\beta^-\beta^-$ decay, the

following constraints can be derived on the effective LQ parameters [Hirsch *et al.* (1996*c*)]:

$$\epsilon_I \leq 2.8 \times 10^{-9} \left(\frac{M_I}{100 \text{ GeV}}\right)^2 \tag{1.32}$$

$$\alpha_I^{(L)} \leq 3.5 \times 10^{-10} \left(\frac{M_I}{100 \text{ GeV}}\right)^2 \tag{1.33}$$

$$\alpha_I^{(R)} \leq 7.9 \times 10^{-8} \left(\frac{M_I}{100 \text{ GeV}}\right)^2 \tag{1.34}$$

These bounds from $0\nu\beta^-\beta^-$ decay are of interest in connection with the discussed evidence for new physics from HERA [Hewett and Rizzo (1997), Babu *et al.* (1997), Kalinowski *et al.* (1997), Choudhury and Raychaudhuri (1997)].

The contribution of sterile neutrino ν_h state to $0\nu\beta^-\beta^-$ decay amplitude is described by the standard Majorana neutrino exchange between the two β-decaying neutrons. The corresponding inverse half-life for $0^+ \to 0^+$ transition is given by [Benes *et al.* (2005)]

$$[T_{1/2}^{0\nu}(0^+ \to 0^+)]^{-1} = G_{01} \left| U_{eh}^2 \frac{m_h}{m_e} M^{0\nu}(m_h) \right|^2 \tag{1.35}$$

where G_{01} is the integrated kinematical factor, U_{eh} is the $\nu_h - \nu_e$ mixing matrix element and $M^{0\nu}(m_h)$ is the NTME.

A typical consequence of the violation of local Lorentz invariance (VLI) is that different species of matter can have different maximum attainable velocities. The constraint on VLI, obtained from the Heidelberg-Moscow experiment, is [Klapdor *et al.* (1998)]

$$\delta v < 4 \times 10^{-16} \qquad for\ \theta_v = \theta_m = 0$$

where $\delta v = v_1 - v_2$ is the measure of VLI in the neutrino sector and θ_v and θ_m are the velocity mixing and weak mixing angles respectively.

1.2.3 Mechanisms of $\beta^-\beta^-$ decay

In nuclear $\beta\beta$ decay, the total angular momentum of four s-wave leptons can be 0,1 or 2 and is equal to the total angular momentum transferred from the nucleus. The lowest 1^+ state in the final nucleus of any $\beta\beta$ decay candidate lies at a much higher level than the first excited 2^+ state; hence the $0^+ \rightarrow 1^+$ transition is much less probable than the $0^+ \rightarrow 0^+$ and $0^+ \rightarrow 2^+$ transitions. The two-nucleon (2n) mechanism is the only possible mechanism in case we restrict the degrees of freedom to nucleons only. In case the pionic degrees of freedom are allowed as well, several other modes, namely $N \leftrightarrow \Delta$ mechanism [Primakoff and Rosen (1969), Smith *et al.* (1973), Picciotto (1978), Halprin *et al.* (1976)], $\Delta \leftrightarrow \Delta$ mechanism [Haxton and Stephenson (1984)] and $\pi^- \leftrightarrow \pi^+$ mechanism [Vergados (1982)] have to be considered. In Fig. 1.1, we present these mechanisms.

It was expected that the contribution of $N \leftrightarrow \Delta$ mechanism to the $2\nu\beta^-\beta^-$decay is negligible because of the large mass difference, and the contribution to the $0\nu\beta^-\beta^-$ decay is significant due to the shorter propagating distance for the virtual neutrino. The consideration of proper selection rules [Doi *et al.* (1981) and Haxton *et al.* (1981)] made it clear that the $0^+ \rightarrow 0^+$ transition is strictly forbidden in the $N \leftrightarrow \Delta$ mechanism even in quark model, while the $0^+ \rightarrow 2^+$ transition is allowed. However, it was shown by Tomoda (1988) that the $N \leftrightarrow \Delta$ mechanism contributes to the $0^+ \rightarrow 0^+$ transition of $0\nu\beta^-\beta^-$ decay, although negligibly in case the recoil current of quarks in addition to the emission of electrons in $s_{1/2}$ and $p_{1/2}$ waves is included. In the $\Delta \leftrightarrow \Delta$ mechanism, the $\Delta^- \leftrightarrow \Delta^+$ and $\Delta^0 \leftrightarrow \Delta^{++}$ transitions are favorable to the $0\nu\beta^-\beta^-$ decay. Due to small probability ($P_\Delta \sim$0.01) of finding a Δ isobar in the tail of either the initial or the final state nuclear

wave function, the $N \leftrightarrow \Delta$ mechanism is suppressed in $0\nu\beta\beta$ decay proportional to $\sqrt{P_\Delta}$ and $\Delta \leftrightarrow \Delta$ mechanism, proportional to P_Δ [Primakoff and Rosen (1969)] with respect to 2n mechanism. Similarly, several transitions are possible in the $\pi^- \leftrightarrow \pi^+$ mechanism [Vergados (1982), Fazely and Liu (1986), (1987)]. However, the contribution are also unimportant [Watanabe and Toki (1986) and Tomoda (1987)]. The above conclusions are not free of ambiguities. Hence, we consider the $2\nu\beta^-\beta^-$ decay and $0\nu\beta^-\beta^-$ decay in 2n mechanism only.

1.3 Objective and motivation of the work

The confirmation of neutrino oscillations has established the fact that neutrinos are massive. The next experimental as well as theoretical challenge is to determine the mass scale and nature of neutrinos. The study of $0\nu\beta\beta$ decay has the potential to take up this challenge and in fact, is the best way of extracting information regarding the nature of neutrinos. In the present work, our aim is to study the $0^+ \rightarrow 0^+$ transition of $0\nu\beta^-\beta^-$ decay of potential $\beta^-\beta^-$ emitters in the mass range $A = 90 - 150$, namely ^{94,96}Zr, ^{100}Mo, ^{110}Pd, ^{128,130}Te and ^{150}Nd isotopes within mechanisms involving light Majorana neutrino mass and right handed current to extract the effective light electron-neutrino mass $< m_\nu >$, the effective weak coupling constants $< \lambda >$ and $< \eta >$ for coupling of right-handed leptonic current with right-handed and left-handed nucleonic currents, respectively. The accurate determination of gauge theoretical parameters in turn depends on the reliability of nuclear wave functions. We also aim to study the $0^+ \rightarrow 2^+$ transition of $2\nu\beta^-\beta^-$ decay of ^{94,96}Zr, ^{104}Ru, ^{100}Mo, ^{110}Pd, ^{128,130}Te and ^{150}Nd isotopes.

The primary goal of nuclear many body theory is to describe as much observed properties of nuclei as possible in a coherent frame. The nuclear $\beta\beta$ decay is not an isolated process and can be studied in the same framework as many other nuclear properties and decays. In the past years, there has been amazing progress in the collection of data concerning level energies as well as electromagnetic properties through experimental studies involving in-beam γ-ray spectroscopy. The availability of data permits a rigorous and detailed critique of the ingredients of the microscopic framework that seeks to provide a description of nuclear $\beta\beta$ decay. Hence, we have studied $0\nu\beta^-\beta^-$ decay not in isolation but together with other observed nuclear phenomena.

Choice of the model and two-body interaction

All the nuclei undergoing $\beta\beta$ decay are even-even type, in which the pairing degrees of freedom play an important role. Moreover, it has been already shown by Griffiths *et al.* (1992) and Suhonen *et al.* (1994) that the deformation can play a crucial role in case of $\beta^-\beta^-$ decay of ^{100}Mo and ^{150}Nd. Hence, it is desirable to have a model in which the pairing and deformation degrees of freedom are included on equal footing in its formalism. For this purpose, the PHFB model is one of the most natural choices. Further, it is well known that the pairing part of the two body interaction is responsible for the sphericity of the nucleus where as the quadrupole-quadrupole (QQ) interaction enhances the collectivity in the nuclear intrinsic wave functions and makes the nucleus deformed. Hence, to examine the explicit role of deformation degrees of freedom vis-à-vis the suppression of NTME $M_{2\nu}$, the pairing plus quadrupole-quadrupole interaction ($PPQQ$) [Baranger *et al.* (1968)] will be the best suited effective two-body interaction.

The PHFB model has been successfully applied to study the $2\nu\beta^{\pm}\beta^{\pm}$ decay as well as $0\nu\beta^{\pm}\beta^{\pm}$ decay for the $0^+ \rightarrow 0^+$ transition in the mass region $A \sim 100$ [Chandra *et al.* (2005), (2009) Raina *et al.* (2006), Rath *et al.* (2010), (2012), (2013)]. It has been shown that the deformations of the intrinsic ground states play a crucial role in reproducing a realistic NTME $M_{2\nu}$ of $2\nu\beta^{-}\beta^{-}$ decay. The PHFB model in conjunction with the pairing plus quadrupole-quadrupole plus hexadecapole-hexadecapole (*PPQQHH*) interaction has been successfully applied to study the yrast spectra of $^{68-76}$Ge, $^{72-78}$Se, $^{74-82}$Kr, $^{100-108}$Zr and $^{100-108}$Mo isotopes [Sawhney *et al.* (2002), War *et al.* (2003), (2003*a*), Chandan *et al.* (2004)]. This has motivated us to carry out the present calculation within PHFB model using four parametrizations of *PPQQHH* interaction.

Organization of the thesis

The present thesis is organized as follows. In Chapter 2, we have calculated the yrast spectra, reduced $B(E2{:}0^+ \rightarrow 2^+)$ transition probabilities, deformation parameters β_2 and gyromagnetic factors $g(2^+)$ of ^{94,96}Zr, ^{94,96,100}Mo, ^{100,104}Ru, ^{104,110}Pd, ^{110}Cd, ^{128,130}Te, ^{128,130}Xe, ^{150}Nd and ^{150}Sm nuclei in the mass range $A = 90 - 150$ participating in the $\beta^{-}\beta^{-}$ decay. The comparison of theoretically calculated properties with the available experimental data tests the "goodness of the PHFB wave functions". In Chapter 3, the same PHFB wave functions are employed to study the $2\nu\beta^{-}\beta^{-}$ decay of ^{94,96}Zr, ^{100}Mo, ^{104}Ru, ^{110}Pd, ^{128,130}Te and ^{150}Nd isotopes for the $0^+ \rightarrow 2^+$ transition. In the same chapter, we have also studied the effect of deformation on NTMEs $M_{2\nu}$. Subsequently, we have studied the $0\nu\beta^{-}\beta^{-}$ decay of same nuclei in the mass range $A = 90-150$ for the $0^+ \rightarrow 0^+$ transition and extracted the limits on gauge parameters $< m_\nu >$, $< \lambda >$ and $< \eta >$ in

Chapter 4. The effect of deformation on NTMEs of $0\nu\beta^-\beta^-$ decay has also been studied in the same chapter. Finally, the concluding remarks are given in Chapter 5 along with a number of necessary improvements to be incorporated in the PHFB model for a more reliable study of the $\beta\beta$ decay in general and $0\nu\beta\beta$ decay in particular.

Table 1.1: List of 35 naturally occuring $\beta^-\beta^-$ emitters along with $Q_{\beta\beta}$ for the $0^+ \rightarrow 0^+$ transition, natural abundance of the parent isotope (P) [Wapstra and Audi (1985) and Lederer and Shirley (1978)] and deformation parameter β_2 [Raman *et al.* (2001)].

Nuclear	$Q_{\beta\beta}$	$P(\%)$	β_2	
Transition	(keV)		Parent	Daughter
$^{46}_{20}$Ca$\rightarrow^{46}_{22}$Ti	987.0±4.0	0.0035	0.152±0.005	0.262±0.032
$^{48}_{20}$Ca$\rightarrow^{48}_{22}$Ti	**4271.0±4.0**	0.187	0.101±0.017	0.269±0.007
$^{70}_{30}$Zn$\rightarrow^{70}_{32}$Ge	1001.0±3.0	0.62	0.228±0.010	0.2245±0.0026
$^{76}_{32}$Ge$\rightarrow^{76}_{34}$Se	**2039.6±0.9**	7.8	0.2623±0.0039	0.3090±0.0037
$^{80}_{34}$Se$\rightarrow^{80}_{36}$Kr	130.0±9.0	**49.8**	0.2318±0.0028	0.265±0.007
$^{82}_{34}$Se$\rightarrow^{82}_{36}$Kr	**2995.0±6.0**	9.2	0.1944±0.0026	0.2022±0.0045
$^{86}_{36}$Kr$\rightarrow^{86}_{38}$Sr	1256.0±5.0	17.3	0.145±0.006	0.128±0.010
$^{94}_{40}$Zr$\rightarrow^{94}_{42}$Mo	1145.3±2.5	17.4	0.090±0.010	0.1509±0.0015
$^{96}_{40}$Zr$\rightarrow^{96}_{42}$Mo	**3350.0±3.0**	2.8	0.081±0.016	0.1720±0.0016
$^{98}_{42}$Mo$\rightarrow^{98}_{44}$Ru	112.0±7.0	**24.1**	0.1684±0.0016	0.1947±0.0030
$^{100}_{42}$Mo$\rightarrow^{100}_{44}$Ru	**3034.0±6.0**	9.6	0.2309±0.0022	0.2172±0.0022
$^{104}_{44}$Ru$\rightarrow^{104}_{46}$Pd	1299.0±4.0	18.7	0.2742±0.0026	0.209±0.007
$^{110}_{46}$Pd$\rightarrow^{110}_{48}$Cd	**2013.0±19.0**	11.8	0.257±0.006	0.1771±0.0039
$^{114}_{48}$Cd$\rightarrow^{114}_{50}$Sn	534.0±4.0	**28.7**	0.1912±0.0035	0.119±0.013
$^{116}_{48}$Cd$\rightarrow^{116}_{50}$Sn	**2802.0±4.0**	7.5	0.1907±0.0034	0.1118±0.0016
$^{122}_{50}$Sn$\rightarrow^{122}_{52}$Te	364.0±4.0	4.56	0.1036±0.0011	0.1848±0.0008
$^{124}_{50}$Sn$\rightarrow^{124}_{52}$Te	**2288.1±1.6**	5.64	0.0953±0.0012	0.1695±0.0009

Table 1.1 continued

Nuclear Transition	$Q_{\beta\beta}$ (keV)	$P(\%)$	β_2	
			Parent	Daughter
$^{128}_{52}$Te$\rightarrow^{128}_{54}$Xe	868.0±4.0	**31.7**	0.1363±0.0011	0.1837±0.0049
$^{130}_{52}$Te$\rightarrow^{130}_{54}$Xe	**2533.0±4.0**	**34.5**	0.1184±0.0014	0.169±0.006
$^{134}_{54}$Xe$\rightarrow^{134}_{56}$Ba	847.0±10.0	10.4	0.120±0.010	0.1636±0.0019
$^{136}_{54}$Xe$\rightarrow^{136}_{56}$Ba	**2479.0±8.0**	8.9	0.086±0.019	0.1242±0.0008
$^{142}_{58}$Ce$\rightarrow^{142}_{60}$Nd	1417.6±2.5	11.1	0.1236±0.0014	0.0926±0.0014
$^{146}_{60}$Nd$\rightarrow^{146}_{62}$Sm	56.0±5.0	17.2	0.1524±0.0030	-
$^{148}_{60}$Nd$\rightarrow^{148}_{62}$Sm	1928.3±1.9	5.7	0.2036±0.0022	0.1423±0.0030
$^{150}_{60}$Nd$\rightarrow^{150}_{62}$Sm	**3367.1±2.2**	5.6	0.2848±0.0021	0.1931±0.0022
$^{154}_{62}$Sm$\rightarrow^{154}_{64}$Gd	1251.9±1.5	**22.6**	0.3410±0.0020	0.3104±0.0020
$^{160}_{64}$Gd$\rightarrow^{160}_{66}$Dy	1729.5±1.4	**21.8**	0.3534±0.0020	0.3365±0.0048
$^{170}_{68}$Er$\rightarrow^{170}_{70}$Yb	653.9±1.6	14.9	0.3363±0.0029	0.3235±0.0047
$^{176}_{70}$Yb$\rightarrow^{176}_{72}$Hf	1078.8±2.7	12.6	0.3078±0.0028	0.2953±0.0028
$^{186}_{74}$W$\rightarrow^{186}_{76}$Os	490.3±2.2	**28.6**	0.2238±0.0020	0.2004±0.0034
$^{192}_{76}$Os$\rightarrow^{192}_{78}$Pt	417.0±4.0	**41.0**	0.1647±0.0028	0.1549±0.0024
$^{198}_{78}$Pt$\rightarrow^{198}_{80}$Hg	1048.0±4.0	7.2	0.1130±0.0027	0.1065±0.0006
$^{204}_{80}$Hg$\rightarrow^{204}_{82}$Pb	416.5±1.9	6.9	0.0686±0.0006	0.0412±0.0005
$^{232}_{90}$Th$\rightarrow^{232}_{92}$U	858.0±6.0	**100**	0.2608±0.0013	0.264±0.011
$^{238}_{92}$U$\rightarrow^{238}_{94}$Pu	1145.8±1.7	**99.275**	0.2863±0.0024	0.2891±0.0033

Table 1.2: Experimental half-life limits $T^{0\nu}_{1/2}$ of $0\nu\beta^-\beta^-$ decay of $A = 48$, 76, 82, 94, 96, 98, 100, 116, 128, 130, 136, 150 and 238 nuclei for the $0^+ \rightarrow 0^+$ transition.

Transition	$T^{0\nu}_{1/2}$ (yr)	C.L.(%)	Project	Reference
^{48}Ca$\rightarrow^{48}$Ti	$>1.3 \times 10^{22}$	90	NEMO 3	[Barabash *et al.*(2011)]
	$>2.7\times10^{22}$	90	GSS+GSE+RCNS	[Umehara *et al.* (2008)]
	$\geq1.4\times10^{22}$	90	ELEGANT VI	[Ogawa *et al.* (2004)]
	$>1.5\times10^{21}$	90	TGV	[Brudanin *et al.* (2000)]
	$>9.5\times10^{21}$	76	HEP Beijing	[You *et al.* (1991)]
	$>2.0\times10^{21}$	80		[Bardin *et al.* (1970)]
^{76}Ge$\rightarrow^{76}$Se	$>3.0\times10^{25}$	90	GERDA	[Agostini *et al.* (2013)]
	$>1.57\times10^{25}$	90	IGEX	[Aalseth *et al.* (2002)]
	$>1.9\times10^{25}$	90	HM	[Klapdor *et al.* (2001)]
	$>1.6\times10^{25}$	90	IGEX	[Gonzalez *et al.* (2000)]
	$>1.6\times10^{25}$	90	HM	[Baudis *et al.* (1999)]
	$>1.2\times10^{25}$	90	MPIH+KIAE	[Morales (1999)]
	$>1.1\times10^{25}$	90	HM	[Baudis *et al.* (1997)]
	$>7.4\times10^{24}$	90	HM	[Gunther *et al.* (1997)]
	$>5.6\times10^{24}$	90	HM	[Balysh *et al.* (1995)]
	$>1.4\times10^{24}$	90	HM	[Balysh *et al.* (1992)]
	$>2.5\times10^{23}$	68	UC+LBL	[Caldwell *et al.* (1986)]
	$>1.0\times10^{23}$	68	PNL+USC	[Avignone *et al.* (1985)]
	$>2.0\times10^{22}$	68		[Forster *et al.* (1984)]

Table 1.2 continued

Transition	$T^{0\nu}_{1/2}$ (yr)	C.L.(%)	Project	Reference
	$>1.2\times10^{23}$	68		[Bellotti *et al.* (1984)]
	$>3.0\times10^{22}$	68		[Simpson *et al.* (1984)]
	$>4.0\times10^{21}$	68		[Leccia *et al.* (1983)]
^{82}Se$\rightarrow^{82}$Kr	$>1.0\times10^{23}$	90	NEMO 3	[Arnold *et al.* (2005)]
	$>1.9\times10^{23}$	90	NEMO 3	[Lalanne (2005)]
	$\geq9.5\times10^{21}$	90	NEMO 2	[Arnold *et al.* (1998)]
	$>5.0\times10^{21}$	90	NEMO 2	[Barabash *et al.* (1998)]
	$>2.7\times10^{22}$	68	UC Irvine	[Elliott *et al.* (1992)]
	$>1.8\times10^{22}$			[Moe *et al.* (1988)]
^{94}Zr$\rightarrow^{94}$Mo	$>1.9\times10^{19}$	90	NEMO 2	[Arnold *et al.* (1999)]
^{96}Zr$\rightarrow^{96}$Mo	$>9.2\times10^{21}$	90	NEMO 3	[A. S. Barabash *et al.*(2011)]
	$>9.2\times10^{21}$	90	NEMO 3	[J. Argyriades *et al.* (2010)]
	$>1.0\times10^{21}$	90	NEMO 2	[Arnold *et al.* (1999)]
	$>8.0\times10^{20}$	90	NEMO 2	[Barabash *et al.* (1998)]
^{98}Mo$\rightarrow^{98}$Ru	$>1.0\times10^{14}$			[Fremlin *et al.* (1952)]

Table 1.2 continued

Transition	$T^{0\nu}_{1/2}$ (yr)	C.L.(%)	Project	Reference
^{100}Mo$\rightarrow^{100}$Ru	$>1.1\times10^{24}$	90	NEMO 3	[Arnold *et al.* (2015)]
	$>4.6\times10^{23}$	90	NEMO 3	[Arnold *et al.* (2005)]
	$>3.5\times10^{23}$	90	NEMO 3	[Lalanne (2005)]
	$>5.5\times10^{22}$	90	ELEGANT V	[Ejiri *et al.* (2001)]
	$>4.9\times10^{21}$	90	ITEP+INFN	[Ashitkov *et al.* (2001)]
	$>2.2\times10^{22}$	90	ELEGANT V	[Kudomi *et al.* (2000)]
	$>2.3\times10^{21}$	90	ITEP+INFN	[Ashitkov *et al.* (1999)]
	$>5.2\times10^{22}$	68	ELEGANT V	[Kudomi *et al.* (1998)]
	$>2.2\times10^{22}$	68	LBL+MHC+ UNM+INEL	[Alston-Garnjost *et al.* (1997)]
	$>1.23\times10^{23}$	90	UC Irvine	[De Silva *et al.* (1997]
	$>5.2\times10^{22}$	68	ELEGANT V	[Ejiri *et al.* (1996)]
	$>6.4\times10^{21}$	90	NEMO 2	[Dassie *et al.* (1995)]
	$>4.4\times10^{22}$	68	LBL+MHC+ UNM+INEL	[Alston-Garnjost *et al.* (1993)]
	$>4.7\times10^{21}$	68	ELEGANT V	[Ejiri *et al.* (1991)]
	$>7.1\times10^{20}$	68	INS Baksan	[Vasilev *et al.* (1990)]
	$>4.0\times10^{21}$	68	LBL+MHC+ UNM+INEL	[Alston-Garnjost *et al.* (1989)]
	$>1.0\times10^{19}$	68	UC Irvine	[Elliott *et al.* (1987)]

Table 1.2 continued

Transition	$T^{0\nu}_{1/2}$ (yr)	C.L.(%)	Project	Reference
^{116}Cd$\rightarrow^{116}$Sn	$>7.0\times10^{22}$	90	INR+INFN	[Danevich *et al.* (2000)]
	$>3.2\times10^{22}$	90	INR+INFN	[Danevich *et al.* (1999)]
	$>5.0\times10^{21}$	90	NEMO 2	[Arnold *et al.* (1996)]
	$>2.9\times10^{22}$	90	INR	[Danevich *et al.* (1995)]
	$>2.9\times10^{21}$	90	Osaka	[Ejiri *et al.* (1995)]
	$>5.4\times10^{21}$	68		[Kume *et al.* (1994)]
	$>2.6\times10^{18}$	90	MPI+ITEP+INFN	[Pipke *et al.* (1994)]
^{128}Te$\rightarrow^{128}$Xe	$>1.1\times10^{23}$	90	INFN+LNGS	[Arnaboldi *et al.* (2003)]
	$>8.6\times10^{22}$	90	INFN+LNGS	[Allessandrello *et al.* (2000)]
	$>7.7\times10^{24}$		Geochemical	[Bernatowicz *et al.* (1992),(1993)]
^{130}Te$\rightarrow^{130}$Xe	$>4.0\times10^{24}$	90	CUORE-0	[Alduino *et al.* (2016)]
	$>4.0\times10^{24}$	90	CUORE-0	[Alfonso *et al.* (2015)]
	$>7.0\times10^{20}$	90	NEMO 3	[Arnold *et al.*(2015)]
	$>1.8\times10^{24}$	90	CUORICINO	[Arnaboldi *et al.* (2005)]
	$>5.5\times10^{23}$	90	CUORICINO	[Arnaboldi *et al.* (2004)]
	$>2.1\times10^{23}$	90	INFN+LNGS	[Arnaboldi *et al.* (2003)]
	$>1.4\times10^{23}$	90	INFN+LNGS	[Allessandrello *et al.* (2000)]
	$>7.7\times10^{22}$	90	Milano	[Morales (1999)]
	$>5.6\times10^{22}$	90	INFN+LNGS	[Allessandrello *et al.* (1998)]
	$>8.2\times10^{21}$	90	INFN+LNGS	[Allessandrello *et al.* (1994)]

Table 1.2 continued

Transition	$T^{0\nu}_{1/2}$ (yr)	C.L.(%)	Project	Reference
^{136}Xe$\rightarrow^{136}$Ba	$>1.1\times10^{25}$		EXO-200	[Albert *et al.* (2014)]
	$>2.6\times10^{24}$	90	KamLAND-Zen	[Gando *et al.* (2012)]
	$>1.2\times10^{24}$	90	INFN	[Bernabei *et al.* (2002)]
	$>4.4\times10^{23}$	90	Caltech+PSI+UN	[Luescher *et al.* (1998)]
	$>4.2\times10^{23}$		Gotthard tunnel	[Busto *et al.* (1996)]
	$>2.6\times10^{23}$	90	Gotthard tunnel	[Vuilleumier *et al.* (1993)]
	$>3.0\times10^{21}$	68	ITEP+INR	[Barabash *et al.* (1989)]
	$>1.0\times10^{21}$	90	Milano+INFN	[Alessandrello *et al.* (1988)]
	$>2.0\times10^{21}$	68		[Barabanov *et al.* (1986)]
^{150}Nd$\rightarrow^{150}$Sm	$>2\times10^{22}$	90	NEMO-3	[Arnold *et al.* (2016)]
	$>1.8\times10^{22}$	90	NEMO 3	[Barabash *et al.*(2011)]
	$>1.8\times10^{22}$	90	NEMO-3	[Argyriades *et al.* (2009)]
	$>1.2\times10^{21}$	90	UC Irvine	[De Silva *et al.* (1997]
	$>2.1\times10^{20}$	90	ITEP +INR	[Artemiev *et al.* (1995)]
	$>2.1\times10^{21}$			[Moe *et al.* (1994)]
	$>1.7\times10^{21}$		INR	[Klimenko *et al.* (1986)]
^{238}U$\rightarrow^{238}$Pu	$>1.0\times10^{12}$	68	INR	[Tretyak *et al.* (2005)]

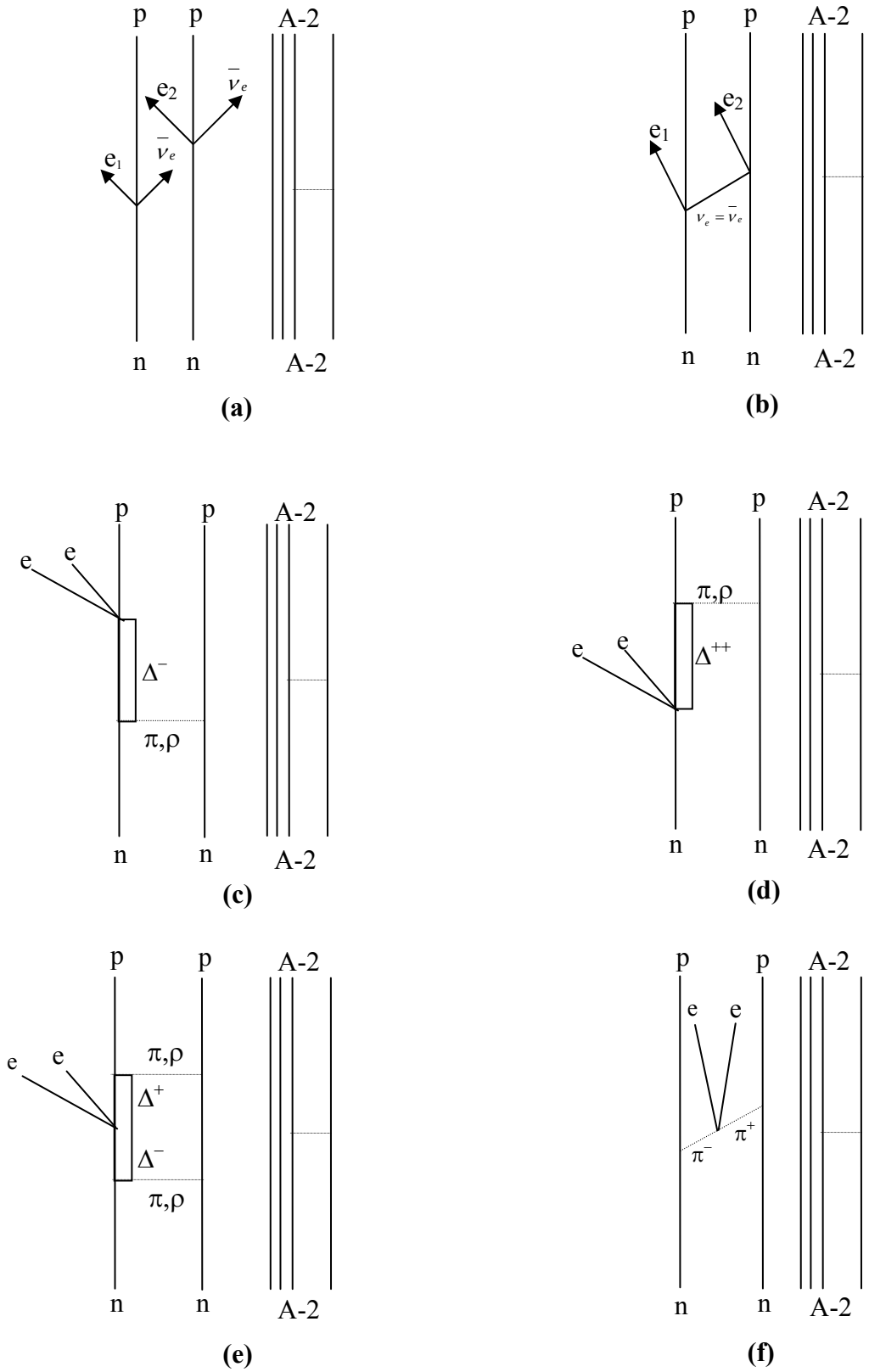

Fig. 1.1: (a) Two nucleon mechanism for $2\nu\beta^-\beta^-$ decay. $0\nu\ \beta^-\beta^-$ decay modes in (b) two nucleon mechanism, (c), (d) $N\leftrightarrow\Delta$ mechanism, (e) $\Delta\leftrightarrow\Delta$ mechanism and (f) $\pi^-\leftrightarrow\pi^+$ mechanism.

Chapter 2

Spectroscopic properties of nuclei participating in $\beta^-\beta^-$ decay

Our aim is to study the $\beta^-\beta^-$ decay of ^{94,96}Zr, ^{100}Mo, ^{104}Ru, ^{110}Pd, ^{128,130}Te and ^{150}Nd isotopes not in isolation but together with other observed nuclear properties in accordance with basic idea of nuclear many-body theory. With the advanced experimental facilities involving in-beam γ-ray spectroscopy, a good amount of data concerning the level energies and electromagnetic properties have been collected [Sakai (1984), Raman *et al.* (2001) and Raghavan (1989)]. The study of energy spectra, electromagnetic static moments, electromagnetic transition probabilities, β-decay rates and spectroscopic factors is the tool to test the contribution of different correlations inside the nucleus as well as the "goodness of wave function". However, it is not possible to study the structure of odd-odd nuclei in the present version of the PHFB model. Hence, the single β-decay rate and the distribution of Gamow-Teller strength can not be calculated. On the other hand, the study of these processes has implications in the understanding of the role of the isoscalar part

of the proton-neutron interaction. This is a serious draw back in the present formalism of the PHFB model. This draw back can be removed by introducing complex Bogoliubov transformations in the PHFB formalism, which will be attempted in the future studies.

The $2\nu\beta^-\beta^-$ decay of ^{94,96}Zr, ^{98,100}Mo, ^{104}Ru, ^{110}Pd, ^{128,130}Te and ^{150}Nd isotopes has been already studied in the PHFB model using pairing plus quadrupole-quadrupole interaction [Chandra *et al.* (2005), Singh *et al.* (2007)] and adding hexadecapole-hexadecapole term in it [Chandra *et al.* (2009)]. The observed decay rates were reproduced quite successfully. In the present study, we use the other two parametrizations of the effective two-body interaction to check the stability of results with respect to the change in parametrization. We calculate reduced $B(E2{:}0^+ \rightarrow 2^+)$ transition probabilities, the deformation parameters β_2 and g-factors $g(2^+)$ and compare them with the experimentally observed values to check the reliability of the wave functions.

The present chapter is organized in the following Sections. In Section 2.1, a brief outline of the PHFB model has been given. A detailed derivation of the HFB method has been given by Baranger (1963), Villars (1966) and Goodman (1979). The formalism to calculate the spectroscopic properties has been presented in Section 2.2. We have compared the calculated yrast spectra and electromagnetic properties with available experimental data for ^{94,96}Zr, ^{94,96,100}Mo, ^{100,104}Ru, ^{104,110}Pd, ^{110}Cd, ^{128,130}Te, ^{128,130}Xe, ^{150}Nd and ^{150}Sm nuclei in Section 2.3. Finally, the conclusions are given in Section 2.4.

2.1 The PHFB model

The PHFB calculation is carried out through the following procedure.

(1) The HFB intrinsic state $|\Phi_K\rangle$ is obtained through a self-consistent solutions of the HFB Hamiltonian [Baranger (1963), Villars (1966) and Goodman (1979)].

(2) States with good angular momentum **J** are projected out from the axially symmetric HFB intrinsic state $|\Phi_K\rangle$ using the standard technique given by Onishi and Yosida (1966).

2.1.1 HFB theory

The nuclear many-body Hamiltonian for non-relativistic point nucleons neglecting three and many-nucleon forces is given by

$$H = \sum_{\alpha\beta} \langle\alpha|\ T\ |\beta\rangle a^\dagger_\alpha a_\beta + \frac{1}{4} \sum_{\alpha\beta\gamma\delta} \langle\alpha\beta|\ V\ |\gamma\delta\rangle a^\dagger_\alpha a^\dagger_\beta a_\delta a_\gamma \tag{2.1}$$

The indices $\alpha\beta\gamma\delta$ span the active valence single particle states of the model space, and $a^\dagger_\alpha$ and a_α are the particle creation and annihilation operators, respectively. The HFB equations are obtained by equating to zero the off diagonal bilinear quasiparticle part of the transformed Hamiltonian after making a canonical transformation from a_α's to quasi-fermions q_α's. The general Bogoliubov transformations are considered to define the quasiparticle creation and destruction operators in terms of particle creation and destruction operators.

$$q^\dagger_\alpha = \sum_\beta \left(u_{\alpha\beta} a^\dagger_\beta + v_{\alpha\beta} a_\beta \right) \tag{2.2}$$

$$q_\alpha = \sum_\beta \left(u^*_{\alpha\beta} a_\beta + v^*_{\alpha\beta} a^\dagger_\beta \right) \tag{2.3}$$

The particle and quasiparticle operators satisfy the fermion anti-commutation relations

$$[a^\dagger_\alpha, a_\beta] = \delta_{\alpha\beta} \; ; \qquad [a^\dagger_\alpha, a^\dagger_\beta] = [a_\alpha, a_\beta] = 0 \tag{2.4}$$

$$[q^\dagger_\alpha, q_\beta] = \delta_{\alpha\beta} \; ; \qquad [q^\dagger_\alpha, q^\dagger_\beta] = [q_\alpha, q_\beta] = 0 \tag{2.5}$$

The transformation coefficients are real and satisfy appropriate orthonormality conditions. The 2n×2n linear transformation

$$\begin{bmatrix} q^\dagger \\ q \end{bmatrix} = \begin{bmatrix} u & v \\ v^* & u^* \end{bmatrix} \begin{bmatrix} a^\dagger \\ a \end{bmatrix} \tag{2.6}$$

is required to be unitary, and it follows from the unitarity condition that

$$uu^\dagger + vv^\dagger = u^\dagger u + \widetilde{v}v^* = I \tag{2.7}$$

$$u\widetilde{v} + v\widetilde{u} = u^\dagger v + \widetilde{v}u^* = 0 \tag{2.8}$$

The quasiparticle vacuum is defined through the relation

$$q_\alpha |\Phi_0\rangle = 0 \tag{2.9}$$

or

$$|\Phi_0\rangle = N \prod_\alpha q_\alpha |0\rangle \tag{2.10}$$

where $|0\rangle$ is the particle vacuum and N is the normalization constant, which is to be inserted appropriately.

The many-body Hamiltonian can be written with respect to the quasiparticle vacuum as

$$H' = H'_0 + H'_2 + H'_4 \tag{2.11}$$

where

$$
\begin{aligned}
H'_0 &= Tr\left[\left(T-\lambda_\pi N_\pi-\lambda_\nu N_\nu+\frac{1}{2}\Gamma\right)\rho+\frac{1}{2}\Delta t^\dagger\right] && (2.12)\\
H'_2 &= \sum_{\alpha\beta}\left(h-\lambda_\pi N_\pi-\lambda_\nu N_\nu\right)_{\alpha\beta}:a^\dagger_\alpha a_\beta: \\
&\quad +\frac{1}{2}\sum_{\alpha\beta}\left[\Delta_{\alpha\beta}:a^\dagger_\alpha a^\dagger_\beta:+\Delta^\dagger_{\alpha\beta}:a_\alpha a_\beta:\right] && (2.13)\\
H'_4 &= \frac{1}{4}\sum_{\alpha\beta\gamma\delta}\langle\alpha\beta|\ V\ |\gamma\delta\rangle:a^\dagger_\alpha a^\dagger_\beta a_\delta a_\gamma: && (2.14)
\end{aligned}
$$

The HF hamiltonian h, the HF potential Γ and the pair potential Δ are given by

$$
\begin{aligned}
h &= T+\Gamma && (2.15)\\
\Gamma_{\alpha\beta} &= \sum_{\gamma\delta}\langle\alpha\gamma|\ V\ |\beta\delta\rangle\rho_{\delta\gamma} && (2.16)\\
\Delta_{\alpha\beta} &= \frac{1}{2}\sum_{\gamma\delta}\langle\alpha\beta|\ V\ |\gamma\delta\rangle t_{\gamma\delta} && (2.17)
\end{aligned}
$$

where the density matrix ρ and the pairing potential t are defined as

$$
\begin{aligned}
\rho_{\alpha\beta} &= \langle\Phi_0|a^\dagger_\beta a_\alpha|\Phi_0\rangle && (2.18)\\
&= \sum_\delta v_{\delta\beta}v^*_{\delta\alpha}=(v^\dagger v)_{\alpha\beta} && (2.19)\\
t_{\alpha\beta} &= \langle\Phi_0|a_\beta a_\alpha|\Phi_0\rangle=v^\dagger u && (2.20)
\end{aligned}
$$

Using Wick's theorem

$$
\begin{aligned}
\langle\Phi_0|H'|\Phi_0\rangle &= \langle\Phi_0|H'_0|\Phi_0\rangle \\
&= Tr\left[\left(T-\lambda_\pi N_\pi-\lambda_\nu N_\nu+\frac{1}{2}\Gamma\right)\rho+\frac{1}{2}\Delta t^\dagger\right] && (2.21)
\end{aligned}
$$

where by construction

$$
\langle\Phi_0|H'_2+H'_4|\Phi_0\rangle=0 \qquad (2.22)
$$

The first term in Eq. (2.21) is the HF binding energy and the second term is the pairing energy. The quasiparticle excitation energies are obtained from H_2' and the remaining H_4' contains the quasiparticle interaction energies, which are neglected in the HFB theory. In time dependent HFB (TDHFB) or the quasiparticle random phase approximation (QRPA), some effects of quasiparticle interaction can be included.

The HFB theory is a generalized HF procedure in which the HF field and the pairing interaction are treated simultaneously and on equal footing. However, the quasiparticle transformations do not conserve the number of particles. Hence, one imposes constraints via the use of Lagrange multipliers while minimizing the complete Hamiltonian H such that the average number of nucleons in the state $|\Phi_0\rangle$ be equal to the given number of nucleons of the nucleus under consideration. That is, one minimizes

$$H' = H - \lambda_\pi N_\pi - \lambda_\nu N_\nu \tag{2.23}$$

where

$$N_\pi = \sum_{\alpha_\pi} a^\dagger_{\alpha_\pi} a_{\alpha_\pi} \quad and \quad N_\nu = \sum_{\alpha_\nu} a^\dagger_{\alpha_\nu} a_{\alpha_\nu} \tag{2.24}$$

possess the expectation values

$$\langle \Phi_0 | N_\pi | \Phi_0 \rangle = Z \ , \ \langle \Phi_0 | N_\nu | \Phi_0 \rangle = A - Z \tag{2.25}$$

Further, the Lagrange's multipliers λ_π and λ_ν turn out to have the physical interpretation of proton and neutron fermi energies.

There are several equivalent methods for deriving the HFB equations such as (i) variational procedure, (ii) the equation of motion and (iii) elimination of dangerous diagrams. Here, we follow the equation of motion method. Further, we use time reversal symmetry

as our concern is with even Z-even N nuclei only. The quasiparticle transformation are rewritten as

$$q_k^\dagger = \sum_\alpha \left(u_{k\alpha} a_\alpha^\dagger + v_{k\alpha} a_{\overline{\alpha}}\right) \tag{2.26}$$

$$q_{\overline{k}}^\dagger = \sum_\alpha \left(u_{k\alpha} a_{\overline{\alpha}}^\dagger - v_{k\alpha} a_\alpha\right) \tag{2.27}$$

and the HFB equations are given by

$$\begin{aligned} E_k u_{k\alpha} &= \sum_\gamma h'_{\alpha\gamma} u_{\alpha\gamma} + \Delta_{\alpha\overline{\gamma}} v_{\alpha\gamma} \\ E_k v_{k\alpha} &= \sum_\gamma \Delta_{\alpha\overline{\gamma}} u_{\alpha\gamma} - h'_{\alpha\gamma} v_{\alpha\gamma} \end{aligned} \tag{2.28}$$

where E_k is the quasiparticle energy. Further

$$h'_{\alpha\gamma} = T_{\alpha\gamma} - \lambda\delta_{\alpha\gamma} + \Gamma_{\alpha\gamma} \tag{2.29}$$

where

$$\Gamma_{\alpha\gamma} = \sum_{\beta\delta} \left[\langle\alpha\beta|\ V\ |\gamma\delta\rangle + \langle\alpha\overline{\beta}|\ V\ |\gamma\overline{\delta}\rangle\right] \sum_{k=1}^{n} v_{k\beta} v_{k\delta} \tag{2.30}$$

$$= \sum_{\beta\delta} \left[\langle\alpha\beta|\ V\ |\gamma\delta\rangle + \langle\alpha\overline{\beta}|\ V\ |\gamma\overline{\delta}\rangle\right] \rho_{\beta\delta} \tag{2.31}$$

and

$$\rho_{\beta\delta} = \sum_k v_{k\beta} v_{k\delta} \tag{2.32}$$

with

$$\Delta_{\alpha\overline{\gamma}} = \sum_{\beta\delta} \langle\alpha\overline{\gamma}|\ V\ |\beta\overline{\delta}\rangle \sum_{k=1}^{n} v_{k\beta} u_{k\delta} \tag{2.33}$$

Using the Bloch-Messiah theorem [Bloch and Messiah (1962)], the coupled HFB equations can be written in a simplified form. We define transformations

$$b_k^\dagger = \sum_\alpha C_{k,\alpha} a_\alpha^\dagger \qquad and \qquad b_{\overline{k}}^\dagger = \sum_\alpha C_{k,\alpha}^* a_{\overline{\alpha}}^\dagger \tag{2.34}$$

where the expansion coefficients appearing in Eq. (2.34) can be obtained by diagonalizing the HF like potential h' in spherical basis

$$h'_{\alpha\beta} = \langle\alpha|T - \lambda_\pi N_\pi - \lambda_\nu N_\nu|\beta\rangle + \sum_k \langle\alpha k|\ V\ |\beta k\rangle v_k^2 \tag{2.35}$$

which includes the appropriate density $\rho_k = v_k^2$. The occupation probabilities v_k^2 are obtained by solving the BCS equation

$$\Delta_k = \Delta_{k\overline{k}} = \sum_{k'} \langle k\overline{k}|\ V\ |k'\overline{k'}\rangle u_{k'} v_{k'} \tag{2.36}$$

The calculation involves iteration between Eqs. (2.35) and (2.36) until a reasonable convergence is achieved in terms of both the expansion coefficients $C_{k,\alpha}$ and v_k^2. Denoting by θ_k the eigenvalue of $h'_{\alpha\beta}$ given by Eq. (2.35), the probability amplitudes u_k and v_k in Eqs. (2.26 and 2.27) are given by

$$u_k^2 = \frac{1}{2}\left[1 + \frac{\theta_k}{E_k}\right] \tag{2.37}$$

and

$$v_k^2 = \frac{1}{2}\left[1 - \frac{\theta_k}{E_k}\right] \tag{2.38}$$

where

$$E_k = \sqrt{\theta_k^2 + \Delta_k^2} \tag{2.39}$$

with

$$\Delta_{k\overline{k}} = \frac{1}{2}\sum_{k'} \langle k\overline{k}|\ V\ |k'\overline{k'}\rangle \left(\frac{\Delta_{k\overline{k'}}}{\sqrt{\theta_{k'}^2 + \Delta_{k'\overline{k'}}^2}}\right) \tag{2.40}$$

The chemical potential λ is obtained by solving the equation

$$\sum_{k=1}^{n}\left[1 - \frac{\theta_k}{\sqrt{\theta_k^2 + \Delta_k^2}}\right] = N \tag{2.41}$$

The ground state energy E_{HFB} is given by

$$E_{HFB} = \sum_{k=1}^{n} (T_{kk} + \lambda - E_k) v_k^2 \tag{2.42}$$

where

$$\begin{aligned} T_{kk} &= \sum_{\alpha\gamma} \langle k\alpha \left| T \right| k\gamma \rangle \\ &= \sum_{\alpha\gamma} T_{\alpha\gamma} C_{k\alpha} \; C_{k\gamma} \end{aligned} \tag{2.43}$$

The quadrupole moment of the axially symmetric HFB intrinsic state is given by

$$Q_{HFB} = 2 \sum_{k=1}^{n} Q_{20} \; v_k^2 \tag{2.44}$$

where

$$Q_{20} = \left(\frac{16\pi}{5} \right)^{1/2} \; r^2 \; Y_{20} \tag{2.45}$$

is the quadrupole moment operator.

The axially symmetric HFB intrinsic state $|\Phi_0\rangle$ can be written as

$$|\Phi_0\rangle = \prod_{im} (u_{im} + v_{im} b_{im}^{\dagger} b_{i\bar{m}}^{\dagger}) |0\rangle \tag{2.46}$$

$$= N \; exp \left(\frac{1}{2} \sum_{\alpha\beta} f_{\alpha\beta} a_{\alpha,m}^{\dagger} a_{\alpha,-m}^{\dagger} |0\rangle \right) \tag{2.47}$$

where the creation operators $b_{im}^{\dagger}$ and $b_{i\bar{m}}^{\dagger}$ are defined as

$$b_{im}^{\dagger} = \sum_{\alpha} C_{i\alpha,m} a_{\alpha,m}^{\dagger} \quad \text{and} \quad b_{i\bar{m}}^{\dagger} = \sum_{\alpha} (-1)^{l+j-m} C_{i\alpha,m} a_{\alpha,-m}^{\dagger} \tag{2.48}$$

with

$$f_{\alpha\beta} = \sum_{i} C_{i,j_\alpha m_\alpha} C_{i,j_\beta m_\beta} \left(\frac{v_{im_\alpha}}{u_{im_\alpha}} \right) \delta_{m_\alpha - m_\beta} \tag{2.49}$$

where N is a normalization constant.

2.1.2 Projection of angular momentum

The intrinsic state $|\Phi_K\rangle$ can be expanded in terms of states of good angular momentum **J** as

$$|\Phi_K\rangle = \sum_J a_J |\Psi_{JK}\rangle \tag{2.50}$$

Applying the rotation operator $R(\Omega)$, one obtains

$$\hat{R}(\Omega)\ |\Phi_K\rangle = \sum_{JM} a_J\ D^J_{MK}(\Omega)\ |\Psi_{JM}\rangle \tag{2.51}$$

where

$$\hat{R}(\Omega) = e^{-i\alpha J_Z} e^{-i\beta J_Y} e^{-i\gamma J_Z} \tag{2.52}$$

and $D^J_{MK}(\Omega)$ is the rotation matrix. Multiplying by D^J_{MK} and integrating, one gets

$$\begin{aligned} |\Psi_{JM}\rangle &= \frac{2J+1}{8\pi^2 a_J} \int d\Omega D^J_{MK}(\Omega) \hat{R}(\Omega)\ |\Phi_K\rangle \\ &= P^J_{MK} |\Phi_K\rangle \end{aligned} \tag{2.53}$$

where

$$P^J_{MK} = \frac{2J+1}{8\pi^2 a_J} \int d\Omega D^J_{MK}(\Omega) \hat{R}(\Omega) \tag{2.54}$$

Restricting to the axially symmetric HFB intrinsic state $|\Phi_0\rangle$ with $K = 0$, one obtains

$$\begin{aligned} |\Psi_{J0}\rangle &= P^J_{00}\, |\Phi_0\rangle \\ &= \frac{2J+1}{8\pi^2} \int D^J_{00}(\Omega) R(\Omega)\, |\Phi_0\rangle\, d\Omega \end{aligned} \tag{2.55}$$

2.2 Spectroscopic properties of yrast states

In the below, we present expressions to calculate various nuclear spectroscopic properties, namely yrast energy spectra, reduced $B(E2{:}J_i \rightarrow J_f)$ transition probabilities [Dixit *et al.*

(2002)], β_2 parameter [Raman *et al.* (1989)] and magnetic dipole moments $\mu(J)$ [Rath *et al.* (1988)].

Yrast spectra

The energy E_J of a state with good angular momentum $\mathbf{J}$ is given by

$$\begin{aligned} E_J &= \frac{\langle \Psi_{J0}|H|\Psi_{J0}\rangle}{\langle \Psi_{J0}|\Psi_{J0}\rangle} \\ &= \frac{\int_0^\pi h(\theta) d^J_{00}(\theta)\sin\theta\ d\theta}{\int_0^\pi n(\theta) d^J_{00}(\theta)\sin\theta\ d\theta} \end{aligned} \tag{2.56}$$

The overlap integrals $h(\theta)$ and $n(\theta)$ are given by

$$\begin{aligned} h(\theta) &= \left\langle \Phi_0|He^{-i\theta J_y}|\Phi_0\right\rangle \\ &= \sum_\alpha \varepsilon_\alpha \left(\frac{M}{1+M}\right)_{\alpha\alpha} + \frac{1}{4}\sum_{\alpha\beta\gamma\delta}\langle\alpha\beta|\ V\ |\gamma\delta\rangle \\ &\quad \times \left\{ 2\left(\frac{M}{1+M}\right)_{\gamma\alpha}\left(\frac{M}{1+M}\right)_{\delta\beta} \right. \\ &\quad \left. + \sum_{\nu\rho}\left(\frac{1}{1+M}\right)_{\gamma\rho} F_{\rho\delta}\left(\frac{1}{1+M}\right)_{\nu\alpha} f_{\nu\beta} \right\} \end{aligned} \tag{2.57}$$

and

$$\begin{aligned} n(\theta) &= \left\langle \Phi_0|e^{-i\theta J_y}|\Phi_0\right\rangle \\ &= \{\det[1+M(\theta)]\}^{1/2} \end{aligned} \tag{2.58}$$

where

$$M(\theta) = F(\theta) f^\dagger \tag{2.59}$$

with

$$F_{\alpha\beta}(\theta) = \sum_{m'_\alpha, m'_\beta} d^{j_\alpha}_{m_\alpha, m'_\alpha}(\theta) d^{j_\beta}_{m_\beta, m'_\beta}(\theta) f_{j_\alpha m'_\alpha, j_\beta m'_\beta} \tag{2.60}$$

and

$$\rho_{\alpha\beta}(\theta) = \left[\frac{M(\theta)}{1+M(\theta)}\right]_{\alpha\beta} = \delta_{\alpha\beta} - \left[\frac{1}{1+M(\theta)}\right]_{\alpha\beta} \tag{2.61}$$

The projection calculation is carried out as follows. In the first step, f matrix is set up using the HFB wave functions. In the next step F, M and $(1/1+M)$ are evaluated for 20 values of Gaussian quadrature points between the range $(0, \pi)$.

Reduced $B(E2{:}J_i \to J_f)$ transition probabilities and β_2 parameter

The reduced $B(E2)$ transition probability is given by

$$B(E2{:}J_i \to J_f) = \left(\frac{5}{16\pi}\right)\left[e_\pi \left\langle Q_{20}\right\rangle_\pi + e_\nu \left\langle Q_{20}\right\rangle_\nu\right]^2 \tag{2.62}$$

where

$$\begin{aligned}
\left\langle Q_{20}\right\rangle_{\tau_3} &= \left\langle \Psi_{J_i K} \left| Q_{20} \right| \Psi_{J_f K} \right\rangle \\
&= \left[n_{J_i} n_{J_f}\right]^{-1/2} \int_0^\pi \sum_\mu \begin{pmatrix} J_i & 2 & J_f \\ -\mu & \mu & 0 \end{pmatrix} \\
&\quad \times d^{J_i}_{-\mu 0}(\theta) n(\theta) \left[b^2 \sum_{\tau_3 \alpha\beta} e_{\tau_3} \left\langle \alpha \left| Q_{2\mu} \right| \beta \right\rangle \rho^{\tau_3}_{\alpha\beta}(\theta)\right] \sin\theta \; d\theta
\end{aligned} \tag{2.63}$$

with

$$n_J = \int_0^\pi n(\theta) d^J_{00}(\theta) \sin\theta \; d\theta \tag{2.64}$$

$$\rho^{\tau_3}_{\alpha\beta}(\theta) = \left[\frac{M(\theta)}{1+M(\theta)}\right]^{\tau_3}_{\alpha\beta} \tag{2.65}$$

and

$$Q_{2\mu} = \sqrt{\frac{16\pi}{5}} \frac{r^2}{b^2} Y_{2\mu}(\theta, \phi) \tag{2.66}$$

The β_2 parameter is given by

$$\beta_2 = \frac{4\pi}{3ZR_0^2}\left[\frac{B(E2)}{e^2}\right]^{1/2} \tag{2.67}$$

where $R_0 = 1.2\ A^{1/3}$ and $B(E2)$ is in units of $\mathrm{e}^2\mathrm{b}^2$.

Magnetic dipole moments $\mu(J)$

Usually, experimentalists prefer to report g-factors defined by $g(J) = \mu(J)/J$. The expression to calculate magnetic diploe moment $\mu(J)$ is given by

$$\begin{aligned}
\mu(J) &= \langle \Psi_{J0} \left| \mu_z \right| \Psi_{J0} \rangle \\
&= n_J^{-1} \int_0^{\pi} n(\theta) \sum_m \begin{pmatrix} J & 1 & J \\ -m & m & 0 \end{pmatrix} \\
&\quad \times d^J_{-m0}(\theta) \sum_{\tau_3 \alpha\beta} \langle \alpha \left| \mu_m \right| \beta \rangle \, \rho^{\tau_3}_{\alpha\beta}(\theta) \sin\theta \; d\theta
\end{aligned} \tag{2.68}$$

where in general [Bohr and Mottelson (1998)]

$$\boldsymbol{\mu} = g_l' \mathbf{l} + g_s' \mathbf{s} + g_p \left(Y^{(2)} \times S^{(2)} \right)^{(1)} \tag{2.69}$$

Here g_l' (g_s') are the effective orbital (spin) g-factors and g_p provides a measure of the spin-polarization effects. In the present calculation, we have neglected the contributions of spin-polarization effects.

2.3 Results and discussions

We use a Hamiltonian with pairing plus quadrupole-quadrupole plus hexadecapole-hexadecapole (*PPQQHH)* type of effective two-body interaction. The Hamiltonian is explicitly written

as

$$H = H_{sp} + V(P) + \zeta_{qq}\,[V(QQ) + V(HH)] \tag{2.70}$$

where ζ_{qq} is an arbitrary parameter and the final results are obtained by setting $\zeta_{qq} = 1$. The purpose of introducing ζ_{qq} is to study the role of deformation by varying the strength of $QQHH$ interaction. Further, H_{sp} denotes the single particle Hamiltonian. The pairing part of the effective two-body interaction $V(P)$ is given by

$$V(P) = -\left(\frac{G}{4}\right)\sum_{\alpha\beta}(-1)^{j_\alpha+j_\beta-m_\alpha-m_\beta}a^\dagger_\alpha a^\dagger_{\bar{\alpha}}a_{\bar{\beta}}a_\beta, \tag{2.71}$$

where α denotes the quantum numbers $(nljm)$ and G is the strength of the pairing interaction. The state $\bar{\alpha}$ is same as α but with the sign of m reversed.

The QQ part of the effective interaction $V(QQ)$ is expressed as

$$V(QQ) = -\left(\frac{\chi_2}{2}\right)\sum_{\alpha\beta\gamma\delta}\sum_{\mu}(-1)^\mu\langle\alpha|q_{2\mu}|\gamma\rangle\langle\beta|q_{2-\mu}|\delta\rangle\ a^\dagger_\alpha a^\dagger_\beta\ a_\delta\ a_\gamma \tag{2.72}$$

where

$$q_{2\mu} = \left(\frac{16\pi}{5}\right)^{1/2} r^2 Y_{2\mu}(\theta,\phi) \tag{2.73}$$

The HH part of the effective interaction $V(HH)$ is given as

$$V(HH) = -\left(\frac{\chi_4}{2}\right)\sum_{\alpha\beta\gamma\delta}\sum_{\nu}(-1)^\nu\langle\alpha|q_{4\nu}|\gamma\rangle\langle\beta|q_{4-\nu}|\delta\rangle\ a^\dagger_\alpha a^\dagger_\beta\ a_\delta\ a_\gamma \tag{2.74}$$

where

$$q_{4\nu} = r^4 Y_{4\nu}(\theta,\phi) \tag{2.75}$$

The relative magnitudes of the parameters of the hexadecapole-hexadecapole part of the two body interaction were calculated from a relation suggested by Bohr and Mottelson

[Bohr and Mottelson (1975)]. According to them the approximate magnitude of these constants for isospin $T = 0$ is given by

$$\chi_\lambda = \frac{4\pi}{2\lambda+1}\frac{m\omega_0^2}{A\left\langle r^{2\lambda-2}\right\rangle} \qquad \text{for } \lambda = 1, 2, 3, 4\cdot\cdot \tag{2.76}$$

and the parameters for the $T = 1$ case are approximately half of their $T = 0$ counterparts. Using $b = 1.0032A^{1/6}$, one obtains

$$\begin{aligned} \chi_4 &= \left[\left(\frac{16}{25}\right)\left(\frac{2}{3}\right)^{2/3}\right]\chi_2 A^{-2/3}b^{-4} \\ &= 0.4884\chi_2 A^{-2/3}b^{-4} \end{aligned} \tag{2.77}$$

In case of $A \leq 110$ nuclei, we treat the doubly even ^{76}Sr ($N = Z = 38$) nucleus as an inert core with the valence space spanned by $1p_{1/2}$, $2s_{1/2,}$ $1d_{3/2}$, $1d_{5/2}$, $0g_{7/2}$, $0g_{9/2}$ and $0h_{11/2}$ orbits for protons and neutrons. The $1p_{1/2}$ orbit is included to examine the role of the $Z = 40$ proton core vis-a-vis the onset of deformation in highly neutron rich isotopes. The set of single particle energies (SPE's) used here are $\varepsilon(1p_{1/2}) = -0.8$, $\varepsilon(0g_{9/2}) = 0.0$, $\varepsilon(1d_{5/2}) = 5.4$, $\varepsilon(2s_{1/2}) = 6.4$, $\varepsilon(1d_{3/2}) = 7.9$, $\varepsilon(0g_{7/2}) = 8.4$ and $\varepsilon(0h_{11/2}) = 8.6$ (in MeV) for proton and neutrons. The same model space and set of SPE's has been employed in the study of 2ν $\beta^-\beta^-$ decay [Chandra *et al.* (2005)] as well as 2ν $\beta^+\beta^+$ decay [Raina *et al.* (2006)] of potential $\beta\beta$ emitters in the mass region $A \sim 100$.

For $A \geq 128$ nuclei, the doubly even ^{100}Sn ($N = Z = 50$) nucleus has been treated as an inert core with the valence space spanned by $2s_{1/2,}1d_{3/2}$, $1d_{5/2}$, $1f_{7/2}$, $0g_{7/2}$, $0h_{9/2}$ and $0h_{11/2}$ orbits for protons and neutrons. The change of model space is forced upon due to the following reason. The number of neutrons increase to about 50 for nuclei occurring in the mass region $A \sim 150$ in the model space with ^{76}Sr as the core. With the increase in neutron number, the yrast energy spectra gets compressed due to increase in the attractive

part of effective two-body interaction. The set of single particle energies (SPE's) used here are (in MeV) $\varepsilon(1d_{5/2}) = 0.0$, $\varepsilon(2s_{1/2}) = 1.4$, $\varepsilon(1d_{3/2}) = 2.0$, $\varepsilon(0g_{7/2}) = 4.0$, $\varepsilon(0h_{11/2}) = 6.5$ (4.8 for ^{150}Nd and ^{150}Sm), $\varepsilon(1f_{7/2}) = 12.0$ (11.5 for ^{150}Nd and ^{150}Sm), $\varepsilon(0h_{9/2}) = 12.5$ (12.0 for ^{150}Nd and ^{150}Sm) for proton and neutrons. This set of SPE's but for the $\varepsilon(0h_{11/2})$, which is increased by 1.5 MeV has been employed for calculations of nuclear properties in the mass region $A \sim 130$ [Singh *et al.* (2007), Rani Devi *et al.* (1997)].

The spectroscopic properties of ^{94,96}Zr, ^{94,96,100}Mo, ^{100,104}Ru, ^{104,110}Pd, ^{110}Cd, ^{128,130}Te, ^{128,130}Xe, ^{150}Nd and ^{150}Sm nuclei have been calculated in PHFB model using two parametrizations of the effective two-body interaction, namely $PPQQ1$ (without hexadecapole-hexadecapole term) [Chandra *et al.* (2005), Singh *et al.* (2007)] and $PPQQHH1$ (with hexadecapole-hexadecapole term) [Chandra *et al.* (2005)]. In $PPQQ1$ and $PPQQHH1$ parametrizations the strengths of the like particle components of the QQ interaction were taken as: $\chi_{2pp} = \chi_{2nn} = -0.0105$ MeV b^{-4}, where b is oscillator parameter and an optimum yrast spectra of ^{94,96}Zr, ^{94,96,100}Mo, ^{100,104}Ru, ^{104,110}Pd, ^{110}Cd, ^{128,130}Te, ^{128,130}Xe, ^{150}Nd and ^{150}Sm nuclei was obtained by varying the strength of proton-neutron (pn) component of the QQ interaction χ_{2pn}. The theoretical spectra was considered to be the optimum if the excitation energy of the 2^+ state E_{2^+} is reproduced as closely as possible in comparison to the experimental results. Thus, χ_{2pn} was fixed through the experimentally available energy spectra for a given model space, SPE's, G_p, G_n and χ_{2pp}. These values of the strength of the QQ interaction were comparable to those suggested by Arima on the basis of an empirical analysis of the effective two-body interactions [Arima (1981)]. All these input parameters were kept fixed to calculate other nuclear spectroscopic properties. In present work we use the other two parametrizations, namely $PPQQ2$ and $PPQQHH2$

parametrizations in which χ_{2pn} is taken as twice of $\chi_{2pp}(=\chi_{2nn})$ i.e. $\chi_{2pn} = 2\chi_{2pp} = 2\chi_{2nn}$ and varying the three parameters together to obtain the E_{2^+} of above nuclei in optimum agreement with the experimental values.

For $A \leq 110$ nuclei, the strengths of the pairing interaction is fixed through the relation $G_p = 30/A$ MeV and $G_n = 20/A$ MeV, which are same as used by Heestand *et al.* (1969) to explain the experimental $g(2^+)$ data of some even-even Ge, Se, Mo, Ru, Pd, Cd and Te isotopes in Greiner's collective model [Greiner (1966)]. For ^{96}Zr in $PQQ2$ parametrization, we have used $G_n = 22/A$ MeV. In $PQQHH2$ parametrization we have used $G_n = 18/A$ MeV and $22/A$ MeV for ^{94}Zr and ^{96}Zr, respectively. The strengths of the pairing interaction fixed for $A \geq 128$ nuclei are $G_p = G_n = 35/A$ MeV.

2.3.1 Yrast spectra

In Table 2.1, we have presented the theoretically calculated ground state energy E_{HFB}, intrinsic quadrupole moments Q_{HFB} and yrast energies for the E_{2^+} to E_{6^+} levels of ^{94,96}Zr, ^{94,96,100}Mo, ^{100,104}Ru, ^{104,110}Pd, ^{110}Cd, ^{128,130}Te, ^{128,130}Xe, ^{150}Nd and ^{150}Sm nuclei in $PPQQ2$ and $PPQQHH2$ parametrizations along with the experimental ones [Sakai (1984)]. We have also presented the results of $PPQQ1$ [Chandra *et al.* (2005), Singh *et al.* (2007)] and $PPQQHH1$ [Chandra *et al.* (2005)] parametrizations in the same table. From Table 2.1, it can be observed that the theoretical spectra is more expanded in comparison to the experimental spectra for all nuclei in all the four parametrizations although the agreement between the theoretically calculated and experimentally observed E_{2^+} is quite good. This can be taken into care by invoking the variation after projection (VAP) prescription [Khosa *et al.* (1982), Tripathi *et al.* (1984), Sharma *et al.* (1988)]. However,

our aim is to reproduce the properties of only low-lying 2^+ state and hence, we have not attempted the VAP calculation. In all cases, an inverse correlation between Q_{HFB} and E_{2^+} is observed except a few exceptions. Such a behavior is due to the enhancement in the collectivity of the intrinsic state with the increase of $\left|\chi_{2pn}\right|$, which decreases the E_{2^+}. This is known as Grodzins's rule [Grodzin (1962)].

2.3.2 Electromagnetic properties

In Table 2.2, the calculated as well as the experimentally observed reduced $B(E2{:}0^+ \rightarrow 2^+)$ transition probabilities, the deformation parameters β_2 and the gyromagnetic factors $g(2^+)$ of the above mentioned nuclei are presented. In column 4, the experimentally observed results are displayed. The calculated and the observed $B(E2{:}0^+ \rightarrow 2^+)$ values are in excellent agreement in case of ^{94}Zr, ^{94,100}Mo, ^{100,104}Ru and ^{104}Pd isotopes for $e_{eff} = 0.60$. In case of ^{96}Zr, ^{96}Mo, ^{128,130}Te, ^{128,130}Xe and ^{150}Nd isotopes, the calculated $B(E2{:}0^+ \rightarrow 2^+)$ agree with experimental limits at $e_{eff} = 0.50$. However, the calculated $B(E2{:}0^+ \rightarrow 2^+)$ differ by approximately 0.04 e^2b^2 in both the parametrizations from the experimental limit in case of ^{110}Pd for $e_{eff} = 0.50$. For ^{110}Cd isotope, the calculated $B(E2{:}0^+ \rightarrow 2^+)$ differ by 0.04 and 0.07 e^2b^2 in $PPQQ2$ and $PPQQHH2$ parametrizations, respectively from the experimental limit. In case of ^{150}Sm isotope, the difference between theoretically calculated and experimental limit of $B(E2{:}0^+ \rightarrow 2^+)$ differ by 0.42 and 0.50 e^2b^2 in $PPQQ2$ and $PPQQHH2$ parametrizations, respectively.

The β_2 parameters have been calculated at the same e_{eff} as in case of $B(E2{:}0^+ \rightarrow 2^+)$ values and presented in column 5 of Table 2.2. The average of experimental values of β_2 parameters are given in column 6 of the same table. The overall agreement be-

tween theoretically calculated values and experimental limits is almost same as in case of $B(E2{:}0^+ \rightarrow 2^+)$ values.

The gyromagnetic factors $g(2^+)$ are calculated with $g_l^\pi = 1.0$, $g_l^\nu = 0.0$, and $g_s^\pi = g_s^\nu = 0.60$. The available experimental $g(2^+)$ values are given in column 8 of Table 2.2. No experimental result is available for ^{96}Zr and ^{94,96}Mo. The theoretical $g(2^+)$ value of ^{94}Zr is a pathological case. The calculated $g(2^+)$ values are 0.565 and 0.068 nm in $PPQQ2$ and $PPQQHH2$ parametrizations, respectively while the most recent measured value is -0.329 ± 0.015 nm [Speidel *et al.* (2002)]. The calculated and experimentally observed $g(2^+)$ values are in overall good agreement for ^{100}Mo, ^{100,104}Ru, ^{104}Pd, ^{110}Cd and ^{128,130}Xe nuclei. The theoretically calculated and experimentally observed $g(2^+)$ values are off in case of ^{110}Pd, ^{128,130}Te, ^{150}Nd and ^{150}Sm nuclei.

Employing either of the four parametrizations, namely $PPQQ1$, $PPQQHH1$, $PPQQ2$ and $PPQQHH2$ method, the experimental excitation energies E_{2^+} of the 2^+ state [Sakai (1984)] can be reproduced within an accuracy of about 2%. The maximum changes in the yrast energies E_{4^+} and E_{6^+} with respect to the $PPQQ1$ interaction [Chandra *et al.* (2005), Singh *et al.* (2007)] are about 8% and 31%, respectively. The maximum changes in the reduced $B(E2{:}0^+ \rightarrow 2^+)$ transition probabilities, deformation parameters β_2 and g-factors $g(2^+)$ with respect to $PPQQ1$ parametrization, are about 13%, 6% and 27%, respectively, except for the case of ^{94}Zr.

2.4 Conclusions

To summarize, the yrast spectra, reduced $B(E2{:}0^+ \rightarrow 2^+)$ transition probabilities, deformation parameters β_2 and g-factors $g(2^+)$ of ^{94,96}Zr, ^{94,96,100}Mo, ^{100,104}Ru, ^{104,110}Pd, ^{110}Cd, ^{128,130}Te, ^{128,130}Xe, ^{150}Nd and ^{150}Sm isotopes have been calculated and compared with the available experimental data as a test of the reliability of the wave functions. The reduced transition probabilities $B(E2{:}0^+ \rightarrow 2^+)$, deformation parameters β_2 and gyromagnetic factors $g(2^+)$ are in overall agreement with the experimental data [Ramen *et al.* (2001), Raghavan (1989)] for all the four parametrizations of the pairing plus multipole type of effective two-body interaction. The overall agreement between the calculated and observed nuclear spectroscopic properties of the above mentioned nuclei suggests that the PHFB wave functions generated by fixing χ_{2pn} to reproduce the E_{2^+} are quite reliable in all the four parametrizations. Hence, we proceed to calculate the NTMEs $M_{2\nu}(2^+)$ and half-lives $T^{2\nu}_{1/2}(2^+)$ of $2\nu\beta^-\beta^-$ decay of ^{94,96}Zr, ^{100}Mo, ^{104}Ru, ^{110}Pd, ^{128,130}Te and ^{150}Nd nuclei for the $0^+ \rightarrow 2^+$ transition using same PHFB wave functions.

Table 2.1: Excitation energies E_{J^π} (MeV) of $J^\pi = 2^+$, 4^+ and 6^+ yrast states of ^{94,96}Zr, ^{94,96,100}Mo, ^{100,104}Ru, ^{104,110}Pd, ^{110}Cd, ^{128,130}Te, ^{128,130} Xe, ^{150}Nd and ^{150}Sm nuclei along with the experimental values.

Nuclei		*PPQQ*2	*PPQQHH*2	*PPQQ*1 [1]	*PPQQHH*1 [2]	Experiment [3]
^{94}Zr	χ_{2pp}	0.01585	0.01179	0.0105	0.0105	
	χ_{2pn}	0.03170	0.02358	0.02519	0.02629	
	E_{HFB}	12.8229	15.3503	15.3101	15.2730	
	Q_{HFB}	39.5518	21.1808	18.4660	22.8912	
	E_{2^+}	0.9065	0.9178	0.9182	0.9165	0.9183
	E_{4^+}	2.0559	2.1332	1.9732	1.9657	1.4688
	E_{6^+}	3.3018	3.1486	2.7993	2.8087	
^{94}Mo	χ_{2pp}	0.01264	0.01228	0.0105	0.0105	
	χ_{2pn}	0.02528	0.02456	0.02670	0.02572	
	E_{HFB}	2.0882	2.1995	2.3260	2.3754	
	Q_{HFB}	31.7867	31.5744	31.1458	31.1272	
	E_{2^+}	0.8706	0.8731	0.8715	0.8713	0.8711
	E_{4^+}	1.9875	1.9864	1.9685	1.9682	1.5737
	E_{6^+}	3.3439	3.3520	3.3136	3.3283	2.4234
^{96}Zr	χ_{2pp}	0.0100	0.00976	0.0105	0.0105	
	χ_{2pn}	0.0200	0.01952	0.01717	0.01918	
	E_{HFB}	26.6187	26.5931	26.5599	26.6366	
	Q_{HFB}	0.7819	1.4231	2.4837	2.2329	
	E_{2^+}	1.7508	1.7351	1.7570	1.7541	1.7507
	E_{4^+}	3.5748	3.6415	3.5269	3.6296	3.1202
	E_{6^+}	-	6.6679	9.7261	9.3686	

Table 2.1 continued

Nuclei		$PPQQ2$	$PPQQHH2$	$PPQQ1$ [1]	$PPQQHH1$ [2]	Experiment [3]
^{96}Mo	χ_{2pp}	0.01213	0.01185	0.0105	0.0105	
	χ_{2pn}	0.02426	0.02373	0.02557	0.02472	
	E_{HFB}	11.5533	11.8941	11.8330	12.0681	
	Q_{HFB}	42.1064	41.2955	41.7271	40.7486	
	E_{2^+}	0.7703	0.7631	0.7779	0.7817	0.7782
	E_{4^+}	2.0299	1.9957	2.0373	0.0220	1.6281
	E_{6^+}	3.5750	3.5029	3.5776	3.5300	2.4406
^{100}Mo	χ_{2pp}	0.00983	0.00980	0.0105	0.0105	
	χ_{2pn}	0.01966	0.01960	0.01906	0.01876	
	E_{HFB}	37.9709	38.0434	37.9451	37.1106	
	Q_{HFB}	48.8102	49.4317	49.1981	48.1273	
	E_{2^+}	0.5369	0.5428	0.5356	0.5357	0.5355
	E_{4^+}	1.4636	1.5088	1.4719	1.4766	1.1359
	E_{6^+}	2.6500	2.7605	2.6738	2.6893	
^{100}Ru	χ_{2pp}	0.00960	0.00960	0.0105	0.0105	
	χ_{2pn}	0.01920	0.01920	0.01838	0.01831	
	E_{HFB}	22.9013	22.8684	22.7892	22.8783	
	Q_{HFB}	45.6087	45.5327	45.6559	45.5799	
	E_{2^+}	0.5397	0.5300	0.5395	0.5402	0.5396
	E_{4^+}	1.5576	1.5605	1.5591	1.5847	1.2265
	E_{6^+}	2.8890	2.9247	2.8940	2.9629	2.0777
^{104}Ru	χ_{2pp}	0.01052	0.01035	0.0105	0.0105	
	χ_{2pn}	0.02104	0.02070	0.02110	0.02053	
	E_{HFB}	46.7079	46.9362	46.6736	46.9232	
	Q_{HFB}	63.9737	63.3099	63.9793	63.2818	
	E_{2^+}	0.3595	0.3579	0.3580	0.3578	0.35799
	E_{4^+}	1.1382	1.1388	1.1339	1.1385	0.8885
	E_{6^+}	2.2357	2.2493	2.2280	2.2486	1.5563

Table 2.1 continued

Nuclei		$PPQQ2$	$PPQQHH2$	$PPQQ1$ [1]	$PPQQHH1$ [2]	Experiment [3]
^{104}Pd	χ_{2pp}	0.00840	0.00849	0.0105	0.0105	
	χ_{2pn}	0.01680	0.01698	0.01486	0.01507	
	E_{HFB}	36.6465	36.3157	36.3457	36.3157	
	Q_{HFB}	48.2701	48.6368	48.8491	49.5676	
	E_{2^+}	0.5516	0.5477	0.5552	0.5560	0.5558
	E_{4^+}	1.5486	1.5713	1.5729	1.6138	1.32359
	E_{6^+}	2.8144	2.8956	2.8790	2.9954	2.2498
^{110}Pd	χ_{2pp}	0.00836	0.00828	0.0105	0.0105	
	χ_{2pn}	0.01672	0.01656	0.01417	0.01393	
	E_{HFB}	78.8593	78.6418	78.5153	78.9177	
	Q_{HFB}	56.9670	56.2252	57.3891	56.8090	
	E_{2^+}	0.3789	0.3673	0.3737	0.3738	0.3738
	E_{4^+}	1.1783	1.1429	1.1563	1.1583	0.9208
	E_{6^+}	2.2796	2.2159	2.2254	2.2359	1.5739
^{110}Cd	χ_{2pp}	0.00827	0.00828	0.0105	0.0105	
	χ_{2pn}	0.01654	0.01656	0.01412	0.01414	
	E_{HFB}	66.1444	66.5745	65.8192	65.6705	
	Q_{HFB}	55.1645	56.8164	54.5945	53.2557	
	E_{2^+}	0.6605	0.6477	0.6576	0.6585	0.6577
	E_{4^+}	1.8818	1.8906	1.8709	1.8921	1.5424
	E_{6^+}	3.4054	3.4849	3.3865	3.4728	2.4799
^{128}Te	χ_{2pp}	0.01210	0.01210	0.0105	0.0105	
	χ_{2pn}	0.02420	0.02420	0.02715	0.2692	
	E_{HFB}	70.6782	70.6535	70.3108	70.3044	
	Q_{HFB}	41.4918	41.3659	41.6187	41.3326	
	E_{2^+}	0.7442	0.7435	0.7436	0.7435	0.7432
	E_{4^+}	2.0307	2.0021	2.0458	2.0130	1.4971
	E_{6^+}	3.6888	3.6267	3.7363	3.6647	1.8111

Table 2.1 continued

Nuclei		$PPQQ2$	$PPQQHH2$	$PPQQ1$ [1]	$PPQQHH1$ [2]	Experiment [3]
^{128}Xe	χ_{2pp}	0.0133	0.01250	0.0105	0.0105	
	χ_{2pn}	0.0266	0.02500	0.0360	0.02662	
	E_{HFB}	50.6626	53.1504	46.1115	53.3671	
	Q_{HFB}	61.8717	59.0051	64.5377	57.9407	
	E_{2^+}	0.4390	0.4506	0.4511	0.4420	0.4429
	E_{4^+}	1.3570	1.3737	1.4263	1.3444	1.0329
	E_{6^+}	2.5915	2.6016	2.7976	2.5404	1.7370
^{130}Te	χ_{2pp}	0.0095	0.00982	0.0105	0.0105	
	χ_{2pn}	0.01900	0.01964	0.01801	0.01890	
	E_{HFB}	87.8821	87.2026	88.1680	87.3017	
	Q_{HFB}	31.9527	33.0609	32.1246	33.1466	
	E_{2^+}	0.8407	0.8392	0.8393	0.8395	0.8395
	E_{4^+}	1.7645	1.8019	1.7741	1.8085	1.6325
	E_{6^+}	3.0718	3.1214	3.0833	3.1283	1.8145
^{130}Xe	χ_{2pp}	0.01151	0.01110	0.0105	0.0105	
	χ_{2pn}	0.02302	0.02220	0.02454	0.02281	
	E_{HFB}	68.0574	69.2260	68.1734	69.2404	
	Q_{HFB}	52.5034	50.5020	52.1713	50.3486	
	E_{2^+}	0.5283	0.5366	0.5385	0.5384	0.5361
	E_{4^+}	1.5210	1.5234	1.5496	1.5268	1.2046
	E_{6^+}	2.7326	2.7355	2.7831	2.7400	1.9444
^{150}Nd	χ_{2pp}	0.01071	0.01100	0.0105	0.0105	
	χ_{2pn}	0.02142	0.02200	0.0216	0.2228	
	E_{HFB}	182.4330	181.0039	182.7331	181.4944	
	Q_{HFB}	83.7499	84.7923	83.7452	84.5975	
	E_{2^+}	0.1297	0.1308	0.1307	0.1300	0.13012
	E_{4^+}	0.4288	0.4335	0.4320	0.4305	0.3815
	E_{6^+}	0.8892	0.9025	0.8960	0.8958	

Table 2.1 continued

Nuclei		$PPQQ2$	$PPQQHH2$	$PPQQ1$ [1]	$PPQQHH1$ [2]	Experiment [3]
^{150}Sm	χ_{2pp}	0.0093	0.00933	0.0105	0.0105	
	χ_{2pn}	0.01860	0.01866	0.01745	0.01730	
	E_{HFB}	171.1474	171.0907	170.7875	170.0885	
	Q_{HFB}	72.9427	73.8965	73.4117	73.5946	
	E_{2^+}	0.3335	0.3319	0.3328	0.3359	0.3339
	E_{4^+}	1.0126	1.0164	1.0156	1.0290	0.7733
	E_{6^+}	1.9040	1.9253	1.9185	1.9504	1.2788

References:

[1] Chandra *et al.* (2005), Singh *et al.* (2007)

[2] Chandra *et al.* (2009)

[3] Sakai (1984)

Table 2.2: Comparison of calculated and experimentally observed reduced transition probabilities $B(E2{:}0^+ \rightarrow 2^+)$, β_2 parameters and g factors $g(2^+)$ of ^{94,96}Zr, ^{94,96,100}Mo, ^{100,104}Ru, ^{104,110}Pd, ^{110}Cd, ^{128,130}Te, ^{128,130} Xe, ^{150}Nd and ^{150}Sm nuclei. The $B(E2)$ is calculated in units of e^2b^2 for effective charge $e_p = 1 + e_{eff}$ and $e_n = e_{eff}$. The $g(2^+)$ has been calculated in units of nuclear magneton for$g_l^\pi = 1.0$, $g_l^\nu = 0.0$ and $g_s^\pi = g_s^\nu = 0.60$. Here (a), (b), (c) and (d) denote $PPQQ2$, $PPQQHH2$, $PPQQ1$ and $PPQQHH1$ parametrizations, respectively.

		$B(E2{:}0^+ \rightarrow 2^+)$ (e^2b^2)		β_2		$g(2^+)$ (nm)	
		Theory	Experiment[1]	Theory	Experiment[1]	Theory	Experiment[2]
^{94}Zr	(a)	0.095	0.066±0.014*	0.109	0.090±0.010	0.565	-0.329±0.015[3]
	(b)	0.085	0.081±0.017	0.102		0.068	-0.26±0.06
	(c)[4]	0.081	0.056±0.014	0.100		0.121	-0.05±0.05
	(d)[5]	0.097		0.110		0.112	
^{94}Mo	(a)	0.241	0.203±0.004*	0.164	0.1509±0.0015	0.348	
	(b)	0.237	0.230±0.040	0.163		0.345	
	(c)[4]	0.232	0.270±0.035	0.161		0.343	
	(d)[5]	0.232		0.161		0.343	
^{96}Zr	(a)	0.061	0.055±0.022*	0.085	0.080±0.017	0.324	
	(b)	0.063		0.087		0.320	
	(c)[4]	0.060		0.085		0.254	
	(d)[5]	0.063		0.087		0.297	
^{96}Mo	(a)	0.338	0.271±0.005*	0.192	0.1720±0.0016	0.552	
	(b)	0.323	0.310±0.047	0.188		0.532	
	(c)[4]	0.335	0.302±0.039	0.191		0.563	
	(d)[5]	0.317		0.186		0.535	

Table 2.2 continued

		$B(E2{:}0^+ \to 2^+)$ (e^2b^2)		β_2		$g(2^+)$ (nm)	
		Theory	Exp.[1]	Theory	Exp.[1]	Theory	Exp.[2]
^{100}Mo	(a)	0.512	0.516±0.010*	0.230	0.2309±0.0022	0.490	0.34±0.18
	(b)	0.527	0.511±0.009	0.233		0.519	
	(c)[4]	0.515	0.526±0.026	0.231		0.477	
	(d)[5]	0.493		0.226		0.467	
^{100}Ru	(a)	0.490	0.490±0.005*	0.215	0.2148±0.0011	0.363	0.47±0.06
	(b)	0.487	0.493±0.003	0.214		0.371	0.51±0.07
	(c)[4]	0.488	0.494±0.006	0.214		0.355	
	(d)[5]	0.484		0.214		0.363	
^{104}Ru	(a)	0.911	0.820±0.012*	0.285	0.2707±0.0020	0.339	0.41±0.05
	(b)	0.892	0.93±0.06	0.282		0.346	
	(c)[4]	0.912	1.04±0.16	0.285		0.339	
	(d)[5]	0.890		0.282		0.345	
^{104}Pd	(a)	0.570	0.535±0.035*	0.216	0.209±0.007	0.483	0.46±0.04
	(b)	0.578	0.61±0.09	0.217		0.491	0.40±0.05
	(c)[4]	0.571	0.535±0.035	0.216		0.439	0.38±0.04
	(d)[5]	0.586		0.219		0.458	
^{110}Pd	(a)	0.621	0.870±0.040*	0.217	0.257±0.006	0.514	0.37±0.03
	(b)	0.611	0.780±0.120	0.215		0.525	0.35±0.03
	(c)[4]	0.614	0.820±0.080	0.216		0.478	
	(d)[5]	0.604		0.214		0.489	

Table 2.2 continued

		$B(E2{:}0^+ \rightarrow 2^+)$ (e^2b^2)		β_2		$g(2^+)$ (nm)	
		Theory	Exp.[1]	Theory	Exp.[1]	Theory	Exp.[2]
^{110}Cd	(a)	0.582	0.450±0.020*	0.201	0.1770±0.0039	0.386	0.31±0.07
	(b)	0.619	0.504±0.040	0.208		0.390	0.285±0.055
	(c)[4]	0.548	0.467±0.019	0.196		0.358	
	(d)[5]	0.522		0.191		0.377	
^{128}Te	(a)	0.378	0.383±0.006*	0.135	0.1363±0.0011	0.516	0.35±0.04
	(b)	0.383	0.380±0.009	0.136		0.526	0.31±0.04
	(c)[4]	0.381	0.378±0.007	0.136		0.514	
	(d)[5]	0.384		0.136		0.526	
^{128}Xe	(a)	0.778	0.750±0.040*	0.187	0.1836±0.0049	0.410	0.41±0.07
	(b)	0.734	0.790±0.040	0.182		0.430	0.31±0.03
	(c)[4]	0.819	0.890±0.230	0.192		0.400	
	(d)[5]	0.729		0.181		0.439	
^{130}Te	(a)	0.288	0.295±0.007*	0.117	0.1184±0.0014	0.682	0.33±0.08
	(b)	0.304	0.290±0.011	0.120		0.668	0.29±0.06
	(c)[4]	0.289	0.260±0.050	0.117		0.679	
	(d)[5]	0.304		0.120		0.667	
^{130}Xe	(a)	0.632	0.65±0.05*	0.167	0.169±0.007	0.461	0.38±0.07
	(b)	0.606	0.631±0.048	0.163		0.476	0.31±0.04
	(c)[4]	0.624	0.640±0.160	0.166		0.463	
	(d)[5]	0.605		0.163		0.478	

Table 2.2 continued

		$B(E2{:}0^+ \rightarrow 2^+)$ (e^2b^2)		β_2		$g(2^+)$ (nm)	
		Theory	Exp.[1]	Theory	Exp.[1]	Theory	Exp.[2]
^{150}Nd	(a)	2.581	2.760±0.040*	0.276	0.2853±0.0021	0.637	0.422±0.039
	(b)	2.640	2.640±0.080	0.279		0.621	0.322±0.009
	(c)[4]	2.580	2.670±0.100	0.276		0.636	
	(d)[5]	2.632		0.279		0.622	
^{150}Sm	(a)	2.010	1.350±0.030*	0.236	0.1931±0.0021	0.578	0.385±0.027
	(b)	2.088	1.470±0.090	0.240		0.593	0.411±0.032
	(c)[4]	2.056	1.440±0.150	0.238		0.592	
	(d)[5]	2.098		0.241		0.604	

*Average $B(E2)$ values [Raman *et al.* (2001)]

References:

[1] Raman *et al.* (2001)

[2] Raghavan (1989)

[3] Speidel *et al.* (2002)

[4] Chandra *et al.* (2005), Singh *et al.* (2007)

[5] Chandra *et al.* (2009)

Chapter 3

$2\nu\beta^-\beta^-$ decay of ^{94,96}Zr, ^{100}Mo, ^{104}Ru, ^{110}Pd, ^{128,130}Te and ^{150}Nd isotopes for the $0^+ \rightarrow 2^+$ transition

The study of $2\nu\beta\beta$ decay is quite interesting from the nuclear structure point of view. The $2\nu\beta^-\beta^-$ decay has been experimentally observed in case of eleven nuclei, namely ^{48}Ca, ^{76}Ge, ^{82}Se, ^{96}Zr, ^{100}Mo, ^{116}Cd, ^{128,130}Te, ^{136}Xe, ^{150}Nd and ^{238}U out of 35 possible candidates for the $0^+ \rightarrow 0^+$ transition [Tretyak and Zdesenko (1995), (2002)] and the NTMEs $M_{2\nu}(0^+)$ extracted from the observed experimental data are available. It is quite a formidable task to understand the observed quenching of the NTMEs $M_{2\nu}$ and reproduce them theoretically. In spite of the best theoretical efforts over the last 30 years, the complete solution of the problem is still unsatisfactory. We are also not going to give a complete solution of the problem. However, we aim at a systematic attempt based on the basic principles of the nuclear many body theory.

In the allowed approximation, the $0^+ \rightarrow 1^+$ transition is much less probable than the $0^+ \rightarrow 0^+$ and $0^+ \rightarrow 2^+$ transitions. The observation of $0\nu\beta\beta$ decay for the $0^+ \rightarrow 2^+$ transition can distinguish between the mechanisms involving the mass of the Majorana neutrinos and the right handed currents [Tomoda (1991)]. The theoretical implications and experimental aspects of the ground to the excited 2^+ state transition of the $\beta\beta$ decay have been excellently reviewed over past years [Suhonen and Civitarese (1998), Barabash (2017)]. Interestingly, it has been shown by Barabash *et al.* (2007) that the decay rates, energy spectra and angular distributions of the $0^+ \rightarrow 0^+$ and $0^+ \rightarrow 2^+$ transitions can be employed to extract limits on the assumed admixture of fermionic and bosonic components of neutrinos.

The $0^+ \rightarrow 2^+$ transition of $2\nu\beta^-\beta^-$ decay has not been experimentally observed so far and only limits are available. All the available experimental limits on half-life $T^{2\nu}_{1/2}(2^+)$ have been presented in Table 3.1. The marked variation in the theoretically calculated NTMEs $M_{2\nu}(2^+)$ for the $0^+ \rightarrow 2^+$ transition using different nuclear models is a general feature [Suhonen and Civitarese (1998)]. For example, the available results for $M_{2\nu}(2^+)$ of ^{96}Zr show that the calculated NTMEs within QRPA [Barabash *et al.* (1996), Raduta and Raduta (2007), Unlu (2013), (2014)], RQRPA(WS) [Toivanen and Suhonen (1997)], RQRPA (AWS) [Toivanen and Suhonen (1997)], and SRPA(WS) [Stoica and Mihut (1995),(1996) differ by a factor of 341. Hence, the observation of the $0^+ \rightarrow 2^+$ transition of $2\nu\beta^-\beta^-$ decay can constrain the validity of different nuclear models employed in the calculation of NTMEs. Alternatively, a reliable theoretical prediction will supplement the experimental designing and planning to study this particular mode of $2\nu\beta^-\beta^-$ decay.

Employing the pnQRPA model, it has been shown by Raduta *et al.* (2007) that the

inclusion of deformation in the mean field can reduce the NTMEs $M_{2\nu}(2^+)$ up to a factor of 341. In the PHFB model, the pairing and deformation degrees of freedom are treated simultaneously on equal footing. However, the structure of intermediate odd-odd nuclei can not be studied in the present version of the PHFB model. In spite of this limitation, the PHFB model has been successfully applied to study the $0^+ \rightarrow 0^+$ transition of $2\nu\beta^-\beta^-$ decay [Chandra *et al.* (2005), Singh *et al.* (2007)] in conjunction with the summation method [Civitarese and Suhonen (1993)]. This has motivated us to apply the PHFB model to study the $0^+ \rightarrow 2^+$ transition of $2\nu\beta^-\beta^-$ decay of ^{94,96}Zr, ^{100}Mo, ^{104}Ru, ^{110}Pd, ^{128,130}Te and ^{150}Nd isotopes in the mass range $90 \leq A \leq 150$.

The present chapter is organized as follows. In Section 3.1, we outline the theoretical formalism to calculate the half life $T^{2\nu}_{1/2}(2^+)$ of $2\nu\beta^-\beta^-$ decay. In Section 3.2, the results of $2\nu\beta^-\beta^-$ decay of ^{94,96}Zr, ^{100}Mo, ^{104}Ru, ^{110}Pd, ^{128,130}Te and ^{150}Nd nuclei for the $0^+ \rightarrow 2^+$ transition are given and discussed. The final conclusions are given in Section 3.3.

3.1 Theoretical framework

The theoretical formalism to calculate the half-life for the $0^+ \rightarrow 2^+$ transition of $2\nu\beta^-\beta^-$ decay $T^{2\nu}_{1/2}(2^+)$ in 2n mechanism has been given in refs. [Tomoda (1991), Haxton and Stephenson Jr. (1984), Doi *et al.* (1985)]. Using the summation method [Civitarese and Suhonen (1993)], the $0^+ \rightarrow 0^+$ and $0^+ \rightarrow 2^+$ transitions of $2\nu\beta^-\beta^-$ mode has already been studied by Hirsch *et al.* in the pseudo-SU(3) model [Hirsch *et al.* (1995), (1995*a*)]. Presently, the summation method applied to the study of $0^+ \rightarrow 0^+$ transition of $2\nu\beta^-\beta^-$ decay within the PHFB model [Chandra *et al.* (2005), Singh *et al.* (2007)] has been

extended to the $0^+ \rightarrow 2^+$ transition. We briefly outline steps to derive the $2\nu\beta^-\beta^-$ decay rate formula following the notations of Doi *et al.* (1985).

3.1.1 Effective Hamiltonian for β^- decay

In left-right symmetric models, the charged-current interaction Lagrangian L_{LR} due to the addition of extra gauge boson W_R is given by

$$L_{LR} = \frac{g}{2\sqrt{2}} \left[j_L^{\mu} W_{L\mu} + j_R^{\mu} W_{R\mu} \right] + h.c. \tag{3.1}$$

where the left and right handed weak leptonic $V \pm A$ currents are written as

$$j_L^{\mu} = \overline{e}\gamma^{\mu} \left(1 - \gamma_5\right) \nu_{eL} \qquad\qquad j_R^{\mu} = \overline{e}\gamma^{\mu} \left(1 + \gamma_5\right) \nu_{eR}^{'} \tag{3.2}$$

with

$$\nu_{eL} = \sum_i U_{ei} N_{ji} \qquad \nu_{eR}^{'} = \sum_i V_{ei} N_{iR} \tag{3.3}$$

The mixing matrices U and V satisfy the following orthonormality conditions.

$$\sum_i |U_{ei}|^2 = 1 \qquad \sum_i |V_{ei}|^2 = 1 \qquad \sum_i U_{ei} V_{ei} = 0 \tag{3.4}$$

The gauge bosons W_L and W_R are related to mass eigenstates W_1 and W_2 with masses M_1 and M_2 respectively by

$$\begin{pmatrix} W_L \\ W_R \end{pmatrix} = \begin{pmatrix} \cos\zeta & \sin\zeta \\ -\sin\zeta & \cos\zeta \end{pmatrix} \begin{pmatrix} W_1 \\ W_2 \end{pmatrix} \tag{3.5}$$

Including hadronic currents, the Lagrangian L_{LR} leads to the weak interaction effective Hamiltonian H_W given by

$$H_W = \left(\frac{G}{\sqrt{2}}\right) \left[j_{L\mu} J_L^{\mu\dagger} + \kappa j_{L\mu} J_R^{\mu\dagger} + \eta j_{R\mu} J_L^{\mu\dagger} + \lambda j_{R\mu} J_R^{\mu\dagger} \right] + h.c. \tag{3.6}$$

where

$$\frac{G}{\sqrt{2}} = \frac{g^2}{8M_1^2}\left[\cos^2\zeta + \left(\frac{M_1}{M_2}\right)^2 \sin^2\zeta\right] \tag{3.7}$$

$$\lambda = \frac{\left[\left(\frac{M_1}{M_2}\right)^2 + \tan^2\zeta\right]}{\left[1 + \left(\frac{M_1}{M_2}\right)^2 \tan^2\zeta\right]} \tag{3.8}$$

and

$$\eta = \kappa = \frac{\left[1 - \left(\frac{M_1}{M_2}\right)^2\right]\tan\zeta}{\left[1 + \left(\frac{M_1}{M_2}\right)^2 \tan^2\zeta\right]} \tag{3.9}$$

Here, the coupling constants κ, η and λ are small ($\ll 1$) parameters and $G = 1.16637\times10^{-5}$ GeV^{-2}. The left and right handed weak $V \pm A$ hadronic currents are given by

$$J_L^{\mu\dagger} = g_V \overline{u}\gamma^\mu (1-\gamma_5)\, d \qquad J_R^{\mu\dagger} = g'_V \overline{u}\gamma^\mu (1+\gamma_5)\, d \tag{3.10}$$

where

$$g_V = \cos\theta_c \qquad g'_V = e^{i\alpha}\cos\theta'_c \tag{3.11}$$

In Eq. (3.11), the θ_c and θ'_c are the Cabibbo-Kobayashi-Maskawa (CKM) mixing angles for the left- and right-handed d and s quarks. The CP violating phase α is due to both the mixing of right handed quarks and the mixing of left and right gauge bosons.

In the nonrelativistic impulse approximation, the left and right handed hadronic currents for nuclear $\beta^-\beta^-$ decay in $V \pm A$ forms are given by

$$J_L^{\mu^\dagger}(x) = \sum_{n=1}^{A}\left[(g_V - g_A C_n)g^{\mu 0} + (g_A\sigma_n^k - g_V \mathbf{D}_n^k)g^{\mu k}\right]\delta(\mathbf{x} - \mathbf{r}_n)\,\tau_n^+ \tag{3.12}$$

$$J_R^{\mu^\dagger}(x) = \sum_{n=1}^{A}\left[(g_V + g_A C_n)g^{\mu 0} + (-g_A\sigma_n^k - g_V \mathbf{D}_n^k)g^{\mu k}\right]\delta(\mathbf{x} - \mathbf{r}_n)\,\tau_n^+ \tag{3.13}$$

The nuclear recoil terms C_n and $\mathbf{D}_n$ are defined as follows

$$C_n = \frac{1}{2M}\left[(\mathbf{P}_n + \mathbf{P}'_n)\cdot\boldsymbol{\sigma}_n - \left(\frac{g_P}{g_A}\right)\ (E_n - E'_n)\,\boldsymbol{\sigma}_n\cdot\mathbf{Q}_n\right] \tag{3.14}$$

$$\mathbf{D}_n = \frac{1}{2M}\left[(\mathbf{P}_n + \mathbf{P}'_n) - i\left(1 - 2M\left(\frac{g_W}{g_V}\right)\right)\boldsymbol{\sigma}_n\times\mathbf{Q}_n\right] \tag{3.15}$$

where $\mathbf{Q}_n = \mathbf{P}_n - \mathbf{P}'_n$. The g_V, g_A, g_P and g_W are vector, axial vector, pseudoscalar and weak magnetism terms. At $q^2 = 0$,

$$g_V(0) = 1.0 \qquad g_A(0) = 1.25 \qquad \frac{g_p}{g_A} = \frac{2M_P}{m_\pi^2} \tag{3.16}$$

where M_P and m_π are the proton and pion masses. By the CVC hypothesis $g_W(0) = \kappa_\beta/2M$ and $\kappa_\beta = 3.70$, where M and κ_β are the mass and isovector anomalous magnetic moment of nucleons respectively.

3.1.2 Decay rate of $2\nu\beta^-\beta^-$ mode for the $0^+ \to 2^+$ transition

The half life for the $0^+ \to 2^+$ transition of $2\nu\beta^-\beta^-$ decay $T^{2\nu}_{1/2}(2^+)$ in 2n mechanism is given by

$$\left[T^{2\nu}_{1/2}(2^+)\right]^{-1} = G_{2\nu}(2^+)\left|M_{2\nu}(2^+)\right|^2 \tag{3.17}$$

where the integrated kinematical factor $G_{2\nu}(2^+)$ has been calculated with good accuracy [Pahomi *et al.* (2014)]. The model dependent NTME $M_{2\nu}(2^+)$ is given by

$$M_{2\nu}(2^+) = \sqrt{\frac{1}{3}}\sum_N \frac{\left\langle 2^+_F \left\| \sigma\tau^+ \right\| 1^+_N \right\rangle \left\langle 1^+_N \left\| \sigma\tau^+ \right\| 0^+_I \right\rangle}{\left[E_0 + E_N - E_I\right]^3} \tag{3.18}$$

where

$$E_0 = \frac{1}{2}(E_I - E_F) = \frac{1}{2}Q_{\beta\beta} + m_e \tag{3.19}$$

Presently, the summation over the intermediate states is performed using the summation method [Civitarese and Suhonen (1993)].

The energy denominator in Eq. (3.18) and $x_N = (E_N - E_I)/E_0$ are always positive. Using

$$[E_0 + E_N - E_I]^{-3} = \frac{1}{2}\frac{\partial^2}{\partial E_0^2}[E_0 + E_N - E_I]^{-1}$$

and the summation method given by Civitarese and Suhonen (1993), the Eq. (3.18) can be written as

$$M_{2\nu}(2^+) = \sqrt{\frac{1}{3}}\frac{1}{2}\frac{\partial^2}{\partial E_0^2}\sum_N \left\langle 2_F^+ \left| \mathbf{\Gamma} \right| N \right\rangle \left\langle N \left| \mathbf{\Gamma} \right| 0_I^+ \right\rangle \int_0^\infty e^{-t(1+x_N)}dt \tag{3.20}$$

where the Gamow-Teller (GT) operator $\mathbf{\Gamma} = \boldsymbol{\sigma}\tau^+$. We change the variable of integration t to $\omega = t/E_0$, which is allowed since $E_0 > 0$. Replacing $e^{-\omega E_N}\ |N\rangle$ by $e^{-\omega H}\ |N\rangle$ and $e^{-\omega E_I}\ \left|0_I^+\right\rangle$ by $e^{-\omega H}\ \left|0_I^+\right\rangle$, which is also allowed since the intermediate states $|N\rangle$ and the initial states $\left|0_I^+\right\rangle$ are eigen states of the nuclear Hamiltonian H, one obtains after summing over all the intermediate states

$$M_{2\nu}(2^+) = \sqrt{\frac{1}{3}}\frac{1}{2}\frac{\partial^2}{\partial E_0^2}\int_0^\infty \left\langle 2_F^+ \left| \mathbf{\Gamma} e^{-\omega H}\mathbf{\Gamma} e^{\omega H} \right| 0_I^+ \right\rangle e^{-\omega E_0}d\omega \tag{3.21}$$

Using the Baker-Hausdorff lemma, one can make the multiple commutators expansion as

$$e^{-\omega H}\mathbf{\Gamma} e^{\omega H} = \sum_{k=0}^{\infty}\frac{(-1)^k\omega^k}{k!}[H,[H,.....,\ [H,\mathbf{\Gamma}].....]]^{(k\ times)} \tag{3.22}$$

The integral given by Eq. (3.21) can be performed resulting in

$$\begin{aligned} M_{2\nu}(2^+) &= \sqrt{\frac{1}{3}}\frac{1}{2}\frac{\partial^2}{\partial E_0^2}\frac{1}{E_0}\left\langle 0_F^+ \left| \sum_\mu (-1)^\mu \Gamma_{-\mu}F_\mu \right| 0_I^+ \right\rangle \\ &= \sqrt{\frac{1}{3}}\frac{1}{E_0^3}\left\langle 0_F^+ \left| \sum_\mu (-1)^\mu \Gamma_{-\mu}F_\mu \right| 0_I^+ \right\rangle \end{aligned} \tag{3.23}$$

where Γ_μ is given by

$$\Gamma_\mu = \sigma_\mu \tau^+ \tag{3.24}$$

and

$$F_\mu = \sum_{\lambda=0}^{\infty} \frac{(-1)^\lambda}{E_0^\lambda} D_\lambda \Gamma_\mu \tag{3.25}$$

with

$$D_\lambda \Gamma_\mu = [H, [H, ..., [H, \Gamma_\mu] .....]^{(\lambda \text{ times})} \tag{3.26}$$

The Eq. (3.23) can be further simplified, when the GT operator commutes with the effective two-body interaction. In the case of pseudo-SU(3) model [Castaños *et al.*(1994), Hirsch *et al.*(1995), Ceron *et al.*(1999)], the GT operator commutes with the two-body interaction and the energy denominator is a well-defined quantity without any free parameter. It has been evaluated exactly for the $2\nu\beta^-\beta^-$ of ^{150}Nd [Hirsch *et al.*(1995*a*)] in the context of pseudo-SU(3) scheme.

3.1.3 NTME $M_{2\nu}(2^+)$ in the PHFB model

In the present work, we use a Hamiltonian with *PPQQHH* type of effective two-body interaction, which does not commute with the GT operator. Hence, the energy denominator is not a well-defined quantity. However, the violation of isospin symmetry for the *QQHH* part of our model Hamiltonian is negligible as is evident from the parameters of the two-body interaction given in Section 2.3. Further, the violation of isospin symmetry for the pairing part of the two-body interaction is presumably small. With these assumptions, the NTME $M_{2\nu}(2^+)$ of $2\nu\beta^-\beta^-$ decay for the $0^+ \rightarrow 2^+$ transition in the PHFB

model in conjunction with the summation method can be derived as follows. Using

$$\begin{aligned}\left[H, a_\pi^\dagger a_\nu\right] &= \left[H_\pi + H_\nu, a_\pi^\dagger a_\nu\right] \\ &= \sum_{nljm} \left(\varepsilon_\pi - \varepsilon_\nu\right) a_\pi^\dagger a_\nu \end{aligned} \tag{3.27}$$

where H_α consists of one-body part of the Hamiltonian only,

$$H_\alpha = \sum_{nljm} \varepsilon_\alpha(n,l,j) a_\alpha^\dagger(nljm) a_\alpha(nljm) \tag{3.28}$$

one obtains

$$\begin{aligned} D_\lambda \Gamma_\mu &= \left[H_\pi + H_\nu, \left[H_\pi + H_\nu, ..., \left[H_\pi + H_\nu, \Gamma_\mu\right] .....\right]\right]^{(\lambda \text{ times})} \\ &= \sum_{nljm} \left[\varepsilon(n_\pi, l_\pi, j_\pi) - \varepsilon(n_\nu, l_\nu, j_\nu)\right]^\lambda \sigma_\mu \tau^+ \end{aligned} \tag{3.29}$$

and F_μ is written as

$$\begin{aligned} F_\mu &= \sum_{\lambda=0}^{\infty} \frac{(-1)^\lambda}{E_0^\lambda} D_\lambda \Gamma_\mu \\ &= \sum_{\pi\nu} \sum_{\lambda=0}^{\infty} \left(\frac{-1}{E_0}\right)^\lambda \left[\varepsilon(n_\pi, l_\pi, j_\pi) - \varepsilon(n_\nu, l_\nu, j_\nu)\right]^\lambda \sigma_\mu \tau^+ \\ &= \sum_{\pi\nu} \frac{E_0^3}{\left[E_0 + \varepsilon(n_\pi, l_\pi, j_\pi) - \varepsilon(n_\nu, l_\nu, j_\nu)\right]^3} \sigma_\mu \tau^+ \end{aligned} \tag{3.30}$$

and the Eq. (3.21) can be further simplified to

$$M_{2\nu}(2^+) = \sqrt{5} \sum_{\pi,\nu} \frac{\left\langle 2_F^+ \left\| \left[\boldsymbol{\sigma} \otimes \boldsymbol{\sigma}\right]^{(2)} \tau^+ \tau^+ \right\| 0_I^+ \right\rangle}{\left[E_0 + \varepsilon(n_\pi, l_\pi, j_\pi) - \varepsilon(n_\nu, l_\nu, j_\nu)\right]^3} \tag{3.31}$$

and this expression is the same as that of Hirsch *et al.* [1995*a*]. We have evaluated the energy denominator as follows. With the assumption that the difference in single particle energies of protons in the intermediate nucleus and neutrons in the parent nucleus is

mainly due to the difference in Coulomb energies, one obtains

$$\varepsilon(n_\pi, l_\pi, j_\pi) - \varepsilon(n_\nu, l_\nu, j_\nu) = \begin{cases} \Delta_C & for \quad n_\nu = n_\pi, l_\nu = l_\pi, j_\nu = j_\pi \\ \Delta_C + \Delta E_{s.o.splitting} & for \quad n_\nu = n_\pi, l_\nu = l_\pi, j_\nu \neq j_\pi \end{cases}, \tag{3.32}$$

where the Coulomb energy difference Δ_C is given by Bohr and Mottelson (1998).

$$\Delta_C = \frac{0.70}{A^{1/3}} \left[(2Z+1) - 0.76 \left\{ (Z+1)^{4/3} - Z^{4/3} \right\} \right] \; MeV \tag{3.33}$$

Finally, one obtains the following expression for the NTME $M_{2\nu}(2^+)$ of $2\nu\beta^-\beta^-$ decay for the $0^+ \rightarrow 2^+$ transition.

$$\begin{aligned} M_{2\nu}(2^+) &= \sum_{\pi,\nu} \frac{\langle \Psi_{00}^{J_f=2} || [\boldsymbol{\sigma} \otimes \boldsymbol{\sigma}]^{(2)} \tau^+ \tau^+ || \Psi_{00}^{J_i=0} \rangle}{[E_0 + \varepsilon(n_\pi, l_\pi, j_\pi) - \varepsilon(n_\nu, l_\nu, j_\nu)]^3} \\ &= \left[n_{(Z,N)}^{Ji=2} n_{(Z+2,N-2)}^{J_f=0} \right]^{-1/2} \int_0^\pi n_{(Z,N),(Z+2,N-2)}(\theta) \\ &\quad \times \sum_\mu \begin{bmatrix} J_i & 2 & J_f \\ -\mu & \mu & 0 \end{bmatrix} d_{\mu 0}^{J_i}(\theta) \\ &\quad \times \sum_{\alpha\beta\gamma\delta} \frac{\left\langle \alpha\beta \left| [\boldsymbol{\sigma} \otimes \boldsymbol{\sigma}]^{(2)} \tau^+ \tau^+ \right| \gamma\delta \right\rangle}{[E_0 + \varepsilon_\alpha(n_\pi, l_\pi, j_\pi) - \varepsilon_\gamma(n_\nu, l_\nu, j_\nu)]^3} \\ &\quad \times \sum_{\varepsilon\eta} \left[\left(1 + F_{Z,N}^{(\pi)}(\theta) f_{Z+2,N-2}^{(\pi)*} \right) \right]_{\varepsilon\alpha}^{-1} \left(f_{Z+2,N-2}^{(\pi)*} \right)_{\varepsilon\beta} \\ &\quad \times \left[\left(1 + F_{Z,N}^{(\nu)}(\theta) f_{Z+2,N-2}^{(\nu)*} \right) \right]_{\gamma\eta}^{-1} \left(F_{Z,N}^{(\nu)*} \right)_{\eta\delta} sin\theta d\theta \end{aligned} \tag{3.34}$$

where

$$n^J = \int_0^\pi \left[det \left(1 + F^{(\pi)} f^{(\pi)\dagger} \right) \right]^{1/2} \left[det \left(1 + F^{(\nu)} f^{(\nu)\dagger} \right) \right]^{1/2} d_{00}^J(\theta) sin(\theta) d\theta \tag{3.35}$$

and

$$n_{(Z,N),(Z+2,N-2)}(\theta) = \left[det \left(1 + F_{Z,N}^{(\nu)} f_{Z+2,N-2}^{(\nu)\dagger} \right) \right]^{1/2} \times \left[det \left(1 + F_{Z,N}^{(\pi)} f_{Z+2,N-2}^{(\pi)\dagger} \right) \right]^{1/2} \tag{3.36}$$

The $\pi(\nu)$ represents the proton (neutron) of nuclei involved in the $2\nu\beta^-\beta^-$ decay process. The matrices $f_{Z,N}$ and $F_{Z,N}(\theta)$ are given by

$$f_{Z,N} = \sum_i C_{ij_\alpha,m_\alpha} C_{ij_\beta,m_\beta} \left(v_{im_\alpha}/u_{im_\alpha}\right) \delta_{m_\alpha,-m_\beta} \tag{3.37}$$

$$F_{Z,N}(\theta) = \sum_{m'_\alpha m'_\beta} d^{j_\alpha}_{m_\alpha,m'_\alpha}(\theta) d^{j_\beta}_{m_\beta,m'_\beta}(\theta) f_{j_\alpha m'_\alpha, j_\beta m'_\beta} \tag{3.38}$$

The results of PHFB calculations are summarized by amplitudes (u_{im}, v_{im}) and expansion coefficients $C_{ij,m}$. The required NTME $M_{2\nu}$ is calculated as follows. In the first step, matrices $f_{Z,N}$ and $F_{Z,N}(\theta)$ given by Eqs. (3.37) and (3.38) are setup for the nuclei involved in the $2\nu\beta^-\beta^-$ decay making use of 20 Gaussian quadrature points in the range $(0, \pi)$. Finally, the required NTME can be calculated in a straightforward manner using the Eq. (3.34). As each proton-neutron excitation is considered according to its spin-flip or non–spin-flip character, the use of the summation method in the present context goes beyond the closure approximation. The spin-orbit splitting is explicitly included in the energy denominator, and hence, the PHFB formalism in conjunction with the summation method goes beyond that previously employed in the pseudo SU(3) model [Hirsch *et al.* (1995), (1995*a*)].

3.1.4 Phase space factors for $2\nu\beta^-\beta^-$ decay the for $0^+ \rightarrow 2^+$ transition

In the following, we give a brief discussion of the theoretical formalism to calculate the phase space factors of $2\nu\beta^-\beta^-$ decay for $0^+ \rightarrow 2^+$ transitions. The detailed derivation of these formulae are given by Doi *et al.* (1985), (1992), Suhonen and Civitarese (1998) and references there in.

The phase space factors of $2\nu\beta^-\beta^-$ decay for the $0^+ \rightarrow 2^+$ transition is given by

$$\begin{aligned} G_{2\nu}(2^+) &= \frac{2(Gg_A)^4}{448\pi^7 m_e^2 \ln(2)} \int_{m_e}^{T+m_e} F_0\left(Z,\varepsilon_1\right) p_1\varepsilon_1 I^{(2)}\left(T,\varepsilon_1\right) d\varepsilon_1 \\ &= g_{2\nu}(2^+) \int_{m_e}^{T+m_e} F_0\left(Z,\varepsilon_1\right) p_1\varepsilon_1 I^{(2)}\left(T,\varepsilon_1\right) d\varepsilon_1 \end{aligned} \tag{3.39}$$

where g_A is the axial vector coupling constant and

$$g_{2\nu}(2^+) = \frac{2(Gg_A)^4}{448\pi^7 m_e^2 \ln(2)} \tag{3.40}$$

$$I^{(2)}\left(T,\varepsilon_1\right) = \int_{m_e}^{T+2m_e-\varepsilon_1} F_0\left(Z,\varepsilon_2\right) p_2\varepsilon_2 \left(\varepsilon_1-\varepsilon_2\right)^2 \left(T+2-\varepsilon_1-\varepsilon_2\right)^7 d\varepsilon_2 \tag{3.41}$$

with $G = 1.16637 \times 10^{-5}\ GeV^{-2}$ and $\alpha = 1/137.06$. Here $\varepsilon_k = \sqrt{p_k^2 + m_e^2}$ is the energy of k^{th} electron. The Fermi function $F_0\left(Z,\varepsilon\right)$ can be approximated as

$$F_0\left(Z,\varepsilon\right) = \frac{4}{\left[\Gamma\left(2\gamma_1+1\right)\right]^2} \left(2pR_A\right)^{2(\gamma_1-1)} \left|\Gamma\left(\gamma_1+iy\right)\right|^2 e^{\pi y} \tag{3.42}$$

where

$$\gamma_k = \sqrt{k^2-\left(\alpha Z\right)^2} \qquad\qquad y = \alpha Z\varepsilon/p \tag{3.43}$$

and the complex gamma function is evaluated using the relation

$$\left|\Gamma\left(\alpha+i\beta\right)\right| = \frac{\Gamma\left(1+\alpha\right)}{\alpha} \prod_{n=0}^{\infty} \left[1+\frac{\beta^2}{\left(\alpha+n\right)^2}\right]^{-\frac{1}{2}} \tag{3.44}$$

Recently the phase space factors $G_{2\nu}(2^+)$ have been calculated by Pahomi *et al.* (2014) using exact Dirac wave functions of electron including finite nuclear size and screening effects.

3.2 Results and discussions

In Table 3.2, the NTMEs $M_{2\nu}(2^+)$ calculated with wave functions generated with four different parametrizations of effective two-body interactions, namely *PPQQ*1, *PPQQHH*1, *PPQQ*2, *PPQQHH*2, are presented. Although, there are only a set of four NTMEs $M_{2\nu}(2^+)$ for a statistical analysis, the estimated average NTMEs $\overline{M}_{2\nu}(2^+)$ and uncertainties $\Delta\overline{M}_{2\nu}(2^+)$ are given in the same Table 3.2. To calculate the uncertainty, a statistical analysis has been done in the following manner. The mean and standard deviation are defined for a finite series of calculations as

$$\overline{M}_i = \frac{\sum_{k=1}^{N} M_i^k}{N} \tag{3.45}$$

and

$$\Delta\overline{M}_i = \frac{1}{\sqrt{N-1}} \left[\sum_{k=1}^{N} \left(\overline{M}_i - M_i^k \right)^2 \right]^{1/2} \tag{3.46}$$

The Eqs. (3.45) and (3.46) define the best estimate of the mean and standard deviation for a Gaussian distribution. The maximum uncertainty $\Delta\overline{M}_{2\nu}(2^+)$ in the average NTMEs $\overline{M}_{2\nu}(2^+)$ turns out to be about 45%, which implies that the NTMEs $M_{2\nu}(2^+)$ are highly sensitive to the deformation content of the intrinsic wave functions. The phase space factors $G_{2\nu}(2^+)$ have been calculated by Pahomi *et al.* (2014) for most of the prospective $2\nu\beta^-\beta^-$ emitters. However, the $G_{2\nu}(2^+)$ of ^{94}Zr and ^{104}Ru isotopes are not available. We calculate them by adopting the prescription of Suhonen and Civitarese (1998) using axial vector coupling constant $g_A = 1.2701$ Beringer *et al.* (2012). The calculated $G_{2\nu}(2^+)$ for the $0^+ \rightarrow 2^+$ transition of $2\nu\beta^-\beta^-$ decay of ^{94}Zr and ^{104}Ru are 6.801×10^{-30} y^{-1} and 9.625×10^{-25} y^{-1}, respectively.

As already mentioned, it has been observed that the inclusion of deformation in the

mean field can reduce the NTMEs $M_{2\nu}(2^+)$ calculated in the pnQRPA model up to a factor of 341 [Raduta and Raduta (2007)]. In Table 3.3, we present the excitation energies E_{2^+}, quadrupole moments $Q(2^+)$ of daughter nuclei along, Q-values of $0^+ \rightarrow 2^+$ transition Q_{2^+} and the $G_{2\nu}(2^+)$. According to the Grodzin's rule [Grodzins (1962)], the excitation energies E_{2^+} and quadrupole moments $Q(2^+)$ are inversely related. Although, a smaller E_{2^+} can give a higher Q-value Q_{2^+} resulting in a larger phase space factor, the NTMEs $M_{2\nu}(2^+)$ are reduced due to a larger $Q(2^+)$. Thus, the $0^+ \rightarrow 2^+$ transition is intrinsically suppressed due to the nuclear structure effects in addition to the cubic dependence of the energy denominator.

A large number of experimental and theoretical studies have been carried out for the $0^+ \rightarrow 2^+$ transition of $2\nu\beta^-\beta^-$ decay. Over the past years, the $0^+ \rightarrow 2^+$ transition of $2\nu\beta^-\beta^-$ decay of ^{94}Zr [Norman and Meekhof (1987), Dokania *et al.* (2017)], ^{96}Zr [Barabash *et al.* (1996), Arpesella *et al.* (1994)], ^{100}Mo [N. Kudomi *et al.* (1992), Blum *et al.* (1992), Barabash *et al.* (1993), Barabash *et al.* (1995), Arnold *et al.* (2014)], ^{110}Pd Lehnert *et al.* (2016), ^{128}Te [Bellotti *et al.* (1987)], ^{130}Te [Bellotti *et al.* (1987), Barabash *et al.* (2001)] and ^{150}Nd [Arpesella *et al.* (1994),(1999), Barabash *et al.* (2009)] isotopes has been experimentally investigated. However, the $2\nu\beta^-\beta^-$ decay of ^{104}Ru for the $0^+ \rightarrow 2^+$ transition has not been experimentally investigated so far. All the available theoretical and experimental results are compiled in Table 3.4. We present only the theoretical $T^{2\nu}_{1/2}(2^+)$ for those models for which no direct or indirect information about $M_{2\nu}(2^+)$ is available to us. As already mentioned, there is a remarkable spread in the calculated NTMEs $M_{2\nu}(2^+)$ within different models. Specifically, the NTMEs $M_{2\nu}(2^+)$ calculated with the QRPA model without and with deformation vary by a factor of 2–341, corresponding

to ^{130}Te and ^{96}Zr isotopes,respectively. The average NTMEs $\overline{M}_{2\nu}(2^+)$ evaluated using the PHFB approach are suppressed by a factor between 1 – 150 with respect to those of Raduta *et al.* (2007) corresponding to ^{96}Zr and ^{128}Te isotopes, respectively. Consideration of the available theoretical and experimental results suggests that the prospective nuclei for the observation of the $0^+ \rightarrow 2^+$ transition of $2\nu\beta^-\beta^-$ decay are ^{96}Zr, ^{100}Mo, ^{110}Pd, ^{130}Te and ^{150}Nd.

3.2.1 Deformation effect

A suppression of NTMEs $M_{2\nu}(0^+)$ for $2\nu\beta^-\beta^-$ decay with respect to the spherical case has been reported when the parent and daughter nuclei have different deformations [Chandra *et al.* (2009), Álvarez-Rodríguez *et al.* (2004), Menéndez *et al.* (2009)]. To investigate this effect for the $0^+ \rightarrow 2^+$ transition, we present the NTMEs $M_{2\nu}(2^+)$ for the $2\nu\beta^-\beta^-$ decay of ^{94,96}Zr, ^{100}Mo, ^{104}Ru, ^{110}Pd, ^{128,130}Te and ^{150}Nd isotopes in Figs. 3.1(a) – 3.1(h) as a function of the difference in the deformation parameter $\Delta\beta_2 = \beta_2(parent) - \beta_2(daughter)$ between the parent and daughter nuclei for the $PPQQ1$ parametrization. The NTMEs $M_{2\nu}(2^+)$ are calculated by keeping the deformation for parent nuclei fixed at $\zeta_{qq} = 1$ and changing the deformation of daughter nuclei by varying ζ_{qq} in the range 0.0 – 1.5. It can be observed that in all cases but for ^{128,130}Te, the largest NTMEs correspond to the $|\Delta\beta_2|$ close to zero. With further increase in deformation, the NTMEs decrease with increase in $|\Delta\beta_2|$. Similar behavior is observed in other three parametrizations of the effective two-body interaction.

3.3 Conclusions

Using a set of reliable wave functions generated with four different parametrizations of the effective two-body interaction namely, $PPQQ1$, $PPQQHH1$, $PPQQ2$ and $PPQQHH2$, sets of four NTMEs $M_{2\nu}(2^+)$ have been calculated to study the $2\nu\beta^-\beta^-$ decay of ^{94,96}Zr, ^{100}Mo, ^{104}Ru, ^{110}Pd, ^{128,130}Te and ^{150}Nd isotopes for the $0^+ \rightarrow 2^+$ transition. It is noticed that the $0^+ \rightarrow 2^+$ transition is intrinsically suppressed due to the cubic dependence of the energy denominator and nuclear structure effects. Specifically, a large phase space factor due a larger Q-value implies a smaller E_{2^+} resulting from a larger $Q(2^+)$, which results in the suppression of NTMEs $M_{2\nu}(2^+)$.

The observation of Raduta *et al.* (2007) that the inclusion of deformation in the mean field can reduce the NTMEs $M_{2\nu}(2^+)$ calculated within pnQRPA up to a factor of 341, motivated us to study the $0^+ \rightarrow 2^+$ transition of $2\nu\beta^-\beta^-$ decay within PHFB approach treating the pairing and deformation degrees of freedom simultaneously on equal footing. It is noticed that with respect to NTMEs $M_{2\nu}(2^+)$ of Raduta *et al.* (2007), the average NTMEs $\overline{M}_{2\nu}(2^+)$ calculated using the PHFB approach are further suppressed by a factor between 1 – 150 corresponding to ^{96}Zr and ^{128}Te isotopes, respectively. In spite of the fact that the $0^+ \rightarrow 2^+$ transition of $2\nu\beta^-\beta^-$ decay is highly suppressed in comparison to the $0^+ \rightarrow 0^+$ transition, the available theoretical and experimental results suggest that the observation of the $0^+ \rightarrow 2^+$ transition of $2\nu\beta^-\beta^-$ decay may be possible in ^{96}Zr, ^{100}Mo, ^{110}Pd, ^{130}Te and ^{150}Nd isotopes.

Table 3.1: Experimental half lives $T^{2\nu}_{1/2}(2^+)$ of $2\nu\beta^-\beta^-$ decay of A = 48, 76, 82, 94, 96, 100, 110, 116, 124, 128, 130, 136, 148, 150, 154, 160, 170, 176 and 186 nuclei for the $0^+ \rightarrow 2^+$ transition.

Transition	$T^{2\nu}_{1/2}(2^+)$ (y)	Project	Reference
^{48}Ca$\rightarrow^{48}$Ti	$> 1.8 \times 10^{20}$	RRCKI+ITEP+FNSPE+JINP	[Bakalyarov *et al.* (2002)]
^{76}Ge$\rightarrow^{76}$Se	$> 3.7 \times 10^{22}$	ITEP+PNPI	[Beck *et al.* (1992)]
	$> 1.1 \times 10^{21}$	IETP	[Barabash *et al.* (1995)]
	$> 1.6 \times 10^{23}$	GERDA	[Agostini *et al.* (2015)]
^{82}Se$\rightarrow^{82}$Kr	$> 1.4 \times 10^{21}$	DPUJ+ITEP	[Suhonen *et al.* (1997)]
	$> 1.0 \times 10^{22}$	LUCIFER	[Beeman *et al.* (2015)]
^{94}Zr$\rightarrow^{94}$Mo	$> 1.3 \times 10^{19}$	NSDLBL	[Norman *et al.* (1987)]
	$> 3.4 \times 10^{19}$	DNAP+INO+DPUL+HBNI	[Dokania *et al.* (2017)]
^{96}Zr$\rightarrow^{96}$Mo	$> 2.0 \times 10^{19}$	NSDLBL	[Norman *et al.* (1987)]
	$> 4.1 \times 10^{19}$	INFN+IETP	[Arpesella *et al.* (1994)]
	$> 7.9 \times 10^{19}$	IETP	[Barabash *et al.* (1996)]

Table 3.1 continued

Transition	$T^{2\nu}_{1/2}(2^+)$(y)	Project	Reference
^{100}Mo$\rightarrow^{100}$Ru	$> 2.3 \times 10^{21}$	-	[Kudomi *et al.* (1992)]
	$> 2.3 \times 10^{21}$	-	[Blum *et al.* (1992)]
	$> 2.3 \times 10^{21}$	ITEP	[Barabash *et al.* (1993)]
	$> 1.6 \times 10^{21}$	ITEP	[Barabash et al (1995)]
	$> 2.5 \times 10^{21}$	NEMO-3	[Arnold *et al.* (2014)]
^{110}Pd$\rightarrow^{110}$Cd	$> 2.9 \times 10^{20}$	-	[Lehnert *et al.* (2016)]
^{116}Cd$\rightarrow^{116}$Sn	$> 2.3 \times 10^{21}$	MPIK+ITEP+INFN	[Piepke *et al.* (1994)]
^{124}Sn$\rightarrow^{124}$Te	$> 4.1 \times 10^{19}$	-	[Smolnikov *et al.*(1985)]
	$> 9.1 \times 10^{20}$	ITEP	[Barabash *et al.* (2009)]
^{128}Te$\rightarrow^{128}$Xe	$> 4.7 \times 10^{21}$	DFU+INFN	[Bellotti *et al.*(1987)]
^{130}Te$\rightarrow^{130}$Xe	$> 4.5 \times 10^{21}$	DFU+INFN	[Bellotti *et al.*(1987)]
	$> 2.8 \times 10^{21}$	INFN	[Bellotti *et al.* (1987)]
	$> 1.6 \times 10^{21}$	ITEP	[Barabash et al (2001)]
^{136}Xe$\rightarrow^{136}$Ba	$> 6.5 \times 10^{21}$	DFU+INFN	[Bellotti *et al.* (1991)]
	$> 4.6 \times 10^{23}$	KamLAND-Zen	[Asakura *et al.* (2016)]

Table 3.1 continued

Transition	$T^{2\nu}_{1/2}(2^+)$(y)	Project	Reference
^{148}Nd$\rightarrow^{148}$Sm	$> 3.0 \times 10^{18}$	IFU+INFN	[Bellotti *et al.* (1982)]
^{150}Nd$\rightarrow^{150}$Sm	$> 8.0 \times 10^{18}$	LNGS+INFN+ITEP+LPI	[Arpesella *et al.* (1994)]
	$> 9.1 \times 10^{19}$	INFN+DFU	[Arpesella *et al.* (1999)]
	$> 2.2 \times 10^{20}$	ITEP	[Barabash *et al.*(2009)]
^{154}Sm$\rightarrow^{154}$Gd	$> 2.3 \times 10^{18}$	-	[Derbin *et al.* (1996)]
^{160}Gd$\rightarrow^{160}$Dy	$> 1.2 \times 10^{17}$	-	[Burachas *et al.*(1993)]
	$> 2.1 \times 10^{19}$	INR	[Danevich et al (2001)]
^{170}Er$\rightarrow^{170}$Yb	$> 3.2 \times 10^{17}$	-	[Derbin *et al.* (1996)]
^{176}Yb$\rightarrow^{176}$Hf	$> 1.6 \times 10^{17}$	-	[Derbin *et al.* (1996)]
^{186}W$\rightarrow^{186}$Os	$> 2.4 \times 10^{20}$	-	[Georgadze *et al.* (1995)]

Table 3.2: Calculated NTMEs $M_{2\nu}(2^+)$ within the PHFB model and their average $\overline{M}_{2\nu}(2^+)$ along with standard deviation $\Delta\overline{M}_{2\nu}(2^+)$.

Nuclei	$M_{2\nu}(2^+)$				$\overline{M}_{2\nu}(2^+)$	$\Delta\overline{M}_{2\nu}(2^+)$
	$PPQQ1$	$PPQQHH1$	$PPQQ2$	$PPQQHH2$		
^{94}Zr	1.44×10^{-4}	1.08×10^{-4}	4.08×10^{-5}	1.02×10^{-4}	9.88×10^{-5}	4.30×10^{-5}
^{96}Zr	9.71×10^{-5}	1.09×10^{-4}	9.15×10^{-5}	1.02×10^{-4}	9.98×10^{-5}	0.74×10^{-5}
^{100}Mo	1.95×10^{-5}	2.52×10^{-5}	2.02×10^{-5}	1.05×10^{-5}	1.89×10^{-5}	0.61×10^{-5}
^{104}Ru	3.30×10^{-5}	4.22×10^{-5}	3.05×10^{-5}	3.96×10^{-5}	3.63×10^{-5}	0.55×10^{-5}
^{110}Pd	1.21×10^{-4}	1.33×10^{-4}	1.12×10^{-4}	1.10×10^{-4}	1.19×10^{-4}	0.10×10^{-4}
^{128}Te	1.19×10^{-6}	2.89×10^{-6}	1.54×10^{-6}	2.65×10^{-6}	2.07×10^{-6}	0.83×10^{-6}
^{130}Te	7.72×10^{-7}	1.86×10^{-6}	8.55×10^{-7}	1.87×10^{-6}	1.34×10^{-6}	0.61×10^{-6}
^{150}Nd	6.32×10^{-6}	5.84×10^{-6}	5.74×10^{-6}	5.54×10^{-6}	5.86×10^{-6}	0.33×10^{-6}

Table 3.3: Excitation energies E_{2^+}, quadrupole moments Q (2^+) of daughter nuclei, Q-values of $0^+ \rightarrow 2^+$ transition Q_{2^+} and the phase space factors $G_{2\nu}(2^+)$ with $g_A = 1.2701$.

Transition	E_{2^+} (MeV)[1]	Q (2^+) eb[2]	Q_{2^+} (MeV)	$G_{2\nu}(2^+)$
^{94}Zr$\rightarrow^{94}$Mo	0.871099	-0.13±0.08	1.145	6.801×10^{-30}
^{96}Zr$\rightarrow^{96}$Mo	0.778213	-0.20±0.08	2.572	1.494×10^{-18}
^{100}Mo$\rightarrow^{100}$Ru	0.53959	-0.54± 0.07	2.494	1.460×10^{-18}
^{104}Ru$\rightarrow^{104}$Pd	0.55579	-0.47± 0.10	0.743	9.625×10^{-25}
^{110}Pd$\rightarrow^{110}$Cd	0.657751	-0.40 ±0.04	1.360	1.228×10^{-20}
^{128}Te$\rightarrow^{128}$Xe	0.4429		0.425	1.429×10^{-24}
^{130}Te$\rightarrow^{130}$Xe	0.5361		1.989	4.632×10^{-19}
^{150}Nd$\rightarrow^{150}$Sm	0.33395	-1.32±0.19	3.037	3.253×10^{-17}

References:

[1] Sakai (1984)

[2] Raghavan (1989)

Table 3.4: Theoretically calculated NTME $M_{2\nu}(2^+)$ and half-life $T^{2\nu}_{1/2}(2^+)$ for the $0^+ \rightarrow 2^+$ transition of ^{94,96}Zr, ^{100}Mo, ^{104}Ru, ^{110}Pd, ^{128,130}Te and ^{150}Nd nuclei along with experimental half-lives $T^{2\nu}_{1/2}(2^+)$. "*" denotes the present calculation with average NTME.

Nuclei	Theory				Experiment	
	Model	Ref.	$\|M_{2\nu}(2^+)\|$	$T^{2\nu}_{1/2}(2^+)$ (y)	$T^{2\nu}_{1/2}(2^+)$ (y)	Ref.
^{94}Zr	PHFB	*	9.884×10^{-5}	1.505×10^{37}	$>1.3\times 10^{19}$	[1]
	QRPA†	[2]	0.0170	5.088×10^{32}	$>3.4\times 10^{19}$	[3]
	QRPA‡	[2]	0.0155	6.120×10^{32}		
^{96}Zr	PHFB	*	9.978×10^{-5}	6.723×10^{25}	$>2.0\times 10^{18}$	[1]
	QRPA	[4]	(0.005-0.038)	2.677×10^{22}-	$>4.1\times 10^{19}$	[5]
				4.635×10^{20}	$>7.9\times 10^{19}$	[4]
	QRPA	[6]	1.113×10^{-4}	5.403×10^{25}		
	QRPA	[7]	0.011	5.532×10^{21}		
	RQRPA†	[8]	0.011	5.532×10^{21}		
	RQRPA‡	[8]	0.010	6.693×10^{21}		
	RQRPA	[9]		$(1.1\text{-}1.4)\times10^{21}$		
	SRPA	[10]	3.117×10^{-4}	6.889×10^{24}		
^{100}Mo	PHFB	*	1.887×10^{-5}	1.924×10^{27}	$>1.5\times 10^{20}$	[11]
	QRPA	[12]	0.033	6.290×10^{20}	$>5.0\times 10^{20}$	[13]
	QRPA	[6]	1.814×10^{-4}	2.081×10^{25}	$>2.3\times 10^{21}$	[14]
	QRPA	[7]	0.0078	1.126×10^{22}	$>1.6\times 10^{21}$	[15]
	RQRPA	[9]		$(1.0\text{-}1.1)\times10^{22}$		
	SRPA	[10]	1.482×10^{-3}	3.119×10^{23}		
	SU(3)$^{+}$	[16]	7.3×10^{-5}	1.285×10^{26}		
	SU(3)$^{++}$	[16]	1.53×10^{-4}	2.926×10^{25}		
	MCM	[17]		$(5.3\text{-}13)\times10^{20}$		

Table 3.4 continued

Nuclei	Theory				Experiment	
	Model	Ref.	$\|M_{2\nu}(2^+)\|$	$T^{2\nu}_{1/2}(2^+)$ (y)	$T^{2\nu}_{1/2}(2^+)$ (y)	Ref.
^{104}Ru	PHFB	*	3.634×10^{-5}	7.867×10^{32}		
	QRPA	[6]	3.736×10^{-3}	7.444×10^{28}		
	QRPA†	[2]	0.00792	1.656×10^{28}		
	QRPA‡	[2]	0.00811	1.580×10^{28}		
^{110}Pd	PHFB	*	1.192×10^{-4}	5.731×10^{27}	$>2.9\times10^{20}$	[18]
	QRPA	[6]	6.671×10^{-3}	1.830×10^{24}		
	QRPA†	[2]	0.0112	6.492×10^{23}		
	QRPA‡	[2]	0.00766	1.388×10^{24}		
	SRPA	[19]	5.621×10^{-3}	2.577×10^{24}		
^{128}Te	PHFB	*	2.068×10^{-6}	1.636×10^{35}	$>4.7\times\ 10^{21}$	[20]
	QRPA	[6]	3.055×10^{-4}	7.498×10^{30}		
	QRPA	[7]	0.00287	8.496×10^{28}		
	SRPA	[19]	1.022×10^{-3}	6.700×10^{29}		
^{130}Te	PHFB	*	1.341×10^{-6}	1.201×10^{30}	$>4.5\times\ 10^{21}$	[20]
	QRPA	[6]	8.272×10^{-5}	3.155×10^{26}	$>1.6\times\ 10^{21}$	[21]
	QRPA	[7]	0.00016	8.433×10^{25}		
	SRPA	[19]	4.088×10^{-3}	1.292×10^{23}		
^{150}Nd	PHFB	*	5.864×10^{-6}	8.940×10^{26}	$>8.0\times\ 10^{18}$	[5]
	SU(3)	[22]	5.38×10^{-5}	1.062×10^{25}	$>9.1\times\ 10^{19}$	[23]

†WS basis; ‡AWS basis; $^{+}$Spherical occupation wave functions; $^{++}$Deformed occupation wave functions

References:

[1] Norman (1987)

[2] Suhonen (2011)

[3] Dokania *et al.* (2017)

[4] Barabash *et al.* (1996)

[5] Arpesella *et al.* (1994)

[6] Raduta *et al.* (2007)

[7] Unlu (2013), (2014)

[8] Toivanen and Suhonen (1997)

[9] Schweiger *et al.* (1998)

[10] Stoica and Mihut (1996)

[11] Kudomi *et al.* (1992)

[12] Suhonen and Civitarese (1994)

[13] Blum *et al.* (1992)

[14] Barabash *et al.* (1993)

[15] Barabash *et al.* (1995)

[16] Hirsch *et al.* (1995)

[17] Suhonen (1998)

[18] Lehnert *et al.* (2016)

[19] Stoica (1994)

[20] Bellotti *et al.* (1987)

[21] Barabash *et al.* (2001)

[22] Hirsch *et al.* (1995*a*)

[23] Arpesella *et al.*(1999)

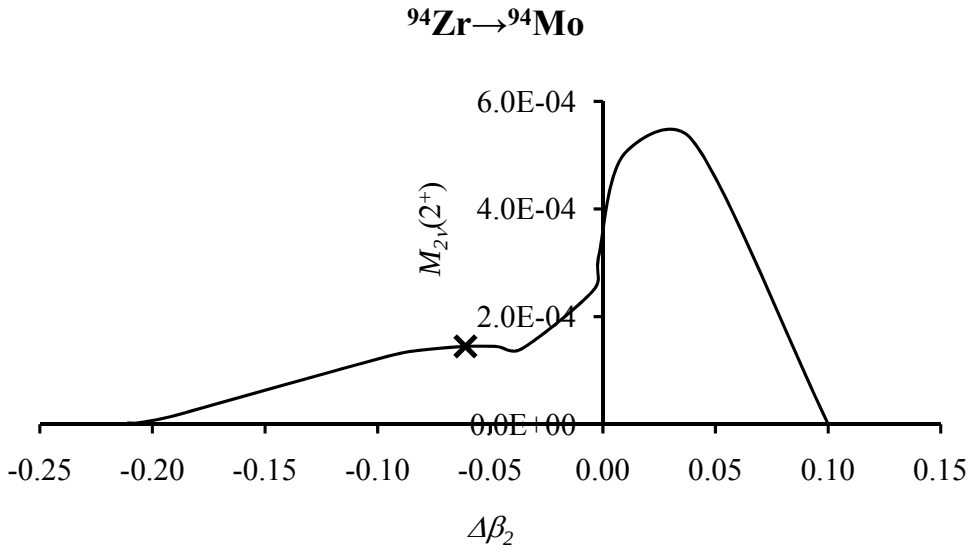

Fig. 3.1(a): NTMEs of $2\nu\beta^-\beta^-$ decay for the $0^+\rightarrow 2^+$ transition of ^{94}Zr as a function of the difference in the deformation parameter $\Delta\beta_2$. "×" denotes the value of calculated NTMEs for $\Delta\beta_2$ at ζ_{qq}=1.0.

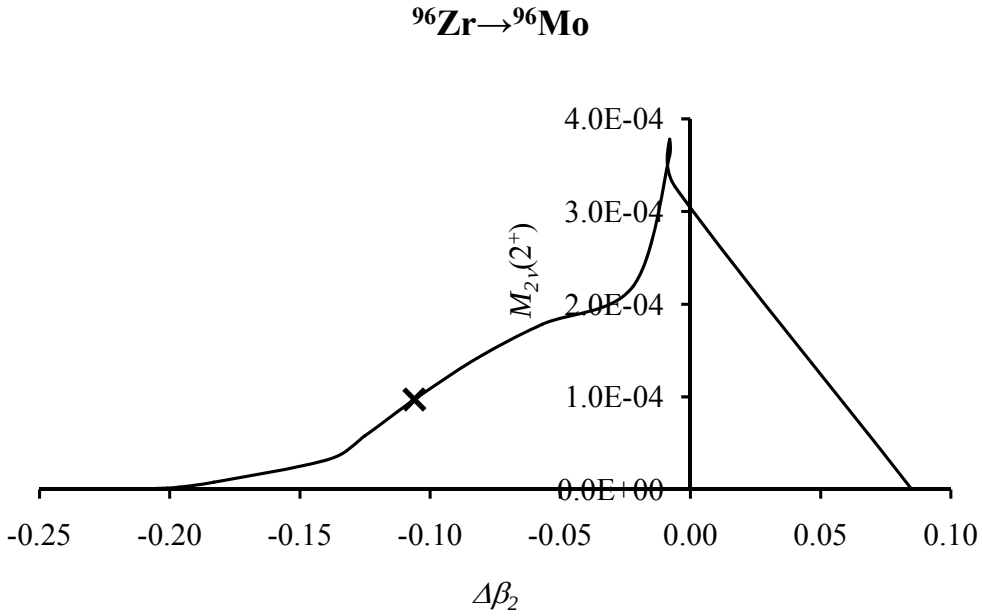

Fig. 3.1(b): NTMEs of $2\nu\beta^-\beta^-$ decay for the $0^+\rightarrow 2^+$ transition of ^{96}Zr as a function of the difference in the deformation parameter $\Delta\beta_2$. "×" denotes the value of calculated NTMEs for $\Delta\beta_2$ at ζ_{qq}=1.0.

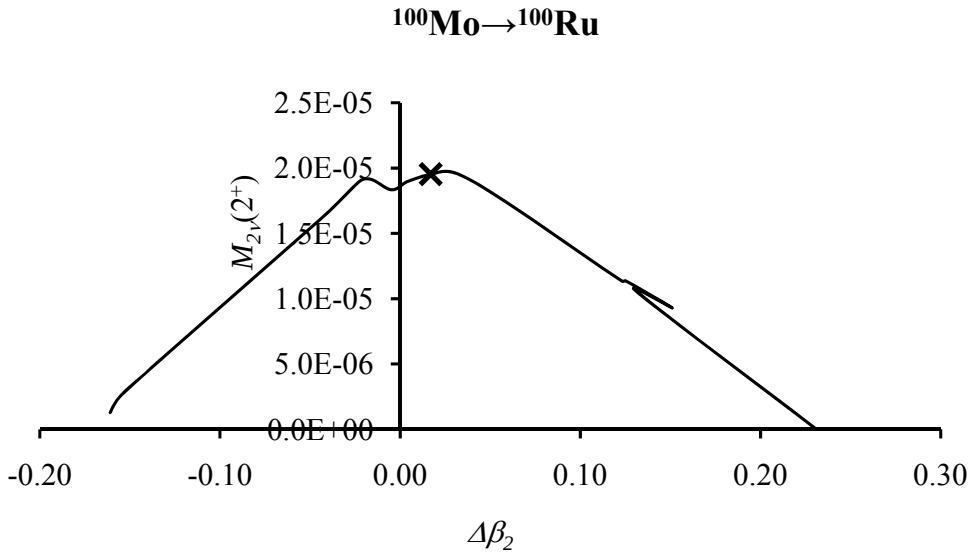

Fig. 3.1(c): NTMEs of $2\nu\beta^-\beta^-$ decay for the $0^+\rightarrow2^+$ transition of ^{100}Mo as a function of the difference in the deformation parameter $\Delta\beta_2$. "×" denotes the value of calculated NTMEs for $\Delta\beta_2$ at ζ_{qq}=1.0.

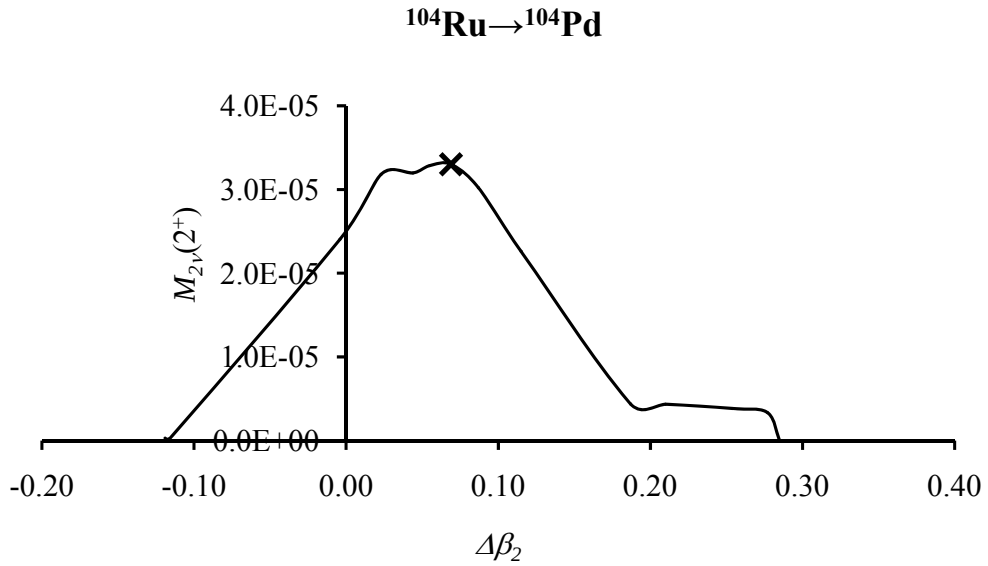

Fig. 3.1(d): NTMEs of $2\nu\beta^-\beta^-$ decay for the $0^+\rightarrow2^+$ transition of ^{104}Ru as a function of the difference in the deformation parameter $\Delta\beta_2$. "×" denotes the value of calculated NTMEs for $\Delta\beta_2$ at ζ_{qq}=1.0.

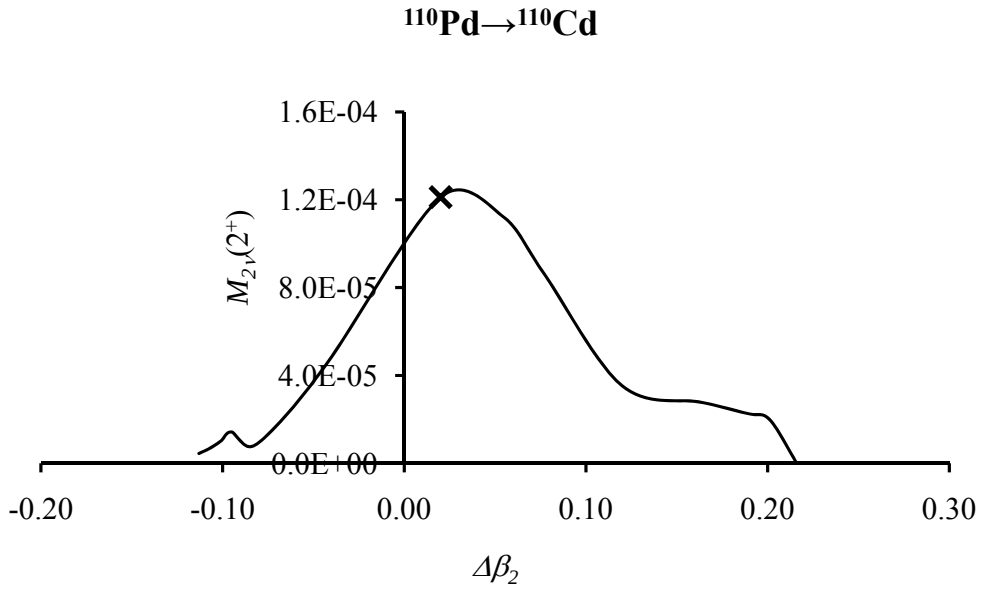

Fig. 3.1(e): NTMEs of $2\nu\beta^-\beta^-$ decay for the $0^+\rightarrow2^+$ transition of ^{110}Pd as a function of the difference in the deformation parameter $\Delta\beta_2$. "×" denotes the value of calculated NTMEs for $\Delta\beta_2$ at ζ_{qq}=1.0.

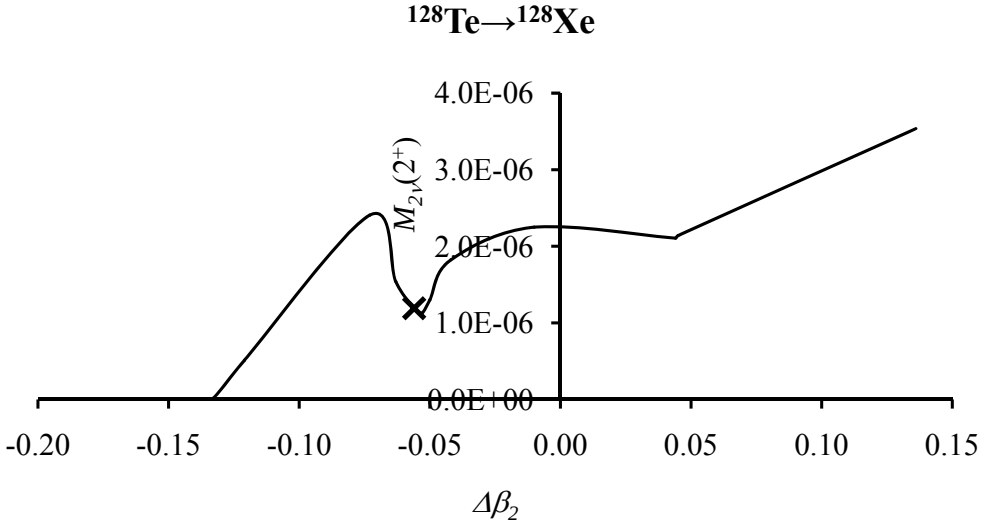

Fig. 3.1(f): NTMEs of $2\nu\beta^-\beta^-$ decay for the $0^+\rightarrow2^+$ transition of ^{128}Te as a function of the difference in the deformation parameter $\Delta\beta_2$. "×" denotes the value of calculated NTMEs for $\Delta\beta_2$ at ζ_{qq}=1.0.

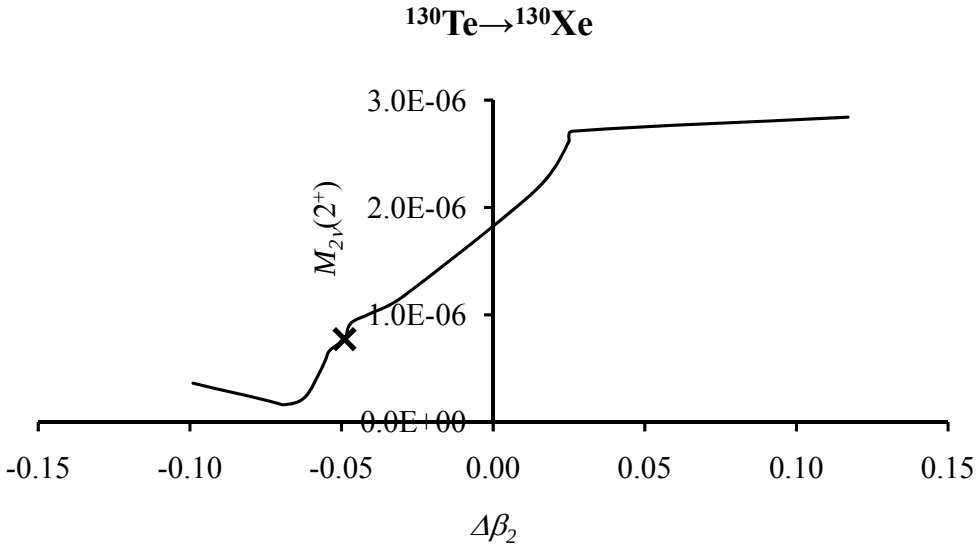

Fig. 3.1(g): NTMEs of $2\nu\beta^-\beta^-$ decay for the $0^+\rightarrow2^+$ transition of ^{130}Te as a function of the difference in the deformation parameter $\Delta\beta_2$. "×" denotes the value of calculated NTMEs for $\Delta\beta_2$ at ζ_{qq}=1.0.

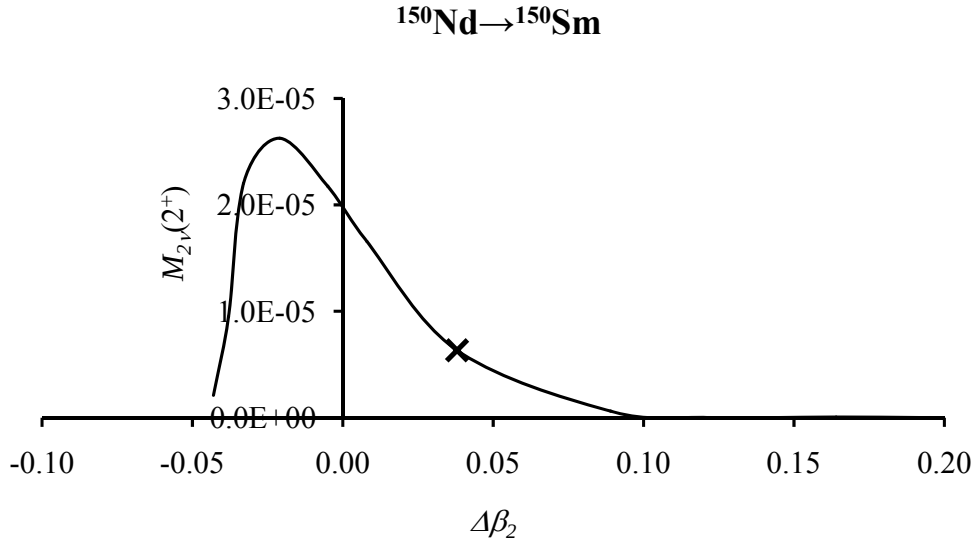

Fig. 3.1(h): NTMEs of $2\nu\beta^-\beta^-$ decay for the $0^+\rightarrow2^+$ transition of ^{150}Nd as a function of the difference in the deformation parameter $\Delta\beta_2$. "×" denotes the value of calculated NTMEs for $\Delta\beta_2$ at ζ_{qq}=1.0.

Chapter 4

$0\nu\beta^-\beta^-$ decay of ^{94,96}Zr, ^{100}Mo, ^{110}Pd, ^{128,130}Te and ^{150}Nd nuclei within mechanisms involving light neutrino mass and right-handed current

Observation of the lepton number L violating neutrinoless double beta ($0\nu\beta\beta$) decay is the most pragmatic approach to establish the Majorana nature of neutrinos. Arguably, the violation of lepton number L conservation and Majorana nature of neutrinos are intimately related [Schechter and Valle (1982)]. In $0\nu\beta\beta$ decay, the neutrino emitted from a nucleon is to be absorbed by another nucleon implying the existence of Majorana neutrino with finite mass. Alternatively, the occurrence of $0\nu\beta\beta$ decay is also possible with the coexistence of right-handed $V+A$ and left-handed $V-A$ currents. In addition, the smallness of neutrino mass as explained by see-saw mechanism requires gauge groups

with right-handed current. In several alternative mechanisms based on various gauge theoretical models beyond the standard model of electroweak unification, the conservation of lepton number L is violated. Specifically, the exchange of light and heavy Majorana neutrinos involving left and right handed currents within the left-right symmetric model (LRSM) is one of such possibilities.

The rate of $0\nu\beta\beta$ decay is a product of appropriate phase-space factors, nuclear transition matrix elements (NTMEs) and parameters of the underlying mechanisms [Vergados *et al.* (2012), (2016), Dell'Oro *et al.* (2016)]. Recently, the phase-space factors have been calculated to good accuracy incorporating the screening correction [Kotila and Iachello (2012), Stoica and Mirea (2013), Štefánik *et al.* (2015)]. The extraction of accurate limits on the parameters of a particular mechanism depends on the reliability of NTMEs. The evaluation of reliable NTMEs is a challenging task. A suitable truncation of unmanageable Hilbert space into a manageable model space with appropriate single-particle energies (SPEs), and effective two-body interaction is required. In addition, alternative considerations of the finite size of nucleons (FNS), short range correlations (SRC) and the effective value of axial vector current coupling constant g_A are also available.

The standard mass mechanism of $0\nu\beta^-\beta^-$ decay has been extensively studied employing a large number of nuclear models, namely shell-model approach [Caurier *et al.* (2008),(2008*a*), Menéndez *et al.* (2009), Brown *et al.* (2014), Neacsu *et al.* (2015), Horoi *et al.* (2010), Horoi *et al.* (2013), Brown *et al.* (2015), Sen'kov *et al.* (2014),(2014*a*),(2016)], QRPA [Šimkovic *et al.* (1999),(2008),(2009), Civitarese (2009), Suhonen and Civitarese (2012)], QRPA with isospin restoration [Šimkovic *et al.* (2013)], deformed QRPA [Faessler *et al.* (2012), Fang *et al.* (2010),(2011), Mustonen and Engel (2013)], projected-Hartree-

Fock-Bogoliubov (PHFB) [Rath *et al.* (2010),(2012)(2013)], energy density functional (EDF) [Rodríguez *et al.* (2010)], covariant density functional theory (CDFT) [Yao *et al.* (2015)], and interacting boson model (IBM) [Barea *et al.* (2009),(2013), Iachello *et al.* (2011),(2011*a*)] with isospin restoration [Barea *et al.* (2015)]. The details about these theoretical studies have been excellently reviewed over the past years in refs. [Suhonen and Civitarese (1998), Faessler and Šimkovic (1998), Engel and Menéndez (2017)] and references there in. In spite of the fact that each model employs different model space, SPEs and two-body residual interactions, the calculated NTMEs $M^{(0\nu)}$ differ by a factor of 2–3.

Uncertainties in NTMEs for $0\nu\beta^-\beta^-$ decay within mechanisms involving light Majorana neutrino mass, classical Majorons and sterile neutrinos have been estimated employing the PHFB approach in conjunctions with four different parametrizations of effective two-body interaction, form factors with two different parametrizations and three different parametrizations of the SRC [Rath *et al.* (2013)]. The uncertainties in NTMEs for $0\nu\beta^-\beta^-$ decay involving heavy Majorana neutrino mass [Rath *et al.* (2012)] and new Majoron models [Rath *et al.* (2016)] have also been investigated. The main objective of the present work is to calculate sets of twelve NTMEs for the $0^+ \rightarrow 0^+$ transition of $0\nu\beta^-\beta^-$ decay involving light neutrino mass and right-handed current by employing sets of four different PHFB wave functions as well as three different parametrizations of SRC and estimate uncertainties therein.

The detailed theoretical formalism of $0\nu\beta^-\beta^-$ decay within the mechanisms of LRSM, namely the exchange of light as well as heavy Majorana neutrino, admixture of $V-A$ and $V+A$ currents, and exchange of right handed heavy neutrino has been developed in refs.

[Doi *et al.* (1985), Tomoda (1991), Doi and Kotani (1993)]. The theoretical formalism of the standard mass mechanisms has been extended by including the contribution of induced currents [Šimkovic *et al.* (1999)]. Including the induced pseudoscalar terms in the nonrelativistic reduction of right-handed $V + A$ current, the light neutrino exchange mechanism of $0\nu\beta^-\beta^-$ decay with left and right handed leptonic and hadronic currents has been investigated in detail [Štefánik *et al.* (2015)]. Presently, the NTMEs are calculated neglecting the induced pseudoscalar terms in the nonrelativistic reduction of right handed $V+A$ current, which will not apparently change the final conclusions as shown by [Štefánik *et al.* (2015)].

The present chapter is organized as follows. In Section 4.1, we present a brief theoretical formalism to study $0\nu\beta^-\beta^-$ decay involving light Majorana neutrino mass and right handed current. The calculated NTMEs required to study $0\nu\beta^-\beta^-$ decay of ^{94,96}Zr, ^{100}Mo, ^{110}Pd, ^{128,130}Te and ^{150}Nd isotopes for the $0^+ \rightarrow 0^+$ transition and the uncertainties in NTMEs are presented in Section 4.2. Further, the extracted limits on the effective light Majorana neutrino mass $< m_\nu >$, the effective weak coupling of right-handed leptonic current with right-handed hadronic current $< \lambda >$, and the effective weak coupling of right-handed leptonic current with left-handed hadronic current $< \eta >$ from the largest available limits on half-lives of $0\nu\beta^-\beta^-$ decay $T^{(0\nu)}_{1/2}(0^+ \rightarrow 0^+)$ are presented in the same section. Conclusions are given in Section 4.3.

4.1 Theoretical formalism

The general form of weak interaction Hamiltonian H_W is given by

$$H_W = \frac{G}{\sqrt{2}}\left[j_{L\mu}J_L^{\mu\dagger} + \kappa j_{L\mu}J_R^{\mu\dagger} + \eta j_{R\mu}J_L^{\mu\dagger} + \lambda j_{R\mu}J_R^{\mu\dagger}\right] + h.c. \tag{4.1}$$

where $j_{L,R}$ and $J_{L,R}$ are left and right handed leptonic and hadronic currents, respectively. Further, κ, η and λ are the parameters for the admixture of $V-A$ and $V+A$ currents. The second term in the Eq. (4.1) is usually neglected as κ enters into $\beta\beta$ decay amplitude always in the combination $1 \pm \kappa$ and it is expected that $|\kappa| \ll 1$.

Using the standard approximations of Doi *et al.* (1985), with CP conservation, the rate for the $0^+ \rightarrow 0^+$ transition of $0\nu\beta^-\beta^-$ decay is given by

$$\begin{aligned}\left[T_{1/2}^{(0\nu)}\right]^{-1} &= \frac{\left|\langle m_\nu\rangle\right|^2}{m_e}C_{mm} + \frac{\left|\langle m_\nu\rangle\right|}{m_e}\langle\lambda\rangle C_{m\lambda} + \frac{\left|\langle m_\nu\rangle\right|}{m_e}\langle\eta\rangle C_{m\eta} \\ &\quad + \langle\lambda\rangle^2 C_{\lambda\lambda} + \langle\eta\rangle^2 C_{\eta\eta} + \langle\lambda\rangle\langle\eta\rangle C_{\lambda\eta}\end{aligned} \tag{4.2}$$

where

$$\langle m_\nu\rangle = {\sum_i}' U_{ei}^2 m_i \tag{4.3}$$

$$\langle\lambda\rangle = \lambda\left|{\sum_i}'\left(\frac{g_V'}{g_V}\right)U_{ei}V_{ei}\right| \tag{4.4}$$

$$\langle\eta\rangle = \eta\left|{\sum_i}' U_{ei}V_{ei}\right| \tag{4.5}$$

and the nuclear structure factors C_{xy} are written as

$$C_{mm} = G_{01}\left|M^{(0\nu)}\right|^2 \tag{4.6a}$$

$$C_{m\lambda} = M^{(0\nu)}\left(G_{04}M_{1+} - G_{03}M_{2-}\right) \tag{4.6b}$$

$$C_{m\eta} = M^{(0\nu)}(G_{03}M_{2+} - G_{04}M_{1-} - G_{05}M_P + G_{06}M_R) \quad (4.6c)$$

$$C_{\lambda\lambda} = G_{02}\left|M_{2-}\right|^2 - \frac{2}{9}G_{03}(M_{1+}M_{2-}) + \frac{1}{9}G_{04}\left|M_{1+}\right|^2 \quad (4.6d)$$

$$C_{\eta\eta} = G_{02}\left|M_{2+}\right|^2 - \frac{2}{9}G_{03}(M_{1-}M_{2+}) + \frac{1}{9}G_{04}\left|M_{1-}\right|^2$$
$$-G_{07}(M_PM_R) + G_{08}\left|M_P\right|^2 + G_{09}\left|M_R\right|^2 \quad (4.6e)$$

$$C_{\lambda\eta} = -2G_{02}(M_{2+}M_{2-}) + \frac{2}{9}G_{03}(M_{2+}M_{1+} + M_{2-}M_{1-})$$
$$-\frac{2}{9}G_{04}(M_{1-}M_{1+}) \quad (4.6f)$$

In addition, the combinations of NTMEs $M^{(0\nu)}$ and $M_{i\pm}$ $(i = 1, 2)$ are defined as

$$M^{(0\nu)} = M_{GT} - M_F + M_T \quad (4.7)$$

$$M_{1\pm} = M_{qGT} - 6M_{qT} \pm 3M_{qF} \quad (4.8)$$

$$M_{2\pm} = M_{\omega GT} \pm M_{\omega F} - \frac{1}{9}M_{1\mp} \quad (4.9)$$

Employing the generally agreed closure approximation in conjunction with the HFB wave functions, the NTMEs M_α ($\alpha = F, GT, T, \omega F, \omega GT, qF, qGT, qT, P$ and R) appearing in the expressions of nuclear structure factors C_{xy} are calculated by using the following expression [Rath *et al.* (2010)].

$$\begin{aligned} M_\alpha &= \left\langle 0_f^+ \left\| O_\alpha(\mathbf{r}, \boldsymbol{\sigma}) \right\| 0_i^+ \right\rangle \\ &= \left[n^{J_f=0}n^{Ji=0}\right]^{-1/2} \int_0^\pi d\theta sin\theta n_{(Z,N),(Z+2,N-2)}(\theta) \times \sum_{\alpha\beta\gamma\delta} \left\langle \alpha\beta \left| O_\alpha(\mathbf{r}, \boldsymbol{\sigma}) \right| \gamma\delta \right\rangle \\ &\quad \times \sum_{\varepsilon\eta} \frac{\left(f^{(\pi)*}_{Z+2,N-2}\right)_{\varepsilon\beta}}{\left[\left(1 + F^{(\pi)}_{Z,N}(\theta) f^{(\pi)*}_{Z+2,N-2}\right)\right]_{\varepsilon\alpha}} \times \frac{\left(F^{(\nu)*}_{Z,N}\right)_{\eta\delta}}{\left[\left(1 + F^{(\nu)}_{Z,N}(\theta) f^{(\nu)*}_{Z+2,N-2}\right)\right]_{\gamma\eta}} \end{aligned} \quad (4.10)$$

where

$$n^J = \int_0^\pi \left[det\left(1 + F^{(\pi)} f^{(\pi)\dagger}\right)\right]^{1/2} \left[det\left(1 + F^{(\nu)} f^{(\nu)\dagger}\right)\right]^{1/2} d^J_{00}(\theta) sin(\theta) d\theta \quad (4.11)$$

and

$$n_{(Z,N),(Z+2,N-2)}(\theta) = \left[det\left(1+F^{(\nu)}_{Z,N}f^{(\nu)\dagger}_{Z+2,N-2}\right)\right]^{1/2} \times \left[det\left(1+F^{(\pi)}_{Z,N}f^{(\pi)\dagger}_{Z+2,N-2}\right)\right]^{1/2} \quad (4.12)$$

The $\pi(\nu)$ represents the proton (neutron) of nuclei involved in the $\left(\beta^-\beta^-\right)_{0\nu}$ decay process. The matrices $f_{Z,N}$ and $F_{Z,N}(\theta)$ are given by

$$f_{Z,N} = \sum_i C_{ij_\alpha,m_\alpha}C_{ij_\beta,m_\beta}\left(v_{im_\alpha}/u_{im_\alpha}\right)\delta_{m_\alpha,-m_\beta} \quad (4.13)$$

$$F_{Z,N}(\theta) = \sum_{m'_\alpha m'_\beta} d^{j_\alpha}_{m_\alpha,m'_\alpha}(\theta)d^{j_\beta}_{m_\beta,m'_\beta}(\theta)f_{j_\alpha m'_\alpha,j_\beta m'_\beta} \quad (4.14)$$

The calculation of n^J, $n_{(Z,N),(Z+2,N-2)}(\theta)$, $f_{Z,N}$ and $F_{Z,N}(\theta)$ require the intrinsic wave functions $|\Phi_0\rangle$ of axially symmetric state with $K = 0$ expressed by the amplitudes (u_{im}, v_{im}) and expansion coefficients $C_{ij,m}$, which are in turn obtained by minimizing the expectation value of the effective Hamiltonian given by [Rath *et al.* (2010)]

$$H = H_{sp} + V(P) + V(QQ) + V(HH) \quad (4.15)$$

in a basis constructed by using a set of deformed states. In Eq.(4.15), the H_{sp}, $V(P)$, $V(QQ)$ and $V(HH)$ denote the single particle Hamiltonian, the pairing, quadrupole-quadrupole and hexadecapole-hexadecapole parts of the effective two-body interaction, respectively. Further, the transition operators have the following general structure

$$O_\alpha\left(\mathbf{r},\boldsymbol{\sigma},\boldsymbol{\tau}\right) = S_\alpha\left(\mathbf{r},\boldsymbol{\sigma}\right)\ \tau^+_n\tau^+_m\ \frac{2R}{\pi}\int h_\alpha(qr)\ f_\alpha(q^2)\ q^2dq \quad (4.16)$$

The NTMEs appearing in Eq.(4.7) have been calculated by Rath *et al.* (2013). Neglecting the induced pseudoscalar terms in the nonrelativistic reduction of right-handed

$V+A$ current [Štefánik *et al.* (2015)], the explicit structure of $S_\alpha(\mathbf{r},\boldsymbol{\sigma})$, $h_\alpha(qr)$ and $f_\alpha(q^2)$ for the rest of the NTMEs M_α is given as follows.

$$O_{\omega F} = \tau_n^+\tau_m^+\frac{2R}{\pi}\int \frac{j_0(qr)}{\left(q+\overline{A}\right)^2}\,\frac{g_V^2(q^2)}{g_A^2}\,q^2dq \tag{4.17a}$$

$$O_{\omega GT} = \boldsymbol{\sigma}_1\cdot\boldsymbol{\sigma}_2\;\tau_n^+\tau_m^+\,\frac{2R}{\pi}\int \frac{j_0(qr)}{\left(q+\overline{A}\right)^2}\,\frac{g_A^2(q^2)}{g_A^2}\,q^2dq \tag{4.17b}$$

$$O_{qF} = \tau_n^+\tau_m^+\frac{2R}{\pi}\int \frac{j_1(qr)qr}{q\left(q+\overline{A}\right)}\,\frac{g_V^2(q^2)}{g_A^2}\,q^2dq \tag{4.17c}$$

$$O_{qGT} = \boldsymbol{\sigma}_1\cdot\boldsymbol{\sigma}_2\;\tau_n^+\tau_m^+\,\frac{2R}{\pi}\int \frac{j_1(qr)qr}{q\left(q+\overline{A}\right)}\,\frac{g_A^2(q^2)}{g_A^2}\,q^2dq \tag{4.17d}$$

$$\begin{aligned} O_{qT} &= \left(3(\boldsymbol{\sigma}_1\cdot\hat{\mathbf{r}}_{12})\,(\boldsymbol{\sigma}_1\cdot\hat{\mathbf{r}}_{12})-\boldsymbol{\sigma}_1\cdot\boldsymbol{\sigma}_2\right)\;\tau_n^+\tau_m^+\,\frac{2R}{\pi} \\ &\quad\times\int \frac{j_1(qr)qr}{q\left(q+\overline{A}\right)}\,\frac{g_A^2(q^2)}{3g_A^2}\,q^2dq \end{aligned} \tag{4.17e}$$

$$\begin{aligned} O_P &= \left(i\frac{R}{2r^2}\,(\boldsymbol{\sigma}_1-\boldsymbol{\sigma}_2)\cdot\left(\frac{\mathbf{r}\times\mathbf{r}_+}{R}\right)\right)\tau_n^+\tau_m^+\frac{2R}{\pi} \\ &\quad\times\int \frac{j_1(qr)qr}{q\left(q+\overline{A}\right)}\frac{g_A(q^2)g_V(q^2)}{g_A^2}q^2dq \end{aligned} \tag{4.17f}$$

$$\begin{aligned} O_R &= \boldsymbol{\sigma}_1\cdot\boldsymbol{\sigma}_2\;\tau_n^+\tau_m^+\,\frac{2R}{\pi} \\ &\quad\times\int \frac{j_0(qr)q^2}{q\left(q+\overline{A}\right)}\,\frac{1}{3m_N}\left(1+\frac{g_M(q^2)}{g_V(q^2)}\right)\frac{g_A(q^2)g_V(q^2)}{g_A^2}\,q^2dq \end{aligned} \tag{4.17g}$$

In the PHFB model, the calculation of nuclear wave functions is based on the independent particle picture. The long range correlations are taken into account through configuration mixing while the short range correlations (SRC) due to the repulsive hard core are usually absent. This effect is quite important for the evaluation of NTMEs since the potentials are still relatively short ranged even after the finite nucleon size effect is taken in to account. The SRC are produced by the repulsive nucleon-nucleon potential generated through the exchange of ω and ρ mesons. They have been included in the calculations of M_α for the $0\nu\beta^-\beta^-$ decay through the Jastrow type of phenomenological correlations with Miller-Spencer parametrization [Miller and Spencer (1976)], effective

operators [Wu *et al.* (1985)], exchange of ω-meson [Hirsch *et al.* (1995*a*)], the Unitary Correlation Operator Method (UCOM) [Šimkovic *et al.* (2008), Kortelainen and Suhonen (2007)] and self-consistent coupled-cluster method (CCM) [Šimkovic *et al.* (2009)]. It has been observed that the effects due to the Jastrow type of correlations with Miller-Spencer parametrization are usually strong [Wu *et al.* (1985)], where as the UCOM and self-consistent CCM have weak effects. Further, it has been shown by Šimkovic *et al.* (2009) that the SRC effects of Argonne V18 and CD-Bonn two nucleon potentials can be parametrized by the Jastrow type of correlations within a few percent of accuracy. Explicitly, this effect of SRC can be incorporated approximately by multiplying the two nucleon wave functions by a correlation function $f(r)$ when calculating NTMEs. This is equivalent to the replacement

$$\langle j_1^\pi \; j_2^\pi \; J \,|O_\alpha|\, j_1^\nu \; j_2^\nu J\rangle \rightarrow \langle j_1^\pi \; j_2^\pi \; J \,|f \; O_\alpha \; f|\, j_1^\nu \; j_2^\nu \; J\rangle \tag{4.18}$$

with

$$f(r) = 1 - ce^{-ar^2}(1 - br^2) \tag{4.19}$$

where $a = 1.1 \; fm^{-2}$, $1.59 \; fm^{-2}$, $1.52 \; fm^{-2}$, $b = 0.68 \; fm^{-2}$, $1.45 \; fm^{-2}$, $1.88 \; fm^{-2}$ and $c = 1.0$, 0.92, 0.46 for Miller-Spencer, Argonne V18 and CD-Bonn NN potentials, respectively.

4.1.1 Phase space factors for $0\nu\beta^-\beta^-$ decay

The formalism to calculate the phase space factors for $0\nu\beta^-\beta^-$ decay have been given in detail by Doi *et al.* (1985),(1993), Tomoda (1991) and Suhonen and Civitarese (1998). Here we briefly outline the steps of derivation following the notations of Doi *et al.* (1993).

The phase space factors for $0\nu\beta^-\beta^-$ decay G_{0k} $(k = 1, 2, ...10)$ can be obtained by evaluating the following integrals

$$G_{0k} = \frac{(Gg_A)^4 m_e^9}{64\pi^5 (m_e R)^2 \ln(2)} \int b_{0k} d\Omega_{0\nu} \tag{4.20}$$

where

$$d\Omega_{0\nu} = 2m_e^{-5} p_1 p_2 \varepsilon_1 \varepsilon_2 \delta (\varepsilon_1 + \varepsilon_2 + E_F - E_I) d\varepsilon_1 d\varepsilon_2 \tag{4.21}$$

Using

$$\begin{pmatrix} \alpha_+ \\ \\ \beta_+ \end{pmatrix} = \frac{1}{2} \left(\varepsilon_1 \varepsilon_2 \pm m_e^2\right) C_{00}, \qquad \begin{pmatrix} \alpha_- \\ \\ \beta_- \end{pmatrix} = \frac{1}{2} (\varepsilon_1 \pm \varepsilon_2) m_e C_{00} \tag{4.22}$$

with

$$C_{00} = \frac{F_0 (Z, \varepsilon_1) F_0 (Z, \varepsilon_2)}{\varepsilon_1 \varepsilon_2} \tag{4.23}$$

and integrating Eq. (4.20), one obtains

$$\begin{aligned} G_{0k} &= \frac{2(Gg_A)^4 m_e^4}{64\pi^5 (m_e R)^2 \ln(2)} \int b_{0k} p_1 p_2 \varepsilon_1 \varepsilon_2 d\varepsilon_1 \\ &= \frac{g^{(0\nu)}}{(m_e R)^2} \int b_{0k}\, p_1 p_2 \varepsilon_1 \varepsilon_2 d\varepsilon_1 \end{aligned} \tag{4.24}$$

where

$$g^{(0\nu)} = \frac{(Gg_A)^4 m_e^4}{32\pi^5 \ln(2)} \tag{4.25}$$

and the nuclear radius

$$R = 1.2A^{1/3}\ fm \tag{4.26}$$

The kinematical factors b_{0k} $(k = 1, 2, ...10)$ are written as follows

$$
\begin{aligned}
b_{01} &= \alpha_+ + \beta_+ \\
&= F_0(Z,\varepsilon_1)F_0(Z,\varepsilon_2) && \text{(4.27a)} \\
b_{02} &= \left(\frac{\varepsilon_{12}}{m_e}\right)^2 \beta_+ \\
&= \frac{1}{2}\left(\frac{\varepsilon_1-\varepsilon_2}{m_e}\right)^2 \frac{(\varepsilon_1\varepsilon_2 - m_e^2)}{\varepsilon_1\varepsilon_2} F_0(Z,\varepsilon_1)F_0(Z,\varepsilon_2) && \text{(4.27b)} \\
b_{03} &= 2\left(\frac{\varepsilon_{12}}{m_e}\right)\beta_- \\
&= \frac{(\varepsilon_1-\varepsilon_2)^2}{\varepsilon_1\varepsilon_2} F_0(Z,\varepsilon_1)F_0(Z,\varepsilon_2) && \text{(4.27c)} \\
b_{04} &= \left(\frac{4}{9}\right)\beta_+ \\
&= \frac{2}{9}\frac{(\varepsilon_1\varepsilon_2 - m_e^2)}{\varepsilon_1\varepsilon_2} F_0(Z,\varepsilon_1)F_0(Z,\varepsilon_2) && \text{(4.27d)} \\
b_{05} &= \frac{4}{3}\frac{(\zeta\alpha_- - 2m_eR\alpha_+)}{(m_eR)} \\
&= \frac{2}{3}\frac{1}{\varepsilon_1\varepsilon_2}\left[\frac{\zeta(\varepsilon_1+\varepsilon_2)m_e}{m_eR} - 2(\varepsilon_1\varepsilon_2 + m_e^2)\right] \\
&\quad \times F_0(Z,\varepsilon_1)F_0(Z,\varepsilon_2) && \text{(4.27e)} \\
b_{06} &= \left(\frac{8}{m_eR}\right)\alpha_- \\
&= \frac{4m_e(\varepsilon_1+\varepsilon_2)}{\varepsilon_1\varepsilon_2\,.\,m_eR} F_0(Z,\varepsilon_1)F_0(Z,\varepsilon_2) && \text{(4.27f)} \\
b_{07} &= \frac{16}{3}\frac{(\zeta\alpha_+ - 2m_eR\alpha_-)}{(m_eR)^2} \\
&= \left(\frac{8}{3m_eR}\right)\frac{1}{\varepsilon_1\varepsilon_2}\left[\frac{\zeta(\varepsilon_1\varepsilon_2 + m_e^2)}{m_eR} - 2m_e(\varepsilon_1+\varepsilon_2)\right] \\
&\quad \times F_0(Z,\varepsilon_1)F_0(Z,\varepsilon_2) && \text{(4.27g)} \\
b_{08} &= \frac{4}{3}\frac{\left[\zeta^2\alpha_+ + 4m_e(Rm_eR\alpha_+ - \zeta\alpha_-)\right]}{(m_eR)^2} \\
&= \frac{8}{9}\frac{1}{\varepsilon_1\varepsilon_2}\left[\left\{\frac{1}{4}\left(\frac{\zeta}{m_eR}\right)^2 + 1\right\}(\varepsilon_1\varepsilon_2 + m_e^2) - \right. \\
&\quad \left.\left(\frac{\zeta}{m_eR}\right)(\varepsilon_1+\varepsilon_2)m_e\right] F_0(Z,\varepsilon_1)F_0(Z,\varepsilon_2) && \text{(4.27h)}
\end{aligned}
$$

$$
\begin{aligned}
b_{09} &= \left(\frac{4}{m_e R}\right)^2 \alpha_+ \\
&= \frac{8}{\varepsilon_1 \varepsilon_2} \frac{(\varepsilon_1 \varepsilon_2 + m_e^2)}{(m_e R)^2} F_0(Z, \varepsilon_1) F_0(Z, \varepsilon_2) \qquad (4.27\text{i}) \\
b_{010} &= 2(\alpha_+ - \beta_+) \\
&= \frac{2m_e^2}{\varepsilon_1 \varepsilon_2} F_0(Z, \varepsilon_1) F_0(Z, \varepsilon_2) \qquad (4.27\text{j})
\end{aligned}
$$

where

$$
\zeta = 3\alpha Z + (T+2)\, m_e R \qquad (4.28)
$$

4.2 Results and discussions

In order to estimate average NTMEs M_α and uncertainties ΔM_α statistically, sets of twelve NTMEs are calculated by using Eq. (4.10) employing four different parametrizations of the two body effective interaction, namely $PPQQ1$, $PPQQHH1$, $PPQQ2$, $PPQQHH2$ and three different parametrizations of the SRC due to Miller-Spencer parametrization, Argonne NN and CD-Bonn potentials and are denoted by SRC1, SRC2 and SRC3, respectively. Specifically, sets of twelve NTMEs, namely $M_{\omega F}$, M_{qF}, $M_{\omega GT}$, M_{qGT}, M_{qT}, M_P and M_R are calculated within the approximations of point nucleons (P), nucleons having finite size ((FNS) and also with SRC (FNS+SRC). These values of NTMEs are presented in Table 4.1. The combination of NTMEs $M^{(0\nu)}$ and $M_{i\pm}$ $(i = 1, 2)$ given by Eqs.(4.7,4.8,4.9) are presented in Table 4.2. In Ref. [Rath *et al.* (2013)], NTMEs $M^{(0\nu)}$ have already been calculated. Presently, we reevaluate them for $g_A = 1.2701$

In Table 4.3, the relative changes in NTMEs M_α (in %) due to the different approximations are presented. Due to FNS, the maximum change in $M_{\omega F}$, M_{qF}, $M_{\omega GT}$, M_{qGT},

M_{qT}, M_P and M_R is about 18%, 40%, and 35%, respectively. With the inclusion of SRC, the NTMEs $M_{\omega F,\omega GT}$ change by about 18%, 2.5% and 4% due to SRC1, SRC2 and SRC3, respectively. The observed changes in $M_{qF,qGT}$ with the inclusion of SRC1, SRC2 and SRC3 are of the same order and the maximum change is about 7%. Due to the inclusion of SRC, the change in M_{qT} is about 2% and M_P can change between 2%-18%. The maximum change in M_R due to SRC1, SRC2 and SRC3 is about 57%, 29% and 11%, respectively.

In Table 4.4 and 4.5, the averages and standard deviations of six NTMEs, namely $M_{\omega F,qF}$, $M_{\omega GT,qGT}$, M_P and M_R are presented. It is observed that the maximum uncertainty in $\overline{M}_{\omega F,qF}$, $\overline{M}_{\omega GT,qGT}$ and $\overline{M}_P$ is about 15% but for ^{150}Nd, in which the standard deviation of $\overline{M}_P$ is about 40%. In ^{94}Zr, ^{100}Mo, and ^{110}Pd isotopes, the NTMEs M_{qT} are quite uncertain due to change of sign in the case of $PPQQHH1$, $PPQQHH2$ and $PPQQ2$ parametrizations. The maximum uncertainty in $\overline{M}_R$ is about 30%. Using the phase space factors calculated by Štefánik *et al.* (2015), reevaluated at $g_A = 1.2701$, sets of twelve nuclear structure factors C_{mm}, $C_{m\lambda}$, $C_{m\eta}$, $C_{\lambda\lambda}$, $C_{\lambda\lambda}$ are computed for ^{96}Zr, ^{100}Mo, ^{110}Pd, ^{130}Te and ^{150}Nd isotopes. The averages of these six nuclear structure factors are reported in Table 4.6. To exhibit the relative role of NTMEs due to different mechanisms, we define $M_{eff}^{(0\lambda)}$ and $M_{eff}^{(0\eta)}$ as

$$C_{\lambda\lambda} = G_{01} \left| M_{eff}^{(0\lambda)} \right|^2 \tag{4.29}$$

$$C_{\eta\eta} = G_{01} \left| M_{eff}^{(0\eta)} \right|^2 \tag{4.30}$$

and present the NTMEs $M_{eff}^{(0\lambda)}$ and $M_{eff}^{(0\eta)}$ along with $M^{(0\nu)}$ [Rath *et al.* (2013)] reevaluated for $g_A = 1.2701$ in Table 4.7. It is observed that NTMEs $M_{eff}^{(0\lambda)}$ are about twice of $M^{(0\nu)}$

and NTMEs $M_{eff}^{(0\eta)}$ are larger by two orders in magnitude than the latter.

Using the average nuclear structure factors $\overline{C}_{mm}$, $\overline{C}_{\lambda\lambda}$, $\overline{C}_{\eta\eta}$, on-axis limits on the effective mass of light neutrino $\langle m_\nu \rangle$, the effective weak coupling of right-handed leptonic current with right-handed hadronic current $< \lambda >$, and the effective weak coupling of right-handed leptonic current with left-handed hadronic current $< \eta >$ are extracted from the largest observed limits on half-lives $T_{1/2}^{(0\nu)}$ of $0\nu\beta^-\beta^-$decay and presented in Table 4.8. The extracted limits on $\langle m_\nu \rangle$, $\langle \lambda \rangle$, and $\langle \eta \rangle$ for ^{130}Te (^{100}Mo) nuclei are 0.33 eV (0.38 eV), 4.57×10^{-7} (4.39×10^{-7}) and 4.72×10^{-9} (5.23×10^{-9}), respectively. In the last two columns of the same Table 4.8, the predicted half-lives $T_{1/2}^{(0\nu)}$ of $0\nu\beta^-\beta^-$decay of ^{96}Zr, ^{100}Mo, ^{110}Pd, ^{130}Te and ^{150}Nd isotopes are given for two sets of parameters (i) $\langle m_\nu \rangle = 50$ meV and (ii) $\langle m_\nu \rangle = 50$ meV, $\langle \lambda \rangle = 10^{-7}$ and $\langle \eta \rangle = 10^{-9}$. It is noticed that the predicted half-lives $T_{1/2}^{(0\nu)}$ are smaller for the latter parametrization than those of pure mass mechanism. By defining $\left[T_{1/2}^{(0\nu)}\right]^{-1} = C^{(0\nu)}$, it is seen that in total $C^{(0\nu)}$, the the contribution of mass mechanism is about 13%–17%, the λ-term contributes 23%–57% and the η-term contributes 24%-41%. Further, the contributions of $m\lambda$ and $m\eta$-term are about 7%-8% and 13%–25%, respectively, while the $\lambda\eta$-term contribute less than 1%.

4.2.1 Deformation effect

To quantify the effect of deformation on M_α, the quantity

$$D_\alpha = \frac{M_\alpha(\zeta_{qq} = 0)}{M_\alpha(\zeta_{qq} = 1)} \tag{4.31}$$

has been defined as the ratio of M_α at zero deformation ($\zeta_{qq} = 0$) and full deformation ($\zeta_{qq} = 1$) [Chaturvedi *et al.* (2008)]. In Table 4.9, we tabulate the values of D_α for

$\alpha = \omega F, qF, \omega GT, qGT, qT, P$ and R. In the mass range $A = 90 - 150$, the NTMEs M_α are suppressed by factor of about 2–7 (D_{qT} and D_P are suppressed by a factor of about 25 and 14, respectively) due to deformation effects and hence, a proper consideration of deformation of participating nuclei is quite crucial in the nuclear structure aspects of $0\nu\beta^-\beta^-$ decay.

4.3 CONCLUSIONS

Using HFB wave functions generated with four different parametrization of pairing plus multipolar type of effective two body interaction, and three different parametrizations of Jastrow SRC, sets of twelve NTMEs, namely $M_{\omega F,qF}$, $M_{\omega GT,qGT}$, M_{qT}, M_P, and M_R are calculated to study the $0\nu\beta^-\beta^-$ decay of ^{94,96}Zr, ^{100}Mo, ^{110}Pd, ^{128,130}Te and ^{150}Nd isotopes within mechanisms involving the light Majorana neutrino and right handed $V+A$ current. The effect due to FNS is maximum (about 40%) for $M_{qF,qGT,qT,P}$. Due to SRC1, SRC2 and SRC3, the maximum change in M_R is about 57%, 29% and 11%, respectively. Effects due to deformation reduce the NTMEs by a factor of 2–7.

The maximum uncertainty in $M_{\omega F,qF}$, $M_{\omega GT,qGT}$ and M_P is about 15% albeit the standard deviation of M_P for ^{150}Nd is about 40%. In the case of M_R, the maximum uncertainty is about 30%. The NTMEs M_{qT} are quite uncertain. Using the average nuclear structure factors $\overline{C}_{mm}$, $\overline{C}_{\lambda\lambda}$, and $\overline{C}_{\eta\eta}$, the most stringent on-axis extracted limits on $\langle m_\nu \rangle$, $\langle \lambda \rangle$, and $\langle \eta \rangle$ from the largest observed limits on half-lives $T^{0\nu}_{1/2}$ of ^{130}Te isotope are 0.33 eV, 4.57×10^{-7} and 4.72×10^{-9}, respectively.

Table 4.1: Theoretically calculated NTMEs M_α ($\alpha = \omega F$, qF, ωGT, qGT, qT, P, R) with the inclusion of SRC (SRC1, SRC2 and SRC3).

Nuclei	Parametrization	NTME	P	F	F+S		
					SRC1	SRC2	SRC3
^{94}Zr	*PPQQ*1	$M_{\omega F}$	0.786	0.663	0.566	0.659	0.686
		M_{qF}	1.021	0.693	0.663	0.724	0.730
		$M_{\omega GT}$	-3.885	-3.485	-2.919	-3.414	-3.576
		M_{qGT}	-5.136	-4.008	-3.743	-4.145	-4.208
		M_{qT}	0.066	0.064	0.064	0.064	0.064
		M_P	2.935	2.604	2.524	2.707	2.726
		M_R	-5.527	-3.653	-1.600	-2.591	-3.250
	*PPQQHH*1	$M_{\omega F}$	0.709	0.595	0.505	0.590	0.616
		M_{qF}	0.917	0.616	0.587	0.643	0.649
		$M_{\omega GT}$	-3.598	-3.226	-2.701	-3.160	-3.311
		M_{qGT}	-4.736	-3.689	-3.443	-3.816	-3.874
		M_{qT}	0.050	0.049	0.049	0.049	0.049
		M_P	2.660	2.360	2.290	2.451	2.468
		M_R	-5.137	-3.389	-1.483	-2.402	-3.014
	*PPQQ*2	$M_{\omega F}$	0.645	0.544	0.463	0.540	0.562
		M_{qF}	0.838	0.568	0.542	0.592	0.598
		$M_{\omega GT}$	-3.688	-3.355	-2.887	-3.306	-3.441
		M_{qGT}	-5.026	-4.077	-3.862	-4.203	-4.254
		M_{qT}	-0.088	-0.087	-0.087	-0.087	-0.087
		M_P	2.451	2.114	2.023	2.218	2.239
		M_R	-4.561	-3.087	-1.373	-2.209	-2.758
	*PPQQHH*2	$M_{\omega F}$	0.680	0.571	0.484	0.566	0.591
		M_{qF}	0.880	0.590	0.562	0.616	0.622
		$M_{\omega GT}$	-3.423	-3.066	-2.561	-3.001	-3.146
		M_{qGT}	-4.501	-3.496	-3.259	-3.617	-3.673
		M_{qT}	0.061	0.059	0.059	0.059	0.059
		M_P	2.559	2.274	2.207	2.360	2.376
		M_R	-4.938	-3.252	-1.421	-2.303	-2.891

Table 4.1 continued

Nuclei	Parametrization	NTME	P	F	F+S		
					SRC1	SRC2	SRC3
^{96}Zr	$PPQQ1$	$M_{\omega F}$	0.593	0.499	0.425	0.496	0.517
		M_{qF}	0.770	0.519	0.496	0.542	0.547
		$M_{\omega GT}$	-2.792	-2.487	-2.054	-2.429	-2.553
		M_{qGT}	-3.713	-2.858	-2.651	-2.957	-3.005
		M_{qT}	0.076	0.073	0.074	0.073	0.073
		M_{P}	2.508	2.236	2.169	2.325	2.341
		M_{R}	-4.245	-2.783	-1.211	-1.967	-2.472
	$PPQQHH1$	$M_{\omega F}$	0.549	0.452	0.375	0.448	0.470
		M_{qF}	0.686	0.428	0.403	0.451	0.457
		$M_{\omega GT}$	-2.849	-2.531	-2.081	-2.470	-2.599
		M_{qGT}	-3.757	-2.869	-2.654	-2.971	-3.021
		M_{qT}	0.026	0.023	0.024	0.024	0.024
		M_{P}	2.683	2.383	2.309	2.477	2.495
		M_{R}	-4.416	-2.890	-1.256	-2.041	-2.566
	$PPQQ2$	$M_{\omega F}$	.567	.477	.406	.474	.494
		M_{qF}	.736	.495	.472	.517	.522
		$M_{\omega GT}$	-2.673	-2.380	-1.963	-2.323	-2.443
		M_{qGT}	-3.551	-2.729	-2.530	-2.823	-2.870
		M_{qT}	0.075	0.072	0.073	0.072	0.072
		M_{P}	2.408	2.147	2.083	2.232	2.247
		M_{R}	-4.082	-2.675	-1.163	-1.890	-2.375
	$PPQQHH2$	$M_{\omega F}$	0.518	0.427	0.353	0.422	0.443
		M_{qF}	0.647	0.403	0.379	0.425	0.430
		$M_{\omega GT}$	-2.680	-2.380	-1.952	-2.321	-2.443
		M_{qGT}	-3.531	-2.689	-2.485	-2.786	-2.833
		M_{qT}	0.032	0.030	0.030	0.030	0.030
		M_{P}	2.533	2.251	2.181	2.340	2.356
		M_{R}	-4.187	-2.737	-1.189	-1.932	-2.429

Table 4.1 continued

Nuclei	Parametrization	NTME	P	F	F+S		
					SRC1	SRC2	SRC3
^{100}Mo	$PPQQ1$	$M_{\omega F}$	1.319	1.131	0.984	1.128	1.170
		M_{qF}	1.741	1.228	1.184	1.279	1.289
		$M_{\omega GT}$	-6.039	-5.427	-4.570	-5.337	-5.583
		M_{qGT}	-8.008	-6.269	-5.871	-6.498	-6.591
		M_{qT}	0.121	0.117	0.117	0.117	0.117
		M_{P}	4.454	3.944	3.797	4.130	4.164
		M_{R}	-8.519	-5.772	-2.567	-4.131	-5.157
	$PPQQHH1$	$M_{\omega F}$	1.180	0.996	0.851	0.992	1.033
		M_{qF}	1.507	1.008	.964	1.057	1.066
		$M_{\omega GT}$	-5.890	-5.290	-4.447	-5.199	-5.441
		M_{qGT}	-7.777	-6.070	-5.678	-6.293	-6.385
		M_{qT}	-0.016	-0.019	-0.019	-0.019	-0.019
		M_{P}	4.557	4.019	3.868	4.206	4.241
		M_{R}	-8.380	-5.663	-2.515	-4.049	-5.058
	$PPQQ2$	$M_{\omega F}$	1.325	1.136	.988	1.133	1.175
		M_{qF}	1.749	1.233	1.189	1.284	1.294
		$M_{\omega GT}$	-6.086	-5.470	-4.607	-5.379	-5.627
		M_{qGT}	-8.073	-6.323	-5.923	-6.554	-6.648
		M_{qT}	0.115	0.111	0.112	0.112	0.112
		M_{P}	4.477	3.963	3.814	4.149	4.184
		M_{R}	-8.574	-5.809	-2.583	-4.157	-5.190
	$PPQQHH2$	$M_{\omega F}$	1.066	0.899	0.767	0.895	0.932
		M_{qF}	1.361	0.908	0.867	0.951	0.960
		$M_{\omega GT}$	-5.327	-4.781	-4.015	-4.699	-4.919
		M_{qGT}	-7.019	-5.467	-5.111	-5.670	-5.754
		M_{qT}	-0.007	-0.009	-0.009	-0.009	-0.009
		M_{P}	4.084	3.600	3.462	3.770	3.802
		M_{R}	-7.616	-5.150	-2.288	-3.684	-4.600

Table 4.1 continued

Nuclei	Parametrization	NTME	P	F	F+S		
					SRC1	SRC2	SRC3
^{110}Pd	$PPQQ1$	$M_{\omega F}$	1.498	1.280	1.109	1.276	1.325
		M_{qF}	2.018	1.421	1.369	1.480	1.491
		$M_{\omega GT}$	-7.057	-6.346	-5.349	-6.243	-6.528
		M_{qGT}	-9.604	-7.574	-7.107	-7.843	-7.952
		M_{qT}	0.140	0.134	0.134	0.134	0.134
		M_P	5.447	4.830	4.659	5.054	5.093
		M_R	-10.217	-6.954	-3.096	-4.982	-6.217
	$PPQQHH1$	$M_{\omega F}$	1.179	0.985	0.833	0.980	1.023
		M_{qF}	1.524	0.999	0.952	1.050	1.060
		$M_{\omega GT}$	-6.111	-5.479	-4.593	-5.385	-5.639
		M_{qGT}	-8.238	-6.435	-6.020	-6.673	-6.770
		M_{qT}	-0.028	-0.032	-0.032	-0.032	-0.032
		M_P	5.251	4.647	4.481	4.861	4.899
		M_R	-9.081	-6.173	-2.746	-4.420	-5.518
	$PPQQ2$	$M_{\omega F}$	1.434	1.225	1.061	1.222	1.268
		M_{qF}	1.935	1.364	1.313	1.420	1.431
		$M_{\omega GT}$	-6.767	-6.085	-5.130	-5.985	-6.259
		M_{qGT}	-9.215	-7.269	-6.822	-7.527	-7.631
		M_{qT}	0.133	0.127	0.127	0.127	0.127
		M_P	5.159	4.570	4.406	4.782	4.819
		M_R	-9.798	-6.662	-2.964	-4.771	-5.955
	$PPQQHH2$	$M_{\omega F}$	1.284	1.084	0.928	1.080	1.124
		M_{qF}	1.699	1.158	1.110	1.211	1.221
		$M_{\omega GT}$	-6.365	-5.715	-4.804	-5.618	-5.879
		M_{qGT}	-8.622	-6.769	-6.342	-7.013	-7.113
		M_{qT}	0.034	0.030	0.030	0.030	0.030
		M_P	5.062	4.476	4.316	4.683	4.720
		M_R	-9.348	-6.343	-2.819	-4.539	-5.668

Table 4.1 continued

Nuclei	Parametrization	NTME	P	F	F+S		
					SRC1	SRC2	SRC3
^{128}Te	$PPQQ1$	$M_{\omega F}$	0.662	0.565	0.489	0.562	0.583
		M_{qF}	0.922	0.658	0.634	0.683	0.688
		$M_{\omega GT}$	-2.987	-2.670	-2.224	-2.616	-2.743
		M_{qGT}	-4.069	-3.163	-2.950	-3.276	-3.326
		M_{qT}	0.212	0.211	0.211	0.211	0.211
		M_{P}	1.037	.863	.816	.914	.924
		M_{R}	-4.860	-3.249	-1.427	-2.310	-2.894
	$PPQQHH1$	$M_{\omega F}$	0.706	0.589	0.497	0.585	0.611
		M_{qF}	0.943	0.628	0.598	0.657	0.663
		$M_{\omega GT}$	-3.411	-3.028	-2.491	-2.965	-3.119
		M_{qGT}	-4.525	-3.431	-3.175	-3.570	-3.629
		M_{qT}	0.172	0.171	0.171	0.171	0.171
		M_{P}	1.439	1.217	1.160	1.282	1.295
		M_{R}	-5.850	-3.930	-1.734	-2.800	-3.504
	$PPQQ2$	$M_{\omega F}$	0.772	0.661	0.573	0.657	0.682
		M_{qF}	1.078	0.774	0.747	0.803	0.809
		$M_{\omega GT}$	-3.539	-3.174	-2.663	-3.115	-3.261
		M_{qGT}	-4.846	-3.803	-3.561	-3.936	-3.993
		M_{qT}	0.193	0.192	0.192	0.192	0.192
		M_{P}	1.220	1.023	.972	1.079	1.091
		M_{R}	-5.572	-3.745	-1.651	-2.668	-3.340
	$PPQQHH2$	$M_{\omega F}$	0.745	0.627	0.533	0.622	0.649
		M_{qF}	1.010	0.688	0.659	0.718	0.725
		$M_{\omega GT}$	-3.561	-3.172	-2.626	-3.107	-3.264
		M_{qGT}	-4.777	-3.665	-3.406	-3.806	-3.867
		M_{qT}	0.182	0.182	0.182	0.182	0.182
		M_{P}	1.377	1.158	1.102	1.220	1.233
		M_{R}	-5.945	-3.991	-1.759	-2.842	-3.557

Table 4.1 continued

Nuclei	Parametrization	NTME	P	F	F+S		
					SRC1	SRC2	SRC3
^{130}Te	$PPQQ1$	$M_{\omega F}$	0.849	0.732	0.641	0.730	0.755
		M_{qF}	1.198	0.879	0.851	0.910	0.916
		$M_{\omega GT}$	-3.931	-3.549	-3.016	-3.493	-3.646
		M_{qGT}	-5.454	-4.354	-4.105	-4.502	-4.561
		M_{qT}	0.089	0.090	0.090	0.090	0.090
		M_{P}	1.658	1.429	1.371	1.499	1.512
		M_{R}	-5.845	-3.976	-1.766	-2.845	-3.553
	$PPQQHH1$	$M_{\omega F}$	0.722	0.607	0.517	0.603	0.629
		M_{qF}	0.975	0.663	0.634	0.692	0.698
		$M_{\omega GT}$	-3.466	-3.089	-2.562	-3.031	-3.182
		M_{qGT}	-4.637	-3.555	-3.306	-3.697	-3.755
		M_{qT}	0.078	0.079	0.079	0.079	0.079
		M_{P}	1.709	1.475	1.416	1.547	1.561
		M_{R}	-5.776	-3.912	-1.735	-2.795	-3.493
	$PPQQ2$	$M_{\omega F}$	0.835	0.720	0.630	0.717	0.743
		M_{qF}	1.178	0.863	0.835	0.893	0.899
		$M_{\omega GT}$	-3.873	-3.496	-2.970	-3.441	-3.592
		M_{qGT}	-5.372	-4.286	-4.040	-4.432	-4.490
		M_{qT}	0.089	0.089	0.089	0.089	0.089
		M_{P}	1.626	1.402	1.346	1.470	1.483
		M_{R}	-5.773	-3.926	-1.743	-2.809	-3.508
	$PPQQHH2$	$M_{\omega F}$	0.720	0.606	0.516	0.602	0.627
		M_{qF}	0.973	0.662	0.634	0.692	0.698
		$M_{\omega GT}$	-3.456	-3.080	-2.555	-3.023	-3.173
		M_{qGT}	-4.628	-3.550	-3.302	-3.691	-3.749
		M_{qT}	0.079	0.079	0.079	0.079	0.079
		M_{P}	1.692	1.460	1.402	1.531	1.545
		M_{R}	-5.751	-3.894	-1.727	-2.783	-3.477

Table 4.1 continued

Nuclei	Parametrization	NTME	P	F	F+S		
					SRC1	SRC2	SRC3
^{150}Nd	$PPQQ1$	$M_{\omega F}$	0.618	0.537	0.475	0.537	0.554
		M_{qF}	0.877	0.651	0.632	0.674	0.678
		$M_{\omega GT}$	-2.795	-2.530	-2.164	-2.496	-2.602
		M_{qGT}	-3.955	-3.184	-3.013	-3.293	-3.334
		M_{qT}	0.044	0.043	0.043	0.043	0.043
		M_{P}	0.483	0.351	0.319	0.380	0.387
		M_{R}	-4.232	-2.925	-1.309	-2.103	-2.620
	$PPQQHH1$	$M_{\omega F}$	0.465	0.400	0.350	0.399	0.413
		M_{qF}	0.638	0.457	0.442	0.475	0.479
		$M_{\omega GT}$	-2.150	-1.938	-1.644	-1.910	-1.994
		M_{qGT}	-3.018	-2.403	-2.265	-2.488	-2.521
		M_{qT}	0.021	0.020	0.020	0.020	0.020
		M_{P}	0.226	0.130	0.107	0.149	0.153
		M_{R}	-3.390	-2.334	-1.043	-1.676	-2.090
	$PPQQ2$	$M_{\omega F}$	0.605	0.526	0.465	0.525	0.543
		M_{qF}	0.859	0.637	0.619	0.660	0.664
		$M_{\omega GT}$	-2.732	-2.473	-2.114	-2.440	-2.543
		M_{qGT}	-3.863	-3.109	-2.941	-3.215	-3.255
		M_{qT}	0.044	0.043	0.043	0.043	0.043
		M_{P}	0.466	0.339	0.309	0.367	0.373
		M_{R}	-4.141	-2.863	-1.281	-2.058	-2.564
	$PPQQHH2$	$M_{\omega F}$	0.481	0.415	0.364	0.414	0.429
		M_{qF}	0.668	0.484	0.469	0.503	0.507
		$M_{\omega GT}$	-2.203	-1.989	-1.692	-1.961	-2.046
		M_{qGT}	-3.099	-2.476	-2.337	-2.563	-2.596
		M_{qT}	0.027	0.026	0.026	0.026	0.026
		M_{P}	0.284	0.184	0.160	0.204	0.209
		M_{R}	-3.428	-2.365	-1.057	-1.699	-2.117

Table 4.2: Combination of NTMEs $M^{(0\nu)}$ and $M_{i\pm}$ $(i = 1, 2)$. The values of $M^{(0\nu)}$ have been taken from Rath *et al.* (2013) and reevaluated at $g_A = 1.2701$.

Nuclei	Parametrization		P	F	F+S		
					SRC1	SRC2	SRC3
^{94}Zr	$PPQQ1$	$M^{(0\nu)}$	-4.788	-4.287	-3.659	-4.214	-4.395
		M_{1+}	-2.470	-2.310	-2.138	-2.358	-2.400
		M_{1-}	-8.595	-6.471	-6.116	-6.699	-6.781
		M_{2+}	-2.145	-2.102	-1.673	-2.011	-2.137
		M_{2-}	-4.397	-3.891	-3.247	-3.810	-3.996
	$PPQQHH1$	$M^{(0\nu)}$	-4.403	-3.936	-3.353	-3.867	-4.035
		M_{1+}	-2.287	-2.135	-1.977	-2.182	-2.221
		M_{1-}	-7.790	-5.829	-5.499	-6.038	-6.114
		M_{2+}	-2.024	-1.983	-1.585	-1.899	-2.016
		M_{2-}	-4.052	-3.584	-2.986	-3.507	-3.680
	$PPQQ2$	$M^{(0\nu)}$	-4.595	-4.167	-3.649	-4.117	-4.267
		M_{1+}	-1.985	-1.854	-1.715	-1.906	-1.941
		M_{1-}	-7.011	-5.261	-4.968	-5.460	-5.527
		M_{2+}	-2.264	-2.226	-1.872	-2.160	-2.264
		M_{2-}	-4.113	-3.693	-3.160	-3.634	-3.788
	$PPQQHH2$	$M^{(0\nu)}$	-4.187	-3.739	-3.179	-3.672	-3.833
		M_{1+}	-2.228	-2.082	-1.929	-2.126	-2.164
		M_{1-}	-7.506	-5.621	-5.303	-5.821	-5.894
		M_{2+}	-1.909	-1.870	-1.488	-1.789	-1.901
		M_{2-}	-3.856	-3.406	-2.831	-3.331	-3.497

Table 4.2 continued

Nuclei	Parametrization		P	F	F+S		
					SRC1	SRC2	SRC3
^{96}Zr	$PPQQ1$	$M^{(0\nu)}$	-3.470	-3.092	-2.610	-3.032	-3.170
		M_{1+}	-1.861	-1.739	-1.605	-1.771	-1.803
		M_{1-}	-6.479	-4.854	-4.579	-5.024	-5.087
		M_{2+}	-1.479	-1.448	-1.120	-1.375	-1.471
		M_{2-}	-3.178	-2.793	-2.300	-2.728	-2.869
	$PPQQHH1$	$M^{(0\nu)}$	-3.46	-3.064	-2.563	-3.000	-3.144
		M_{1+}	-1.855	-1.723	-1.586	-1.758	-1.792
		M_{1-}	-5.968	-4.294	-4.005	-4.466	-4.532
		M_{2+}	-1.636	-1.602	-1.261	-1.526	-1.626
		M_{2-}	-3.192	-2.792	-2.279	-2.722	-2.869
	$PPQQ2$	$M^{(0\nu)}$	-3.318	-2.955	-2.491	-2.897	-3.029
		M_{1+}	-1.794	-1.677	-1.548	-1.707	-1.738
		M_{1-}	-6.208	-4.646	-4.382	-4.809	-4.870
		M_{2+}	-1.416	-1.386	-1.070	-1.315	-1.407
		M_{2-}	-3.041	-2.671	-2.196	-2.608	-2.744
	$PPQQHH2$	$M^{(0\nu)}$	-3.251	-2.877	-2.402	-2.816	-2.952
		M_{1+}	-1.784	-1.659	-1.528	-1.691	-1.724
		M_{1-}	-5.665	-4.078	-3.804	-4.240	-4.303
		M_{2+}	-1.532	-1.500	-1.177	-1.428	-1.522
		M_{2-}	-3.000	-2.622	-2.135	-2.555	-2.695

Table 4.2 continued

Nuclei	Parametrization		P	F	F+S		
					SRC1	SRC2	SRC3
^{100}Mo	$PPQQ1$	$M^{(0\nu)}$	-7.550	-6.790	-5.838	-6.701	-6.975
		M_{1+}	-3.511	-3.286	-3.023	-3.364	-3.428
		M_{1-}	-13.956	-10.654	-10.127	-11.038	-11.161
		M_{2+}	-3.169	-3.113	-2.461	-2.982	-3.173
		M_{2-}	-6.968	-6.193	-5.218	-6.092	-6.372
	$PPQQHH1$	$M^{(0\nu)}$	-7.244	-6.490	-5.554	-6.399	-6.668
		M_{1+}	-3.157	-2.931	-2.674	-3.011	-3.074
		M_{1-}	-12.201	-8.981	-8.458	-9.351	-9.472
		M_{2+}	-3.354	-3.296	-2.656	-3.168	-3.356
		M_{2-}	-6.720	-5.960	-5.001	-5.856	-6.132
	$PPQQ2$	$M^{(0\nu)}$	-7.609	-6.844	-5.886	-6.753	-7.029
		M_{1+}	-3.518	-3.291	-3.027	-3.370	-3.435
		M_{1-}	-14.011	-10.689	-10.158	-11.076	-11.199
		M_{2+}	-3.204	-3.147	-2.491	-3.016	-3.208
		M_{2-}	-7.020	-6.240	-5.259	-6.138	-6.420
	$PPQQHH2$	$M^{(0\nu)}$	-6.537	-5.852	-5.001	-5.769	-6.014
		M_{1+}	-2.896	-2.690	-2.457	-2.763	-2.821
		M_{1-}	-11.062	-8.135	-7.660	-8.471	-8.581
		M_{2+}	-3.032	-2.978	-2.397	-2.863	-3.033
		M_{2-}	-6.071	-5.380	-4.509	-5.287	-5.537

Table 4.2 continued

Nuclei	Parametrization		P	F	F+S		
					SRC1	SRC2	SRC3
^{110}Pd	$PPQQ1$	$M^{(0\nu)}$	-8.928	-8.050	-6.939	-7.946	-8.265
		M_{1+}	-4.391	-4.113	-3.807	-4.208	-4.283
		M_{1-}	-16.499	-12.639	-12.020	-13.089	-13.232
		M_{2+}	-3.726	-3.662	-2.905	-3.512	-3.733
		M_{2-}	-8.068	-7.169	-6.035	-7.052	-7.377
	$PPQQHH1$	$M^{(0\nu)}$	-7.560	-6.773	-5.785	-6.678	-6.961
		M_{1+}	-3.499	-3.244	-2.975	-3.333	-3.399
		M_{1-}	-12.640	-9.240	-8.684	-9.631	-9.759
		M_{2+}	-3.527	-3.467	-2.795	-3.335	-3.532
		M_{2-}	-6.900	-6.103	-5.095	-5.995	-6.284
	$PPQQ2$	$M^{(0\nu)}$	-8.566	-7.724	-6.659	-7.623	-7.929
		M_{1+}	-4.205	-3.939	-3.646	-4.030	-4.102
		M_{1-}	-15.816	-12.120	-11.526	-12.551	-12.687
		M_{2+}	-3.575	-3.514	-2.788	-3.369	-3.581
		M_{2-}	-7.734	-6.873	-5.785	-6.759	-7.071
	$PPQQHH2$	$M^{(0\nu)}$	-7.970	-7.160	-6.145	-7.062	-7.353
		M_{1+}	-3.730	-3.473	-3.194	-3.562	-3.630
		M_{1-}	-13.923	-10.422	-9.852	-10.825	-10.956
		M_{2+}	-3.534	-3.473	-2.782	-3.336	-3.538
		M_{2-}	-7.234	-6.414	-5.377	-6.302	-6.599

Table 4.2 continued

Nuclei	Parametrization		P	F	F+S		
					SRC1	SRC2	SRC3
^{128}Te	$PPQQ1$	$M^{(0\nu)}$	-3.786	-3.388	-2.889	-3.333	-3.477
		M_{1+}	-2.573	-2.451	-2.312	-2.491	-2.525
		M_{1-}	-8.106	-6.401	-6.117	-6.590	-6.655
		M_{2+}	-1.425	-1.394	-1.055	-1.322	-1.421
		M_{2-}	-3.363	-2.962	-2.455	-2.901	-3.046
	$PPQQHH1$	$M^{(0\nu)}$	-4.187	-3.704	-3.103	-3.639	-3.812
		M_{1+}	-2.725	-2.575	-2.409	-2.627	-2.668
		M_{1-}	-8.385	-6.341	-5.997	-6.568	-6.647
		M_{2+}	-1.774	-1.734	-1.327	-1.650	-1.769
		M_{2-}	-3.814	-3.331	-2.720	-3.258	-3.433
	$PPQQ2$	$M^{(0\nu)}$	-4.506	-4.047	-3.476	-3.988	-4.152
		M_{1+}	-2.768	-2.629	-2.471	-2.677	-2.716
		M_{1-}	-9.234	-7.276	-6.953	-7.497	-7.571
		M_{2+}	-1.740	-1.705	-1.317	-1.624	-1.738
		M_{2-}	-4.003	-3.542	-2.962	-3.475	-3.641
	$PPQQHH2$	$M^{(0\nu)}$	-4.422	-3.931	-3.321	-3.865	-4.041
		M_{1+}	-2.843	-2.692	-2.523	-2.744	-2.785
		M_{1-}	-8.900	-6.822	-6.474	-7.053	-7.133
		M_{2+}	-1.827	-1.787	-1.374	-1.701	-1.822
		M_{2-}	-3.990	-3.499	-2.879	-3.425	-3.603

Table 4.2 continued

Nuclei	Parametrization		P	F	F+S		
					SRC1	SRC2	SRC3
^{130}Te	$PPQQ1$	$M^{(0\nu)}$	-5.088	-4.602	-4.007	-4.547	-4.718
		M_{1+}	-2.395	-2.255	-2.090	-2.310	-2.350
		M_{1-}	-9.586	-7.529	-7.196	-7.770	-7.847
		M_{2+}	-2.017	-1.980	-1.575	-1.900	-2.019
		M_{2-}	-4.514	-4.031	-3.425	-3.966	-4.140
	$PPQQHH1$	$M^{(0\nu)}$	-4.320	-3.840	-3.251	-3.782	-3.951
		M_{1+}	-2.183	-2.040	-1.877	-2.093	-2.133
		M_{1-}	-8.033	-6.017	-5.682	-6.246	-6.323
		M_{2+}	-1.852	-1.813	-1.414	-1.734	-1.851
		M_{2-}	-3.946	-3.469	-2.870	-3.401	-3.573
	$PPQQ2$	$M^{(0\nu)}$	-5.010	-4.530	-3.942	-4.475	-4.645
		M_{1+}	-2.369	-2.231	-2.068	-2.285	-2.325
		M_{1-}	-9.438	-7.407	-7.078	-7.645	-7.721
		M_{2+}	-1.989	-1.953	-1.553	-1.874	-1.991
		M_{2-}	-4.445	-3.968	-3.370	-3.904	-4.076
	$PPQQHH2$	$M^{(0\nu)}$	-4.311	-3.833	-3.246	-3.774	-3.943
		M_{1+}	-2.181	-2.038	-1.876	-2.091	-2.131
		M_{1-}	-8.020	-6.012	-5.679	-6.241	-6.318
		M_{2+}	-1.845	-1.807	-1.409	-1.727	-1.844
		M_{2-}	-3.934	-3.459	-2.863	-3.392	-3.563

Table 4.2 continued

Nuclei	Parametrization		P	F	F+S		
					SRC1	SRC2	SRC3
^{150}Nd	$PPQQ1$	$M^{(0\nu)}$	-3.658	-3.326	-2.915	-3.293	-3.412
		M_{1+}	-1.585	-1.489	-1.374	-1.528	-1.556
		M_{1-}	-6.849	-5.394	-5.168	-5.573	-5.626
		M_{2+}	-1.416	-1.394	-1.115	-1.341	-1.422
		M_{2-}	-3.237	-2.902	-2.486	-2.863	-2.983
	$PPQQHH1$	$M^{(0\nu)}$	-2.772	-2.507	-2.178	-2.480	-2.575
		M_{1+}	-1.232	-1.154	-1.062	-1.185	-1.208
		M_{1-}	-5.060	-3.896	-3.714	-4.037	-4.080
		M_{2+}	-1.123	-1.105	-.882	-1.062	-1.127
		M_{2-}	-2.478	-2.209	-1.876	-2.177	-2.273
	$PPQQ2$	$M^{(0\nu)}$	-3.574	-3.249	-2.847	-3.217	-3.333
		M_{1+}	-1.551	-1.457	-1.345	-1.495	-1.523
		M_{1-}	-6.704	-5.280	-5.058	-5.455	-5.507
		M_{2+}	-1.382	-1.361	-1.087	-1.308	-1.388
		M_{2-}	-3.165	-2.837	-2.430	-2.799	-2.916
	$PPQQHH2$	$M^{(0\nu)}$	-2.854	-2.586	-2.253	-2.559	-2.655
		M_{1+}	-1.259	-1.180	-1.087	-1.212	-1.234
		M_{1-}	-5.265	-4.087	-3.903	-4.231	-4.273
		M_{2+}	-1.138	-1.120	-.894	-1.076	-1.142
		M_{2-}	-2.544	-2.273	-1.935	-2.241	-2.338

Table 4.3: Change in the NTME M_α of $0\nu\beta^-\beta^-$decay (in %) due to the exchange of light Majorana neutrino, and admixture of $V-A$ and $V+A$ currents, with the inclusion of FNS and SRC (SRC1, SRC2, and SRC3) for all four parametrizations of the effective two-body interaction.

NTME	FNS	FNS+SRC		
		SRC1	SRC2	SRC3
$M_{\omega F}$	13.1–17.7	11.6–17.3	0.1–1.1	3.1–3.8
M_{qF}	25.8–37.7	2.9–5.9	3.5–5.3	4.2–6.6
$M_{\omega GT}$	9.0–11.2	13.9–18.0	1.3–2.5	2.6–3.0
M_{qGT}	18.9–24.2	5.3–7.6	3.1–4.0	4.3–5.8
M_{qT}	0.2–34.2	0.0–2.4	0.0–2.3	0.0–2.0
M_P	10.8–42.5	2.9–17.8	3.8–14.1	4.5–17.9
M_R	30.9–34.6	55.2–56.6	28.1–29.4	10.4–11.2

Table 4.4: Average values for NTMEs $\overline{M}_\alpha$ (uncertainty $\Delta\overline{M}_\alpha$) ($\alpha = \omega F$, qF, ωGT, qGT) for the $0\nu\beta^-\beta^-$ decay of ^{94,96}Zr, ^{100}Mo, ^{110}Pd, ^{128,130}Te and ^{150}Nd isotopes.

Nuclei	$M_{\omega F}$	M_{qF}	$M_{\omega GT}$	M_{qGT}
^{94}Zr	0.569(0 .066)	0.627(0 .058)	-3.119(0 .312)	-3.841(0 .318)
^{96}Zr	0.443(0.050)	0.470(0.055)	-2.303(0.230)	-2.799(0.183)
^{100}Mo	1.004(0.130)	1.115(0.156)	-4.985(0.516)	-6.081(0.483)
^{110}Pd	1.102(0.150)	1.259(0.185)	-5.618(0.596)	-7.068(0.591)
^{128}Te	0.587(0.061)	0.699(0.065)	-2.849(0.335)	-3.541(0.325)
^{130}Te	0.642(0.081)	0.779(0.114)	-3.140(0.360)	-3.969(0.455)
^{150}Nd	0.456(0.071)	0.567(0.094)	-2.134(0.324)	-2.819(0.398)

Table 4.5: Average values for NTMEs $\overline{M}_\alpha$ (uncertainty $\Delta\overline{M}_\alpha$) ($\alpha = qT$, P, R) for the $0\nu\beta^-\beta^-$ decay of ^{94,96}Zr, ^{100}Mo, ^{110}Pd, ^{128,130}Te and ^{150}Nd isotopes.

Nuclei	M_{qT}	M_P	M_R
^{94}Zr	0.021(0.065)	2.382(0.207)	-2.274(0 .664)
^{96}Zr	0.050(0.024)	2.296(0.121)	-1.874(0.542)
^{100}Mo	0.050(0.067)	3.966(0.245)	-3.832(1.097)
^{110}Pd	0.065(0.073)	4.731(0.241)	-4.474(1.279)
^{128}Te	0.189(0.015)	1.091(0.156)	-2.541(0.753)
^{130}Te	0.084(0.005)	1.474(0.073)	-2.686(0.758)
^{150}Nd	0.033(0.011)	0.260(0.106)	-1.801(0.545)

Table 4.6: Average nuclear structure factors $\overline{C}_{mm}$, $\overline{C}_{m\lambda}$, $\overline{C}_{m\eta}$, $\overline{C}_{\lambda\lambda}$, and $\overline{C}_{\eta\eta}$ for the $0\nu\beta^-\beta^-$ decay of ^{96}Zr, ^{100}Mo, ^{110}Pd, ^{130}Te and ^{150}Nd isotopes.

Nuclei	C_{mm}	$C_{m\lambda}$	$C_{m\eta}$	$C_{\lambda\lambda}$	$C_{\eta\eta}$	$C_{\lambda\eta}$
^{96}Zr	4.37×10^{-13}	-2.26×10^{-13}	5.02×10^{-11}	1.51×10^{-12}	1.15×10^{-8}	-1.54×10^{-12}
^{100}Mo	1.62×10^{-12}	-8.45×10^{-13}	1.80×10^{-10}	4.76×10^{-12}	3.52×10^{-8}	-4.63×10^{-12}
^{110}Pd	6.42×10^{-13}	-2.48×10^{-13}	9.14×10^{-11}	8.21×10^{-13}	1.45×10^{-8}	-7.76×10^{-13}
^{130}Te	6.09×10^{-13}	-2.69×10^{-13}	6.97×10^{-11}	1.21×10^{-12}	1.19×10^{-8}	-1.10×10^{-12}
^{150}Nd	1.32×10^{-12}	-6.85×10^{-13}	1.05×10^{-10}	4.55×10^{-12}	1.89×10^{-8}	-4.08×10^{-12}

Table 4.7: Effective NTMEs $M_{eff}^{(0\lambda)}$ and $M_{eff}^{(0\eta)}$ along with $M^{(0\nu)}$ for the $0\nu\beta^-\beta^-$ decay of ^{96}Zr, ^{100}Mo, ^{110}Pd, ^{130}Te and ^{150}Nd isotopes.

Nuclei	$M^{(0\nu)}$	$M_{eff}^{(0\lambda)}$	$M_{eff}^{(0\eta)}$
^{96}Zr	2.85	5.30	463.07
^{100}Mo	6.25	10.71	920.40
^{110}Pd	7.15	8.08	1072.80
^{130}Te	4.05	5.71	567.26
^{150}Nd	2.84	5.26	338.85

Table 4.8: Experimental limits on half-lives $T_{1/2}^{(0\nu)}$ and the extracted on-axis limits on the effective mass of light neutrino $\langle m_\nu \rangle$, $\langle \lambda \rangle$, and $\langle \eta \rangle$ for the $0\nu\beta^-\beta^-$ decay of ^{96}Zr, ^{100}Mo, ^{110}Pd, ^{130}Te and ^{150}Nd isotopes. Predicted half-lives $T_{1/2}^{(0\nu)}$ of $0\nu\beta^-\beta^-$decay for two sets of parameters (i) $\langle m_\nu \rangle = 50$ meV (Case I) and (ii) $\langle m_\nu \rangle = 50$ meV, $\langle \lambda \rangle = 10^{-7}$ and $\langle \eta \rangle = 10^{-9}$ (Case II).

Nuclei	$T_{1/2}^{(0\nu)}$(Ex)	Ref.	$< m_\nu >$	$< \lambda >$	$< \eta >$	$T_{1/2}^{(0\nu)}$(I)	$T_{1/2}^{(0\nu)}$(II)
^{96}Zr	9.2×10^{21}	[1]	8.09	8.53×10^{-6}	1.00×10^{-7}	2.39×10^{26}	3.00×10^{25}
^{100}Mo	1.1×10^{24}	[2]	0.38	4.39×10^{-7}	5.23×10^{-9}	6.45×10^{25}	9.34×10^{24}
^{110}Pd	6.0×10^{17}	[3]	8.27×10^{2}	1.43×10^{-3}	1.10×10^{-5}	1.63×10^{26}	2.84×10^{25}
^{130}Te	4.0×10^{24}	[4]	0.33	4.57×10^{-7}	4.72×10^{-9}	1.72×10^{26}	2.95×10^{25}
^{150}Nd	2.0×10^{22}	[5]	3.17	3.35×10^{-6}	5.36×10^{-8}	7.88×10^{25}	1.25×10^{25}

References:

[1] Argyriades *et al.* (2010) [2] Arnold *et al.* (2015) [3] Winter (1952)

[4] Alduino *et al.* (2016) [5] Arnold *et al.* (2016)

Table 4.9: Minimum and maximum values of D_α ($\alpha = \omega F$, qF, ωGT, qGT, qT, P, R) using all four parametrizations of the effective two-body interaction with the inclusion of SRC (SRC1, SRC2, and SRC3).

NTME	D_α		
	SRC1	SRC2	SRC3
$M_{\omega F}$	1.9–6.9	1.8–6.9	1.8–6.9
M_{qF}	1.9–6.9	1.9–6.9	1.9–6.9
$M_{\omega GT}$	1.9–7.2	1.9–7.2	1.9–7.2
M_{qGT}	2.0–7.2	1.9–7.1	1.9–7.1
M_{qT}	-0.8–25.0	-0.8–24.9	-0.8–25.0
M_P	1.8–13.6	1.8–12.1	1.8–11.9
M_R	1.8–7.1	1.8–7.1	1.8–7.0

Chapter 5

Conclusions

One of the striking events in history of particle physics is the discovery of neutrino mass, the evidences for which came from the neutrino oscillation experiments. However, the access to neutrino mass from the data of oscillation experiments is not an easy task as these experiments provide only mass-squared differences of neutrino mass eigenstates. Naturally, the next step should be the determination of the mass and nature of the neutrinos. The only proof for the Majorana nature of the neutrinos would be the discovery of $0\nu\beta\beta$ decay of potential even Z-even N emitters. The experimental search of $0\nu\beta\beta$ decay requires a huge amount of expensive enriched isotopes, and low background setup situated deep underground. Klapdor and his collaborators have claimed that $0\nu\beta^-\beta^-$ decay of ^{76}Ge has been observed in Heidelberg-Moscow experiment [Klapdor *et al.* (2001), (2004)]. However, this claim could not be universally accepted as other experimental groups were sceptical about the results. Many experiments are running world wide for the observation of $0\nu\beta^-\beta^-$ decay of potential $\beta^-\beta^-$ emitters and several projects have been proposed to achieve this goal.

In the present work, our aim was to study the $2\nu\beta^-\beta^-$ decay for the $0^+ \rightarrow 2^+$ transition as well as the $0\nu\beta^-\beta^-$ decay for the $0^+ \rightarrow 0^+$ transition within mechanisms involving light Majorana neutrino mass and right handed current of some potential nuclei in the mass range $A = 90 - 150$. The required NTMEs for both the modes of $\beta^-\beta^-$ decay have been calculated by employing the PHFB model in conjunction with four different parametrizations of pairing plus multipolar effective two body interaction, namely $PPQQ1$, $PPQQHH1$, $PPQQ2$, $PPQQHH2$ and three different parametrizations of the SRC due to Miller-Spencer parametrization, Argonne NN and CD-Bonn potentials. As the $0\nu\beta^-\beta^-$ has not been observed so far, the nuclear models predict half-lives $T^{0\nu}_{1/2}$ of $0\nu\beta^-\beta^-$ decay assuming certain value of neutrino mass or conversely, limits on various lepton number violating gauge-theoretical parameters are extracted from the observed experimental half-life limits by calculating the appropriate NTMEs. Prior to the calculation of NTMEs of $0\nu\beta^-\beta^-$ decay, the "goodness of the wave functions" has been checked by calculating nuclear spectroscopic properties, namely the yrast spectra, reduced $B(E2{:}0^+ \rightarrow 2^+)$ transition probabilities, β_2 parameters and g-factors $g(2^+)$ of the nuclei under going $\beta^-\beta^-$ decay and comparing them with the experimental values. After obtaining an overall agreement between the calculated and experimentally observed values, the NTMEs $M_{2\nu}(2^+)$ and half-lives $T^{2\nu}_{1/2}(2^+)$ of $2\nu\beta^-\beta^-$ decay for the $0^+ \rightarrow 2^+$ transition of the ^{94,96}Zr, ^{100}Mo, ^{104}Ru, ^{110}Pd, ^{128,130}Te and ^{150}Nd nuclei have been calculated and the results have been compared with the other existing theoretical calculations as well as experimental results. It was noticed that the validity of the nuclear models can not be uniquely established in the absence of experimental results as well as uncertainty in g_A, and further work is necessary both in the experimental as well as theoretical front to judge the relative ap-

plicability, success and failure of these nuclear models employed for the nuclear structure calculations.

Finally, the NTMEs of $0\nu\beta^-\beta^-$ decay for the $0^+ \rightarrow 0^+$ transition within mechanisms involving the light Majorana neutrino, and right handed $V + A$ current using the same HFB wave functions that were used in the calculation of spectroscopic properties and NTMEs $M_{2\nu}(2^+)$ of $2\nu\beta^-\beta^-$ decay. We have also extracted limits on the effective light Majorana neutrino mass $< m_\nu >$, the effective weak coupling of right-handed leptonic current with right-handed hadronic current $< \lambda >$ and the effective weak coupling of right-handed leptonic current with left-handed hadronic current $< \eta >$ from the observed limit on half-life $T^{0\nu}_{1/2}$. The best limit comes from the $0\nu\beta^-\beta^-$ decay of ^{130}Te nucleus studied experimentally under the CUORE-0 experiment combined with Cuoricino data. The limits extracted on $\langle m_\nu \rangle$, $\langle \lambda \rangle$, and $\langle \eta \rangle$ with the NTMEs calculated in the PHFB model are 0.33 eV, 4.57×10^{-7} and 4.72×10^{-9}, respectively.

Uncertainty in NTMEs

In order to extract lepton number violating gauge-theoretical parameters accurately, reliable calculation of NTMEs is required. On the one hand, there is a large variation in the calculated NTMEs in different nuclear models. Even in the same type of generic model, the calculated NTMEs have noticeable uncertainty. Further, there is no objective way to judge the correctness of these theoretical calculations. The uncertainty in NTMEs is mainly due to different approaches employed in the existing theoretical calculations [Engel (2015)]. The two basic ingredients of any nuclear model are the model space and the effective two-body interaction. In the absence of any general guiding principles to fix these

two ingredients, there is no clear cut prescription in practice for this purpose. Hence, the nuclear models employed to calculate the NTMEs use different model spaces and different effective interactions. In addition, the basic approach to fix the single particle energies and parameters of the two-body interactions are quite different even for the same model space. Moreover, Šimkovic *et al.* (2009) have shown that the choice of g_A and SRC is also source of uncertainty in the NTMEs. We discuss briefly this uncertainty aspect in the following.

Vogel (2000) has used the spread between the calculated NTMEs to estimate the theoretical uncertainty. He showed that for the case of ^{76}Ge, which is a well studied case, the calculated rates differ by a factor of about $6-7$. The effective neutrino mass $\langle m_\nu \rangle$ is inversely proportional to the square root of $T^{0\nu}_{1/2}$. Hence, the uncertainty in the effective neutrino mass is about 2 to 3.

Bilenky and Grifolos (2002) have suggested a method, which allows to check the calculations of NTMEs of the $0\nu\beta^-\beta^-$ decay of different nuclei by confronting them with the experimental data. They have defined a ratio $R\left(A, Z/A^{'}, Z^{'}\right)$ of the half-lives as

$$\begin{aligned} R\left(A, Z/A^{'}, Z^{'}\right) &= \frac{T^{0\nu}_{1/2}\left(A, Z\right)}{T^{0\nu}_{1/2}\left(A^{'}, Z^{'}\right)} \\ &= \frac{\left|M^{(0\nu)}\left(A^{'}, Z^{'}\right)\right|^2 G_{01}(E^{'}_0, Z^{'})}{\left|M^{(0\nu)}\left(A, Z\right)\right|^2 G_{01}\left(E_0, Z\right)} \end{aligned} \tag{5.1}$$

If, the calculated ratio R in a certain nuclear model is in agreement with experimental data, this could only mean that the model is correct up to a possible factor, which does not depend on A and Z. Thus, the calculated ratios of the corresponding NTMEs-squared can be confronted with the experimental data if the $0\nu\beta^-\beta^-$ decay of different nuclei will

be observed. It is predicted that the calculated ratios are very sensitive to the nuclear models and vary within about one order of magnitude.

Rodin *et al.* [Rodin *et al.* (2003), (2005)] have calculated the variance in NTMEs $M^{(0\nu)}$ for the $0\nu\beta^-\beta^-$ decay of ^{76}Ge, ^{82}Se, ^{96}Zr, ^{100}Mo, ^{116}Cd, ^{128}Te, ^{130}Te, ^{136}Xe and ^{150}Nd nuclei considering two models, namely QRPA and RQRPA with three sets of basis states along with three realistic effective interactions. The parameter g_{pp} has been fixed by reproducing the observed half-lives $T^{2\nu}_{1/2}$ of $2\nu\beta^-\beta^-$ decay. It has been shown that the calculated NTMEs $M^{(0\nu)}$ do not depend noticeably on the form of the nucleon-nucleon potential used. Even more importantly, with the choice of g_{pp} the results are also essentially independent on the size of the single particle basis. The calculated values of $M^{(0\nu)}$ differ between the small and large bases by a factor of 2 or more. They have also shown that not only is the variance substantially less than the average value, but the results of QRPA, albeit slightly larger, are quite close to the RQRPA values.

Improvements in the PHFB model

In the PHFB model, two most important features of nuclei, namely pairing and deformation are treated on equal footing. In earlier work [Chandra *et al.* (2005), Singh *et al.* (2007)] it has been shown that the deformations of the intrinsic ground states play a crucial role in reproducing a realistic NTME in the case of $2\nu\beta^-\beta^-$ decay. We have studied the deformation effect on the NTME M_α of $0\nu\beta^-\beta^-$decay due to admixture of $V-A$ and $V+A$ currents, and it is noticed that nuclear structure effects are also important in the case of $0\nu\beta^-\beta^-$ decay. However, the trend of results suggests that it is necessary to incorporate a number of improvements in our study of $\beta^-\beta^-$ decay in general and $2\nu\beta^-\beta^-$

decay in particular, which are discussed in the below.

(1) The proton-neutron pairing should be included in the Hamiltonian to make it isospin symmetric so that the summation method will be exact.

(2) The study of single β-decay rates and the distribution of Gamow-Teller strength has implications in the understanding of the role of the isoscalar part of the proton-neutron interaction. It is not possible to study these aspects presently as the structure of odd-odd nuclei can not be calculated in the present version of the PHFB model. This is a serious draw back in the present formalism of the PHFB model. However, this limitation can be over come by extending the HFB formalism using complex Bogoliubov transformation.

(3) The fluctuations in average particle numbers is around 5%. None the less, it is necessary that number projection should be carried out for consistency.

(4) It is realized from the study of $2\nu\beta^-\beta^-$ decay that a reasonably large model space is more effective in reproducing the observed quenching of NTMEs. An appropriate effective two-body interaction is needed for a large model space. Therefore, it will be illustrative to study $\beta^-\beta^-$ decay in the PHFB model using a large model space in conjunction with appropriate two-body effective interaction.

(5) In the deformed Hartree-Fock (DHF) model [Ripka (1968), Brink (1966), Guney and Warke (1967), Praharaj (1988)], Ahlpara *et al.* (1985) have shown that it is possible to get the shell-model results by mixing a few intrinsic states. Moreover, it is advantageous to work with such a basis instead of a large shell model basis needed to study even the low lying spectra of nuclei [Pandya *et al.* (1985)]. Hence, the band mixing in the PHFB model is one of the best alternatives to study the medium-heavy and heavy nuclei, for which it is difficult to perform a shell-model calculation without truncating the model

space severely.

Further studies on $0\nu\beta^-\beta^-$ decay

The possible occurrence of $0\nu\beta^-\beta^-$ decay in grand unified theories (GUT) requires the existence of Majorana neutrino with non-vanishing mass and/or right handed lepton current. However, the $0\nu\beta^-\beta^-$ decay is also possible in various other gauge theoretical models besides GUT like Majoron models, R_p-violating minimal supersymmetric standard model (*MSSM*), lepto-quark exchange mechanism and compositeness scenario, and has the potential to assess the validity of different gauge models as well as to probe the physics beyond the standard model. The study of other decay processes like positron emission, electron capture and double electron capture ($e^+\beta\beta$) of $\beta\beta$ decay will be interesting both from experimental as well as theoretical point of view. A reliable and timely prediction of the half-life of $e^+\beta\beta$ modes will be helpful in designing the experimental set up and data analysis. Moreover, $e^+\beta\beta$ processes would play a crucial role in discriminating the finer issues like dominance of Majorana neutrino mass or the right handed current once the $0\nu\beta\beta$ decay is observed. Last but not the least, a study of $0\nu\beta\beta$ decay can draw inferences regarding exotic phenomena such as dark energy, dark matter and violation of weak equivalence principle.

Bibliography

[1] C. E. Aalseth *et al.,* Phys. Rev. D 65, 092007 (2002).

[2] K. Ackerstaff *et al.,* Eur. Phys. J. C 5, 229 (1998).

[3] M Agostini *et al.,* Phys. Rev. Lett 111 122503 (2013).

[4] M. Agostini *et al.,* J. Phys. G 42, 115201 (2015).

[5] D. P. Ahalpara, K. H. Bhatt and R. Sahu, J. Phys. G: Nucl. Phys. 11, 735 (1985).

[6] Q. R. Ahmed *et al.,* Phys. Rev. Lett., 87, 071301 (2001).

[7] Q. R. Ahmed *et al.,* Phys. Rev. Lett., 89, 011301 (2002).

[8] M. H. Ahn *et al.,* Phys. Rev. Lett. 90, 041801 (2002).

[9] J. B. Albert *et al.* Nature 510, 229-234 (2014).

[10] C. Alduino *et al.,* Phys. Rev. C 93, 045503 (2016).

[11] A. Alessandrello *et al.,* Nucl. Phys. A 478, 453 (1988).

[12] K. Alfonso *et al.,* Phys. Rev. Lett. 115, 102502 (2015).

[13] M. Alston-Garnjost *et al.,* Phys. Rev. C 55, 474 (1997).

[14] M. Alston-Garnjost *et al.,* Phys. Rev. Lett. 63, 1671 (1989).

[15] M. Alston-Garnjost *et al.,* Phys. Rev. Lett. 71, 831 (1993).

[16] R. Álvarez-Rodríguez, P. Sarriguren, E. Moya de Guerra, L. Pacearescu, A. Faessler, F. Šimkovic, Phys. Rev. C 70, 064309 (2004).

[17] M. Apollonio *et al.,* Eur. Phys. J. C 27, 331 (2003).

[18] J. Argyriades *et al.* Phys.Rev.C80:032501 (2009).

[19] J. Argyriades *et al.* Nucl. Phys. A 847 168-179,(2010).

[20] A. Arima, Nucl. Phys. A 354, 19 (1981).

[21] R. Arnold *et al.,* Z. Phys. C 72, 239 (1996).

[22] R. Arnold *et al.,* Nucl. Phys. A 765, 483 (2006).

[23] R. Arnold *et al.,* Phys. Rev. Lett. 107, 062504 (2011).

[24] R. Arnold, *et al.,* Nucl. Phys. A 925, 25 (2014).

[25] R. Arnold *et al.* Phys. Rev. D 92, 072011 (2015).

[26] R. Arnold *et al.* Phys. Rev. D 94, 072003 (2016).

[27] C. Arpesella, A.S. Barabash, E. Bellotti, C. Brofferio, E. Fiorini, P.P. Sverzellati, and V.I. Umatov, Europhys. Lett. 27, 29 (1994).

[28] C. Arpesella, E. Bellotti, N. Ferrari, L. Zanotti, Nucl. Phys. B (Proc. Suppl.) 70, 249 (1999).

[29] V. Artemiev *et al.,* Phys. Lett. B 345, 564 (1995).

[30] K. Asakura *et al.,*Nucl. Phys. A 946, 171 (2016).

[31] V. N. Aseev *et al.,* Phy. Rev. D 84, 112003 (2011).

[32] V. D. Ashitkov *et al.,* Phys. At. Nucl. 62, 2044 (1999).

[33] F. T. Avignone III *et. al.*, Phys. Rev. Lett. 54, 2309 (1985); Phys. Lett. B 256, 559 (1991).

[34] F. T. Avignone III *et. al.*, Rev. Of Mod Phys., Vol 80, April–June (2008)

[35] M. Aunola, O. Civitarese, J. Kauhanen and J. Suhonen, Nucl. Phys. A 596, 187 (1996).

[36] K. S. Babu *et al.,* preprint Phys. Lett. B 402, 367-373 (1997).

[37] J. N. Bahcall, P. I. Krastev and A. Yu. Smirnov, Phys. Rev. D 58, 096016 (1998).

[38] A. Bakalyarov *et al.,* Pis'ma Zh. Eksp. Teor. Fiz. 76, 643 (2002) [JEPT Lett. 76, 545 (2002)].

[39] A. Balysh *et al.,* Phys. Lett. B 283, 32 (1992); ibid 322, 176 (1994); ibid 356, 450 (1995), Phys. Rev. Lett. 77, 5186 (1996).

[40] A. Balysh *et al.,* Phys. Lett. B 283, 32 (1992); ibid 322,176 (1994); ibid 356, 450 (1995); Phys. Rev. Lett. 77, 5186 (1996).

[41] I. R. Barabanov *et al.,* Pis'ma Zh. Eksp. Teor. Fiz 43, 166 (1986).

[42] A. S. Barabash, F. T. Avignoue III, C. K. Guerard, R. L. Brodzinski, H. S. Miley, J. H. Reeves, and V. I. Umatov, Proc. 3-rd Int. Syrup. on Weak and Electromagn. Interactions in Nuclei WEIN-92. Dubna, Russia, June 16-22, 1992 p.582 (World Sci. Publ. Co., 1993).

[43] A. S. Barabash *et al.,* Phys. Lett. B 345, 408 (1995).

[44] A. S. Barabash *et al.,* Z. Phys. A 352, 231 (1995)a.

[45] A. S. Barabash, R. Gurriaran, F. Hubert, Ph. Hubert, J. L. Reyss, J. Suhonen, V. I. Umatov, J. Phys. G 22, 487 (1996).

[46] A. S. Barabash, F. Hubert, Ph. Hubert, V.I. Umatov, Eur. Phys. J. A 11, 143 (2001).

[47] A. S. Barabash, Talk at the 13th Lomonosov Confrence on Elementary Partricle Physics Moscow-Russia,(2007)

[48] A. S. Barabash *et al.,* Phys. Rev. C 79, 045501 (2009).

[49] A. S. Barabash *et al.,* Phys. of At Nuc , 74, Issue 2, 312–317, (2011)

[50] A. S. Barabash, Nuclear Physics, A 935, 52 (2015).

[51] A. S. Barabash, $arXiv$: 1702.06340v1.

[52] M. Baranger, Phys. Rev. 120, 957 (1960); Cargese lectures in theoretical physics, 1962 (W.A. Benjamin,New York, 1963).

[53] R. Barate *et al.,* Eur. Phys. J. C 2, 395 (1998).

[54] R. K. Bardin, P. J. Gollon, J. D. Ullman and C. S. Wu Nucl. Phys. A 158, 337 (1970).

[55] J. Barea and F. Iachello, Phys. Rev. C 79, 044301 (2009).

[56] J. Barea, J. Kotila, and F. Iachello, Phys. Rev. C 87, 014315 (2013).

[57] J. Barea, J. Kotila, F. Iachello, Phys. Rev. C 91, 034304 (2015).

[58] L. Baudis *et al.,* Phys. Lett. B 407, 219 (1997).

[59] L. Baudis *et al.,* Nuc. Phys. B 70 Pages 106-110 (1999).

[60] L. Baudis *et al.,* Phys. Lett. B 407, 219 (1997).

[61] M. Beck *et al*, Z. Phys. A 343, 397 (1992).

[62] R. Becker-Szendy *et al.,* Nucl. Phys. B (Proc. Suppl.) 38, 331 (1995).

[63] J. W. Beeman *et al.,* Eur. Phys. J. C 75, 591 (2015).

[64] E. Bellotti, *et al.* , Lett. Nuovo Cimento 33, 273 (1982).

[65] E. Bellotti, C. Cattadori, O. Cremonesi, E. Fiorini, C. Liguori, A. Pullia, P. P. Sverzellati and L. Zanotti, Euro. Phys. Lett. 3, 889 (1987).

[66] E. Bellotti, *et al.,* J. Phys. G 17, S 231 (1991).

[67] P. Benes, A. Faessler, S. Kovalenko and F. Simkovic, Phys. Rev. D 71, 077901 (2005).

[68] J. Beringer *et al.,* Particle Data Group, Phys. Rev. D 86, 01001 (p. 1266) (2012).

[69] J. Bernabeu, B. Desplanques and J. Navarro, Z. Phys. C 46, 323 (1990).

[70] S. M. Bilenky and B. Pontecorvo, Phys. Lett. 102B, 32 (1981).

[71] S. M. Bilenky and S. T. Petcov, Rev. Mod. Phys. 59, 671 (1987); ibid 60, 575 (E) (1988); ibid 61, 169 (E) (1989).

[72] S. M. Bilenky and J. A. Grifols, Phys. Lett. B 550, 154 (2002).

[73] C. Bloch and A. Messiah, Nucl. Phys. 39, 95 (1962).

[74] D. Blum *et al*, Phys. Lett. B 275, 506 (1992).

[75] F. Boehm *et al.,* Phys. Rev. D 62, 072002 (2000).

[76] A. Bohr and B. R. Mottelson, Nuclear Structure Vol. II p. 356 (New York, Benjamin, 1975).

[77] B. A. Brown, M. Horoi, and R. A. Sen'kov, Phys. Rev. Lett. 113, 262501 (2014).

[78] B. A. Brown, D. L. Fang, and M. Horoi, Phys. Rev. C 92, 041301(R) (2015).

[79] V. B. Brudanin, N. I. Rukhadze, Ch. Briancon, V. G. Egorov, V. E. Kovalenko, A. Kovalik, A. V. Salamatin, I. Stekl, V. V. Tsoupko-Sitnikov, Ts. Vylov and P. Sermak, Phys. Lett. B 495, 63 (2000).

[80] S. F. Burachas, F. A. Danevich, Yu. G. Zdesenko, V. D. Ryzhikov and V. I. Tretyak, preprint KINR-93-2 (Kiev, 1993).

[81] D. O. Caldwell *et al.,* Phys. Rev. D 33, 2737 (1986).

[82] O. Castanos, J. G. Hirsch, O. Civitarese, P. O. Hess, Nucl. Phys. A 571, 276 (1994).

[83] E. Caurier, A. Poves, A. P. Zuker, Phys. Lett. B 252, 13 (1990).

[84] E. Caurier, A. Poves, A. P. Zuker, Phys. Lett. B 1517, 74 (1995).

[85] E. Caurier, F. Nowacki, A. Poves and J. Retamosa, Phys. Rev. Lett. 77, 1954 (1996).

[86] E. Caurier, F. Nowacki, A. Poves and J. Retamosa, Nucl. Phys. A 654, 973 (1999).

[87] E. Caurier, J. Menéndez, F. Nowacki, and A. Poves, Phys. Rev. Lett. 100, 052503 (2008).

[88] E. Caurier, F. Nowacki, and A. Poves, Eur. Phys. J. A 36, 195 (2008*a*)

[89] V. E. Ceron, J. G. Hirsch, Phys. Lett. B 471, 1 (1999).

[90] R. Chandra, J. Singh, P. K. Rath, P. K. Raina and J. G. Hirsch, Euro. Phys. J. A 23, 223 (2005).

[91] R. Chandra, K. Chaturvedi, P.K. Rath, P.K. Raina, J.G. Hirsch, Europhys. Lett. 86, 32001 (2009).

[92] K. Chaturvedi, R. Chandra, P.K. Rath, P.K. Raina, and J. G. Hirsch, Phys. Rev. C 78, 054302 (2008).

[93] M. K. Cheoun, A. Bobyk, A. Faessler, F. Simkovic and G. Teneva, Nucl. Phys. A 561, 74 (1993); Nucl. Phys. A 564, 329 (1993).

[94] M. K. Cheoun, A. Faessler, F. Simkovic, G. Teneva and A. Bobyk, Nucl. Phys. A 587, 301 (1995).

[95] C. Ching, T. Ho and X. Wu, Phys. Rev. C 40, 304 (1989).

[96] D. Choudhury and S. Raychaudhuri, preprint hep-ph/9702392.

[97] O. Civitarese *et al.,* Phys. Lett. B 25, 333 (1990).

[98] O. Civitarese, A. Faessler, J. Suhonen and X. R. Wu, Nucl. Phys. Lett. A 524, 404 (1991); J. Phys. G 17, 943 (1991).

[99] O. Civitarese and J. Suhonen, Phys. Rev. C 47, 2410 (1993).

[100] O. Civitarese and J. Suhonen, Nucl. Phys. A 575, 251 (1994).

[101] O. Civitarese, J. Suhonen and A. Faessler, Nucl. Phys. A 591, 195 (1995).

[102] O. Civitarese and J. Suhonen, Phys. Rev. C 58, 1535 (1998).

[103] O. Civitarese and J. Suhonen, Nucl. Phys. A 653, 321 (1999).

[104] O. Civitarese, J. Phys.: Conference Series 173, 012012 (2009).

[105] F. A. Danevich, A. Sh. Georgadze, V. V. Kobyachev, B. N. Kropivyanskey, V. N. Kuts, A. S. Nikolaiko, V. I. Tretyak and Yu. Zdesenko, Phys. Lett. B 344, 72 (1995).

[106] F. A. Danevich *et al.* Nucl. Phys. B (Proc. Suppl.) 70, 246 (1999).

[107] F. A. Danevich, A. Sh. Georgadze, V. V. Kobychev, B. N. Kropivyansky, A. S. Nikolaiko, O. A. Ponkratenko, V. I. Tretyak, S. Yu. Zdesenko and Yu. G. Zdesenko, Phys. Rev. C 62, 045501 (2000).

[108] Dassie *et al.* (NEMO Collaboration), Phys. Rev. D 51, 2090 (1995).

[109] S. Dell'Oro, S. Marcocci, M. Viel, and F. Vissani, Advances in High Energy Physics 2016, 2162659 (2016).

[110] A. De Silva, M. K. Moe, M. A. Nelson and M. A. Vient, Phys. Rev. C 56, 2451 (1997).

[111] A. V. Derbin, A. I. Egorov, V. N. Muratova, and S. V. Bakhlanov, Phys. At. Nucl.59, 2037 (1996).

[112] Rani Devi, S. P. Sarswat, A. Bharti and S. K. Khosa, Phys. Rev. C 55, 2433 (1997).

[113] B. M. Dixit, P. K. Rath and P. K. Raina, Phys. Rev. C 65, 034311 (2002); ibid 67, 059901 (E) (2003).

[114] B. M. Dixit Ph.D. Thesis, University of Lucknow (2002).

[115] M. Doi, T. Kotani, H. Nishiura, K. Okuda and E. Takasugi, Phys. Lett.B 102, 323 (1981); ibid 103, 219 (1981); ibid 113, 513(E) (1982)

[116] M. Doi, T. Kotani, H. Nishiura, K. Okuda and E. Takasugi, Prog. Theor. Phys. 66, 1739-1765 (1981); ibid 68, 340(E), 347(E) (1982).

[117] M. Doi, M. Kenmoku, T. Kotani, H. Nishiura and E. Takasugi, Prog.Theor. Phys. 70, 1331 (1983).

[118] M. Doi, M. Kenmoku, T. Kotani, and E. Takasugi, Phys. Rev. D 30, 626 (1984).

[119] M. Doi, T. Kotoni and E. Takasugi, Prog. Theor. Phys. Suppl. 83, 1 (1985).

[120] M. Doi and T. Kotani, Prog. Theor. Phys. 87, 1207 (1992).

[121] M. Doi and T. Kotani, Prog. Theor. Phys., 89, 139 (1993).

[122] N. Dokania *et al.,* Eur. Phys. J. A 53: 74 (2017).

[123] K. Eguchi *et al.,* Phys. Rev. Lett. 90, 021802 (2003).

[124] H. Ejiri *et al.,* J. Phys. G 17, 155 (1991).

[125] H. Ejiri *et al.,* Nucl. Phys. A 611, 85 (1996).

[126] S. R. Elliott, A. A. Hann and M. K. Moe, Phys. Rev. Lett. 59, 2020 (1987); ibid 59, 1649 (1987).

[127] J. Engel, W. C. Haxton and P. Vogel, Phys. Rev. C 46, 2153 (1992).

[128] J. Engel, S. Pittel, M. Stoitsov, P. Vogel and J. Dukelsky, Phys. Rev. C 46, 1781 (1997).

[129] J. Engel, and J. Menéndez, Reports on Progress in Physics 80, 046301 (2017).

[130] J. Engel, J. Phys. G: Nucl. Part. Phys. 42 034017 (2017).

[131] A. Faessler and F. Simkovic, J. Phys. G 24, 2139 (1998).

[132] A. Faessler, Th. Gutsche, S. Kovalenko, and F. Simkovic Phys. Rev. D 77, 113012 (2008).

[133] A. Faessler, V. Rodin, F. Šimkovic, J. Phys. G: Nucl. Part. Phys. 39, 124006 (2012).

[134] D L. Fang, A. Faessler, V. Rodin and F. Šimkovic, Phys. Rev. C 82, 051301(R) (2010).

[135] D L. Fang, A. Faessler, V. Rodin and F. Šimkovic, Phys. Rev. C 83, 034320 (2011).

[136] Dong-Liang Fang, Amand Faessler and Fedor Simkovic. Phys. Rev. C 92, 044301 (2015).

[137] A. Fazely and L. C. Liu, Phys. Rev. Lett. 57, 968 (1986).

[138] A. Fazely and L. C. Liu, Phys. Rev. Lett. 59, 2384 (1987).

[139] A. Forster *et al.,* Phys. Lett 138 B, 301 (1984).

[140] Y. Fukuda *et al.,* Phys. Lett. B 335, 237 (1994).

[141] Y. Fukuda *et al.,* Phys. Rev. Lett. 81, 1562 (1998).

[142] Y. Fukuda *et al.,* Phys. Rev. Lett. 82, 1810 (1999); ibid 82, 2430 (1999); ibid 82, 2644 (1999).

[143] W. Furry, Phys. Rev. 56, 1184 (1939).

[144] A. Sh. Georgadze, F. A. Danevich, Yu. G. Zdesenko, V. V. Kobychev, B. N. Kropivyanskki, V. N. Kuts, V. V. Nikolaiko and V. I. Tretyak, Phys. At. nucl. 58, 1093 (1995).

[145] M.C. Gonzalez-Garcia Jour. of H. E. P. 11 052(2014).

[146] D. Gonzalez *et al.,* Nucl. Phys. B(Proc. Suppl.), 87, 278 (2000).

[147] A. L. Goodman, "Advances in Nuclear Physics", Ed. J. W. Negele and E. Voget (Plenum, New York, 1979).

[148] W. Greiner, Nucl. Phys. 80, 417 (1966).

[149] L. Grodzins, Phys. Lett. 2, 88 (1962).

[150] D. E. Groom *et al.,* (Particle data group) Eur. Phys. J. C 15, 1 (2000).

[151] M. R. Guney and C. S. Warke, Phys. Rev. 155, 108 (1967).

[152] M. Gunther *et al.,* Phys. Rev. D 55, 54 (1997).

[153] A. Halprin, P. Minkowski, H. Primakoff and S. P. Rosen, Phys. Rev.D 13, 2567 (1976).

[154] W. C. Haxton, G. J. Stephenson Jr. and D. Strottman, Phys. Rev. Lett. 47, 153 (1981).

[155] W. C. Haxton and G. J. Stephenson Jr., Prog. Part. Nucl. Phys. 12, 409 (1984).

[156] J. L. Hewett and T. G. Rizzo, preprint hep-ph/9703337.

[157] J. G. Hirsch, O. Castanos, P. O. Hess and O. Civitarese, Phys. Rev. C 51, 2252 (1995).

[158] J. G. Hirsch, O. Castanos, P. O. Hess and O. Civitarese, Nucl. Phys. A 589, 445 (1995*a*).

[159] J. G. Hirsch, P. O. Hess and O. Civitarese, Phys. Rev. C 54, 1976 (1996).

[160] J. G. Hirsch, P. O. Hess and O. Civitarese, Phys. Lett. B 390, 36 (1997); Phys. Rev. C 56, 199 (1997).

[161] J. G. Hirsch, O. Castanos, P. O. Hess and O. Civitarese, Phys. Lett. B 534, 57 (2002).

[162] M. Hirsch, X. Wu, H. V. Klapdor, C. Ching, T. Ho, Z. Phys. A 345, 163 (1993).

[163] M. Hirsch *et al.,* Z. Phys. A 347, 51 (1994).

[164] M. Hirsch, H. V. Klapdor-Kleingrothaus and S. G. Kovalenko, Phys. Rev. Lett. 75, 17 (1995).

[165] M. Hirsch, H. V. Klapdor-Kleingrothaus and O. Panella, Phys. Lett. B 374, 7 (1996).

[166] M. Hirsch, H. V. Klapdor-Kleingrothaus, S. G. Kovalenko and H. Päs, Phys. Lett. B 372, 8 (1996*a*).

[167] M. Hirsch, H. V. Klapdor-Kleingrothaus and S. G. Kovalenko, Phys. Lett. B 372, 181 (1996*b*).

[168] M. Hirsch, H. V. Klapdor-Kleingrothaus and S. G. Kovalenko, Phys. Rev. D 54, R4207 (1996*c*).

[169] M. Horoi and S. Stoica, Phys. Rev. C 81, 024321 (2010).

[170] M. Horoi and B. A. Brown, Phys. Rev. Lett. 110, 222502 (2013).

[171] Mihai Horoi and Andrei Neacsu, Phys. Rev. C 93, 024308 (2016)

[172] F. Iachello and J. Barea, Nucl. Phys. B Proc. Suppl. 217, 5 (2011).

[173] F. Iachello, J. Barea, and J. Kotila, AIP Conf. Proc. 1417, 62 (2011)a.

[174] Y. Iwata, N. Shimizu, T. Otsuka, Y. Utsuno, J. Menéndez, M. Honma, and T. Abe, Phy. Rev. Lett. 116, 112502 (2016).

[175] J. M. Jauch, Helv. Phys. Acta 27, 89 (1954).

[176] J. Kalinowski *et al.,* Z.Phys. C 74 595-603 (1997).

[177] S. K. Khosa and P. K. Mattu, Phys. Rev. C 43, 634 (1991).

[178] H. V. Klapdor-Kleingrothaus, Int. J. Mod. Phys. A 13, 3953 (1998).

[179] H. V. Klapdor-Kleingrothaus *et al.,* Mod. Phys. Lett. A 16, 2409 (2001); Eur. Phys. J. A 12 147-154 (2001).

[180] H. V. Klapdor-Kleingrothaus and U. Sarkar, Mod. Phys. Lett. A 16 2469-2482 (2001).

[181] H. V. Klapdor-Kleingrothaus, A. Dietz, H. L. Harney and I. V. Krivoshina, Mod. Phys. Lett. A 16 2409-2420 (2001); hep-ph/0205228.

[182] H. V. Klapdor-Kleingrothaus, A. Dietz, H. L. Harney and I. V. Krivoshina, Mod. Phys. Lett. A 16 2409-2420 (2001); hep-ph/0205228.

[183] H. V. Klapdor-Kleingrothaus, A. Dietz and I. V. Krivoshina, Phys. Rev. D 70, 078301 (2004).

[184] H. V. Klapdor-Kleingrothaus, I. V. Krivoshina, A. Dietz and O. Chkvorets, Phys. Lett. B 586, 198 (2004).

[185] A. A. Klimenko, A. A. Pomansky and A. A. Smolnikov, Nucl. Instrum. Meth. B 17, 445 (1986).

[186] M. Kobayashi and K. Maskawa, Prog. Theor. Phys. 49, 652 (1973).

[187] S. E. Koonin, D. J. Dean and K. Langanke, Phys. Rep. 278, 1 (1997).

[188] J. Kotila, and F. Iachello, Phys. Rev. C 85, 034316 (2012).

[189] T. Kotani, Proceedings of the Fourth Moriond Workshop, ed. by Tran Thanh Van (Editions Frontieres, France, 1984), p. 397; Proceedings of International

Symposium on Nuclear Spectroscopy and Nuclear Interactions, ed. by Ejiri and Fukuda p. 259. (World Scientific Pub, Sigapore, 1984).

[190] Ch. Kraus *et al.*, Eur. Phys. J C 40, 447 (2005).

[191] F. Krmpotic, A. Mariano, T. T. S. Kuo and K. Nakayama, Phys. Lett. B 319, 393 (1993).

[192] N. Kudomi, H. Ejiri, K. Nagata, K. Okada, T. Shibata, T. Shima, and J. Tanaka, Phys. Rev. C 461 2132 (1992).

[193] N. Kudomi *et al*, Nucl. Phys. B(Proc. Suppl.) 87, 301 (2000).

[194] E. J. Konopinski and H. Mahmoud, Phys. Rev. 92, 1045 (1953).

[195] B. Lehnert *et al*, J. Phys G: Nucl. Part. Phys. 43, 115201 (2016).

[196] C. N. Leung and S.T. Petcov, Nucl. Phys. B 125, 461 (1983).

[197] B. Maier *et al.,* in Proceedings of the international workshop on double beta decay and related topics, Trento, edited by H.V. Klapdor-Kleingrothaus and S. Stoica (World Scientific, Singapore), p. 455 (1995).

[198] E. Majorana, Nuovo Cim. 5, 171 (1937).

[199] Z. Maki, M. Nakagawa and S. Sakata, Prog. Theor. Phys. 28, 870 (1962).

[200] J. Menéndez, A. Poves, E. Caurier, F. Nowacki, Nucl. Phys. A 818, 139 (2009).

[201] J Men´endez, Tom´as R. Rodr´ıguez,Gabriel Mart´ınez-Pinedo, Alfredo Poves, Phy. Rev. C 90, 024311 (2014).

[202] G. A. Miller and J. E. Spencer, Annals Phys. 100, 562 (1976).

[203] M. Moe and P. Vogel, Ann. Rev. Nucl. Part. Sci. 44, 247 (1994).

[204] M. Moe and P. Vogel, Ann. Rev. Nucl. Part. Sci. 44, 247 (1994).

[205] R. N. Mohapatra and P. B. Pal, Massive Neutrinos in Physics and Astophysics, World Scientific, Singapore, (1991).

[206] A. Morales, Nucl. Phys. B (Proc. Suppl.) 77, 335 (1999).

[207] M. T. Mustonen and J. Engel, Phys. Rev. C. 87, 064302 (2013).

[208] A. Neacsu and M. Horoi, Phys. Rev. C 91, 024309 (2015).

[209] E. B. Norman, D. M. Meekhof, Phys. Lett. B 195, 126 (1987).P. Raghavan, Atomic Data and Nuclear Data Table 42, 189 (1989).

[210] F. Nowacki, A. Poves, E. Caurier and B. Bounthong, Phys. Rev. Lett. 117, 272501 (2016).

[211] K. Ogawa, H. Horie, in: M. Morita, H. Ejiri, H. Ohtsubo, T. Sato (Eds.), Nuclear Weak Process and Nuclear Structure, World Scientific, Singapore, p. 308 (1989).

[212] I. Ogawa *et al.,* Nucl. Phys. A 730, 215 (2004).

[213] N. Onishi and S. Yoshida, Nucl. Phys. A260, 226 (1966), Nucl. Phys. 80, 367 (1966).

[214] I. Ostrovskiy, Mod. Phys. Lette. A 3, 1630017 (2016).

[215] T. E. Pahomi, A. Neacsu, M. Mirea, S. Stoica, Romanian Reports in Physics, 66, 370 (2014)

[216] S. P. Pandya, R. Sahu and A. K. Rath, Ind. J. Phys. 70 A, 69 (1996).

[217] O. Panella and Y. N. Srivastava, Phys. Rev. D 52, 5308 (1995).

[218] O. Panella, C. Carimalo, Y. N. Srivastava and A. Widom, Phys. Rev. D 56, 5766 (1997).

[219] S. T. Petcov, Phys. Lett. 110B, 245 (1982)

[220] C. Picciotto, Can. J. Phys. 56, 399 (1978).

[221] A. Piepke *et al.,* Nucl. Phys. A577, 493 (1994).

[222] B. Pontecorvo, Zh. Eksp. Teor. Fiz. 33, 549 (1957).

[223] C. R. Praharaj, J. Phys. G14, 843 (1988).

[224] H. Primakoff, Phys. Rev. 85, 888 (1952).

[225] H. Primakoff and S. P. Rosen, Report Prog. in Phys. 22, 121 (1959).

[226] H. Primakoff and S. P. Rosen, Proc. Phys. Soc. (London) 78, 464 (1961).

[227] H. Primakoff and S. P. Rosen, Phys. Rev. 184 1925 (1969).

[228] G. Racah, Nuovo Cim. 4, 322 (1937).

[229] P. B. Radha, D. J. Dean, S. E. Koonin, T. T. S. Kuo, K. Langanke, A. Poves, J. Retamosa and P. Vogel, Phys. Rev. Lett. 76, 2642 (1996).

[230] P. B. Radha, D. J. Dean, S. E. Koonin, K. Langanke and P. Vogel, Phys. Rev. C 56, 3079 (1997).

[231] A. A. Raduta, A. Faessler and S. Stoica, Nucl. Phys. A 534, 149 (1991).

[232] A. A. Raduta, D. S. Delion and A. Faessler, Phys. Rev. C 51, 3008 (1995).

[233] A. A. Raduta, C. M. Raduta, Phys. Lett. B 647, 265 (2007).

[234] P. Raghavan, Atomic Data and Nuclear Data Table, 42, 189 (1989).

[235] P. K. Raina, A. Shukla, S. Singh, P. K. Rath and J. G. Hirsch, Eur. Phys. J. A 28, 27 (2006).

[236] S. Raman, C. W. Nestor Jr., S. Kahane and K. H. Bhatt, Atomic Data and Nuclear Data Table, 42, 1 (1987).

[237] S. Raman, C. W. Nestor Jr. and P. Tikkanen, Atomic Data and Nuclear Data Table, 78, 1 (2001).

[238] P. K. Rath, R. Chandra, K. Chaturvedi, P.K. Raina, and J.G. Hirsch, Phys. Rev. C. 82, 064310 (2010).

[239] P. K. Rath, R. Chandra, P.K. Raina, K. Chaturvedi, and J.G. Hirsch, Phys. Rev. C. 85, 014308 (2012).

[240] P. K. Rath, R. Chandra, K. Chaturvedi, P. Lohani, P. K. Raina, and J. G. Hirsch, Phys. Rev. C 88, 064322 (2013).

[241] P. K. Rath, R. Chandra, K. Chaturvedi, P. Lohani, and P. K. Raina, Phys. Rev. C 93, 024314 (2016).

[242] J. Retamosa, E. Caurier and F. Nowacki, Phys. Rev. C 51, 371 (1995);Review of Particle Physics, Phys. Lett. B, 592 (2004).

[243] G. Ripka, In Advances in Nuclear Physics, Ed. M. Baranger and E. Vogt, (Plenum, New York) Vol. I, p183 (1968).

[244] V. A. Rodin, A. Fassler, F. Simkovic, and P. Vogel, Phys. Rev. C 68, 044302 (2003).

[245] V. A. Rodin, A. Fassler, F. Simkovic, and P. Vogel, $nucl-th/0503063$.

[246] T.R. Rodríguez and G. Martínez-Pinedo, Phys. Rev. Lett. 105, 252503 (2010).

[247] O. A. Rumyantsev and M. H. Urin, JETP Lett. 61, 361 (1995).

[248] R. Saakyan, Annu. Rev. Nucl. Part. Sci. 63, 503 (2013).

[249] M. Sakai, Atomic Data and Nuclear Data Tables 31, 400 (1984).

[250] M. Sambataro and J. Suhonen, Phys. Rev. C 56, 782 (1997).

[251] J. Schechter and J. W. F. Valle, Phys. Rev. D 25, 2951 (1982).

[252] J. Schwieger, F. Simkovic and A. Faessler, Nucl. Phys. A 600, 179 (1996).

[253] J. Schweiger, F. Simkovic, A. Faessler, W.A. Kominski, Phys. Rev. C 57, 1738 (1998).

[254] R. A. Sen'kov and M. Horoi, Phys. Rev. C 88, 064312 (2013).

[255] R. A. Sen'kov, M. Horoi, and B. A. Brown, Phys. Rev. C 89, 054304 (2014).

[256] R. A. Sen'kov and M. Horoi, Phys. Rev. C 90, 051301(R) (2014)a.

[257] R. A. Sen'kov and M. Horoi, Phys. Rev. C 93, 044334 (2016).

[258] S. K. Sharma, P. N. Tripathi and S. K. Khosa, Phys. Rev. C 38, 2935 (1988).

[259] F. Simkovic, JINR communications 39, 21 (1989).

[260] F. Simkovic, G. Teneva, A. Bobyk, M. K. Cheoun, A. Faessler and S. B. Khadkikar, Prog. Part. Nucl. Phys. 32, 329 (1994).

[261] F. Simkovic, J. Schwieger, G. Pantis and A. Faessler, Found.Phys. 27 1275 (1997).

[262] F. Simkovic and G. Pantis, Czech. J. Phys. B 48, 235 (1998).

[263] F. Simkovic and Veselesky, Proc. Int. Workshop MEDEX97, Praha, June 1997, Czech. J. Phys. B48, 245 (1998).

[264] F. Simkovic, G. Pantis, J. D. Vergados and A. Faessler, Phys. Rev. C 60, 055502 (1999).

[265] F. Šimkovic, Larisa Pacearescu and Amand Faessler, Nuclear Physics A 733 321–350 (2004).

[266] F. Šimkovic, A. Faessler, V. Rodin, P. Vogel, and J. Engel, Phys. Rev. C 77, 045503 (2008).

[267] F. Šimkovic, A. Faessler, H. Müther, V. Rodin, and M. Stauf, Phys. Rev. C 79, 055501 (2009).

[268] F. Šimkovic, V. Rodin, A. Faessler, and P. Vogel, Phys. Rev. C 87, 045501 (2013).

[269] S. Singh, R. Chandra, P. K. Rath, P. K. Raina, J. G. Hirsch, Eur. Phys. J. A 33, 375 (2007).

[270] L. D. Skouras and J. D. Vergados, Phys. Rev. C 28, 2122 (1983).

[271] D. Smith, C. Picciotto and D. Bryman, Phys. Lett. B 46, 157 (1973).

[272] A. A. Smolnikov, Ph. D. Thesis, INR AN SSSR (Moscow, 1985).

[273] K. H. Speidel, O. Kenn and F. Nowacki Prog. Part. Nucl. Phys. 49, 91 (2002).

[274] D. Štefánik, R. Dvornický, F. Šimkovic, and P. Vogel, Phys. Rev. C 92, 055502 (2015)

[275] S. Stoica and W. A. Kaminski, Phys. Rev. C 47, 867 (1993).

[276] S. Stoica, Phys. Rev. C 49, 2240 (1994).

[277] S. Stoica, Phys. Lett. B 350, 152 (1995).

[278] S. Stoica and I. Mihut, Nucl. Phys. A 602, 197 (1996); S. Stoica, Phys. Lett. B 350, 152 (1995).

[279] S. Stoica and H. V. Klapdor-Kleingrothaus, Eur. Phys. J. A 9, 345 (2000).

[280] S. Stoica and H. V. Klapdor-Kleingrothaus, Phys. Rev. C 63, 064304 (2001); Nucl. Phys. A654, 269 (2001).

[281] S. Stoica, and M. Mirea, Phys. Rev. C 88, 037303 (2013).

[282] J. Suhonen, Nucl. Phys. A 563, 205 (1993).

[283] J. Suhonen and O. Civitarese, Phys. Lett. B 308, 212 (1993); ibid 312, 367 (1993).

[284] J. Suhonen, O. Civitarese, Phys. Rec. C 49, 3055 (1994).

[285] J. Suhonen, P. C. Divari, L. D. Skouras and I. P. Johnstone, Phys. Rev.C 55, 714 (1997).

[286] J. Suhonen, O. Civitarese, Phys. Rep. 300, 123 (1998).

[287] J. Suhonen, Nucl. Phys. A 864, 63 (2011).

[288] J. Suhonen and O. Civitarese, J. Phys. G 39, 124005 (2012).

[289] G. Teneva, F.Simkovic, A. Bobyk, M. K. Cheoun, A. Faessler and S. B. Khadkikar, Nucl. Phys. A 249, 586 (1995).

[290] T. Thummler, Nucl. Phys. B, 229-332, 146 (2012).

[291] J. Toivanen and J. Suhonen, Phys. Rev. Lett. 75, 410 (1995).

[292] J. Toivanen and J. Suhonen, Phys. Rev. C 55, 2314 (1997).

[293] T. Tomoda and A. Faessler, Phys. Lett. B 157, 4 (1985).

[294] T. Tomoda, A. Faessler, K. W. Schmid and F. Gruemmer, Nucl. Phys. A452, 591 (1986).

[295] T. Tomoda, A. Faessler, K. W. Schmid and F. Gruemmer, Phys. Lett. B 199, 475 (1987).

[296] T. Tomoda, Nucl. Phys. A 484, 635 (1988).

[297] T. Tomoda, Rep. Prog. Phys. 54, 53 (1991).

[298] V. I. Tretyak and Y. G. Zdesenko, Atomic data and Nuclear data Tables, 61, 43 (1995), ibid 80, 83 (2002).

[299] V. I. Tretyak, F. A. Danevich, S. S. Nagorny and Yu. G. Zdesenko Europhys. Lett. 69, 41 (2005).

[300] P. N. Tripathi, Ph.D. Thesis, I.I.T. Kanpur, (1984).

[301] P. N. Tripathi, S. K. Sharma and S. K. Khosa, Phys. Rev. C 29, 1951 (1984).

[302] S. Umehara *et al.* Phys. Rev. C 78 058501(2008) .

[303] S. Unlu , Chin. Phy. Lett. 31, 4, 042101(2014); Phys. Scr. 87, 045202 (2013).

[304] J. W. F. Valle, Phys. Rev. D27, 1672 (1983).

[305] J. W. F. Valle and M. Singer Phys. Rev. D28, 540 (1983).

[306] S. I. Vasilev *et al.,* JETP Lett. 51, 622 (1990); 58, 178 (1993).

[307] J. D. Vergados, Phys. Rev. C 13, 865 (1976).

[308] J. D. Vergados, Phys. Rev. D 25, 914 (1982).

[309] J. D. Vergados, Phys. Rep. 361, 1 (2002).

[310] J. D. Vergados, H. Ejiri and F. Šimkovic, Int. J. Mod. Phys. E 25, 1630007 (2016); Rep. Prog. Phys. 75, 106301 (2012).

[311] F. Villars, Proceedings of International School of Physics, "Enrico Fermi" Course 36 edited by C. Bloch Academic, New York (1966).

[312] D. M. Vladimirov and Yu. V. Gaponov, Sov. J. Nucl. Phys. 55, 1010 (1992).

[313] P. Vogel and M. R. Zirnbauer, Phys. Rev. Lett. 57, 3148 (1986).

[314] P. Vogel, $arXiv : nucl - th/0005020$.

[315] P. Vogel, J. Phys. G: Nucl. Part. Phys. 39 124002 (2012)

[316] M. Watanabe and H. Toki, Proc. Int. Symp. on Nuclear Beta Decays and Neutrino (Osaka) , ed. T. Kotani, H. Ejiri and E. Takasugi (Singapore: World Scientific) p 212.11-13 June (1986)

[317] L.J. Wen, J. Cao, and Y.F. Wang, Annu. Rev. Nucl. Part. Sci. 67:183–211 (2017).

[318] R. G. Winter, Phys. Rev. 85, 687 (1952).

[319] H. F. Wu *et al.* Phys. Lett. B 162, 227 (1985).

[320] X. Wu, A. Staudt, H. V. Klapdor, C. Ching and T. Ho, Phys. Lett. B 272, 169 (1991).

[321] X. Wu, A. Staudt, T. T. S. Kuo and H. V. Klapdor, Phys. Lett. B 276, 274 (1992).

[322] D. Wyler and L. Wolfstein, Nucl. Phys.B 218, 205 (1983).

[323] N. Yosida and F. Iachello, arXiv:1301.7172v1 [nucl-th].

[324] K. You *et al.,* Phys. Lett. B 265, 53 (1991).

[325] Ya. B. Zeldovich, S.Yu. Lukyanov and Ya. A. Smorodinskii, Usp. Fiz.Nauk 59, 361 (1954).

[326] J. M. Yao, L. S. Song, K. Hagino, P. Ring and J. Meng, Phys. Rev. C91, 024316 (2015).

[327] L. Zhao, B. A. Brown and W.A. Richter, Phys. Rev. C 42, 1120 (1990).

[328] L. Zhao and B.A. Brown, Phys. Rev. C 47, 2641 (1993).

I. List of Publications

1. 'Two neutrino double-β decay of $94 \leq A \leq 150$ nuclei for the $0^+ \rightarrow 2^+$ transition', Yash Kaur Singh, R. Chandra, P.K. Raina and P.K. Rath, Eur. Phys. J. A 53, 244 (2017).

2. 'Neutrinoless double beta decay and Physics beyond the Standard Model', Yash Kaur Singh *et al.*, DAE-BRNS Symp. on Nucl. Phys. 61, 286 (2016).

3. 'Study of neutrinoless double beta decay in R-parity violating supersymmetric models via exchange of gluinos', Yash Kaur Singh, T. K. Yadav, R. Chandra, P.K. Rath and P.K. Raina, DAE-BRNS Symp. on Nucl. Phys. 60, 104 (2015).

4. 'Study of Majoron accompanied neutrinoless double beta decay', R. Chandra, K. Chaturvedi, Yash Kaur Singh, T. K. Yadav, P.K. Rath and P.K. Raina, DAE-BRNS Symp. on Nucl. Phys. 59, 122 (2014).

5. 'Nuclear transition matrix elements for neutrinoless double-β decay within mechanisms involving light Majorana neutrino mass and right-handed current' Yash Kaur Singh, R. Chandra, K. Chaturvedi, Tripti Avasthi, P.K. Raina and P.K. Rath (communicated)

II. Participation in Conference /Workshop/Schools/Symposium

1. Participated and presented a paper in International Conference on Nanoscience and Nanotechnology (ICNN-2013) 18-20 November , 2013 held at BBAU, Lucknow.

2. Participated in Winter School on Accelerator Nuclear and Particle Physics , held between 29-3-2014 to 04-04-2014 at BHU Varanasi.

3. Participated in DST- SERC School on Nuclear structure on High Angular Momentum and Isospin at TIFR, Mumbai between October 5-24, 2014.

4. Given oral presentation at 59th DAE- BRNS symposium on nuclear physics during December 08-12, 2014 held at BHU, Varanasi.

5. Participated in SERC School on Modern Theories of Nuclear structure, during Feb 23- March 5, 2015 at IIT Roorkee, Utrakhand.

6. Given a poster presentation in 3rd Lucknow Science Congress and National Conference between 31stoct- 2nd Nov 2015, held at BBAU Lucknow.

7. Given oral presentation in 60th DAE- BRNS Symposium on Nuclear Physics between December 07-11 2015 held at Sai Institute of higher learning , Prasanthi Nilayam.

8. Participated in "Winter school on Beyond Standard Model Physics " held at BHU, Varanasi held between 21 th January- 14th February 2016.

9. Participated in "NDBD- 2016" workshop held at IIT Ropar, Rupnagar, Punjab held between October 17-21, 2016.

10. Presented poster in 61st DAE- BRNS Symposium on Nuclear Physics during December 05- 09, 2016 at SINP, Kolkata.

11. Participated in XXXVII Annual IAPT convention 2017 and National Symposium on Recent Trends in Physics at different scales held at Gurukul Kangri Vishwavidyalaya, Haridwar during October 29-31, 2017.

Eur. Phys. J. A (2017) **53**: 244
DOI 10.1140/epja/i2017-12445-8

THE EUROPEAN PHYSICAL JOURNAL A

Regular Article – Theoretical Physics

Two neutrino double-β decay of $94 \leq A \leq 150$ nuclei for the $0^+ \longrightarrow 2^+$ transition

Yash Kaur Singh[1], R. Chandra[1,a], P.K. Raina[2], and P.K. Rath[3]

[1] Department of Applied Physics, Babasaheb Bhimrao Ambedkar University, Lucknow, India
[2] Department of Physics, Indian Institute of Technology, Ropar, Rupnagar - 140001, India
[3] Department of Physics, University of Lucknow, Lucknow-226007, India

Received: 1 October 2017 / Revised: 6 December 2017
Published online: 22 December 2017 –
Communicated by M. Anselmino

Abstract. Within the PHFB approach, the $0^+ \rightarrow 2^+$ transition of two neutrino double-β decay of ^{94,96}Zr, ^{100}Mo, ^{104}Ru, ^{110}Pd, ^{128,130}Te and ^{150}Nd isotopes is studied employing wave functions generated with four different parametrizations of the pairing plus multipole type of two-nucleon interaction and the summation method. In comparison to the $0^+ \rightarrow 0^+$ transition, the nuclear transition matrix elements $M_{2\nu}(2^+)$ are quite sensitive to the deformation of the yrast 2^+ state. Consideration of the available theoretical and experimental results suggests that the observation of the $0^+ \rightarrow 2^+$ transition of $2\nu\beta^-\beta^-$ decay may be possible in ^{96}Zr, ^{100}Mo, ^{130}Te and ^{150}Nd isotopes. The effect of deformation on the $M_{2\nu}(2^+)$ is also studied.

1 Introduction

The nuclear double beta ($\beta\beta$) decay is a convenient tool to test the validity of models employed in the nuclear structure studies and probe the physics beyond standard model of electroweak unification (SM). Over the past years, the theoretical as well as experimental studies of the $\beta\beta$ decay has attracted a lot of attention and has been excellently reviewed in refs. [1–6] and references therein. The two neutrino double beta ($2\nu\beta\beta$) decay is a second order process in weak interaction and is allowed in the SM. The neutrinoless double beta ($0\nu\beta\beta$) decay is far more interesting as it involves the Majorana neutrinos and violation of the lepton number conservation by two units. The observation of the $0\nu\beta\beta$ decay can not only establish the Majorana nature of neutrinos but also provide information on the physics beyond the SM [7,8].

The $\beta\beta$ decay can occur in four different modes namely, double-electron ($\beta^-\beta^-$) emission, double-positron ($\beta^+\beta^+$) emission, electron positron conversion ($\varepsilon\beta^+$) and double-electron capture ($\varepsilon\varepsilon$). The latter three processes are energetically competing. In the allowed approximation, the $0^+ \rightarrow 1^+$ transition is much less probable than the $0^+ \rightarrow 0^+$ and $0^+ \rightarrow 2^+$ transitions. The observation of $0\nu\beta\beta$ decay for the $0^+ \rightarrow 2^+$ transition can distinguish between the mechanisms involving the mass of the Majorana neutrinos and the right handed currents [9]. The theoretical implications and experimental aspects of the ground to the excited 2^+ state transition of the $\beta\beta$ decay have been excellently reviewed over the past years [10,11]. Interestingly, it has been shown by Barabash *et al.* [12] that the decay rates, energy spectra and angular distributions of the $0^+ \rightarrow 0^+$ and $0^+ \rightarrow 2^+$ transitions can be employed to extract limits on the assumed admixture of fermionic and bosonic components of neutrinos.

Out of 35 possible candidates, the $0^+ \rightarrow 0^+$transition of $2\nu\beta^-\beta^-$ decay has been observed for twelve nuclei [3, 13] and limits on the half-lives $T^{2\nu}_{1/2}$ of a number of isotopes for the $0^+ \rightarrow 0^+$ and $0^+ \rightarrow 2^+$ transitions have already been given [14,15]. The inverse half-life of $2\nu\beta^-\beta^-$ decay is a product of the phase space factor and model dependent nuclear transition matrix elements (NTMEs) $M_{2\nu}$. The phase space factors have been calculated employing the exact Dirac wave functions in conjunction with finite nuclear size and screening effects [16,17]. Using the observed experimental half-lives for the $0^+ \rightarrow 0^+$ transition, the NTMEs $M_{2\nu}$ has been extracted [13] and in all cases of $2\nu\beta^-\beta^-$ decay, it has been observed that the NTMEs $M_{2\nu}(0^+)$ are sufficiently quenched [18]. The main motive of all theoretical calculations is to understand the physical mechanism responsible for the observed suppression of $M_{2\nu}(0^+)$. Hence, the validity of different nuclear models can be tested by calculating $M_{2\nu}(0^+)$ and comparing them with the experimental value.

The $0^+ \rightarrow 2^+$ transition of $2\nu\beta^-\beta^-$ decay has not been experimentally observed so far. The marked variation in the theoretically calculated NTMEs $M_{2\nu}(2^+)$ for the $0^+ \rightarrow 2^+$ transition using different nuclear models is a general feature [10]. For example, the available results for

[a] e-mail: ramesh.luphy@gmail.com

$M_{2\nu}(2^+)$ of ^{96}Zr show that the calculated NTMEs within QRPA [19–22], RQRPA (WS) [23], RQRPA (AWS) [23], and SRPA (WS) [24,25], differ by a factor of 341. Hence, the observation of the $0^+ \to 2^+$ transition of $2\nu\beta^-\beta^-$ decay can constrain the validity of different nuclear models employed in the calculation of NTMEs. Alternatively, a reliable theoretical prediction will supplement the experimental designing and planning to study this particular mode of $2\nu\beta^-\beta^-$ decay.

Employing the pnQRPA model, it has been shown by Raduta *et al.* [20] that the inclusion of deformation in the mean field can reduce the NTMEs $M_{2\nu}(2^+)$ up to a factor of 341. In the PHFB model, the pairing and deformation degrees of freedom are treated simultaneously on equal footing. However, the structure of intermediate odd-odd nuclei cannot be studied in the present version of the PHFB model. In spite of this limitation, the PHFB model has been successfully applied to study the $0^+ \to 0^+$ transition of $2\nu\beta^-\beta^-$ decay [26,27] in conjunction with the summation method [28]. This has motivated us to apply the same set of wave functions to study the $0^+ \to 2^+$ transition of $2\nu\beta^-\beta^-$ decay of ^{94,96}Zr, ^{100}Mo, ^{104}Ru, ^{110}Pd, ^{128,130}Te and ^{150}Nd isotopes in the mass range $90 \leq A \leq 150$.

The theoretical formalism to calculate the half-life for the $0^+ \to 2^+$ transition of $2\nu\beta^-\beta^-$ decay $T^{2\nu}_{1/2}(0^+ \to 2^+)$ in 2n mechanism has been given in refs. [9,29,30]. Using the summation method [28], the $0^+ \to 0^+$ and $0^+ \to 2^+$ transitions of $2\nu\beta^-\beta^-$ mode has already been studied by Hirsch *et al.* in the pseudo-$SU(3)$ model [31,32]. Presently, the summation method applied to the study of $0^+ \to 0^+$ transition of $2\nu\beta^-\beta^-$ decay within the PHFB model [26, 27] has been extended to the $0^+ \to 2^+$ transition. In sect. 2, we outline the theoretical formalism to calculate the half life $T^{2\nu}_{1/2}(2^+)$ of $2\nu\beta^-\beta^-$ decay. The results are presented and discussed in sect. 3. The final conclusions are given in sect. 4.

2 Theoretical framework

The half life for the $0^+ \to 2^+$ transition of $2\nu\beta^-\beta^-$ decay $T^{2\nu}_{1/2}(2^+)$ in 2n mechanism is given by

$$\left[T^{2\nu}_{1/2}(2^+)\right]^{-1} = G_{2\nu}(2^+)\left|M_{2\nu}(2^+)\right|^2, \quad (1)$$

where the integrated kinematical factor $G_{2\nu}(2^+)$ has been calculated with good accuracy [33]. The model dependent NTME $M_{2\nu}(2^+)$ is given by

$$M_{2\nu}(2^+) = \sqrt{\frac{1}{3}}\sum_N \frac{\langle 2^+\|\sigma\tau^+\|1^+_N\rangle\langle 1^+_N\|\sigma\tau^+\|0^+\rangle}{[E_0 + E_N - E_I]^3}, \quad (2)$$

where

$$E_0 = \frac{1}{2}(E_I - E_F) = \frac{1}{2}Q_{\beta\beta} + m_e. \quad (3)$$

Presently, the summation over the intermediate states is performed using the summation method [28]. Extending the summation method already applied to the $0^+ \to 0^+$ transition of $2\nu\beta^-\beta^-$ decay [26,27] to the $0^+ \to 2^+$ transition, the NTME $M_{2\nu}(2^+)$ is written as

$$M_{2\nu}(2^+) = \sqrt{5}\sum_{\pi,\nu} \frac{\langle 2^+_F\|[\boldsymbol{\sigma}\otimes\boldsymbol{\sigma}]^{(2)}\tau^+\tau^+\|0^+_I\rangle}{[E_0 + \varepsilon(n_\pi, l_\pi, j_\pi) - \varepsilon(n_\nu, l_\nu, j_\nu)]^3} \quad (4)$$

and this expression is the same as that of Hirsch *et al.* [32].

As each proton-neutron excitation is considered according to its spin-flip or non–spin-flip character, the use of the summation method in the present context goes beyond the closure approximation. The spin-orbit splitting is explicitly included in the energy denominator, and hence, the PHFB formalism in conjunction with the summation method goes beyond that previously employed in the pseudo $SU(3)$ model [31,32]. In the PHFB model, the NTME $M_{2\nu}(2^+)$ for the $0^+ \to 2^+$ transition of $2\nu\beta^-\beta^-$ decay is calculated using

$$\begin{aligned} M_{2\nu} &= \sum_{\pi,\nu} \frac{\langle \Psi^{J_f=2}_{00}|||[\boldsymbol{\sigma}\otimes\boldsymbol{\sigma}]^{(2)}\tau^+\tau^+||\Psi^{J_i=0}_{00}\rangle}{[E_0 + \varepsilon(n_\pi, l_\pi, j_\pi) - \varepsilon(n_\nu, l_\nu, j_\nu)]^3} \\ &= \left[n^{Ji=2}_{(Z,N)} n^{J_f=0}_{(Z+2,N-2)}\right]^{-1/2} \int_0^\pi n_{(Z,N),(Z+2,N-2)}(\theta) \\ &\quad \times \sum_\mu \begin{bmatrix} J_i & 2 & J_f \\ -\mu & \mu & 0 \end{bmatrix} d^{J_i}_{\mu 0}(\theta) \\ &\quad \times \sum_{\alpha\beta\gamma\delta} \frac{\langle \alpha\beta|[\boldsymbol{\sigma}\otimes\boldsymbol{\sigma}]^{(2)}\tau^+\tau^+|\gamma\delta\rangle}{[E_0 + \varepsilon_\alpha(n_\pi, l_\pi, j_\pi) - \varepsilon_\gamma(n_\nu, l_\nu, j_\nu)]^3} \\ &\quad \times \sum_{\varepsilon\eta} \left[\left(1 + F^{(\pi)}_{Z,N}(\theta) f^{(\pi)*}_{Z+2,N-2}\right)\right]^{-1}_{\varepsilon\alpha} \left(f^{(\pi)*}_{Z+2,N-2}\right)_{\varepsilon\beta} \\ &\quad \times \left[\left(1 + F^{(\nu)}_{Z,N}(\theta) f^{(\nu)*}_{Z+2,N-2}\right)\right]^{-1}_{\gamma\eta} \left(F^{(\nu)*}_{Z,N}\right)_{\eta\delta} \sin\theta\, \mathrm{d}\theta \end{aligned} \quad (5)$$

and the expressions for n^J, $n_{(Z,N),(Z+2,N-2)}(\theta)$, $f_{Z,N}$ and $F_{Z,N}(\theta)$ are given in refs. [26,27].

3 Results and discussions

The model space, single particle energies (SPEs), parameters of pairing plus multipolar type of effective two-body interaction have already been discussed in refs. [26,27, 34,35]. Specifically, the effective Hamiltonian is written as [34]

$$H = H_{sp} + V(P) + \zeta_{qq}\left[V(QQ) + V(HH)\right], \quad (6)$$

where H_{sp}, $V(P)$, $V(QQ)$ and $V(HH)$ denote the single particle Hamiltonian, the pairing, quadrupole-quadrupole and hexadecapole-hexadecapole parts of the effective two-body interaction, respectively. The ζ_{qq} is an arbitrary parameter and the final results are obtained by setting the $\zeta_{qq} = 1$. The purpose of introducing ζ_{qq} is to study the role of deformation by varying the strength of the QQ

Table 1. Calculated NTMEs $M_{2\nu}(2^+)$ within the PHFB model and their average $\overline{M}_{2\nu}(2^+)$ along with standard deviation $\Delta\overline{M}_{2\nu}(2^+)$.

Nuclei	$M_{2\nu}(2^+)$				$\overline{M}_{2\nu}(2^+)$	$\Delta\overline{M}_{2\nu}(2^+)$
	PQQ1	*PQQHH1*	*PQQ2*	*PQQHH2*		
^{94}Zr	1.44×10^{-4}	1.08×10^{-4}	4.08×10^{-5}	1.02×10^{-4}	9.88×10^{-5}	4.30×10^{-5}
^{96}Zr	9.71×10^{-5}	1.09×10^{-4}	9.15×10^{-5}	1.02×10^{-4}	9.98×10^{-5}	0.74×10^{-5}
^{100}Mo	1.95×10^{-5}	2.52×10^{-5}	2.02×10^{-5}	1.05×10^{-5}	1.89×10^{-5}	0.61×10^{-5}
^{104}Ru	3.30×10^{-5}	4.22×10^{-5}	3.05×10^{-5}	3.96×10^{-5}	3.63×10^{-5}	0.55×10^{-5}
^{110}Pd	1.21×10^{-4}	1.33×10^{-4}	1.12×10^{-4}	1.10×10^{-4}	1.19×10^{-4}	0.10×10^{-4}
^{128}Te	1.19×10^{-6}	2.89×10^{-6}	1.54×10^{-6}	2.65×10^{-6}	2.07×10^{-6}	0.83×10^{-6}
^{130}Te	7.72×10^{-7}	1.86×10^{-6}	8.55×10^{-7}	1.87×10^{-6}	1.34×10^{-6}	0.61×10^{-6}
^{150}Nd	6.32×10^{-6}	5.84×10^{-6}	5.74×10^{-6}	5.54×10^{-6}	5.86×10^{-6}	0.33×10^{-6}

Table 2. Excitation energies E_{2^+}, quadrupole moments $Q(2^+)$ of daughter nuclei, Q-values of $0^+ \to 2^+$ transition Q_{2^+} and the phase space factors $G_{2\nu}(2^+)$ with $g_A = 1.2701$.

Transition	E_{2^+} (MeV) [36]	Q (2^+) (eb) [37]	Q_{2^+} (MeV)	$G_{2\nu}(2^+)$
^{94}Zr $\to$ ^{94}Mo	0.871099	-0.13 ± 0.08	1.145	6.801×10^{-30}
^{96}Zr $\to$ ^{96}Mo	0.778213	-0.20 ± 0.08	2.572	1.494×10^{-18}
^{100}Mo $\to$ ^{100}Ru	0.53959	-0.54 ± 0.07	2.494	1.460×10^{-18}
^{104}Ru $\to$ ^{104}Pd	0.55579	-0.47 ± 0.10	0.743	9.625×10^{-25}
^{110}Pd $\to$ ^{110}Cd	0.657751	-0.40 ± 0.04	1.360	1.228×10^{-20}
^{128}Te $\to$ ^{128}Xe	0.4429		0.425	1.429×10^{-24}
^{130}Te $\to$ ^{130}Xe	0.5361		1.989	4.632×10^{-19}
^{150}Nd $\to$ ^{150}Sm	0.33395	-1.32 ± 0.19	3.037	3.253×10^{-17}

and *HH* interactions. In the *QQ* part of the effective two-body interaction $V(QQ)$, the strengths of the proton-proton, the neutron-neutron and the proton-neutron interactions are denoted by χ_{2pp}, χ_{2nn} and χ_{2pn}, respectively. By reproducing the experimental excitation energies E_{2^+} of the 2^+ state in two alternative ways provides two different parametrization of the *QQ* interaction, namely *PQQ*1 [26,27] and *PQQ*2 [35]. The inclusion of the hexadecapolar *HH* part of the effective interaction adds two additional parametrizations, namely *PQQHH*1 [34] and *PQQHH*2 [35].

In refs. [26,27,34,35], the reliability of wave functions generated with four different parametrizations of the effective two-body interaction, namely *PQQ*1, *PQQHH*1, *PQQ*2 and *PQQHH*2 was tested by comparing the theoretically calculated results for a number of spectroscopic properties, namely the yrast spectra, reduced $B(E2 : 0^+ \to 2^+)$ transition probabilities, quadrupole moments $Q(2^+)$ and g-factors $g(2^+)$ of ^{94,96}Zr, ^{94,96,100}Mo, ^{100,104}Ru, ^{104,110}Pd, ^{110}Cd, ^{128,130}Te, ^{128,130}Xe, ^{150}Nd and ^{150}Sm isotopes with the available experimental data. In addition, the calculated $M_{2\nu}$ and corresponding $T^{2\nu}_{1/2}$ for the $0^+ \to 0^+$ transition were compared with the available experimentally observed results. Presently, the same set of wave functions are employed to calculate the NTMEs $M_{2\nu}(2^+)$.

In table 1, the NTMEs $M_{2\nu}(2^+)$ calculated with wave functions generated with four different parametrizations of effective two-body interactions are presented. Although, there are only a set of four NTMEs $M_{2\nu}(2^+)$ for a statistical analysis, the estimated average NTMEs $\overline{M}_{2\nu}(2^+)$ and uncertainties $\Delta\overline{M}_{2\nu}(2^+)$ are given in the same table 1. The maximum uncertainty $\Delta\overline{M}_{2\nu}(2^+)$ in the average NTMEs $\overline{M}_{2\nu}(2^+)$ turns out to be about 45%, which implies that the NTMEs $M_{2\nu}(2^+)$ are highly sensitive to the deformation content of the intrinsic wave functions. The phase space factors $G_{2\nu}(2^+)$ have been calculated by Pahomi *et al.* [33] for most of the prospective $2\nu\beta^-\beta^-$ emitters. However, the $G_{2\nu}(2^+)$ of ^{94}Zr and ^{104}Ru isotopes are not available. We calculate them by adopting the prescription of Suhonen and Civitarese [10] using axial vector coupling constant $g_A = 1.2701$ [38]. The calculated $G_{2\nu}(2^+)$ for the $0^+ \to 2^+$ transition of $2\nu\beta^-\beta^-$ decay of ^{94}Zr and ^{104}Ru are $6.801 \times 10^{-30}\,\mathrm{y}^{-1}$ and $9.625 \times 10^{-25}\,\mathrm{y}^{-1}$, respectively.

A suppression of NTMEs $M_{2\nu}(0^+)$ for $2\nu\beta^-\beta^-$ decay with respect to the spherical case has been reported when the parent and daughter nuclei have different deformations [34,39,40]. To investigate this effect for the $0^+ \to 2^+$ transition, we present the NTMEs $M_{2\nu}(2^+)$ for the $2\nu\beta^-\beta^-$ decay of ^{94,96}Zr, ^{100}Mo, ^{104}Ru, ^{110}Pd, ^{128,130}Te and ^{150}Nd isotopes in fig. 1 as a function of the difference in the deformation parameter $\Delta\beta_2 = \beta_2(parent) - \beta_2(daughter)$ between the parent and daughter nuclei. The NTMEs $M_{2\nu}(2^+)$ are calculated by keeping the deformation for parent nuclei fixed at $\zeta_{qq} = 1$ and changing the deformation of daughter nuclei by varying ζ_{qq} in the range 0.0–1.5. It can be observed that in all cases but for ^{128,130}Te, the largest NTMEs correspond to the $|\Delta\beta_2|$ close to zero. With further increase in deformation, the NTMEs decrease with increase in $|\Delta\beta_2|$.

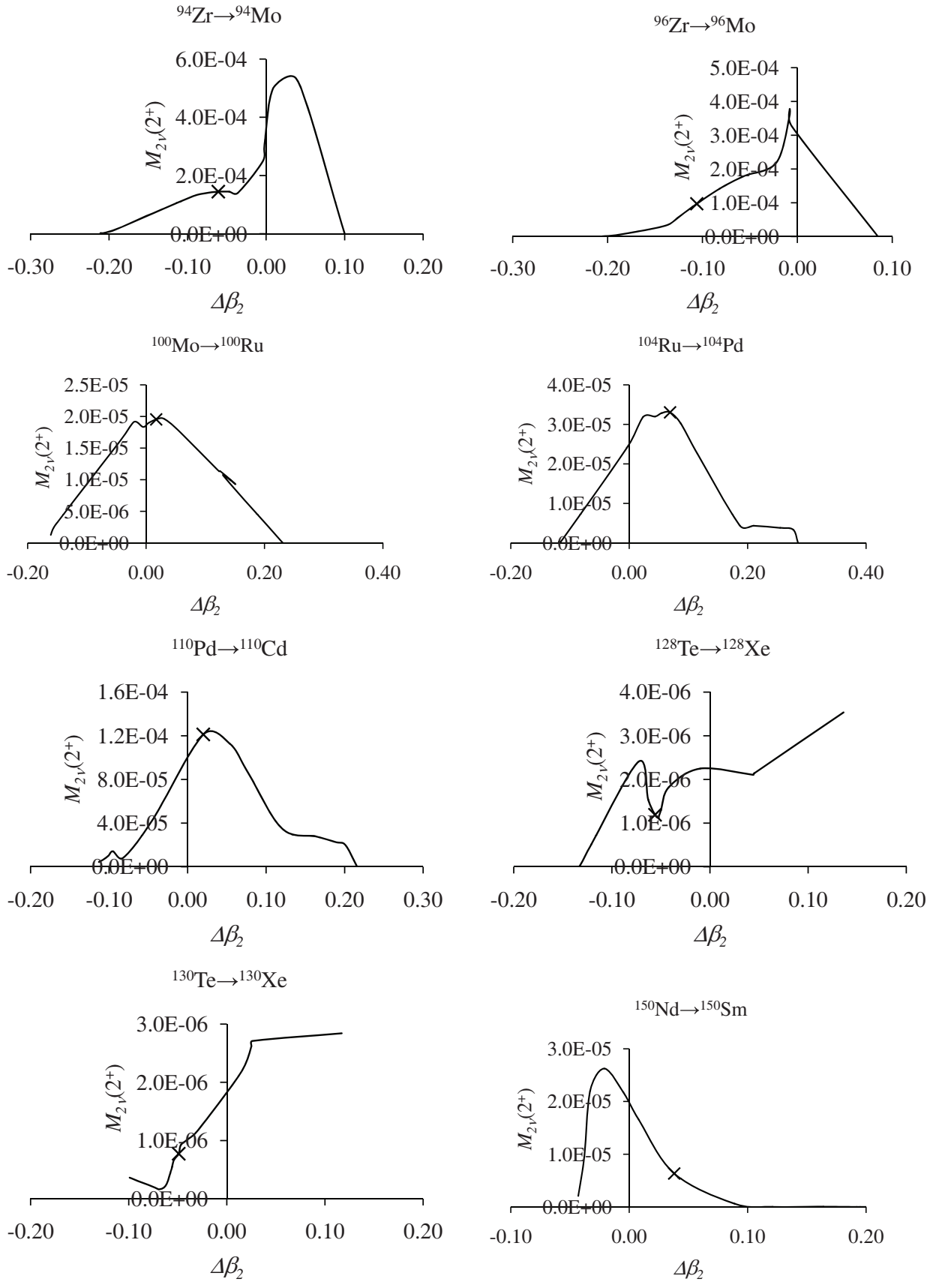

Fig. 1. NTMEs as a function of the difference in the deformation parameter $\Delta\beta_2$. "×" denotes the value of calculated NTMEs for $\Delta\beta_2$ at $\zeta_{qq} = 1.0$.

Table 3. Theoretically calculated NTMEs $M_{2\nu}(2^+)$ and half-lives $T^{2\nu}_{1/2}(2^+)$ for the $0^+ \to 2^+$ transition of ^{94,96}Zr, ^{100}Mo, ^{104}Ru, ^{110}Pd, ^{128,130}Te and ^{150}Nd nuclei along with experimental half-lives $T^{2\nu}_{1/2}(2^+)$. "*" denotes the present calculation with the average NTME.

Nuclei	Theory				Experiment	
	model	ref.	$\lvert M_{2\nu}(2^+)\rvert$	$T^{2\nu}_{1/2}$ (y)	$T^{2\nu}_{1/2}$ (y)	ref.
^{94}Zr	PHFB	*	9.88×10^{-5}	1.505×10^{37}	$> 1.3 \times 10^{19}$	[41]
	QRPA†	[42]	0.0170	5.088×10^{32}	$> 3.4 \times 10^{19}$	[43]
	QRPA‡	[42]	0.0155	6.120×10^{32}		
^{96}Zr	PHFB	*	9.98×10^{-5}	6.723×10^{25}	$> 2.0 \times 10^{18}$	[41]
	QRPA	[19]	(0.005–0.038)	2.677×10^{22}	$> 4.1 \times 10^{19}$	[44]
				4.635×10^{20}	$> 7.9 \times 10^{19}$	[19]
	QRPA	[20]	1.113×10^{-4}	5.403×10^{25}		
	QRPA	[21,22]	0.011	5.532×10^{21}		
	RQRPA†	[23]	0.011	5.532×10^{21}		
	RQRPA‡	[23]	0.010	6.693×10^{21}		
	RQRPA	[45]		$(1.1–1.4) \times 10^{21}$		
	SRPA	[24,25]	3.117×10^{-4}	6.889×10^{24}		
^{100}Mo	PHFB	*	1.89×10^{-5}	1.924×10^{27}	$> 1.5 \times 10^{20}$	[46]
	QRPA	[47]	0.033	6.290×10^{20}	$> 5.0 \times 10^{20}$	[48]
	QRPA	[20]	1.814×10^{-4}	2.081×10^{25}	$> 2.3 \times 10^{21}$	[49]
	QRPA	[21,22]	0.0078	1.126×10^{22}	$> 1.6 \times 10^{21}$	[50]
	RQRPA	[45]		$(1.0–1.1) \times 10^{22}$	$> 2.5 \times 10^{21}$	[51]
	SRPA	[24,25]	1.482×10^{-3}	3.119×10^{23}		
	$SU(3)^{+}$	[31]	7.3×10^{-5}	1.285×10^{26}		
	$SU(3)^{++}$	[31]	1.53×10^{-4}	2.926×10^{25}		
	MCM	[52]		$(5.3–13) \times 10^{20}$		
^{104}Ru	PHFB	*	3.63×10^{-5}	7.867×10^{32}		
	QRPA	[20]	3.736×10^{-3}	7.444×10^{28}		
	QRPA†	[42]	0.00792	1.656×10^{28}		
	QRPA‡	[42]	0.00811	1.580×10^{28}		
^{110}Pd	PHFB	*	1.19×10^{-4}	5.731×10^{27}	$> 2.9 \times 10^{20}$	[53]
	QRPA	[20]	6.671×10^{-3}	1.830×10^{24}		
	QRPA†	[42]	0.0112	6.492×10^{23}		
	QRPA‡	[42]	0.00766	1.388×10^{24}		
	SRPA	[54]	5.621×10^{-3}	2.577×10^{24}		
^{128}Te	PHFB	*	2.07×10^{-6}	1.636×10^{35}	$> 4.7 \times 10^{21}$	[55]
	QRPA	[20]	3.055×10^{-4}	7.498×10^{30}		
	QRPA	[21,22]	0.00287	8.496×10^{28}		
	SRPA	[54]	1.022×10^{-3}	6.700×10^{29}		
^{130}Te	PHFB	*	1.34×10^{-6}	1.201×10^{30}	$> 4.5 \times 10^{21}$	[55]
	QRPA	[20]	8.272×10^{-5}	3.155×10^{26}	$> 1.6 \times 10^{21}$	[56]
	QRPA	[21,22]	0.00016	8.433×10^{25}		
	SRPA	[54]	4.088×10^{-3}	1.292×10^{23}		
^{150}Nd	PHFB	*	5.86×10^{-6}	8.940×10^{26}	$> 8.0 \times 10^{18}$	[44]
	$SU(3)$	[32]	5.38×10^{-5}	1.062×10^{25}	$> 9.1 \times 10^{19}$	[57]
					$> 2.2 \times 10^{20}$	[58]

† WS basis.
‡ AWS basis.
$^{+}$ Spherical occupation wave functions.
$^{++}$ Deformed occupation wave functions.

As already mentioned, it has been observed that the inclusion of deformation in the mean field can reduce the NTMEs $M_{2\nu}(2^+)$ calculated in the pnQRPA model up to a factor of 341 [20]. In table 2, we present the excitation energies E_{2^+}, quadrupole moments $Q(2^+)$ of daughter nuclei along, Q-values of $0^+ \rightarrow 2^+$ transition Q_{2^+} and the $G_{2\nu}(2^+)$. According to the Grodzin's rule [59], the excitation energies E_{2^+} and quadrupole moments $Q(2^+)$ are inversely related. Although, a smaller E_{2^+} can give a higher Q-value Q_{2^+} resulting in a larger phase space factor, the NTMEs $M_{2\nu}(2^+)$ are reduced due to a larger $Q(2^+)$. Thus, the $0^+ \rightarrow 2^+$ transition is intrinsically suppressed due to the nuclear structure effects in addition to the cubic dependence of the energy denominator.

A large number of experimental and theoretical studies have been carried out for the $0^+ \rightarrow 2^+$ transition of $2\nu\beta^-\beta^-$ decay. Over the past years, the $0^+ \rightarrow 2^+$ transition of $2\nu\beta^-\beta^-$ decay of ^{94}Zr [41,43], ^{96}Zr [19,44], ^{100}Mo [46,48–51], ^{110}Pd [53], ^{128}Te [55], ^{130}Te [55,56] and ^{150}Nd [44,57,58] isotopes has been experimentally investigated. However, the $2\nu\beta^-\beta^-$ decay of ^{104}Ru for the $0^+ \rightarrow 2^+$ transition has not been experimentally investigated so far. All the available theoretical and experimental results are compiled in table 3. We present only the theoretical $T^{2\nu}_{1/2}(2^+)$ for those models for which no direct or indirect information about $M_{2\nu}(2^+)$ is available to us. As already mentioned, there is a remarkable spread in the calculated NTMEs $M_{2\nu}(2^+)$ within different models. Specifically, the NTMEs $M_{2\nu}(2^+)$ calculated with the QRPA model without and with deformation vary by a factor of 2–341, corresponding to ^{130}Te and ^{96}Zr isotopes, respectively. The average NTMEs $\overline{M}_{2\nu}(2^+)$ evaluated using the PHFB approach are suppressed by a factor between 1–150 with respect to those of Raduta *et al.* [20] corresponding to ^{96}Zr and ^{128}Te isotopes, respectively. Consideration of the available theoretical and experimental results suggests that the prospective nuclei for the observation of the $0^+ \rightarrow 2^+$ transition of $2\nu\beta^-\beta^-$ decay are ^{96}Zr, ^{100}Mo, ^{110}Pd, ^{130}Te and ^{150}Nd.

4 Conclusions

Using a set of reliable wave functions generated with four different parametrizations of the effective two-body interaction, namely, $PQQ1$, $PQQHH1$, $PQQ2$ and $PQQHH2$ [26,27,34,35], sets of four NTMEs $M_{2\nu}(2^+)$ have been calculated to study the $2\nu\beta^-\beta^-$ decay of ^{94,96}Zr, ^{100}Mo, ^{104}Ru, ^{110}Pd, ^{128,130}Te and ^{150}Nd isotopes for the $0^+ \rightarrow 2^+$ transition. It is noticed that the $0^+ \rightarrow 2^+$ transition is intrinsically suppressed due to the cubic dependence of the energy denominator and nuclear structure effects. Specifically, a large phase space factor due to a larger Q-value implies a smaller E_{2^+} resulting from a larger $Q(2^+)$, which results in the suppression of NTMEs $M_{2\nu}(2^+)$.

The observation of Raduta *et al.* [20] that the inclusion of deformation in the mean field can reduce the NTMEs $M_{2\nu}(2^+)$ calculated within pnQRPA up to a factor of 341, motivated us to study the $0^+ \rightarrow 2^+$ transition of $2\nu\beta^-\beta^-$ decay within the PHFB approach treating the pairing and deformation degrees of freedom simultaneously on an equal footing. It is noticed that with respect to NTMEs $M_{2\nu}(2^+)$ of Raduta *et al.* [20], the average NTMEs $\overline{M}_{2\nu}(2^+)$ calculated using the PHFB approach are further suppressed by a factor between 1–150 corresponding to ^{96}Zr and ^{128}Te isotopes, respectively. In spite of the fact that the $0^+ \rightarrow 2^+$ transition of $2\nu\beta^-\beta^-$ decay is highly suppressed in comparison to the $0^+ \rightarrow 0^+$ transition, the available theoretical and experimental results suggest that the observation of the $0^+ \rightarrow 2^+$ transition of $2\nu\beta^-\beta^-$ decay may be possible in ^{96}Zr, ^{100}Mo, ^{110}Pd, ^{130}Te and ^{150}Nd isotopes.

This work is partially supported by DST-SERB, India vide sanction No. SR/FTP/PS-085/2011, SB/S2/HEP-007/2013 and Council of Scientific and Industrial Research (CSIR), India vide sanction No. 03(1216)/12/EMR-II.

References

1. J.D. Vergados, H. Ejiri, F. Šimkovic, Int. J. Mod. Phys. E **25**, 1630007 (2016).
2. J.D. Vergados, H. Ejiri, F. Šimkovic, Rep. Prog. Phys. **75**, 106301 (2012).
3. R. Saakyan, Annu. Rev. Nucl. Part. Sci. **63**, 503 (2013).
4. Reyco Henning, Rev. Phys. **1**, 29 (2016).
5. I. Ostrovskiy, Mod. Phys. Lett. A **31**, 1630017 (2016).
6. J. Engel, J. Menéndez, Rep. Prog. Phys. **80**, 046301 (2017).
7. H.V. Klapdor-Kleingrothaus, I.V. Krivosheina, I.V. Titkova, Int. J. Mod. Phys. A **21**, 1159 (2006).
8. H.V. Klapdor-Kleingrothaus, I.V. Krivosheina, Mod. Phys. Lett. A **21**, 1547 (2006).
9. T. Tomoda, Rep. Prog. Phys. **54**, 53 (1991).
10. J. Suhonen, O. Civitarese, Phys. Rep. **300**, 123 (1998).
11. A.S. Barabash, AIP Conf. Proc. **1894**, 020002 (2017).
12. A.S. Barabash, A.D. Dolgov, R. Dvornický, F. Šimkovic, A.Yu. Smirnov, Nucl. Phys. B **783**, 90 (2007).
13. A.S. Barabash, Nucl. Phys. A **935**, 52 (2015).
14. V.I. Tretyak, Y.G. Zdesenko, At. Data Nucl. Data Tables **80**, 83 (2002).
15. V.I. Tretyak, Y.G. Zdesenko, At. Data Nucl. Data Tables **61**, 43 (1995).
16. J. Kotila, F. Iachello, Phys. Rev. C **85**, 034316 (2012).
17. S. Stoica, M. Mirea, Phys. Rev. C **88**, 037303 (2013).
18. J. Barea, J. Kotila, F. Iachello, Phys. Rev. C **91**, 034304 (2015).
19. A.S. Barabash, R. Gurriaran, F. Hubert, Ph. Hubert, J.L. Reyss, J. Suhonen, V.I. Umatov, J. Phys. G Nucl. Part. Phys. **22**, 487 (1996).
20. A.A. Raduta, C.M. Raduta, Phys. Lett. B **647**, 265 (2007).
21. S. Unlu, Chin. Phys. Lett. **31**, 042101 (2014).
22. S. Unlu, Phys. Scr. **87**, 045202 (2013).
23. J. Toivanen, J. Suhonen, Phys. Rev. C **55**, 2314 (1997).
24. S. Stoica, I. Mihut, Nucl. Phys. A **602**, 197 (1996).
25. S. Stoica, Phys. Lett. B **350**, 152 (1995).
26. R. Chandra, J. Singh, P.K. Rath, P.K. Raina, J.G. Hirsch, Eur. Phys. J. A **23**, 223 (2005).

27. S. Singh, R. Chandra, P.K. Rath, P.K. Raina, J.G. Hirsch, Eur. Phys. J. A **33**, 375 (2007).
28. O. Civitarese, J. Suhonen, Phys. Rev. C **47**, 2410 (1993).
29. W.C. Haxton, G.J. Stephenson jr., Prog. Part. Nucl. Phys. **12**, 409 (1984).
30. M. Doi, T. Kotani, E. Takasugi, Prog. Theor. Phys. Suppl. **83**, 1 (1985).
31. J.G. Hirsch, O. Castanos, P.O. Hess, O. Civitarese, Phys. Rev. C **51**, 2252 (1995).
32. J.G. Hirsch, O. Castaños, P.O. Hess, O. Civitarese, Nucl. Phys. A **589**, 445 (1995).
33. T.E. Pahomi, A. Neacsu, M. Mirea, S. Stoica, Romanian Rep. Phys. **66**, 370 (2014).
34. R. Chandra, K. Chaturvedi, P.K. Rath, P.K. Raina, J.G. Hirsch, EPL **86**, 32001 (2009).
35. P.K. Rath, R. Chandra, K. Chaturvedi, P.K. Raina, J.G. Hirsch, Phys. Rev. C **82**, 064310 (2010).
36. M. Sakai, At. Data Nucl. Data Tables **31**, 400 (1984).
37. P. Raghavan, At. Data Nucl. Data Tables **42**, 189 (1989).
38. Particle Data Group (J. Beringer *et al.*), Phys. Rev. D **86**, 010001 (2012).
39. R. Álvarez-Rodríguez, P. Sarriguren, E. Moya de Guerra, L. Pacearescu, A. Faessler, F. Šimkovic, Phys. Rev. C **70**, 064309 (2004).
40. J. Menéndez, A. Poves, E. Caurier, F. Nowacki, Nucl. Phys. A **818**, 139 (2009).
41. E.B. Norman, D.M. Meekhof, Phys. Lett. B **195**, 126 (1987).
42. J. Suhonen, Nucl. Phys. A **864**, 63 (2011).
43. N. Dokania *et al.*, Eur. Phys. J. A **53**, 74 (2017).
44. C. Arpesella, A.S. Barabash, E. Bellotti, E. Brofferio, E. Fiorini, P.P. Sverzellati, V.I. Umatov, Europhys. Lett. **27**, 29 (1994).
45. J. Schweiger, F. Simkovic, A. Faessler, W.A. Kominski, Phys. Rev. C **57**, 1738 (1998).
46. N. Kudomi, H. Ejiri, K. Nagata, K. Okada, T. Shibata, T. Shima, J. Tanaka, Phys. Rev. C **46**, R2132 (1992).
47. J. Suhonen, O. Civitarese, Phys. Rev. C **49**, 3055 (1994).
48. D. Blum *et al.*, Phys. Lett. B **275**, 506 (1992).
49. A.S. Barabash, F.T. Avignoue III, C.K. Guerard, R.L. Brodzinski, H.S. Miley, J.H. Reeves, V.I. Umatov, in *Proceedings of 3rd Int. Symp. on Weak and Electromagn. Interactions in Nuclei WEIN-92. Dubna, Russia, June 16-22, 1992* (World Sci. Publ. Co., 1993) p. 582.
50. A.S. Barabash *et al.*, Phys. Lett. B **345**, 408 (1995).
51. R. Arnold *et al.*, Nucl. Phys. A **925**, 25 (2014).
52. J. Suhonen, Phys. At. Nucl. **61**, 1186 (1998).
53. B. Lehnert *et al.*, J. Phys. G: Nucl. Part. Phys. **43**, 115201 (2016).
54. S. Stoica, Phys. Rev. C **49**, 2240 (1994).
55. E. Bellotti, C. Cattadori, O. Cremonesi, E. Fiorini, C. Liguori, A. Pullia, P.P. Sverzellati, L. Zanotti, Europhys. Lett. **3**, 889 (1987).
56. A.S. Barabash, F. Hubert, Ph. Hubert, V.I. Umatov, Eur. Phys. J. A **11**, 143 (2001).
57. C. Arpesella, E. Bellotti, N. Ferrari, L. Zanotti, Nucl. Phys. B (Proc. Suppl.) **70**, 249 (1999).
58. A.S. Barabash, Ph. Hubert, A. Nachab, V.I. Umatov, Phys. Rev. C **79**, 045501 (2009).
59. L. Grodzins, Phys. Lett. B **2**, 88 (1962).

Neutrinoless double beta decay and Physics beyond the Standard Model

Yash Kaur Singh[1], Pooja Lohani[2], V. K. Nautiyal[1], R. Gautam[1], R. Chandra[1],* K. Chaturvedi[3], P. K. Rath[2] and P. K. Raina[4]

[1] *Department of Applied Physics, Babasaheb Bhimrao Ambedkar University, Lucknow - 226025, INDIA*
[2]*Department of Physics, University of Lucknow, Lucknow, 226007, INDIA*
[3] *Department of Physics, Bundelkhand University, Jhansi – 284128, INDIA*
[4]*Department of Physics, IIT Ropar, Nangal Road, Rupnagar, Punjab – 140001, INDIA*
* *email: ramesh.luphy@gmail.com*

Introduction

The nuclear ββ decay, in which the charge *Z* of an even *Z*-even *N* nucleus is changed by two units while the mass number *A* remains the same, is a rare and spontaneous process of weak interaction in nature. The ββ decay can be categorized in mainly two modes, namely two neutrino double beta $(\beta\beta)_{2\nu}$ decay and neutrinoless double beta $(\beta\beta)_{0\nu}$ decay. The $(\beta\beta)_{2\nu}$ decay establishes the validity of different nuclear models employed for nuclear structure calculations by calculating the nuclear transition matrix elements (NTMEs) $M_{2\nu}$. The $(\beta\beta)_{0\nu}$ decay violates the lepton number conservation by two units and can be studied in any theory in which lepton number conservation is not exact. Hence $(\beta\beta)_{0\nu}$ decay is an excellent process to probe the new physics beyond the standard model (SM) of electroweak unification. Apart from the well studied left-right symmetric model, the $(\beta\beta)_{0\nu}$ decay can also be studied in Majoron models, R-parity violating as well as conserving supersymmetric (SUSY) models. Further, the $(\beta\beta)_{0\nu}$ decay can verify issues like compositeness, leptoquarks, sterile neutrinos and violation of weak equivalence principle. The detailed progress of experimental as well as theoretical studies on ββ decay in general and $(\beta\beta)_{0\nu}$ decay in particular can be found in references [1,2] and references there in.

The PHFB model in conjunction with pairing plus multipole type of two-body effective interaction has been successfully applied to study the $(\beta\beta)_{0\nu}$ decay [3-7]. In present work the same PHFB model has been applied to study the $(\beta\beta)_{0\nu}$ decay in various theories beyond the SM.

Theoretical framework

The details about the model space, single particle energies, *PQQ* type of effective two-body interaction and the procedure to fix its parameters have been given in Refs. [3,4]. The Hamiltonian of the effective two-body interaction used in the present work is given as

$$H = H_{s.p.} + V(P) + V(QQ) + V(HH) \quad (1)$$

where $H_{s.p.}$, $V(P)$, $V(QQ)$ and $V(HH)$ denote the single particle Hamiltonian, pairing, quadrupole-quadrupole and hexadecapole-hexadecapole parts of the effective two-body interaction. We use four different parametrizations of the interaction Hamiltonian, namely *PQQ*1, *PQQ*2, *PQQHH*1 and *PQQHH*2 [5]. Further, we use the Jastrow type of short range correlations with Miller-Spencer, Argonne V18 and CD-Bonn NN potentials [5,8]. The detailed theoretical formalism to study the $(\beta\beta)_{0\nu}$ decay in Majoron and SUSY models are given in refs. [9,10,11]. Further, the theory of compositeness and leptoquark in connection with $(\beta\beta)_{0\nu}$ decay is given in refs. [12,13].

Results and discussions

The NTMEs involved in $(\beta\beta)_{0\nu}$ decay in various theories stated above are calculated within PHFB model using pairing plus multipole type of two-body interaction. The NTMEs have been calculated by considering the finite size of nucleon (F) and Jastrow type of short range correlations (SRC) with Miller-Spencer, Argonne V18 and CD-Bonn NN potentials for $(\beta\beta)_{0\nu}$ decay of ^{94,96}Zr, ^{100}Mo, ^{128,130}Te and ^{150}Nd isotopes for the $0^+ \rightarrow 0^+$ transition. At present, some results are presented for the case of ^{100}Mo

with *PQQ1* parametrization. The detailed results will be presented in the symposium.

Table 1: NTMEs for the Majoron accompanied $(\beta\beta)_{0\nu}$ decay of ^{100}Mo for the *PQQ1* parametrization.

NTME	F	F+S		
		SRC1	SRC2	SRC3
$M^{(\chi)}_{Fm_\nu}$	2.15	1.89	2.15	2.22
$M^{(\chi)}_{GTm_\nu}$	-5.52	-4.72	-5.43	-5.66
$M^{(\chi)}_{Tm_\nu}$	0.05	0.05	0.05	0.05
$M^{(\chi)}_{CR}$	-0.26	-0.23	-0.26	-0.27
$M^{(\chi)}_{F\omega^2}$ $\times 10^3$	1.18	1.14	1.19	1.20
$M^{(\chi)}_{GT\omega^2}$ $\times 10^3$	-5.79	-5.60	-5.86	-5.91

Table 2: NTMEs of $(\beta\beta)_{0\nu}$ decay in SUSY models via exchange of gluinos for ^{100}Mo with in PHFB model using *PQQ1* interaction.

NTME	F	F+S		
		SRC1	SRC2	SRC3
M^N_F	0.716	0.037	0.056	0.067
M^P_F	0.007	0.003	-0.002	0.002
M^N_{GT}	-0.210	-0.108	-0.164	-0.196
M^P_{GT}	-0.023	0.009	0.004	-0.007
$M^{1\pi}_{GT}$	5.422	2.169	3.80	4.831
$M^{2\pi}_{GT}$	2.613	1.856	2.45	2.661
M^P_T	0.001	0.001	0.001	0.001
$M^{1\pi}_T$	0.285	0.285	0.302	0.302
$M^{2\pi}_T$	0.130	0.132	0.134	0.134

Table 3: NTMEs of $(\beta\beta)_{0\nu}$ decay in SUSY models via exchange of squark for ^{100}Mo with in PHFB model using *PQQ1* interaction.

NTME	F	F+S		
		SRC1	SRC2	SRC3
M_F	-258.7	-131.7	-201.4	-241.1
$M_{GT\text{-}MT}$	412.4	207.4	318.8	382.1
$M_{GT\text{-}AP}$	-25.77	-20.00	-24.92	-26.57
$M_{GT\text{-}\pi}$	506.4	441.8	511.2	528.9
$M_{T\text{-}MT}$	-10.33	-10.36	-10.85	-10.83
$M_{T\text{-}AP}$	-1.13	-1.14	-1.15	-1.15
$M_{T\text{-}\pi}$	17.90	18.06	18.09	18.07

In Table 1, 2 and 3, SRC1, SRC2 and SRC3 denote the Jastrow type of short range correlations (SRC) with Miller-Spencer, Argonne V18 and CD-Bonn NN potentials, respectively.

References

[1] F. T. Avignone III, S. R. Elliott, and J. Engel, Rev. Mod. Phys.**80**, 481 (2008).

[2] J. D. Vergados, H. Ejiri, and F. Simkovic, Rep. Prog. Phys. **75**,106301 (2012).

[3] R. Chandra, J. Singh, P. K. Rath, P. K. Raina, and J. G. Hirsch, Eur. Phys. J. A **23**, 223 (2005).

[4] S. Singh, R. Chandra, P. K. Rath, P. K. Raina, and J. G. Hirsch, Eur. Phys. J. A **33**, 375 (2007).

[5] P. K. Rath, R. Chandra, K. Chaturvedi, P. K. Raina, and J. G. Hirsch, Phys. Rev. C. **82**, 064310 (2010).

[6] P. K. Rath, R. Chandra, K. Chaturvedi, P. Lohani, P. K. Raina, and J. G. Hirsch, Phys. Rev. C **88**, 064322 (2013).

[7] P. K. Rath, R. Chandra, K. Chaturvedi, P. Lohani, and P. K. Raina, Phys. Rev. C **93**, 024314 (2016).

[8] F. Simkovic, A. Faessler, H. Muther, V. Rodin, and M. Stauf, Phys. Rev. C **79**, 055501 (2009).

[9] M. Hirsch, H. V. Klapdor-Kleingrothaus, S. G. Kovalenko and H. Pas, Phys. Lett. B **372**, 8 (1996).

[10] M. Hirsch, H. V. Klapdor-Kleingrothaus and S. G. Kovalenko, Phys. Lett. B **372**, 181 (1996).

[11] A. Faessler, T. Gutsche, S. Kovalenko and F. Simkovic, Phys. Rev. D **77**, 113012 (2008).

[12] O. Panella, C. Carimalo, Y.N. Srivastava and A. Widom, Phys. Rev. D **56**, 5766 (1997).

[13] M. Hirsch, H.V. Klapdor-Kleingrothaus and S.G. Kovalenko, Phys. Rev. D **54**, R4207 (1996).

Acknowledgment

One of the authors RC thanks DST-SERB, India for financial support vide Dy. No. SERB/F/6190/2015-16.

Study of neutrinoless double beta decay in R-parity violating supersymmetric models via exchange of gluinos

Yash Kaur Singh[1], T. K. Yadav[2], R. Chandra[1],* P. K. Rath[2] and P. K. Raina[3]
[1] *Department of Applied Physics, Babasaheb Bhimrao Ambedkar University, Lucknow - 226025, INDIA*
[2]*Department of Physics, University of Lucknow, Lucknow, 226007, INDIA*
[3] *Department of Physics, IIT Ropar, Nangal Road, Rupnagar, Punjab – 140001, INDIA*
* *email: ramesh.luphy@gmail.com*

Introduction

The $(\beta^-\beta^-)_{0\nu}$ decay mode is far more interesting since it violates the conservation of lepton number L by two units ($\Delta L=2$). The $(\beta^-\beta^-)_{0\nu}$ decay process requires massive Majorana neutrino and the Majorana mass term requires the breaking of lepton number L. However, the only gauge-anomaly free combination of quantum numbers in general gauge theories is B-L. Therefore, one considers the breaking of B-L symmetry. The B-L conservation is exact in the standard model (SM) of electroweak unification and hence the $(\beta^-\beta^-)_{0\nu}$ decay is not allowed in the SM. However, the B-L violation is expected in the gauge theories beyond the SM. Besides the exchange of a Majorana neutrino, the $(\beta^-\beta^-)_{0\nu}$ decay can also proceed through other mechanisms which involve B-L violation.

Out of such several mechanisms responsible for $(\beta^-\beta^-)_{0\nu}$ decay, we consider here the contribution of R-parity violating Minimal supersymmetric standard model (R_p MSSM). In supersymmetry theories the R-parity (R_p) is a discrete, multiplicative symmetry defined as $R_p=(-1)^{3B+L+2S}$, where S, B and L are the spin, baryon number and lepton number, respectively. The $R_p=+1$ for ordinary particles and $R_p=-1$ for their superpartners. The R-parity violating supersymmetric models have been widely reviewed in the literature because of their interesting phenomenological and cosmological implications.

In the R_p-violating MSSM [1,2], the exchange of gluinos, photinos etc. contributes to $(\beta^-\beta^-)_{0\nu}$ decay and leads to a very stringent limit on the first generation Yukawa coupling and combination of the intergeneration Yukawa couplings. Constraint on the Yukawa coupling constant is given as

$$\lambda'_{11i}\lambda'_{1i1} \leq \varepsilon'_i\left(\frac{\Lambda_{SUSY}}{100GeV}\right)^3$$

Here, Λ_{SUSY} is effective SUSY breaking scale. The current upper bound for the R_p violating SUSY interaction constant λ_{111}' is $\leq 1.2\times10^{-4}$ ($\leq 3.8\times10^{-2}$) [3] assuming masses of SUSY particles to be on the scale of 100 GeV (1 TeV) for the case of ^{76}Ge. For the same inputs and using the best fit value of half-life $T_{1/2}^{0\nu}=1.19\times10^{25}$ yr [4], one gets $\lambda_{111}'=1.3\times10^{-4}$ (4.1×10^{-2}) assuming the scale of SUSY particles to be 100 GeV (1 TeV).

In the present work, the relevant nuclear transition matrix elements (NTMEs) necessary to extract SUSY parameters from $(\beta^-\beta^-)_{0\nu}$ decay of nuclei in the mass range 94–150 are calculated using Projected Hartree-Fock Bogoliubov (PHFB) model in conjunction with pairing plus multi pole type of two body interaction. The PHFB model has been successfully applied to study the $(\beta^-\beta^-)_{0\nu}$ decay in left-right symmetric models and majoron models [5]. Finally the constraints on the combination of lepton number violating parameters are derived from the available half-life limits of $(\beta^-\beta^-)_{0\nu}$ decay.

Theoretical framework

The inverse half life of $(\beta^-\beta^-)_{0\nu}$ decay in Rp MSSM is given by [2]

$$T_{1/2}^{-1}(0\nu\beta\beta) = G_{01}\,M_1^{\nu}(m_e R)^{-1}\left(4\overline{\eta}_{(i)} - \overline{\eta}_{(q)} + \eta_{(q)}\right)^2 \quad (1)$$

where the two body nuclear transition matrix elements are

$$M_F^{(i)} = \left\langle 0_f^+ \left\| h_+(\mu,\mathbf{r})\tau_n^+\tau_m^+ \right\| 0_i^+ \right\rangle \quad (2)$$

$$M_{GT}^{(i)} = \left\langle 0_f^+ \left\| h_+(\mu,\mathbf{r})\tau_n^+\tau_m^+\boldsymbol{\sigma}_n\,\boldsymbol{\sigma}_m \right\| 0_i^+ \right\rangle \quad (3)$$

$$M_{GT'}^{(i)} = \left\langle 0_f^+ \left\| h_R(\mu,\mathbf{r})\tau_n^+\tau_m^+\boldsymbol{\sigma}_n\,\boldsymbol{\sigma}_m \right\| 0_i^+ \right\rangle \quad (4)$$

$$M_{T'}^{(i)} = \left\langle 0_f^+ \left\| h_{T'}(\mu,\mathbf{r})\, S_{nm}\ \tau_n^+\tau_m^+ \right\| 0_i^+ \right\rangle \quad (5)$$

where h_α denotes the neutrino potentials

$$h_+(\mu,\mathbf{r}) = \frac{2}{\pi} R \int_0^\infty dq \cdot q^2 \frac{j_0(qr)\, f^2(q^2)}{\omega(\omega+\bar{A})} \quad (6)$$

$$h_R(\mu,\mathbf{r}) = \frac{2}{\pi}\frac{R^2}{m_p}\int_0^\infty dq \cdot q^4 \frac{j_0(qr)\, f^2(q^2)}{\omega(\omega+\bar{A})} \quad (7)$$

$$h_{T'}(\mu,\mathbf{r}) = \frac{2}{\pi}\frac{R^2}{m_p}\int_0^\infty dq \cdot q^4 \frac{j_0(qr) - 3j_1(qr)}{\omega(\omega+\bar{A})} f^2(q^2) \quad (8)$$

Results and discussions

The appropriate NTMEs involved in $(\beta^-\beta^-)_{0\nu}$ decay in Rp MSSM calculated within PHFB model using pairing plus quadrupole-quadrupole (PQQ) interaction is presented in Table 1. Further, the NTMEs have been calculated by considering the finite size of nucleon (F) and Jastrow type of short range correlations (SRC) with Miller-Spencer, Argonne V18 and CD-Bonn NN potentials for the SUSY accompanied $(\beta^-\beta^-)_{0\nu}$ decay of ^{94,96}Zr, ^{98,100}Mo, ^{104}Ru, ^{110}Pd, ^{128,130}Te and ^{150}Nd isotopes for the $0^+\rightarrow0^+$ transition. At present, the results are presented for the case of ^{100}Mo.

Table 1: Calculated NTMEs M_α of SUSY accompanied $(\beta^-\beta^-)_{0\nu}$ decay of ^{100}Mo in the PHFB model using PQQ interaction.

$\mathbf{M_\alpha}$	**F+SRC**		
	SRC1	**SRC2**	**SRC3**
M_{FN}	3.74×10^{-2}	5.64×10^{-2}	6.71×10^{-2}
M_F	-3.32×10^{-3}	-1.69×10^{-3}	2.22×10^{-3}
M_{GTN}	-0.108	-0.164	-0.196
M_{GT}	9.14×10^{-3}	4.25×10^{-3}	-7.44×10^{-3}
$M_{GT}^{1\pi}$	2.17	3.80	4.83
$M_{GT}^{2\pi}$	1.86	2.45	2.67
M_T	1.24×10^{-3}	1.50×10^{-3}	1.53×10^{-3}
$M_T^{1\pi}$	0.285	0.302	0.302
$M_T^{2\pi}$	0.132	0.134	0.134

In Table 1, SRC1, SRC2 and SRC3 denote the Jastrow type of short range correlations (SRC) with Miller-Spencer, Argonne V18 and CD-Bonn NN potentials, respectively. The calculation of NTMEs for rest of the nuclei stated above along with the extracted limits on SUSY parameters will be presented in the symposium.

Conclusions

To summarize, we study the $(\beta^-\beta^-)_{0\nu}$ decay of ^{94,96}Zr, ^{98,100}Mo, ^{104}Ru, ^{110}Pd, ^{128,130}Te and ^{150}Nd isotopes for the $0^+\rightarrow0^+$ transition in R_p-violating MSSM via exchange of gluinos. The relevant NTMEs are calculated within PHFB model using pairing plus multi pole type of two-body effective interaction. The SUSY parameters of R_p-violating MSSM using calculated NTMEs and experimental data will be extracted and presented in the symposium.

References

[1] R. N. Mohapatra and P. B. Pal, Massive Neutrinos in Physics and Astophysics, World Scientific, Singapore, (1991).

[2] M. Hirsch, H. V. Klapdor-Kleingrothaus and S. G. Kovalenko, Phys. Lett. B **372**, 181 (1996).

[3] A. Faessler and F. Simkovic, Prog. Part. Nucl. Phys. **46**, 233 (2001).

[4] H. V. Klapdor-Kleingrothaus, I. V. Krivoshina, A. Dietz and O. Chkvorets, Phys. Lett. B **586**, 198 (2004).

[5] P. K. Rath, R. Chandra, K. Chaturvedi, P. Lohani, P. K. Raina, and J. G. Hirsch, Phys. Rev. C **88**, 064322 (2013).

Acknowledgment

One of the authors RC thanks DST-SERB, India for financial support vide Dy. No. SERB/F/5139/2013-14.

Study of Majoron accompanied neutrinoless double beta decay

R. Chandra[1],* K. Chaturvedi[2], Yash Kaur Singh[1], T. K. Yadav[1], P. K. Rath[3] and P. K. Raina[4]

[1] *Department of Applied Physics, Babasaheb Bhimrao Ambedkar University, Lucknow - 226025, INDIA*
[2] *Department of Physics, Bundelkhand University, Jhansi – 284128, INDIA*
[3] *Department of Physics, University of Lucknow, Lucknow, 226007, INDIA*
[4] *Department of Physics, IIT Ropar, Nangal Road, Rupnagar, Punjab – 140001, INDIA*
* *email: ramesh.luphy@gmail.com*

Introduction

In the last decade, the confirmation of neutrino flavor oscillations and the reported observation of neutrinoless double beta $(\beta\beta)_{0\nu}$ decay have together played an extremely inspirational role in the advancement of a vast amount of experimental as well as theoretical studies on nuclear double-β decay in general and $(\beta\beta)_{0\nu}$ decay in particular [1,2].

In the left-right symmetric model [3,4], the possible mechanisms of $(\beta^-\beta^-)_{0\nu}$ decay are the exchange of left handed light as well as heavy Majorana neutrinos and the exchange of right handed heavy Majorana neutrinos. Alternatively, the occurrence of lepton number violating Majoron accompanied $(\beta\beta)_{0\nu}$ decay is also a possibility. The Majorons, in a general sense, are massless or light bosons carrying leptonic charge L. The existence of Majorons can play a crucial role in many areas namely Physics beyond the Standard Model, history of early universe, evolution of steller objects, supernovae astrophysics and the solar neutrino problem.

Following Bamert et al. [5], the nine different Majoron models are summarized in Table 1:

Table 1: Nine Majoron models according to Bamert et al. [5].

Mode	Case	n	L	M_α
$\beta\beta\phi$	IB	1	0	M_F-M_{GT}
$\beta\beta\phi$	IC	1	0	M_F-M_{GT}
$\beta\beta\phi$	IIB	1	-2	M_F-M_{GT}
$\beta\beta\phi$	IIC	3	-2	M_{CR}
$\beta\beta\phi$	IIF	3	-2	M_{CR}
$\beta\beta\phi\phi$	ID	3	0	$M_{F\omega2}$-$M_{GT\omega2}$
$\beta\beta\phi\phi$	IE	3	0	$M_{F\omega2}$-$M_{GT\omega2}$
$\beta\beta\phi\phi$	IID	3	-1	$M_{F\omega2}$-$M_{GT\omega2}$
$\beta\beta\phi\phi$	IIE	7	-1	$M_{F\omega2}$-$M_{GT\omega2}$

It can be noticed from Table 1 that the proposed Majoron models can be broadly classified as single Majoron emission $(\beta\beta\phi)_{0\nu}$ and double Majoron emission $(\beta\beta\phi\phi)_{0\nu}$ depending upon the number of Majorons emitted. In table 1, n, L and M_α denote the spectral index of the sum energy spectrum, leptonic charge and nuclear transition matrix elements (NTMEs), respectively.

The projected Hartree-Fock Bogoliubov (PHFB) model in conjunction with pairing plus quadrupole-quadrupole (PQQ) interaction has been successfully applied to study the $(\beta\beta)_{0\nu}$ decay as well as classical Majoron models i.e. the case IB, IC and IIB [6]. In the present case we apply the same model to calculate the NTMEs of rest of the Majoron models i.e. the case IIC, IIF, ID, IE, IID and IIE.

Theoretical framework

The details about the model space, single particle energies, *PQQ* type of effective two-body interaction and the procedure to fix its parameters have been given in Rath et al. [6] and references there in. In the approximation of light neutrino mass, the inverse half-life formula for Majoron emitting $(\beta\beta)_{0\nu}$ decay is given by [7]

$$\left[T_{1/2}^{(0\nu\phi)}(0^+ \to 0^+)\right]^{-1} = \left|\langle g_\alpha \rangle\right|^m \left|M_\alpha\right|^2 G_{\beta\beta\alpha}$$

with m=2 for $(\beta\beta\phi)_{0\nu}$ and m=4 for $(\beta\beta\phi\phi)_{0\nu}$ decay modes. Here $<g_\alpha>$ and $G_{\beta\beta\alpha}$ denote the effective Majoron-neutrino coupling constant and phase space factors, respectively. The index α indicates that effective Majoron-neutrino coupling constant, NTMEs and phase space factors are different for different Majoron models. In closure approximation the NTMEs M_α are defined as

$$M_\alpha = \sum_{n,m} \left\langle 0_F^+ \left\| O_{\alpha,nm} \tau_n^+ \tau_m^+ \right\| 0_I^+ \right\rangle$$

The required nuclear transition operators are given by Hirsch et al. [7].

Results and discussions

We have calculated the NTMEs involved in different Majoron models listed in Table 1 using PHFB wave functions. Further, the NTMEs have been calculated by considering the finite size of nucleon (F) and Jastrow type of short range correlations (SRC) with Miller-Spencer, Argonne V18 and CD-Bonn NN potentials for the Majoron accompanied $(\beta\beta)_{0\nu}$ decay of ^{94,96}Zr, ^{98,100}Mo, ^{104}Ru, ^{110}Pd, ^{128,130}Te and ^{150}Nd isotopes for the $0^+ \rightarrow 0^+$ transition. The results are presented in Table 2 for the case of ^{100}Mo.

Table 2: Calculated NTMEs M_α of Majoron accompanied $(\beta\beta)_{0\nu}$ decay of ^{100}Mo in the PHFB model using PQQ type of two-body interaction.

$\mathbf{M_\alpha}$	**F**	**F+SRC**		
		SRC1	**SRC2**	**SRC3**
M_F	1.3662	1.2026	1.3667	1.4128
M_{GT}	-5.5167	-4.7220	-5.4265	-5.6564
M_{CR}	-0.2078	-0.1802	-0.2071	-0.2148
$M_{F\omega 2}$	0.0012	0.0011	0.0012	0.0012
$M_{GT\omega 2}$	-0.0058	-0.0056	-0.0059	-0.0059

In Table 2, SRC1, SRC2 and SRC3 denote the Jastrow type of short range correlations (SRC) with Miller-Spencer, Argonne V18 and CD-Bonn NN potentials, respectively. The calculation of NTMEs for rest of the nuclei stated above along with the extracted limits on effective Majoron-neutrino coupling will be presented in the symposium.

Conclusions

To summarize, we study the Majoron accompanied $(\beta\beta)_{0\nu}$ decay of ^{94,96}Zr, ^{98,100}Mo, ^{104}Ru, ^{110}Pd, ^{128,130}Te and ^{150}Nd isotopes for the $0^+ \rightarrow 0^+$ transition within PHFB model using pairing plus quadrupole-quadrupole type of two-body effective interaction and calculate the appropriate NTMEs of nine different Majoron models for extracting the effective Majoron-neutrino coupling from available half-life limits.

References

[1] F. T. Avignone III, S. R. Elliott, and J. Engel, Rev. Mod. Phys. 80, 481 (2008).
[2] J. D. Vergados, H. Ejiri, and F. Simkovic, Rep. Prog. Phys. 75, 106301 (2012).
[3] M. Doi and T. Kotani, Prog. Theor. Phys. 89, 139 (1993).
[4] M. Hirsch, H. V. Klapdor-Kleingrothaus, and O. Panella, Phys. Lett. B 374, 7 (1996).
[5] P. Bamert, C. P. Burgess and R. N. Mohapatra, Nucl. Phys. B 449, 25 (1995)
[6] P. K. Rath, R. Chandra, K. Chaturvedi, P. Lohani, P. K. Raina, and J. G. Hirsch, Phys. Rev. C 88, 064322 (2013).
[7] M. Hirsch, H. V. Klapdor-Kleingrothaus, S. G. Kovalenko and H. Pas, Phys. Lett. B 372, 8 (1996).